



McGinley & Associates

5690 Riggins Court
Suite C
Reno, NV 89502

ph: 775.829.2245
fax: 775.829.2213
www.mcgin.com

LAS VEGAS WASH INITIAL PERCHLORATE MODELING REPORT

Las Vegas Wash
Henderson, Nevada

Prepared for:

*Nevada Division of Environmental Protection
333 W. Nye Lane
Carson City, NV 89706*

October 20, 2003

| Soil and Groundwater Remediation

| Regulatory Compliance

| Environmental Audits

| Hydrogeology

| Hazmat Response

TABLE OF CONTENTS

1.	INTRODUCTION.....	1
1.1	Background.....	1
1.1.1	Study Area Description	2
1.1.2	Remediation History.....	2
1.2	Objectives	2
2.	CONCEPTUAL MODEL	3
2.1	Geology.....	3
2.1.1	Stratigraphy.....	3
2.1.2	Structure.....	4
2.1.3	Geophysical Survey	4
2.2	Hydrogeology.....	4
2.2.1	Hydrologic and Hydrogeologic Control Features	5
2.2.2	Aquifer Hydraulic Properties	5
2.3	Water Budget.....	6
2.3.1	Surface Water Flow.....	6
2.3.2	Groundwater Flow.....	7
2.4	Perchlorate Distribution and Mass Flux	9
2.4.1	Surface Water	9
2.4.2	Groundwater	9
2.4.3	Mass Flux in Paleochannel.....	10
3.	GROUNDWATER MODELING METHODS	11
3.1	Numerical Codes, Software Selections, and Modeling Technique.....	11
3.1.1	Groundwater Flow Code	11
3.1.2	Solute Transport Code.....	12
3.1.3	Modeling Technique.....	12
3.2	Domain and Grid.....	12
3.3	Boundary Conditions.....	13
3.4	Aquifer Parameters	14
3.5	Initial Conditions, State, Simulation Time, and Solvers	15
3.6	Pore Volume Calculations.....	15
3.7	Base Case and Best-Estimate Models	16
3.8	Sensitivity Analyses	16
4.	GROUNDWATER MODELING RESULTS	16
4.1	Groundwater Flow.....	16
4.2	Solute Transport	17
4.2.1	Base Case Analysis Results	17
4.2.2	Sensitivity Analysis Results	17
5.	DISCUSSION AND CONCLUSIONS	18
6.	RECOMMENDATIONS.....	20
7.	REFERENCES	22

8.	LIMITATIONS	24
9.	CLOSING	25

LIST OF TABLES

Table 1	Sheet Piling Beneath Erosion Control Structures
Table 2	Summary of Aquifer Test Results for Wash Gravels
Table 3	Summary of Aquifer Test Results for Paleochannel
Table 4	Average Surface Water Flows and Discharges to Las Vegas Wash for 2002
Table 5	Summary of Discharges to Disposal Basins, City of Henderson
Table 6	Groundwater Flow and Discharges to Groundwater
Table 7	Cross Section Analysis and Mass Flux at Athens Road
Table 8	Cross Section Analysis and Mass Flux at Seep Area
Table 9	Athens Road and Seep Area Pumping Summary
Table 10	Mass Flux at LM-6 and Northshore Road
Table 11	Selected Perchlorate Concentrations for Alluvium South of Wash
Table 12	Perchlorate Concentrations for Groundwater from Wash Alluvium
Table 13	Numerical Model Grid Bottom Data
Table 14	Boundary Assignment Values
Table 15	Solute Concentration Input Function Variables
Table 16	Erosion Control Structure Hydraulic Conductivity Multipliers
Table 17	Northshore Road Field Data

LIST OF FIGURES

Figure 1	Project Location Map Showing Las Vegas Wash Study Area
Figure 2	Geologic Map of Study Area
Figure 3	Alluvium/Tertiary Formation Contact Elevation Contours
Figure 4	Isopach of Alluvium
Figure 5	Groundwater Elevations and Contours in Alluvium
Figure 6	Location of Conceptual Model Elements
Figure 7	Schematic of Conceptual Model
Figure 8	Numerical Model Grid Bottom Contours
Figure 9	Numerical Model Boundary Assignments

LIST OF PLOTS

Plot 1	Reach (2) Solute Concentration Input Function
Plot 2	Reach (3) Solute Concentration Input Function
Plot 3	Reach (4) Solute Concentration Input Function
Plot 4	Relative Solute Concentration Input Functions
Plot 5	Breakthrough Curve: Wash Concentrations
Plot 6	Breakthrough Curve: Wash Concentrations Versus Pore Volumes
Plot 7	Breakthrough Curve: Aquifer Concentrations
Plot 8	Breakthrough Curve: Wash Mass
Plot 9	Breakthrough Curve: 90%-Efficient Model
Plot 10	Breakthrough Curve: 95%-Efficient Model
Plot 11	Breakthrough Curve: Reach (4) Zero-Flux Model

LIST OF APPENDICES

Appendix A	Geophysical Survey Report
Appendix B	Modifications and New Source Code for MT3D

Appendix C Model Results
Appendix D Sensitivity Analyses Results

1. INTRODUCTION

This report describes the methods and results of an investigation of the fate and transport of perchlorate in the Las Vegas Wash, near Henderson, Nevada, by request of the Nevada Division of Environmental Protection (NDEP). The purpose of the investigation was to develop a predictive tool, via data compilation and conceptual and numerical model development, to address temporal distributions of perchlorate in the Las Vegas Wash.

The conceptual and numerical models described herein focus on the alluvial aquifer system of the study area. Therefore, data from the deeper perchlorate plume in the Tertiary Formation southwest of the subject study area is not addressed herein.

The quality of this project has been greatly enhanced by data and concepts made readily available by numerous entities. McGinley and Associates, Inc (MGA) would like to acknowledge, in particular, the NDEP (Doug Zimmerman, Todd Croft), Southern Nevada Water Authority (SNWA; Joseph Leising, Jerry Hester), and Kerr-McGee (KMG; Susan Crowley, Ed Krish) for their willingness to participate. Contributions were also made by Basic Remediation Company (BRC), City of Henderson, City of Las Vegas, and Clark County Sanitation District.

1.1 Background

The history of perchlorate production at the BMI Industrial Complex has been summarized in several previous reports including Geraghty & Miller (1993), Leising and Mace (2001), and NDEP (2003). Production of perchlorate compounds began within the BMI Industrial Complex in 1945. Initially, both the U.S. Navy and Western Electrochemical Company (WECCO) produced perchlorate compounds. In 1955, WECCO merged with American Potash and Chemical Company (AM&CC). The Navy ceased their operations in 1962 and sold that portion of the plant to AP&CC. Kerr-McGee purchased AP&CC in 1967 and continued perchlorate compound production until ceasing manufacturing in 1998. The remaining perchlorate compounds were recovered from the on-site lined ponds and process equipment, and the perchlorate production process was dismantled by March 2002.

High concentrations of Perchlorate are found dissolved in groundwater within the gravels of the Las Vegas Wash near Henderson, NV. The presence of the perchlorate is a result of past industrial activities which occurred over a large area of the alluvial fan above the wash, specifically, the BMI Industrial Complex and the BMI Upper and Lower Ponds (Ponds). The BMI Complex is still active; however, use of the Ponds for the disposal of process effluent was discontinued in 1976.

Groundwater characterization efforts at the BMI Complex and vicinity have identified two perchlorate plumes south of the Wash. One plume originates from the former Pacific Engineering & Production Company of Nevada (PEPCON) facility and extends northeasterly towards the Wash. The second plume originates from the KMG facility within the BMI Complex and extends north-north easterly towards the Wash. Groundwater flowing through the wash gravels encounters a series of fault structures at the east end of the subject study area, daylights, and combines with surface water flow, which continues to Lake Mead and the Colorado River.

1.1.1 Study Area Description

The study area encompasses an approximately two-mile reach of Las Vegas Wash (Wash) located in the southeastern portion of Las Vegas Valley as shown in Figure 1. Surface water in the Wash generally flows west to east, discharging into Lake Mead. Groundwater in the Wash gravels generally flows west to east, before encountering a fault zone and being re-directed to surface water flows. Wash gravels are comprised of unconsolidated sandy pebble to cobble gravel overlying fine grained Tertiary deposits (Bell and Smith, 1980; Bingler, 1977). The Wash gravels range in width from over 2,000 feet on the west side of the study area to approximately 1,000 feet on the east as shown on Figure 2.

Land surface generally slopes from the BMI Complex and Ponds to the north toward the Wash with an approximate gradient of 0.020. Groundwater flows north to the Wash with an approximate gradient of 0.010. At the present time groundwater flow from the BMI Complex and Ponds occurs primarily within fairly well defined paleochannels. The paleochannels are incised into underlying lower permeability, fine grained Tertiary deposits. Quaternary alluvium comprised chiefly of silts, sands, and gravels overlie and fill the paleochannels. Perchlorate-impacted groundwater originating from the KMG facility flows within one of the paleochannels and discharges to the Wash as both a surface and subsurface discharge.

1.1.2 Remediation History

Groundwater characterization and remediation efforts related to the occurrence of perchlorate in surface water and groundwater in the Las Vegas Valley have been underway since July 1997. Capture and treatment of the surface water flow at the Seep Area was initiated in November 1999 and has continued to date. The seep flow varies seasonally but has been routinely gauged in excess of 300 gallons per minute (gpm). The captured surface water is treated through an ion exchange system and is discharged to the Wash down stream of the capture point.

Groundwater has been pumped from Seep Area Wells since October 2001 in an effort to reduce the amount of perchlorate entering the Wash system. Groundwater extraction at the Seep Area was increased from four wells and the seep to nine wells and the seep in early 2003. Pumping rates from October 2002 through March 2003 have varied between approximately 324 gpm and 584 gpm.

A line of eight pumping wells across the paleochannel was installed at Athens Road approximately one mile up-gradient from the Seep Area to achieve plume capture. Pumping and treatment of perchlorate-impacted groundwater at Athens Road was initiated in July 2002. However, the wells did not operate on a continuous basis until October 2002 as a result of several equipment problems related to the treatment system. A separate ion exchange system was installed and became operational in mid-October 2002 to allow for continuous operation of the Athens Road wells. Pumping rates from October 2002 through March 2003 have varied between approximately 230 gpm and 250 gpm.

1.2 Objectives

The overall project objective was to develop an understanding of how reduced mass loading of perchlorate from the main paleochannel affects perchlorate loading within the Wash. Four specific project objectives were defined, as follows:

1. Develop an understanding of the geological and hydrogeologic setting of the Wash gravels;

2. Identify other potential sources (paleochannels);
3. Estimate time required for perchlorate to flush from Wash gravels; and
4. Assess the need for remediation in the Wash based on simulated temporal perchlorate distributions at the discharge location of the study area.

To accomplish these objectives, four tasks were identified:

1. Data Compilation and Review
 - collect, review, and analyze existing information;
2. Geophysical Survey
 - conduct a geophysical survey at strategic locations across Las Vegas Wash;
3. Conceptual Model
 - develop a conceptual model (including identification and description of pertinent materials, geometries and structures, and fluid and contaminant mass balances) based on results of data review and geophysical survey; and
4. Numerical Model
 - develop a groundwater flow and solute transport model to evaluate perchlorate flushing from the wash gravels following source removal.

2. CONCEPTUAL MODEL

The conceptual model summarizes the current understanding of hydrogeologic conditions within the main paleochannel contributing perchlorate to the Wash, wastewater discharges to and surface water flow in the Wash, groundwater flow in the Wash gravels, and groundwater flow from the area between the BMI Upper and Lower Ponds and the Wash. The conceptual model is based fundamentally upon reports by Leising (2001), Kerr-McGee (2001), memoranda by the NDEP (2003), and data furnished by SNWA, BRC, City of Henderson, City of Las Vegas, and Clark County Sanitation District.

Reviewed water level, perchlorate, and surface water flow data were collected by SNWA, NDEP, KMG, and BRC over a period of approximately five years from various wells and surface water locations. Data sets provided by each entity are not individually comprehensive of all data stations, and are not collectively contemporaneous. Additionally, some data stations have been abandoned. Other data (e.g., aquifer hydraulic properties) were generated by separate entities over a time period of approximately 20 years. MGA, for the purposes of this investigation, has assumed that all the data are of equal quality, unless otherwise specified.

2.1 Geology

2.1.1 Stratigraphy

The study area lies on coalesced alluvial fans from the McCullough Range and River Mountains south of the Wash and from Frenchman Mountain north of the Wash (Bell and Smith, 1980). The alluvial fans are Quaternary deposits that uncomfortably overlay the Tertiary Formation.

The upper portion of the Tertiary Formation south of the Wash that was penetrated by monitor wells and geotechnical boreholes on and adjacent to the site is composed of gypsiferous clays, silts, and fine sands. The surface of the Tertiary Formation slopes to the north toward the Wash and appears to be erosional with incised channels. The surface map of the Tertiary Formation was developed from KMG's well database and results from the geophysical survey lines across the Wash. Figure 3 shows contours on top of the Tertiary Formation within the study area and model domain. Further discussion regarding the development of this map is included in Section 3.2. The surface of the Tertiary Formation forms the lower boundary of the model.

South of the Wash, Quaternary alluvial fan deposits are primarily composed of poorly sorted sand and gravel with silts and clay that grade to finer material toward the Wash. Locally the alluvium is cemented by caliche. Within the study area the fan deposits range in thickness from about 20 to 60 feet.

Recent deposits comprised of unconsolidated, poorly sorted, sandy pebble to cobble gravel occur within the Wash across the site (Bell and Smith, 1980 and Bingler, 1977). Thickness of the Wash gravels range from about 50 feet on the west to over 100 feet on the east. Figure 4 shows an alluvium isopach map that was developed from KMG's well data base and results from the geophysical survey lines across the Wash.

2.1.2 Structure

On the eastern boundary of the study area, a fault zone cuts across the Wash. Basement rock material is exposed in the Wash about 1.8 miles downstream of the Pabco Weir at this location. Bell and Smith (1980) mapped a concealed fault about 2,500 feet upstream of this location (Figure 2).

2.1.3 Geophysical Survey

A geophysical investigation was conducted along five profiles across the Wash utilizing both time domain electromagnetic (TDEM) soundings with a Geonics EM-47 and frequency domain electromagnetic (FDEM) profiles with a Geonics EM-34 terrain conductivity meter. The results of the geophysical survey are provided in Appendix A. A total of 76 TDEM soundings were conducted along the five profiles totaling 9450 feet in length to map the depth to the top of the Tertiary clay unit underlying the Wash gravels. FDEM profiles were acquired along the profiles to map lateral changes in deep resistivity structure potentially associated with changes in depth to the clay unit.

2.2 Hydrogeology

The principal inflows to the groundwater system study area include subsurface inflow from up-gradient Wash gravels, main paleochannel, area south of the Wash and north of the former BMI Ponds, and Rapid Infiltration Basins (RIBs) south of the Wash. Primary groundwater outflow from the system is conceptualized as discharge to the Wash channel at the fault zone on the east side of the site. Groundwater within the alluvium occurs under unconfined conditions and flows north to the Wash at an average gradient of 0.010 as shown on Figure 5. At the present time groundwater flow from the BMI Complex and Ponds occurs primarily within fairly well defined paleochannels. The paleochannels are incised into underlying lower permeability, fine grained Tertiary deposits. Quaternary alluvium comprised chiefly of silts, sands, and gravels overlie and fill the paleochannels. Perchlorate impacted groundwater originating from the KMG facility flows within one of the paleochannels (herein referred to

as the main paleochannel) and discharges to the Wash as both a surface and subsurface discharge.

2.2.1 Hydrologic and Hydrogeologic Control Features

Erosion Control Structures

Erosion control structures are used to stabilize the channel of the Wash. Three erosion control structures have been installed within the study area. These are the Pabco Weir, the Historic Lateral Weir, and the Bostic Weir. Three additional erosion control structures are planned within the study area. These are the Sunrise Mountain Weir, the Landfill Weir, and the Lower Narrows Weir. The weir structures control surface water elevations behind them and, to some degree, groundwater flow around and beneath them. Structure locations are shown on Figure 6.

The erosion control structures are generally constructed with sheet piling driven into the soil at the weir and toe of the structure. Present-structure weir and toe elevations and separation are summarized in Table 1. The sheet piling has the effect of reducing the area for groundwater flow within the Wash gravels. The sheet piling is typically present to approximately 15 feet below ground surface, and extends from bank to bank of the Wash. At the Historic Lateral the original 90-inch pipeline serves the purpose of the up-stream sheet piling.

Paleochannels

Gravel mining operations in the area north of the Upper Ponds in Sections 29 and 32 resulted in removal of the alluvium overlying the fine grained Tertiary Formation. As a result, the mapped paleochannels in this area were destroyed (Figure 6). The paleochannels in the western portion of the Upper Ponds in Section 6 appear to trend north-northwest toward the main paleochannel beneath the Lower Ponds area. These features appear to converge as they approach the Seep Area.

Fault Zone

The fault zone identified on the east end of the study area controls groundwater flow by truncating the Wash gravels and forcing groundwater to flow to the surface (Leising, 2001).

2.2.2 Aquifer Hydraulic Properties

Aquifer tests were conducted at three locations within the study area in Wash gravels by Kerr-McGee (2001) and Converse (1986 and 2002). Reported transmissivity values for the tests from the Seep Area and Rainbow Gardens were in reasonable agreement (Table 2). However, the reported value for the test at the Historic Lateral was higher by a factor of approximately four. For the purpose of the conceptual model analysis, the transmissivity for the aquifer test at the Historical Lateral was estimated based on the specific capacity of the pumping well by the method developed by Theis (1935) as described in Fetter (2001). The resulting transmissivity was estimated at 20,000 ft²/day which is in agreement with the other aquifer tests' results. Using aquifer thickness values ranging from 35 to 38 ft, the geometric mean hydraulic conductivity from the three tests is 485 ft/day (Table 2). Reported aquifer storativity ranged from about 0.08 to 0.22. These values are consistent with typical values of specific yield for medium sand to coarse gravel (from 0.20 to 0.25).

The results of aquifer tests conducted in the vicinity of the paleochannel at Athens Road and at the northeastern corner of the City of Henderson aeration ponds (Kerr-McGee, 2001) are provided in Table 3.

Slug tests in the Tertiary Formation were conducted in five piezometers at the Historic Lateral Wash Crossing (Converse, 1986). Hydraulic conductivity values calculated from these tests ranged from 1.18×10^{-1} to 2.74×10^{-2} feet/day. Converse noted that these values appeared high for clayey soils, and that sand lenses or porous gypsum layers may have influenced the results. The reported values are typical for silt or silty, fine sand.

2.3 Water Budget

Measured and estimated sources of surface water and groundwater inflow into and outflow from the Wash were inventoried to develop an initial water budget for the study area. Table 4 summarizes surface water flows, Table 5 summarizes groundwater flows, and Figure 7 shows a schematic of the conceptual model. Describing and estimating flows into and out of the system is necessary prior to developing a numerical flow model.

Within the study area groundwater flow was assumed to have four components: groundwater inflow in the Wash from upstream, flow within the main paleochannel, City of Henderson RIBs, and groundwater inflow from the area north of the Ponds between Pabco Road and the narrows. Groundwater flow from north of the Wash and discharge from the Tertiary Formation were assumed negligible for the conceptual model.

2.3.1 Surface Water Flow

Surface water flows in the Wash were evaluated for 2002 based on measured flows and compared to known discharges during 2002 to the Wash.

Surface Inflows

The locations for surface water gauging stations are shown on Figure 6. Stream flow data obtained from eight U.S. Geological Survey (U.S.G.S.) gauging stations in the Wash, including:

- Vegas Valley Drive,
- Wasteway,
- Duck Creek,
- Pabco Road, and
- Northshore Road.

Table 4 shows average flows for the surface water gauging stations. The U.S.G.S. data are provisional and subject to revision.

Surface Discharges to Wash

Municipal and industrial wastewater discharges to Wash inventoried included:

- Clark County,
- City of Las Vegas,
- City of Henderson,
- Pittman Bypass Pipeline, and
- Perchlorate Treatment System.

Table 4 shows average discharges from municipal and industrial facilities. Total average discharge from municipal and industrial sources to the Wash for 2002 was 218 cfs.

Surface Outflow

Surface water outflow was measured at the Northshore Road gauging station located about 5 miles downstream from Pabco Weir. Average daily flow measured in 2002 at Northshore Road was 244 cfs.

Average daily flow at Pabco was estimated at 230 cfs. The difference in flow between Pabco Weir and Northshore Road was approximately 14 cfs; the difference being assumed to be groundwater outflow from the Wash gravels into Las Vegas Wash surface flow.

2.3.2 Groundwater Flow

Monitor well location coordinates, measuring point elevation, and depth to water data were provided by KMG and SNWA for wells they routinely monitor. These data were screened for wells located within the study area and a combined data set was developed for use in modeling. Additional well location and monitoring data were provided by the City of Henderson. For several locations where there were no current data, location and elevation information were developed from the SNWA GIS data base. Most of the data were from 2002 and 2003; a few data points, e.g., the former Rhodes Ranch area represent monitor well locations and water level elevation data that were from the GIS data base.

Groundwater Inflow

Subsurface inflow was evaluated for the Wash below Duck Creek, the main paleochannel, and the area east of Pabco Road to the Narrows.

Effluent Disposal Basins

The City of Henderson operates three effluent disposal basins (P2 RIBs, Birding Preserve, and Pabco RIBs) south of the Wash. Discharge to these disposal basins is summarized in Table 5. Adjusting the discharge for evaporative losses of approximately 8.2 ft/year (Shevenell, 1996) the recharge to groundwater is about 4.8 cfs (Tables 5 and 6) total for all three basins.

Wash Below Duck Creek

Data from the Las Vegas SE Folio Geologic Map (Bingler, 1977), log for SNWA well WMW7.8, and data for well LG030 (Figure 6), and the geophysical cross section at Line 1 (Figures 3 and 4) were used to develop an estimate for groundwater flow upstream of the study area. These data indicated that the depth to the base of the alluvium was greater than 30 feet, depth to water was about 12 feet, and the width of the recent Wash deposits was about 1750 feet. Using the geometric mean hydraulic conductivity of 485 ft/day from aquifer tests for the Wash, the subsurface inflow was estimated at 3.0 cfs shown on Table 6.

Paleochannel at Athens Road

Groundwater flow in the main paleochannel at Athens Road was estimated for the geologic cross section B-B' developed by Kerr-McGee (2001) (Figure 6). The cross section, about 2100 feet in length, was digitized across the channel in segments separated by perchlorate concentration intervals of 10, 100, 200, 300, and 400 mg/L to estimate areas, Table 7. Aquifer hydraulic properties from Table 3 and a measured hydraulic gradient (Kerr-McGee, 2001; Plate 1) were used to estimate the flow at 83,061 ft³/d or 0.961 cfs.

Paleochannel at Seep Area

In the Seep Area about 6,500 feet north of Athens Road groundwater flow in the main paleochannel was estimated for the geologic cross section A-A' developed by Kerr-McGee (2001; Figure 2). The cross section, about 2510 feet in length, was digitized across the channel at perchlorate concentration intervals of 10, 20, 40, 60, and 80 mg/L to estimate areas, Table 8. Aquifer hydraulic properties from Table 2 and a measured hydraulic gradient (Kerr-McGee, 2001; Plate 1) were used to estimate the flow at 487,100 ft³/d or 5.64 cfs.

Based on maps of the top of the Tertiary Formation (Figure 3) and water table map for the alluvium (Figure 5), all the water from the Birding Preserve and P2 RIBs, and about one-half the water from the Pabco RIBs was assumed to flow to the Seep Area. Summing the groundwater flow at Athens Road plus the discharges to groundwater corrected for evaporation yields 4.8 cfs. The combined flows compare favorably with the total flow at the Seep Area.

Alluvium South of the Wash

Within the area described as south of the Wash and north of the BMI Ponds and east of the Pabco RIBs there are few monitor wells completed in the alluvium. Thus, site characterization in the area is inadequate in terms of hydraulic properties, water levels, and perchlorate data for the alluvium. Some data for this area comes from wells that have been abandoned, thus data cannot be verified and in some cases dates back to 1998.

However, an initial estimate for the hydrologic conditions was made based on two key assumptions: 1) the City of Henderson Pabco RIBs are assumed to create a hydraulic barrier in the alluvium such that groundwater from the main paleochannel does not migrate eastward; and 2) that a few wells immediately adjacent to the Wash represent average conditions for the area. Groundwater flows north to the Wash with an approximate gradient of 0.010. Based on an estimated average saturated thickness of 25 feet, section length of 3,950 feet, and estimated range for hydraulic conductivity from 10 to 100 feet/day (assumed lower and upper bounds) for the alluvium, groundwater discharge was estimated to range from 0.11 to 1.1 cfs (Table 6).

Groundwater Outflow

Groundwater Pumping for Remediation

KMG operates a pumping and treatment system for the removal of perchlorate from groundwater before it enters the Wash gravels. A line of eight pumping wells was installed across the paleochannel at Athens Road approximately one mile up-gradient from the Seep Area. Pumping and treatment of perchlorate-impacted groundwater at Athens Road was initiated in July 2002; however, continuous operation did not occur until October 2002. In addition, KMG also has been pumping from a seep and a line of nine wells immediately up-gradient of the Seep Area. Pumping from the seep began in November 1999. Pumping from the initial four Seep Area wells began in October 2001 south of the Seep. Pumping from this area increased in October 2002 when all well fields began delivery of water to the ion exchange treatment systems. Pumping from the Seep Area was further increased in March 2003 when five additional wells were placed in operation. Pumping data for the period from October 2002 through March 2003 is summarized in Table 9. For the period pumping at Athens Road averaged 0.53 cfs and pumping at the Seep and Seep Area wells averaged 1.07 cfs for a total groundwater removal of 1.60 cfs.

Groundwater Discharge to Las Vegas Wash

Groundwater flow within the Wash gravels is truncated at the fault. Based on review of surface water flows in the Wash (Table 4) the groundwater discharge at this point was estimated at about 14 cfs. Assuming that all subsurface inflow and groundwater recharge from infiltration basins discharge at the fault zone, groundwater outflow is estimated to range from 8.9 to 9.9 cfs (Table 6).

The groundwater discharge to the Wash therefore appears to be constrained between 8.9 cfs (Table 6) and 14 cfs (Table 4). Of these two discharge estimates, the groundwater inventory range of 8.9 to 9.9 cfs is favored, due to the inherent inaccuracy of the surface water flows recorded for wide weirs, and the averaging techniques employed in the surface water inventory.

Tertiary Formation

Hydraulic head relationships between the alluvium and Tertiary Formation have not been clearly defined over the study area. Southwest of the study area and down-gradient of the former PEPCON Facility hydraulic head was found to increase with depth (Kleinfelder, 1999 and 2000). Preliminary data from two wells in the Wash indicate a downward gradient downstream of Pabco Weir (SNWA, 2003). At this time there appears insufficient data to draw conclusions about the patterns of these trends. However, in terms of this investigation, because the hydraulic conductivity of the underlying Tertiary in the study area is very low, the contribution of groundwater from or loss of groundwater to the Tertiary was assumed to be insignificant.

2.4 Perchlorate Distribution and Mass Flux

Perchlorate contributions to the Wash from groundwater sources evaluated included the paleochannel at Athens Road and Seep Area, discharge from the area north of the former BMI Ponds east of the Pabco RIBs and narrows. The effect of the City of Henderson effluent disposal basins on perchlorate concentration at the Seep Area was evaluated. Perchlorate contributions from north of the Wash and from the Tertiary Formation were assumed negligible for the conceptual model.

2.4.1 Surface Water

Perchlorate mass flux in the Wash has been shown to increase between SNWA monitoring stations LM-6 and Northshore Road (Leising, 2001). Based on the differences in flow and flux between the two stations, the required input concentration was estimated to be 3.5 mg/L to achieve the difference in mass flux (Leising, 2001). The estimated perchlorate input required to achieve the mass flux difference was reevaluated using a later data set from December 2001 to February 2003 as shown in Table 10. Data for the evaluation were obtained from SNWA. The time of grab sample collection and Wash flow measurement interval occurred at the same time of day to reduce error due to fluctuations in flow (Leising, 2001). For the second data set, the required perchlorate input was estimated at 3.5 mg/L also.

2.4.2 Groundwater

Alluvium

Alluvium South of the Wash

Perchlorate data collected for the area is sparse and covers the time period from 1999 through 2002. A few wells selected to represent the area are listed in Table 11. Also on Table 11, the

well designated LMW/RMW represents the geometric mean of data from eleven wells in the City of Henderson former landfill and the Rhodes Ranch areas. A perchlorate value of 1.0 mg/L was used to represent this area, which is in general agreement with the data.

Wash Gravels

Limited groundwater sampling for perchlorate in the Wash gravels has been conducted down stream from the Seep Area to date. However, discharge water from dewatering operations during construction of the Pabco Weir (UNLV, 2000) and Bostic Weir (SNWA, 2003) was monitored for concentrations of perchlorate (Table 12). Perchlorate concentration of the discharge water from the Pabco dewatering operation ranged from 1.0 to 45 mg/L, with an average of 10 mg/L. During recent dewatering at the Bostic Weir perchlorate concentration ranged from 1.1 to 7.2 mg/L, with an average of 3 mg/L. The average value for perchlorate from dewatering at both weirs represents a very large volume of groundwater sampled and is assumed to be representative of respective reaches of the Wash gravels. The SNWA has monitored selected wells and seeps along the Wash since 1999; Table 12 provides a summary of that perchlorate data. Based on this data for the Wash gravels, initial conditions are assumed to be 10 mg/L between the Seep and Pabco Weir and 3.0 mg/L below Pabco Weir to the fault zone.

Tertiary Formation South of Wash

Downstream from Pabco Weir one monitoring well WMW 5.58S(d) has been completed in the Tertiary Formation (SNWA, 2003). The well was sampled two times in 2002 and the perchlorate concentration ranged from 3.1 to 4.9 mg/L.

2.4.3 Mass Flux in Paleochannel

Based on the evaluation of groundwater flow at the cross sections at Athens Road B-B' and the Seep Area A-A' (Figure 6), mass flux was evaluated for perchlorate within the main paleochannel. The low end perchlorate concentration for the section width was set at 10 mg/L with the assumption it would account for the majority of the mass.

Paleochannel at Athens Road

The concentration mid-point for the digitized cross section intervals of 10, 100, 200, 300, and 400 mg/L and the groundwater flow for each segment were used to estimate mass flux for the section A-A' at 1,104 pounds per day, Table 7. An area weighted concentration of 213 mg/L was estimated for the cross section.

Paleochannel at Seep Area

Based on maps of the top of the Tertiary Formation (Figure 3) and water table map for the alluvium (Figure 5), all the water from the Birding Preserve and P2 RIBs, and about one-half the water from the Pabco RIBs was assumed to flow to the Seep Area at about 3.74 cfs. The flow at the disposal basins was adjusted for evaporation. The concentration mid-point for the digitized cross section intervals of 10, 20, 40, 60, and 80 mg/L and the groundwater flow for each segment were used to estimate mass flux for the section B-B' at 1,170 pounds per day, Table 8. An area weighted concentration of 39 mg/L was estimated for the cross section

The mass fluxes at both cross sections are comparable as would be expected assuming that there are no additional inflows with significant perchlorate concentration. The average perchlorate mass flux due to groundwater flow at Athens Road (1,104 lbs/day) and the Seep Area (1,170 lbs/day) compares favorably with the combined average mass recovered from the Athens Road and Seep Area Recovery Systems (1,384 lbs/day).

However, the area weighted concentrations for the Athens Road and Seep Area cross sections are significantly different. The area weighted concentration at the Seep was evaluated using a dilution model accounting for the flows and concentrations at Athens Road and the City of Henderson effluent disposal basins, as follows.

$$C_M = \frac{(C_A \times Q_A + C_P \times Q_P)}{(Q_A + Q_P)} \quad (1)$$

where C_M is resultant concentration, C_A is the concentration at Athens Road, Q_A is the flow at Athens Road, C_P is the concentration for the disposal basins, and Q_P is the flow from the disposal basins.

For Athens Road both flow and concentration were taken from the cross section evaluation. For the effluent disposal basins, the flow and concentration were estimated as described below. Based on the top of Tertiary contours and alluvial water level elevations, the total flow for the Birding Preserve and P2 Ponds and one-half the flow from the Pabco RIBs were used as the flow rate (discharge to groundwater). Inflows to the ponds were adjusted for evaporation to estimate discharge to groundwater. Because the wastewater has not been typically analyzed for perchlorate, an input concentration was estimated at 0.010 mg/L based on the Alfred M. Smith Water Treatment Facility finished water and monitoring data from the Wash upstream of the Seep Area. The resultant concentration of the mix was calculated as 44 mg/L. This number compares favorably with the area weighted concentration at the Seep Area of 39 mg/L.

3. GROUNDWATER MODELING METHODS

3.1 Numerical Codes, Software Selections, and Modeling Technique

The codes selected for groundwater flow and solute transport modeling, respectively, were MODFLOW2000 and MT3D. Beyond modeling codes, pre- and post-processing software was utilized for model input file preparation and model output visualization, including Scientific Software, Inc. *Groundwater Vistas* and Golden Software, Inc. *Surfer*.

3.1.1 Groundwater Flow Code

The U.S. Geological Survey modular finite-difference ground-water flow model, MODFLOW2000 (Harbaugh et al., 2000) was used for the purpose of simulating groundwater flow. This code is the latest release of MODFLOW (McDonald and Harbaugh, 1988), which is the most widely used program for simulating ground-water. The popularity of the program is attributed to the ease of understanding and use, and extensive model verification and documentation (Anderson and Woessner, 1992). MODFLOW2000 will be referred to as MODFLOW herein. MODFLOW may be used to approximate the solution to the partial-differential equation for three-dimensional transient groundwater flow in heterogeneous and anisotropic media, assuming constant fluid density and alignment of the principal axes of hydraulic conductivity with the coordinate system (McDonald and Harbaugh, 1988; Harbaugh et al., 2000). MODFLOW is modular in structure: it uses a suite of subroutines for the solution of the groundwater flow problem and simulation of various hydrologic system components. An in-depth treatment of the methods and applications of MODFLOW are readily available.

3.1.2 Solute Transport Code

MT3D (Zheng, 1990) is a three-dimensional solute transport model for simulation of advection, dispersion and chemical reactions of contaminants in groundwater systems. MT3D was first developed by S.S. Papadopoulos & Associates, Inc. with partial support from the U.S. Environmental Protection Agency (USEPA). Since 1990, MT3D has been available as a public domain code from the USEPA. MT3D is based on a modular structure to simulate solute transport. MT3D interfaces directly with MODFLOW for the head solution, and supports all the hydrologic and discretization features of MODFLOW. MT3D has been widely accepted and applied in numerous field-scale modeling studies throughout the world. An in-depth treatment of the methods and applications of MT3D are readily available.

MT3D Modifications

Modifications to the MT3D code set were required to maintain mass conservation and correctly simulate mass pathways over gaining and losing reaches of the wash. Two of the stock version source files were modified (mt3dms4.for, and mt_ssm4.for) and three new source files were created (ade.for, erfc.for, and river_flow.for). The code modifications and new source codes are presented in Appendix B. These modifications simulate the removal of solute mass from the wash gravels to the wash over gaining reaches of the wash, allow for mixing with wash flow and concentrations using Equation (1), and input the resultant concentrations from the wash to the wash gravels over down-stream losing reaches of the wash.

3.1.3 Modeling Technique

The groundwater flow and solute transport models (model-sets) were run using a Monte Carlo, or stochastic, technique. The model-sets were run together for 1,800 simulations (or realizations), with each model-set run using a randomly generated set of model parameters. The parameters specified to be variable (or uncertain) included hydraulic conductivity, porosity, dispersivity, the initial concentration term for the solute concentration input function over Reach (2) (discussed below), and the velocity and groundwater flux terms for the solute concentration input function over Reach (4) (discussed below). Each uncertain parameter value was chosen from a uniform range defined by a minimum and maximum value.

The results of the suite of solute transport realizations were generated as the median (i.e., 50 percentile) breakthrough curve and the 95% confidence interval breakthrough curves, based on the ranges of parameters input.

3.2 Domain and Grid

The areal dimensions of the model domain are shown on Figures 1 through 6. The areal extents of the modeling domain were designed to incorporate critical site conceptual model components, particularly the location of the main paleochannel adjacent to the wash in the southwest, and the location of the fine-grained materials outcropping along the fault zone within the wash in the northeast. The southeast vertex of the domain is given as Northing 26,731,866 feet, Easting 829,039 feet, State Plane Coordinate system (Nevada East). The domain extends 5,900 feet north and 12,000 feet east from the southeast vertex.

The domain was discretized into a two-dimensional model grid with regular row and column spacing of 50 feet (118 rows and 240 columns). The grid spacing was chosen to provide

sufficiently fine resolution for discretizing the extents of the active channel while minimizing computational time requirements for solution.

The top of the model grid is defined as land surface. Grid top elevations were extracted from the U.S.G.S. Henderson 1:24,000 scale 10-meter Digital Elevation Model (DEM). The uppermost boundary of the models, however, are “free-surface” boundaries. The elevation of the top of each stochastic model realization is determined in an iterative fashion as the aquifer is simulated as an unconfined aquifer.

Grid bottom contours and elevations are shown on Figure 8. The bottom of the model grid is defined as the contact between the wash gravels and underlying fine grained materials. Grid bottom elevations were interpolated from the results of the geophysical survey and from well log interpretations. A summary of the spatial data used to interpolate the grid bottom elevations is provided in Table 13.

3.3 Boundary Conditions

A schematic showing boundary-type assignments for the numerical model is provided in Figure 9. A summary of boundary assignment values is provided in Table 14.

Groundwater Flow Model

The Neumann-type boundary condition (specified no-flow) was used to de-activate all cells with nodes located outside of the areas mapped as Quaternary Alluvium (Qa) on the Nevada Bureau of Mines and Geology (NBMG) Henderson Quadrangle (Figure 2). This delineation is also shown with a red line in Figures 2 through 7. The remaining active cells are also shown on Figure 9.

The use of Neumann-type boundaries was employed model-wide to simulate the groundwater inventory-derived fluid fluxes.

The Neumann-type boundary condition (specified-flow) was used to simulate groundwater flow into the west and south edges of the active model domain, using the MODFLOW Well Package. These specified-flow boundaries were subdivided into four reaches corresponding to elements of the groundwater budget on Table 6. Groundwater entering the western edge of the model within the wash (3 cfs) was simulated using Reach (1). Groundwater entering the wash from the main paleochannel (5.273 cfs) was calculated by subtracting the average pumping at Athens Road (0.527 cfs, Table 9) from the estimated groundwater flux at Athens Road (1.0 cfs) and adding the inflow from the RIBs (4.8 cfs). The resulting flow was simulated by apportioning the total flow between Reaches (2) (2.933 cfs) and (3) (2.34 cfs). The range of the groundwater flux over Reach (4) used for the stochastic suite was defined with a minimum and maximum value of 0.11 and 1.1 cfs (Table 6). These cells are shown in red on Figure 9.

The Cauchy-type (mixed) boundary condition was used to simulate wash stage heads, using the River Package. This boundary condition was assigned to cells that contained the trace of the south edge of the wash; the head value assigned was interpolated from the SNWA-provided GIS. These cells are shown in blue on Figure 9. Treatment water discharge to the study area were indirectly simulated using the MT3D code modifications as described in Section 3.1.3 above. The location of simulated treatment water discharge to the model is shown on Figure 9.

The Neumann-type boundary condition (specified-flow) was also used to simulate groundwater extraction at the seep and the seep wells, using the Well Package. These specified-flow boundaries were designated with two reaches. Groundwater extraction at the seep (-0.406 cfs) was simulated using Reach (9). Groundwater extraction at the seep wells (-0.667 cfs) was simulated using Reach (10). These cells are shown in red on Figure 9.

Solute Transport Model

Solute inputs to the model domain were simulated using the Well Package over Reaches (1) through (4). Concentrations of solute were assigned over Reach (1) as a constant 10 µg/L. Concentrations of solute were generated using a one-dimensional solute transport equation as an input function, for assignment over Reaches (2) through (4), as follows:

$$C(t) = \frac{1}{2} \operatorname{erfc} \left[\frac{L - vt}{\sqrt{4D_L t}} \right] [C_1 - C_0] + C_0,$$

where C [µg/L] is the concentration value assigned at time t [d], L is the length between the source and boundary [ft], v is the groundwater velocity [ft/d], D_L is the coefficient of longitudinal dispersion [ft²/d], C_1 is the initial concentration [µg/L], and C_0 is the final concentration [µg/L]. A summary of the variables used for each Reach input function is provided in Table 15, and a plot of each input function is provided in Plots 1 through 3. Plot 4 shows the relative magnitude and timing of solute inputs for Reaches (2) through (4). The initial concentrations along each Reach were as follows: Reach (2) (50,000 µg/L), and Reaches (3) and (4) (1,000 µg/L).

The range of the initial concentration term for the solute concentration input function over Reach (2) used for the stochastic suite was defined with a minimum and maximum value of 40,000 and 50,000 µg/L, respectively. The range of the velocity term for the solute concentration input function over Reach (4) used for the stochastic suite was defined with a minimum and maximum value of 0.07 to 7 ft/d, respectively.

Solute inputs were also simulated using the River Package and the MT3D code modifications as described in Section 3.1.3 above. Treatment water solute flux to the study area was indirectly simulated using the MT3D code modifications. The location of simulated treatment water solute concentrations input is shown on Figure 9.

3.4 Aquifer Parameters

Groundwater Flow Model

Hydraulic conductivity was modeled as a homogeneous and isotropic field for each realization, with the exception of the vicinities of the erosion control structures. The range of hydraulic conductivity values used for the stochastic analysis was defined with a minimum and maximum of 450 and 550 ft/d, respectively.

Simulation of the erosion control structures (the Pabco, Bostic, and Historic Lateral structures) was accomplished using a hydraulic conductivity multiplier for each cell in which a structure was present. Each multiplier was calculated based on the percent of the cell that the erosion control structure sheet piling occupies. The Pabco structure has sheet piling only on the up-stream side. The Bostic structure has sheet piling on the up- and down-stream sides. The Historic Lateral structure has sheet piling on the down-stream side only, and the Historic Lateral pipeline serves as the stabilizer on the up-stream side (the multiplier for the pipeline was calculated using the equation for the volume of a cylinder). The average of the

erosion control structure multipliers was 0.77, with the exception of the average multiplier for the Historic Lateral pipeline of 0.97. A summary of the erosion control structure multipliers is provided in Table 16.

Solute Transport Model

Porosity was modeled as a homogeneous field for each realization. The range of porosity values used for the stochastic suite was defined with a minimum and maximum of 0.10 and 0.30, respectively.

Dispersivity was modeled as a homogeneous and isotropic field for each realization. The range of dispersivity values used for the stochastic suite was defined with a minimum and maximum of 500 and 1,000 ft, respectively.

3.5 Initial Conditions, State, Simulation Time, and Solvers

Groundwater Flow Model

For each realization, initial hydraulic heads were assigned as a constant field of 1,700 ft, and the groundwater flow model was run as a steady-state simulation. The PCG2 solver was used with a head change criterion for convergence of 0.001 and a residual criterion for convergence of 1.

Solute Transport Model

For each realization, initial concentrations were assigned as a field of 10,000 $\mu\text{g/L}$ for areas upstream of the Pabco erosion control structure and 3,000 $\mu\text{g/L}$ for areas downstream of the same structure (Table 12) as discussed in Section 2.4.2. The solute transport model was run as a transient simulation of 9,131 days (25 years) duration. The third-order TVD solver was used with a closure criterion of 0.001.

Model Time

The specified concentrations assigned to Reach (2) begin to decay when the toe of “fresh” groundwater from the Athens Road extraction well array is simulated to reach that boundary. Therefore, time zero for the model-sets is inferred to be the approximate date that continuous groundwater treatment began at Athens Road: October 2002.

3.6 Pore Volume Calculations

Predicted Wash concentrations versus Wash gravel pore volumes through-flow was calculated by relating pore volumes to the time required for a pore volume to discharge from the model domain. Although the breakthrough curves can be converted from a time scale to a pore-volume scale as noted, complex groundwater/surface water interactions at the site allow for a significant amount of perchlorate transport interaction with the wash. Therefore, the use of a pore-volume representation is not strictly valid.

First, the head solution was obtained from the best-estimate model run. Next, the total model pore volume (simulated aquifer volume within area of study) was calculated by subtracting each cell bottom elevation from the corresponding calculated head, and multiplying this difference by the cell areal dimension and a value for porosity of 0.20 (the best-estimate value). The total model cell volume was calculated to be 198,297,343 ft^3 . The fluid flux discharging from the best-estimate model was calculated to be 670,753 ft^3/d . The time to flush one pore volume from the Wash gravels in the area of study is estimated using:

$$T_{pore} = \frac{198,297,343 \text{ ft}^3}{670,753 \text{ ft}^3/\text{d}} = 295.63 \text{ days.}$$

Therefore, one can convert a breakthrough curve in days, to a breakthrough curve in pore volumes by dividing the breakthrough curve time by 295.63 d/pore-volume.

3.7 Base Case and Best-Estimate Models

The base case groundwater flow and transport model-set are comprised of the inputs and methods described in Sections 3.1 through 3.6 above. This model-set represents the culmination of the literature review, results of the geophysical survey and the conceptual model presented herein. The base case model is separate from the best-estimate and sensitivity analyses models.

The best-estimate model, referred to only in Section 4.1, is a deterministic model (not stochastic) with the otherwise-variable parameters assigned values from the median of their stochastic suite ranges. The best-estimate model was generated in order to ascertain specific model behaviors.

3.8 Sensitivity Analyses

Three stochastic sensitivity analyses were performed: a “90% efficient remediation system” analysis, a “95% efficient remediation system” analysis, and an analysis with zero flux along Reach (4). Each of these models were modified from the base case model.

The “90% efficient remediation system” analysis (90%-efficient model) was set up with the solute mass flux for Reach (3) assigned a constant value equal to 10% of the initial solute flux from Reach (2), in order to simulate solute movement past the groundwater extraction well array at Athens Road. The “95% efficient remediation system” analysis (95%-efficient model) was set up in a similar manner.

The analysis with zero flux along Reach (4) (Reach (4) zero-flux model) was run after removing the specified flux boundary assignment from the cells included in Reach (4).

4. GROUNDWATER MODELING RESULTS

4.1 Groundwater Flow

The best-estimate groundwater flow model ran without error, and with very few cells deactivated due to simulated drying (less than 0.01%). The model ran with a calculated percent discrepancy (mass budget error) of $-0.02 \text{ ft}^3/\text{day}$. The output volumetric budget included approximately 29.4 cfs of simulated Wash discharge/recharge within the study area. The simulated net groundwater discharge to the wash (as used for the pore volumes calculation above) was calculated as 7.76 cfs. This value is also the net groundwater flux applied to specified-flux boundaries, minus model error.

The sensitivity of the best-estimate model to the simulation of the erosional control structures is relatively insignificant. The global discrepancy between modeled hydraulic heads with and without the simulation of the structures was less than 0.05 ft.

The global mass balance errors for the stochastic groundwater flow suite were less than 0.05% for all realizations.

4.2 Solute Transport

4.2.1 Base Case Analysis Results

A summary of the predicted Wash and aquifer perchlorate concentration and Wash mass time-series (and pore volume series) data for the base case model-set is provided in Appendix C. The Wash and aquifer observation points referred to herein occupy the eastern-most cell of the model assigned as a boundary in the River Package, where groundwater is simulated to daylight into surface water flow; this is the model discharge area. Predicted breakthrough curves of perchlorate for the Wash (time-series and pore volume series) and aquifer, and a mass breakthrough curve of perchlorate for the Wash, are provided in Plots 5 through 8, respectively. Field data obtained by NDEP for the Northshore Road location are plotted on Plot 5 as well. A summary of the NDEP Northshore Road field data is provided in Table 17.

Concentrations of perchlorate in the Wash are predicted to have remained between 300 and 400 $\mu\text{g/L}$ for approximately 0.5 years (April 2003; approximately 0.7 pore volumes) following time zero. Concentrations are predicted to decline relatively sharply between 0.5 and 3 years (November 2005; approximately 3.7 pore volumes) following time zero, until they level out at approximately 13 to 11 $\mu\text{g/L}$. Concentrations decline approximately 95% during this period. Concentrations are not simulated to decline below 10 $\mu\text{g/L}$ (background concentration).

The shape of the breakthrough curve for concentrations of perchlorate in the aquifer is similar to that of the Wash. However predicted aquifer concentrations begin greater than 1,000 $\mu\text{g/L}$. Concentrations are predicted to decline at a greater rate during the first 0.5 years following time zero, and at a much greater rate between 0.5 and 3 years. At approximately 3 years following time zero, concentrations are predicted to decline to approximately 20 $\mu\text{g/L}$. Concentrations decline greater than 98% during this period.

The shape of the mass flux breakthrough curve, and its characteristics, is identical to that of the Wash concentrations. Mass flux is predicted to decline from approximately 450 lbs/day after 0.5 years following time zero, to approximately 16 to 13 lbs/day after approximately 3 years.

4.2.2 Sensitivity Analysis Results

A summary of the predicted Wash perchlorate concentration time-series data for the sensitivity analyses is provided in Appendix D. Predicted breakthrough curves of perchlorate for the Wash for the 90%-efficient, 95%-efficient, and Reach (4) zero-flux model are provided in Plots 9 through 11, respectively.

The inflection point times for the 90%-efficient and 95%-efficient model median breakthrough curves are essentially identical to that of the base case model median curve. The 90%-efficient model predicts that concentrations in the Wash will decline to approximately 70 $\mu\text{g/L}$ after three years following time zero. The 95%-efficient model predicts that concentrations in the Wash will decline to approximately 40 $\mu\text{g/L}$ after three years following time zero. These concentrations are predicted to decline gradually over the remainder of model time to approximately 65 and 38 $\mu\text{g/L}$, respectively.

The median breakthrough curve for the Reach (4) zero-flux model follows that of the base case model median curve until approximately 1.8 years following time zero. This model

predicts that concentrations decline to approximately 11 µg/L three years after time zero, and that concentrations will continue to decline to approximately 10 µg/L (background concentration) within four years.

5. DISCUSSION AND CONCLUSIONS

MGA believes the conceptual model described herein is well-suited for the purpose of the initial investigation presented herein. The conceptual model provides a suitable framework on which to pose a relatively simple “mixing cell” model, as discussed below. Furthermore, uncertainty in the model results are believed to be primarily due to the current level of understanding of conditions in the vicinity of the main paleochannel (i.e., remediation system efficiency, and groundwater and perchlorate flux) than to most other components of the conceptual model, as discussed below. However, the conceptual model presented herein does contain uncertainty due to limitations of temporal and spatial data distributions, and therefore is still somewhat limited in terms of its application beyond that presented herein. The data compilation and review resulted in the identification of relatively few monitor wells within the confines of the Wash banks, no monitor wells in the area of the fault zone, no monitor wells north of the Wash, and very limited data for the area south of the eastern reaches of the Wash. Furthermore, the breadth of data (i.e., water levels, measuring point elevations, perchlorate concentrations, etc.) identified for given locations was inconsistent and non-contemporaneous across the entire population, and in some cases non-reproducible.

MGA believes sufficient data were available to develop an overall water budget for the Wash for the purpose of this project, including surface water flows, and discharges to surface water and groundwater. The results of the conceptual model water budget compare relatively favorably with that of previous investigations (Leising, personal communication, 2003).

The conceptual model mass flux budget indicates that the primary source for the perchlorate plume originates from the KMG facility within the BMI Complex and extends north-northeasterly within the main paleochannel to the Wash. Other groundwater contributions appear to be less significant with respect to the total load in the Wash. This conclusion may be weighted by the relatively sparse data available in other areas of the subject study area. The area south of the eastern reaches of the Wash has been identified as a potential source area for groundwater and perchlorate flux. The model-sets described herein account for this potential to varying degrees. Neither the conceptual model nor the numerical models included an evaluation of the perchlorate plume originating from the former PEPCON facility.

The relatively large volume of water simulated as Wash discharge/recharge may indicate the importance of groundwater/surface water interactions in the study area to solute transport. The integrity of the model in predicting this phenomenon is uncertain. However, the integrity of the modeling of the process may be relatively important to understanding perchlorate transport in the Wash. Although the groundwater/surface water interactions were simulated, a degree of uncertainty exists in the models ability to properly simulate this process. The relative agreement between simulated and observed net fluid provides some level of model verification. However, additional data describing the groundwater/surface water interactions is necessary to provide a higher level of model verification.

The base case transport model fairly consistently under-predicts field concentration data. Only three of the eight plotted data points falls within the 95% model certainty range.

However, the model results show a general agreement with the trend of an exponential fit to the field data.

The more rapid decline in predicted aquifer concentrations than Wash concentrations during the first 0.5 years following time zero may be due to the model-predicted phenomena of a large degree of groundwater/surface water interaction. Higher concentration groundwater may be predicted to discharge to surface water early in its travel path, where it is relatively quickly removed from the study area.

Although the shape of the mass flux and Wash concentrations breakthrough curves are identical, the model predicts field mass flux data much better. Four of the plotted data points fall within the 95% model certainty range. The model results show a general agreement with the trend and values of an exponential fit to the field flux data. The last half of the trend-line falls entirely within the 95% model certainty. Mid-time field data (collected during the second year following time zero, over the critical rate times on the breakthrough curves) will ultimately indicate the integrity of the model-set to predict concentrations and mass flux.

The results of the sensitivity models may provide an indication of the range of perchlorate concentrations to be expected in the Wash as a result of variation in effectiveness of the remedial system in the main paleochannel, or negligible contributions of fluid and/or mass flux from Reach (4). The 90% and 95% efficient models predict a median value of about 65 $\mu\text{g/L}$ and 38 $\mu\text{g/L}$, respectively, after 25 years as compared to about 10 $\mu\text{g/L}$ for the base case model. The Reach (4) zero-flux model predicts approximately 10 $\mu\text{g/L}$ within 4 years, owing to potentially favorable conditions south of the eastern reaches of the Wash, where conditions are poorly understood.

The product of the investigation presented herein is, essentially, a mixing cell model; the resulting solutions of the models are largely modifications to the solute input functions applied over Reaches (2) through (4). The most important of perchlorate inputs identified in this investigation and incorporated into the numerical models occurs in the vicinity of the main paleochannel, along Reach (2). That is to say, the numerical models are most sensitive to the application of the one-dimensional solute transport equation (an analytical model) for the simulation of solute input along Reach (2). Furthermore, the models presented herein have been designed under the assumption that the one-dimensional solute transport equation is an appropriate model for solute inputs along Reaches (2) through (4). The potentially slow release of perchlorate mass from the areas south of the eastern reaches of the Wash, along Reach (4) of the model domain, is also notably significant to model results.

MGA's conclusion regarding the need for perchlorate remediation in the Wash gravels is based upon the criteria of perchlorate concentrations and/or mass flux to approach approximately 10 $\mu\text{g/L}$ or 13 lbs/day. The median results of the base case model predict that perchlorate concentrations and mass flux will be reduced to 10.04 $\mu\text{g/L}$ and 12.98 lbs/day via natural attenuation processes (dispersion and dilution) in approximately 22.25 years (approximately November 2025) following time zero. However, perchlorate concentrations and mass flux are predicted to decline approximately 97% from time zero values (to 13.21 $\mu\text{g/L}$ and 17.08 lbs/day) in approximately 3.1 years (approximately November 2005) following time zero. The process of implementation of active remediation in the Wash gravels (including site characterization studies, remedial alternative and feasibility evaluation, engineering design, equipment evaluation and procurement, contractor bid solicitation, contractor selection, system construction and installation, and troubleshooting/start-up) is estimated to require at least two to three years following regulatory

direction. Based on the above stated criteria, assumptions and results of modeling presented herein, MGA does not believe that active remedial efforts are needed to address dissolved perchlorate in groundwater within the gravels of the Las Vegas Wash at this time.

6. RECOMMENDATIONS

MGA recommends the continuation of monitoring in areas of known groundwater contamination in order to track the progress of perchlorate plume capture within the main paleochannel. The continuation of surface water monitoring is equally important. The implementation of this recommendation may allow for conceptual and numerical model verification. Similarly, a synoptic groundwater/surface water sampling event performed at strategically selected locations within the study area is recommended in order to develop a current (and concurrent) status appraisal of perchlorate distribution and groundwater elevation/Wash stage. The synoptic event should be scheduled following the completion of additional monitor well construction activities recommended below.

Expansion of the model domain to include the areas south of the current model domain, in the vicinity of the main paleochannel and south to Athens Road and areas south of the eastern reaches of the Wash, is recommended in order to limit the greatest degree of uncertainty to the models presented herein. Replacing the solute input functions with individual calibration-ready model elements (plume capture at Athens Road and fluid and solute flux distributions to the Wash from the RIBs and south of the eastern reaches of the Wash) will allow for much greater modeling flexibility and certainty.

Additional site characterization is recommended in order to provide a greater quality and quantity of data to refine the initial conceptual model and strengthen the numerical model-set presented herein, as well as benefit future modeling efforts. These recommendations are summarized in the remainder of this section and are not necessarily listed by priority.

1. An additional geophysical survey is recommended for areas extending west of Line 5 and Line 1 to further define Wash gravel contacts in the vicinity of the fault zone and channel geometry near the confluence of Duck Creek with the Wash.
 - Rationale – Extending the east-west-trending Line 5 will provide information for locating new monitor wells at the fault zone and refine the numerical model grid bottom geometry. This will improve the numerical model at this location with information on geology, hydraulic head relationships, and perchlorate concentration at the point of groundwater discharge. The additional geophysical cross section west of Line 1 will provide information to improve the estimation of groundwater inflow within the channel.
2. Additional monitor wells are recommended to be constructed adjacent to the Wash (including the vicinity of the fault zone), completed within the Wash gravels.
 - Rationale – The sparse data within the boundaries of the Wash banks limits the certainty and use of the conceptual model, as well as necessitates the use of assumptions with regards to perchlorate concentrations for initial conditions in the numerical model. Additional data in these areas will allow for more certainty in model results. Also, hydraulic head data made available in the study area may enable greater flexibility of future modeling efforts (i.e., the use of specified-head boundary assignments and the calibration of such models).

3. Strategically located multi-level monitor well clusters (completed at three separate horizons) are recommended to be constructed.
 - Rationale – There is insufficient data regarding hydraulic head relationships between the Wash gravels and the underlying Tertiary Formation. Also, there is insufficient data to determine if there is a density gradient with the perchlorate plume in the Wash gravels. The models presented herein do not account for the potential of the Tertiary Formation to be a source/sink for groundwater and perchlorate. The inclusion of such conditions may produce substantially different model results than that presented herein.
4. Monitor wells for water level elevation and perchlorate data north of the Wash are recommended to be constructed.
 - Rationale – There are no data from which to determine groundwater inflow from the area north of the Wash. The areas north of the wash may provide a source of groundwater input to the study area, which could reduce the times to predicted Wash perchlorate concentrations at the study area discharge.
5. Monitor wells south of the Wash and along the eastern reaches of the Wash (east of Pabco Road) are recommended to be constructed.
 - Rationale – Groundwater elevation and perchlorate concentration data for this area are very limited. The availability of additional data in this area may enable the substitution of the variable boundary condition for Reach (4) discussed above, and/or verification of the Reach (4) zero-flux sensitivity analysis- wherein background concentrations are predicted to be reached within approximately four years.
6. Adequate testing of the hydraulic properties of the alluvium in the areas south of the eastern reaches of the Wash (east of Pabco Road) in conjunction with #5 above.
 - Rationale – The evaluation of groundwater flux for this area required making assumptions about the hydraulic conductivity for this area. These assumptions are directly related to the shape of the solute concentration input function along Reach (4).

7. REFERENCES

- Anderson, M.P., and W.W. Woessner, 1992. Applied Groundwater Modeling: Simulation of Flow and Advective Transport. Academic Press, Inc.
- Bell, J. W. and Smith, E. I., 1980, Geologic Map of the Henderson Quadrangle, Nevada, Nevada Bureau of Mines and Geology Map 67.
- Bingler, E.C., 1977, Las Vegas SE Folio Geologic Map, Nevada. Nevada Bureau of Mines and Geology Map.
- Converse, 1986, Geotechnical Site Investigation, Las Vegas Wash Crossing of the Las Vegas Valley Lateral Pipeline, Las Vegas, Nevada, prepared for Boyle Engineering, Las Vegas, Nevada, June.
- Converse, 2000, Geotechnical Data Report, Southern Nevada Water Authority, Rainbow Gardens Weir W-3.5, Las Vegas Wash, ½ Mile Upstream of Lake Las Vegas, Clark County, Nevada prepared for Boyle Engineering, Las Vegas, Nevada.
- Converse, 2002, Geotechnical Data Report, Southern Nevada Water Authority East Valley Transmission System, prepared for Boyle Engineering, Las Vegas, Nevada.
- Fetter, C.W., 2001, Applied Hydrogeology, Prentice Hall, Upper Saddle River, New Jersey, pp. 598.
- Geraghty & Miller, 1993, Phase I Environmental Conditions Assessment for Basic Management, Inc., Industrial Complex, Clark County, Nevada, April.
- Harbaugh, A.W., Banta, E.R., Hill, M.C., and McDonald, M.G., 2000, MODFLOW-2000, the U.S. Geological Survey modular ground-water model -- User guide to modularization concepts and the Ground-Water Flow Process: U.S. Geological Survey Open-File Report 00-92, 121 p.
- Hill, M.C., Banta, E.R., Harbaugh, A.W., and Anderman, E.R., 2000, MODFLOW-2000, the U.S. Geological Survey modular ground-water model -- User guide to the Observation, Sensitivity, and Parameter-Estimation Processes and three post-processing programs: U.S. Geological Survey Open-File Report 00-184, 210 p.
- Kerr-McGee, 2003, Letter to U.S. EPA, Reporting Treatment System Operation, April 22.
- Kerr-McGee, 2001, Seep Area Groundwater Characterization Report, prepared for the Nevada Division of Environmental Protection, January, 18, 19 pp. plus Appendices.
- Kleinfelder. 1999. Hydrogeologic Investigations: American Pacific Corporation (Former PEPCON Facility) Henderson, Nevada. April
- Kleinfelder. 2000. Supplemental Hydrogeologic Investigations: American Pacific Corporation (Former PEPCON Facility) Henderson, Nevada. January.
- Leising, J.F., and Mace, J.T., 2001. Results of Perchlorate Monitoring in the Las Vegas Wash, Nevada. Proceedings of the 36th Symposium, Engineering Geology & Geotechnical Engineering, Las Vegas, Nevada, March.

- Longwell, C. R., Pampeyan, E. H., Bowyer, B., and Roberts, R. J., 1965, Geology and Mineral Deposits of Clark County, Nevada, Nevada Bureau of Mines and Geology Bulletin 62, 218 pp.
- McDonald, J.M., and A.W. Harbaugh, 1988. A Modular Three-Dimensional Finite-Difference Ground-Water Flow Model. U.S. Geological Survey Techniques of Water Resources Investigations Book 6 Chapter A1, 586 pp.
- Nevada Division of Environmental Protection, 2003, Fact Sheet – Perchlorate in the Las Vegas Valley, NV, Significant Controls Are Operating, January.
- Nevada Division of Environmental Protection, 2002 – 2003, Las Vegas Wash Monitoring Data for Northshore Road Station, Las Vegas office.
- Plume, R.W. 1989. Ground-Water Conditions in Las Vegas Valley, Clark County, Nevada, Part 1, Hydrogeologic Framework. U.S. Geological Survey Water Supply Paper 2320-A
- Pollard, J., 2000, Sampling results during dewatering of the Pabco Road erosion control structure; unpublished tabulated data, University of Nevada, Las Vegas, Harry Reid Center for Environmental Research.
- SNWA, 2003, Sampling results during dewatering of the Bositc Weir erosion control structure; unpublished tabulated data.
- Shevenell, L., 1996, Statewide Potential Evapotranspiration Maps for Nevada, Nevada Bureau of Mines and Geology, Report 48, pp. 32.
- Standard Methods for the Evaluation of Water and Wastewater, 1995. American Public Health association, American Water Works Association, Water Environment Federation: 19th ed.
- Theis, C.V., 1935. The relation between the lowering of the piezometric surface and the rate and duration of a well using groundwater storage. Trans. Amer. Geophys. Union, 2, pp. 519-524.
- Trudeau, D.A. 1981. Memorandum Report Exploratory Well Drilling Program, Las Vegas Wash Unit, Colorado River Basin Salinity Control Project. U.S. Department of the Interior, Water and Power Resources Services, April
- Westphal, J.A. and Nork, W.E. 1972. Reconnaissance Analysis of Effects of Waste Water Discharge on the Shallow Ground-Water Flow System, Lower Las Vegas Valley, Nevada.
- Wyman, R.V., 1993. Geology of Las Vegas, Nevada. Bulletin of the Association of Engineering Geologists. Vol. XXX, No. 1, pp33 – 78.
- Zheng, C., 1990. MT3D: A modular three-dimensional transport model for simulation of advection, dispersion and chemical reactions of contaminants in ground-water systems, U.S. EPA, R.S. Kerr Environmental Research Laboratory, Ada, Oklahoma.

8. LIMITATIONS

The conclusions and recommendations presented herein are based, in part, on analytical data, field measurements, survey data and results of previous environmental assessment and/or remediation activities conducted by others. MGA makes no warranties or guarantees as to the accuracy or completeness of information provided or compiled by others. Changes in site conditions may occur as a result of rainfall, water usage, or other factors.

It should be recognized that definition and evaluation of environmental conditions is a difficult and inexact science. Judgments and opinions leading to conclusions and recommendations are generally made with an incomplete knowledge of the conditions present. More extensive studies, including additional environmental investigations, can tend to reduce the inherent uncertainties associated with such studies. Additional information not found or available to MGA at the time of writing this report may result in a modification to the conclusions and recommendations contained herein.

The presentation of data in plots presented herein is intended for the purpose of the visualization of environmental conditions. A greater degree of spatial and temporal data density may result in a more accurate representation of environmental conditions. Although such data visualization techniques may aid in providing a conceptual understanding of environmental conditions, such presentations are not intended to completely depict environmental conditions.

This report is not a legal opinion. The services performed by MGA have been conducted in a manner consistent with the level of care ordinarily exercised by members of our profession currently practicing under similar conditions. No other warranty, expressed or implied, is made.

9. CLOSING

MGA anticipates that the information provided herein satisfies the NDEP at this time. Please do not hesitate to call the Project Manager, at (775) 322-2022, or MGA, at (775) 829-2245, with any questions or concerns.

Respectfully submitted,

McGinley and Associates, Inc.

I hereby certify that I am responsible for the services described in this document and for the preparation of this document. The services described in this document have been provided in a manner consistent with the current standards of the profession and to the best of my knowledge comply with all applicable federal, state and local statutes, regulations, and ordinances.

The use of the word "certify" in this document constitutes an expression of professional opinion regarding those facts or findings which are the subject of the certification and does not constitute a warranty or guarantee, either expressed or implied.

Paul Hackenberry, P.G., C.E.M. #1823, Exp. 4/15/05
Project Manager, Consulting Hydrogeologist

Brian Giroux, C.E.M., R.G., C.Hg.
Hydrogeologist

Greg Pohll, Ph.D.
Consulting Hydrogeologist

Reviewed by:

Joseph McGinley, P.E., C.E.M.
Principal

Table 1. Sheet Piling Beneath Erosion Control Structures			
Structure	Elevation (ft, msl)	Horizontal Separation (ft)	
Pabco			
Weir	1530 - 1517	NA	
Toe	Gabion Structure		
Historic Lateral			
Weir	1514 - 1506	94	
Toe	1512 - 1502		
Bostic			
Weir	1506 - 1486	339	
Toe	1491 - 1474		

Table 2. Summary of Aquifer Test Results for Wash Gravels.							
Test Location	Discharge During Test (gpm)	Test Duration (hrs)	Aquifer Thickness (ft)	Maximum Drawdown Observed in Pumping Well (ft)	Transmissivity (ft ² /day)	Hydraulic Conductivity (ft/day)	Storativity
Seep Area	65	36	35	0.94	16,000	457	NA
Historic Lateral	950	24	38	10.8	20,000	526	0.08
Rainbow Gardens	223	24	38	5.32	18,000	474	0.10 – 0.22

Table 3. Summary of Aquifer Test Results for Paleochannel							
Test Location	Discharge During Test (gpm)	Test Duration (hrs)	Aquifer Thickness (ft)	Maximum Drawdown Observed in Pumping Well (ft)	Transmissivity (ft ² /day)	Hydraulic Conductivity (ft/day)	Storativity
Athens Road	45	48	32	2.36	6,880	215	0.07
Northeast Corner Birding Preserve	52	30	25	2.02	8,000	320	0.08

Table 4. Average Surface Water Flows and Discharges to Las Vegas Wash for 2002			
Station Location	Discharge Source	Surface Water Flow (ft³/sec)	Discharge to Wash (ft³/sec)
Inflow			
Vegas Valley Dr.		12.8	
	City of Las Vegas		83
	Clark County		121
Wasteway		225	
Duck Creek		6.1	
	City of Henderson (surface water)		8.6
	Pitman Bypass Pipeline		4.4
	Perchlorate Treatment System		1.6
Pabco Weir		230	
Outflow			
Northshore Road		244	
Groundwater Outflow		14	
Total Municipal and Industrial Discharge to Wash in 2002			218

Table 5. Summary of Discharges to Disposal Basins, City of Henderson.				
Year	Pabco RIBs Discharge (cfs)	Birding Preserve Discharge (cfs)	P2 RIBs Discharge (cfs)	Total Discharge (cfs)
2000	2.73	3.64	0.77	7.14
2001	2.73	3.74	0.45	6.92
2002	2.54	3.29	0.85	6.68

Table 6. Groundwater Flow and Discharges to Groundwater			
Location	Discharge Source	Groundwater Flow (ft³/sec)	Discharge to Groundwater (ft³/sec)
Inflow			
Wash Below Duck Creek	Groundwater	3.0	
Paleochannel at Athens Road	Groundwater	1.0	
City of Henderson	Effluent Disposal Basins		4.8
Area North of Ponds	Groundwater	0.11 - 1.1	
Total		8.9 - 9.9	

Table 7. Cross Section Analysis and Mass Flux at Athens Road

Concentration Interval (mg/L)	Average Concentration (mg/L)	WT Elev. (ft)	Base Alluvium Elev. (ft)	Area (ft ²)	Q (ft ³ /day)	Mass Flux (lbs/day)
10	55	1601	1574	2,528	5,982	21
100	150	1601	1570.5	6,158	14,572	136
200	250	1599.5	1563	3,258	7,710	120
300	350	1598.5	1566	2,819	6,671	146
400	400	1600	1569	1,268	3,001	75
400	350	1600	1571	5,697	13,481	294
300	250	1599.5	1590	5,133	12,147	189
200	150	1598	1586	4,043	9,567	89
100	55	1599	1581	4,196	9,929	34
10		1599.5	1583.5			
Totals				35,100	83,061	1,104
Groundwater flow (cfs)		0.961				
Total length of section (ft)		2,072				
Aquifer Test & Hydraulic Data						
Aquifer Thickness (ft)		32				
Transmissivity (gpd/ft)		51,500				
Hydraulic Conductivity (ft/day)		215				
Hydraulic Gradient		0.011				
Area Weighted Conc.						
Perchlorate (mg/L)		213				

Table 8. Cross Section Analysis and Mass Flux at Seep Area

Concentration Interval (mg/L)	Average Concentration (mg/L)	WT Elev. (ft)	Base Alluvium Elev. (ft)	Area (ft ²)	Q (ft ³ /day)	Mass Flux (lbs/day)
10	15	1556	1516	15,237	62,849	59
20	30	1555	1518	31,815	131,228	245
40	50	1553	1481	12,733	52,520	164
60	70	1552	1483	8,981	37,044	162
80	80	1552	1506	4,215	17,386	87
80	70	1551	1506	8,955	36,937	161
60	50	1550	1501	9,916	40,901	127
40	30	1549	1500	16,568	68,339	128
20	15	1548	1506	9,672	39,894	37
10		1546	1511			
Totals				118,092	487,098	1,170
Groundwater flow (cfs)		5.64				
Total Length of Section (ft)		2,510				
Aquifer Test & Hydraulic Data						
Aquifer Thickness (ft)		35				
Transmissivity (gpd/ft)		120,000				
Hydraulic Conductivity (ft/day)		458				
Hydraulic Gradient		0.009				
Area Weighted Conc.						
Perchlorate (mg/L)		39				
Dilution Model (Flow adjusted for evaporation from COH RIBs)						
Athens Rd + COH RIBs (mg/L)		44				

Table 9. Athens Road and Seep Area Pumping Summary

DATE	Discharge			Conc. ClO ₄ (mg/L)	Mass Removed (lbs/day)
	(gpm)	(cfs)	(ft ³ /day)		
Athens Rd Wells (Monthly Averages)					
Oct-02	229.3	0.511	44,147	263	723
Nov-02	250.0	0.557	48,113	334	1,001
Dec-02	246.7	0.550	47,486	393	1,164
Jan-03	231.7	0.516	44,603	386	1,074
Feb-03	224.0	0.499	43,126	291	783
Mar-03	237.8	0.530	45,770	287	819
Oct 2002-Mar 2003	237.7	0.527	45,541		963
Seep Wells (Monthly Averages)					
Oct-02	191			159.0	365
Nov-02	203			113.6	277
Dec-02	241			45.5	132
Jan-03	338			60.9	247
Feb-03	395			40.7	193
Mar-03	427			66.8	342
Oct 2002-Mar 2003	299				259
Seep (Monthly Averages)					
Oct-02	133			74.0	118
Nov-02	272			74.0	241
Dec-02	201			74.0	179
Jan-03	175			74.0	155
Feb-03	156			74.0	139
Mar-03	156			74.0	139
Oct 2002-Mar 2003	182				162
Total Seep System (Monthly Averages)					
Oct-02	324	0.722	62,359	124	483
Nov-02	475	1.059	91,483	91	519
Dec-02	442	0.986	85,171	58	310
Jan-03	513	1.142	98,678	65	402
Feb-03	552	1.229	106,227	50	332
Mar-03	584	1.300	112,317	69	481
Oct 2002-Mar 2003	482	1.073	92,706		421
Total Athens Road Wells and Seep System					
Average Total Mass Removed					1,384
Total Average Discharge		1.60			

Table 10. Mass Flux at LM-6 and Northshore Road

DATE	LM-6	Pabco	Pabco/LM-6		Northshore	
	ClO ₄ (µg/L)	Flow (cfs) *	Mass Flux (lbs/day)	ClO ₄ (µg/L)	Flow (cfs) *	Mass Flux (lbs/day)
12/19/01	530	173	494	1100	189	1,122
01/09/02	240	289	374	550	261	772
01/16/02	190	265	271	480	252	652
01/20/02	210	245	277	260	284	398
01/23/02				780	222	932
01/30/02	150	260	210	360	243	472
02/06/02	150	262	212	350	254	479
02/13/02	140	292	220	400	257	554
02/20/02	140	254	192	410	261	575
02/27/02	160	267	230			
03/14/02	130	237	166	360	205	397
04/10/02	160	172	148	300	205	331
05/08/02	150	162	131	420	213	481
06/05/02	200	232	250	500	232	626
07/10/02	130	234	164	360	232	449
08/08/02	190	287	293	290	417	651
09/04/02	240	265	343	350	249	470
09/25/02	130	234	164			
10/02/02	110	224	133	330	227	404
10/09/02	100	224	121	230	211	262
10/16/02	170	254	232	290	228	357
10/23/02	160	264	228	330	233	415
10/30/02	120	264	171	320	274	472
11/03/02				200	275	296
11/05/02	120	264	171	290	247	386
11/13/02	87	274	128			
11/20/02	130	196	137	270	257	374
11/27/02				290	251	392
12/04/02	150	203	164	300	278	449
12/11/02	150	201	162	310	269	448
12/24/02	210	220	248	410	278	613
12/31/02	120	228	147	280	289	436
01/08/03	120	203	131	300	285	460
01/15/03	110	225	133	310	282	471
01/22/03	220	201	238	500	264	710
01/29/03	97	268	140			
02/05/03	97	258	135	230	292	362
02/19/03	85	261	120			
Average	160	239	202	378	255	505
Maximum	530	292	494	1,100	417	1,122
Minimum	85	162	120	200	189	262
Number of Samples	35	35	35	33	33	33

* Average flow for the time interval 11:00AM - 4:00 PM

Table 11. Selected Perchlorate Concentrations for Alluvium South of Wash

Location	Date	Concentration Range (mg/L)
RRMW-1	Mar-02	1
HMW-7	Apr-02	1.1
LG010	6/2000 – 12/1999	0.950 – 2.2
WMW5.5S	5/2002 – 10/2002	0.340 – 0.900
WMW4.9s	5/2002 – 11/2002	1.9
LMW/RMW		1.0 *

* Geomean of data from SNWA GIS database

Table 12. Perchlorate Concentrations for Groundwater from Wash Alluvium

Location	Concentration Range (mg/L)	Average (mg/L)
Seep Area (2003)	0.260 – 153*	
Pabco Weir Dewatering (2000)	1.0 – 45	10
Bostic Weir Dewatering (2003)	1.1 – 7.2	3
LM-8 Seeps	0.400 – 3.5	
New C1 Channel	1.2 – 9.9	4

* Depth weighted average for wells in cluster

Table 13. Numerical Model Grid Bottom Data

Location ID	Northing (ft)	Easting (ft)	GS Elev. (ft msl)	A/T Elev. (ft msl)	Source
1_1612	26734546.00	831212.00	1549.54	1484.88	GP Survey
1_2150	26735077.00	831128.00	1554.13	1530.78	GP Survey
1_2250	26735175.00	831112.00	1558.07	1532.65	GP Survey
1_2350	26735274.00	831096.00	1566.93	1534.91	GP Survey
1_2450	26735373.00	831081.00	1562.99	1537.72	GP Survey
1_2560	26735482.00	831064.00	1568.90	1538.35	GP Survey
1_2650	26735570.00	831049.00	1573.49	1537.63	GP Survey
1_2745	26735664.00	831035.00	1577.43	1534.94	GP Survey
1N_1000	26734016.00	830904.00	1550.85	1480.71	GP Survey
1N_1100	26734103.00	830954.00	1550.53	1489.58	GP Survey
1N_1200	26734189.00	831004.00	1550.53	1492.34	GP Survey
1N_1300	26734276.00	831055.00	1550.85	1488.03	GP Survey
1N_1400	26734362.00	831105.00	1549.54	1491.26	GP Survey
2_1060	26734013.00	834748.00	1529.53	1477.29	GP Survey
2_1160	26734112.00	834766.00	1526.90	1476.09	GP Survey
2_1470	26734417.00	834822.00	1523.95	1475.26	GP Survey
2_1570	26734515.00	834840.00	1523.95	1473.02	GP Survey
2_1670	26734613.00	834858.00	1523.95	1473.99	GP Survey
2_1770	26734712.00	834876.00	1523.95	1479.91	GP Survey
2_1870	26734810.00	834894.00	1523.29	1478.20	GP Survey
2_1970	26734910.00	834913.00	1521.98	1480.88	GP Survey
2_2170	26735106.00	834948.00	1521.65	1465.99	GP Survey
2_2520	26735449.00	835012.00	1534.78	1470.79	GP Survey
2_2625	26735553.00	835031.00	1535.11	1470.42	GP Survey
2_380	26733345.00	834625.00	1530.84	1476.36	GP Survey
2_580	26733542.00	834661.00	1541.34	1482.46	GP Survey
2_800	26733752.00	834734.00	1539.37	1473.73	GP Survey
2_960	26733915.00	834729.00	1531.50	1474.81	GP Survey
3_1000	26734306.00	837006.00	1541.34	1490.32	GP Survey
3_1100	26734403.00	836982.00	1540.68	1483.20	GP Survey
3_1200	26734500.00	836957.00	1537.73	1476.12	GP Survey
3_1320	26734616.00	836928.00	1531.50	1468.60	GP Survey
3_1420	26734713.00	836904.00	1524.28	1461.22	GP Survey
3_1520	26734810.00	836880.00	1523.62	1456.74	GP Survey
3_1620	26734878.00	836863.00	1523.95	1456.80	GP Survey
3_1750	26735038.00	836858.00	1508.86	1454.31	GP Survey
3_1850	26735118.00	836856.00	1506.89	1453.98	GP Survey
3_1930	26735218.00	836853.00	1505.91	1450.10	GP Survey
3_2030	26735319.00	836851.00	1506.23	1444.47	GP Survey
3_2315	26735603.00	836843.00	1508.86	1438.83	GP Survey
3_2455	26735743.00	836839.00	1522.64	1454.13	GP Survey
3_2555	26735843.00	836836.00	1522.64	1454.56	GP Survey
3_2655	26735942.00	836834.00	1521.98	1451.38	GP Survey
3_2755	26736042.00	836831.00	1523.62	1449.57	GP Survey
3_2855	26736143.00	836828.00	1524.61	1449.77	GP Survey
3_2955	26736242.00	836825.00	1525.59	1457.97	GP Survey
4_1410	26736271.00	840694.00	1483.60	1483.60	GP Survey
4_1530	26736387.00	840662.00	1478.35	1458.97	GP Survey
4_1850	26736671.00	840520.00	1476.38	1418.24	GP Survey

Table 13. Numerical Model Grid Bottom Data					
Location ID	Northing (ft)	Easting (ft)	GS Elev. (ft msl)	A/T Elev. (ft msl)	Source
4_1900	26736714.00	840494.00	1477.69	1429.82	GP Survey
4_1950	26736757.00	840469.00	1478.35	1435.96	GP Survey
4_2100	26736874.00	840399.00	1505.25	1442.75	GP Survey
4_2200	26736971.00	840340.00	1505.58	1451.44	GP Survey
4_2300	26737057.00	840289.00	1505.58	1478.30	GP Survey
4_2400	26737147.00	840235.00	1506.56	1472.18	GP Survey
4_2500	26737229.00	840186.00	1508.86	1491.83	GP Survey
4_2600	26737314.00	840135.00	1510.50	1510.50	GP Survey
4-5_1625	26736479.00	840635.00	1477.69	1419.09	GP Survey
5_1000	26736352.00	840937.00	1477.36	1477.36	GP Survey
5_1300	26736429.00	840753.00	1476.71	1413.73	GP Survey
5_1545	26736465.00	840519.00	1480.97	1390.30	GP Survey
5_1645	26736453.00	840419.00	1481.30	1364.97	GP Survey
5_1755	26736440.00	840310.00	1481.30	1365.46	GP Survey
5_1845	26736429.00	840221.00	1478.35	1363.67	GP Survey
5_2300	26736299.00	839902.00	1481.30	1383.87	GP Survey
5_2400	26736242.00	839827.00	1481.30	1378.31	GP Survey
5_2600	26736157.00	839656.00	1483.27	1390.98	GP Survey
5_2700	26736113.00	839567.00	1483.92	1371.23	GP Survey
ESE-B2	26732341.80	839248.60	NA	1554.00	KMG
ESE-B3	26731961.20	837860.90	NA	1561.00	KMG
HSC-1	26733118.44	829167.32	NA	1503.00	KMG
HSC-2	26733408.75	830557.59	NA	1482.00	KMG
HSC-3	26735919.80	835538.40	NA	1480.00	KMG
LG009	26734572.85	836000.00	NA	1458.00	KMG
LG016	26735115.80	830725.70	NA	1529.00	KMG
LG017	26732682.70	833420.30	NA	1506.00	KMG
LG019	26733097.80	831713.10	NA	1507.00	KMG
LG235	26734661.40	835955.73	NA	1467.30	KMG
LG236	26734856.71	835937.50	NA	1468.00	KMG
LMW1	26734846.00	839446.56	NA	1478.70	KMG
LMW3	26735454.00	840599.06	NA	1495.30	KMG
LMW4	26733546.00	838291.63	NA	1520.10	KMG
LMW5	26733562.00	840503.00	NA	1531.80	KMG
PC113	26732302.72	829176.92	NA	1543.71	KMG
PC114	26732303.16	829700.65	NA	1544.83	KMG
PC115	26733155.24	831044.52	NA	1505.00	KMG
PC115R	26733131.33	831148.64	NA	1504.79	KMG
PC116	26733213.14	831364.81	NA	1505.50	KMG
PC116R	26733203.15	831348.43	NA	1503.04	KMG
PC56	26732289.43	830645.29	NA	1516.99	KMG
PC57	26732239.50	830831.27	NA	1518.21	KMG
PC58	26732118.26	831123.84	NA	1536.79	KMG
PC59	26732452.69	830150.30	NA	1536.34	KMG
PC60	26732358.75	830405.14	NA	1529.80	KMG
PC61	26732323.18	830524.66	NA	1523.70	KMG
PC62	26732733.52	829764.28	NA	1533.45	KMG
PC63	26732553.25	829925.71	NA	1533.95	KMG
PC68	26732906.82	829616.96	NA	1517.66	KMG

Table 13. Numerical Model Grid Bottom Data

Location ID	Northing (ft)	Easting (ft)	GS Elev. (ft msl)	A/T Elev. (ft msl)	Source
PC69	26733074.08	829478.05	NA	1516.19	KMG
PC74	26734003.52	829203.52	NA	1508.54	KMG
PC75	26734004.98	829194.53	NA	1508.48	KMG
PC76	26734006.74	829183.79	NA	1508.51	KMG
PC79	26733246.69	829815.28	NA	1519.33	KMG
PC80	26733250.46	829823.75	NA	1519.07	KMG
PC81	26733254.71	829833.37	NA	1519.03	KMG
PC82	26733194.85	830317.05	NA	1503.44	KMG
PC83	26733201.29	830325.65	NA	1503.47	KMG
PC84	26733208.53	830332.58	NA	1503.14	KMG
PC85	26733185.56	830816.05	NA	1506.70	KMG
PC86	26733185.76	830826.99	NA	1507.08	KMG
PC87	26733185.37	830837.82	NA	1507.09	KMG
PC88	26733178.42	831259.41	NA	1499.91	KMG
PC89	26733184.33	831264.70	NA	1499.90	KMG
PC90	26733192.63	831271.92	NA	1499.53	KMG
PC91	26733110.85	831729.99	NA	1512.42	KMG
PC92	26733109.85	831749.30	NA	1512.12	KMG
PC93	26733117.81	832179.60	NA	1508.86	KMG
PC94	26733122.48	832189.05	NA	1508.84	KMG
PC95	26733449.91	831227.21	NA	1507.61	KMG
PC96	26733450.83	830896.56	NA	1505.69	KMG
PC97	26733441.54	831565.69	NA	1505.78	KMG
PC99R	26733143.32	831244.93	NA	1500.17	KMG
PC99R2	26733155.42	831258.73	NA	1500.18	KMG
PC99R3	26733160.44	831255.55	NA	1499.90	KMG
PG217A	26732525.30	834363.80	NA	1514.00	KMG
PG229	26732377.64	830459.01	NA	1532.00	KMG
PG234	26732021.69	834960.18	NA	1548.00	KMG
PG256	26732045.40	832117.78	NA	1546.00	KMG
RB-17	26732142.90	836014.10	NA	1540.00	KMG
RB-18	26733459.90	836202.60	NA	1524.00	KMG
RMW-1	26733349.00	836590.90	NA	1517.00	KMG
RMW-10	26732382.80	838327.30	NA	1540.00	KMG
RMW-7	26732460.00	839535.20	NA	1501.00	KMG
GS Elev.	Ground surface elevation above mean sea level.				
A/T Elev.	Alluvium/Tertiary Formation contact elevation above mean sea level.				

Table 14. Boundary Assignment Values					
Boundary	Type	Value or Range Specified			
		Head (ft)	Flow (cfs)	Concentration (ug/L)	
				Minimum	Maximum
Reach (1)	Flux	--	3	10	--
Reach (2)	Flux	--	2.933	10	40,000 to 50,000
Reach (3)	Flux	--	2.34	10	1,000
Reach (4)	Flux	--	0.11 to 1.1	10	1,000
Reach (9)	Flux	--	-0.406	--	--
Reach (10)	Flux	--	-0.667	--	--
Wash	Mixed	GIS	Calculated	Calculated	Calculated

Table 15. Solute Concentration Input Function Variables						
Variable	C ₀ (ug/L)	C ₁ (ug/L)	L (ft)	Velocity (ft/d)	α _L (ft)	DI (ft ² /d)
Reach (2)	10	50000	5000	32	500	16000
Reach (3)	10	1000	10000	1	1000	1000
Reach (4)	10	1000	10000	7	1000	7000

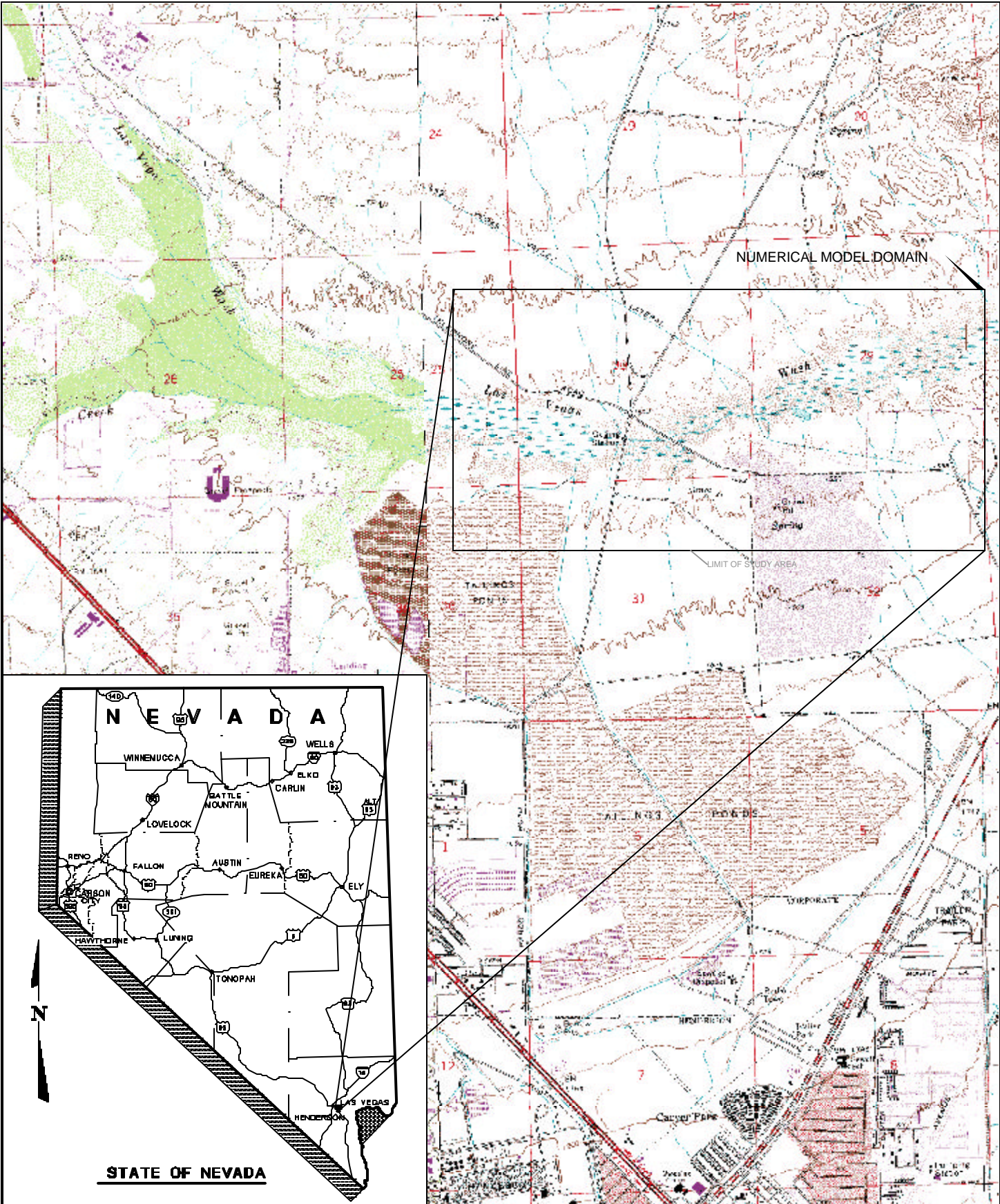
Table 16. Erosion Control Structure Hydraulic Conductivity Multipliers						
Structure ID	Row	Column	Stage (GIS) (ft)	A/T Elev. (ft)	Structure Bottom (ft)	Multiplier (-)
Pabco U	63	76	1531.20	1482.00	1517.00	0.7114
Pabco U	64	76	1531.17	1481.00	1517.00	0.7176
Pabco U	65	76	1531.13	1480.00	1517.00	0.7236
Pabco U	66	76	1531.10	1481.00	1517.00	0.7186
Pabco U	67	76	1531.07	1482.00	1517.00	0.7133
Pabco U	68	76	1531.02	1482.00	1517.00	0.7140
Pabco U	69	75	1531.48	1484.00	1517.00	0.6950
Pabco U	70	75	1531.44	1485.00	1517.00	0.6891
Pabco U	71	75	1531.38	1486.00	1517.00	0.6831
Pabco U	72	75	1531.24	1486.00	1517.00	0.6852
Pabco U	73	75	1530.99	1487.00	1517.00	0.6820
Pabco U	74	74	1531.71	1489.00	1517.00	0.6556
Pabco U	75	74	1530.88	1490.00	1517.00	0.6605
Pabco U	76	74	1531.70	1490.00	1517.00	0.6475
Pabco U	77	74	1532.07	1491.00	1517.00	0.6331
Pabco U	78	74	1532.35	1492.00	1517.00	0.6196
Historic Lateral U	46	132	1515.31	1475.00	*	0.9751
Historic Lateral U	47	133	1514.86	1474.00	*	0.9754
Historic Lateral U	48	133	1514.87	1474.00	*	0.9754
Historic Lateral U	49	133	1514.99	1473.00	*	0.9761
Historic Lateral U	50	134	1514.52	1473.00	*	0.9758
Historic Lateral U	51	134	1514.73	1472.00	*	0.9765
Historic Lateral U	52	134	1514.96	1471.00	*	0.9771
Historic Lateral U	53	134	1515.20	1471.00	*	0.9773
Historic Lateral U	54	135	1514.75	1470.00	*	0.9775
Historic Lateral U	55	135	1515.00	1470.00	*	0.9777
Historic Lateral U	56	135	1515.25	1469.00	*	0.9783
Historic Lateral U	57	136	1514.61	1468.00	*	0.9784
Historic Lateral U	58	136	1514.67	1468.00	*	0.9785
Historic Lateral U	59	136	1514.44	1469.00	*	0.9779
Historic Lateral U	60	136	1518.00	1469.00	*	0.9795
Historic Lateral U	61	136	1519.56	1469.00	*	0.9801
Historic Lateral U	62	137	1517.48	1468.00	*	0.9797
Historic Lateral U	63	137	1517.39	1468.00	*	0.9797
Historic Lateral U	64	137	1517.36	1463.00	*	0.9815
Historic Lateral U	65	138	1516.51	1459.00	*	0.9825
Historic Lateral U	66	138	1516.79	1462.00	*	0.9817
Historic Lateral D	52	137	1512.84	1470.00	1502.00	0.7470
Historic Lateral D	53	137	1513.06	1470.00	1502.00	0.7431
Historic Lateral D	54	137	1513.28	1470.00	1502.00	0.7394
Historic Lateral D	55	138	1512.74	1469.00	1502.00	0.7545
Historic Lateral D	56	138	1512.90	1469.00	1502.00	0.7517
Historic Lateral D	57	138	1513.01	1469.00	1502.00	0.7498
Historic Lateral D	58	138	1513.01	1468.00	1502.00	0.7554
Historic Lateral D	59	139	1512.14	1467.00	1502.00	0.7754
Historic Lateral D	60	139	1513.19	1466.00	1502.00	0.7629
Historic Lateral D	61	139	1513.99	1464.00	1502.00	0.7602
Historic Lateral D	62	139	1514.52	1465.00	1502.00	0.7472
Bostic U	37	171	1496.70	1431.00	1486.00	0.8371
Bostic U	38	171	1496.90	1432.00	1486.00	0.8320

Table 16. Erosion Control Structure Hydraulic Conductivity Multipliers

Structure ID	Row	Column	Stage (GIS) (ft)	A/T Elev. (ft)	Structure Bottom (ft)	Multiplier (-)
Bostic U	39	171	1497.13	1432.00	1486.00	0.8291
Bostic U	40	170	1497.67	1429.00	1486.00	0.8301
Bostic U	41	170	1497.85	1424.00	1486.00	0.8395
Bostic U	42	170	1497.95	1425.00	1486.00	0.8362
Bostic U	43	170	1498.06	1430.00	1486.00	0.8228
Bostic U	44	170	1498.03	1434.00	1486.00	0.8121
Bostic U	45	171	1497.75	1437.00	1486.00	0.8066
Bostic U	46	171	1497.82	1442.00	1486.00	0.7882
Bostic U	47	171	1497.90	1446.00	1486.00	0.7707
Bostic U	48	171	1498.00	1450.00	1486.00	0.7500
Bostic U	49	172	1497.76	1451.00	1486.00	0.7485
Bostic U	50	172	1497.87	1452.00	1486.00	0.7412
Bostic D	37	180	1493.15	1419.00	1484.00	0.8766
Bostic D	38	180	1493.28	1417.00	1484.00	0.8783
Bostic D	39	180	1493.41	1412.00	1484.00	0.8844
Bostic D	40	179	1494.00	1413.00	1484.00	0.8765
Bostic D	41	179	1494.14	1417.00	1484.00	0.8686
Bostic D	42	179	1494.38	1421.00	1484.00	0.8585
Bostic D	43	179	1494.46	1425.00	1484.00	0.8494
Bostic D	44	179	1494.53	1430.00	1484.00	0.8368
Bostic D	45	180	1494.18	1433.00	1484.00	0.8336
Bostic D	46	180	1494.28	1438.00	1484.00	0.8173
U	Up-stream					
D	Down-stream					
A/T Elev.	Alluvium/Tertiary Formation contact elevation above mean sea level.					
*	No structure bottom used. Calculation based on volume of 6 foot diameter pipeline.					


Table 17. Northshore Road Field Data

Date	Time (d)	Time (yr)	Concentration	
			(ug/L)	Mass (lb/d)
11/26/02 9:30 AM	26	0.07	480	459
12/26/02 9:20 AM	56	0.15	530	615
1/28/03 9:30 AM	89	0.24	590	627
2/28/03 11:30 AM	120	0.33	390	686
3/28/03 9:15 AM	148	0.41	460	285
4/28/03 9:30 AM	179	0.49	500	405
5/28/03 9:30 AM	209	0.57	400	492
6/27/03 9:15 AM	239	0.66	230	266
7/28/03 9:30 AM	270	0.74	220	325



DESIGNED	BB	8/03
DRAWN	TAD	8/03
CHECKED		
APPROVED		
No.	DESCRIPTION	BY DATE

FIGURE 1
PROJECT LOCATION MAP
 -SHOWING-
LAS VEGAS WASH
STUDY AREA
HENDERSON, NEVADA



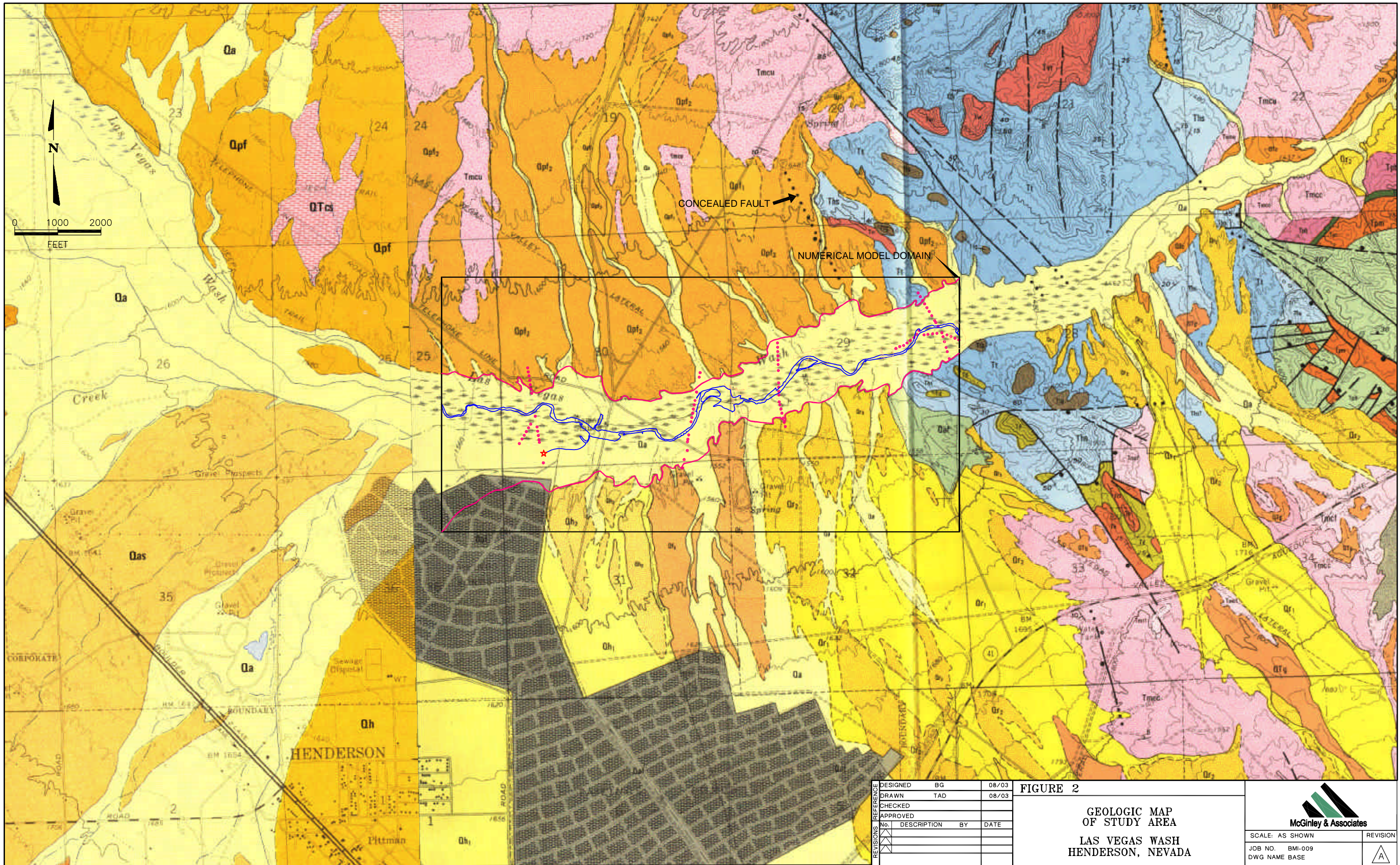
SCALE: AS SHOWN

JOB NO. BMI-009

DWG NAME BASE

REVISION

A




CONCEALED FAULT

NUMERICAL MODEL DOMAIN

DESIGNED	BG	08/03
DRAWN	TAD	08/03
CHECKED		
APPROVED		
NO.	DESCRIPTION	BY DATE

FIGURE 2
GEOLOGIC MAP
OF STUDY AREA
LAS VEGAS WASH
HENDERSON, NEVADA



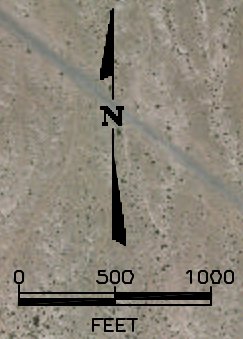
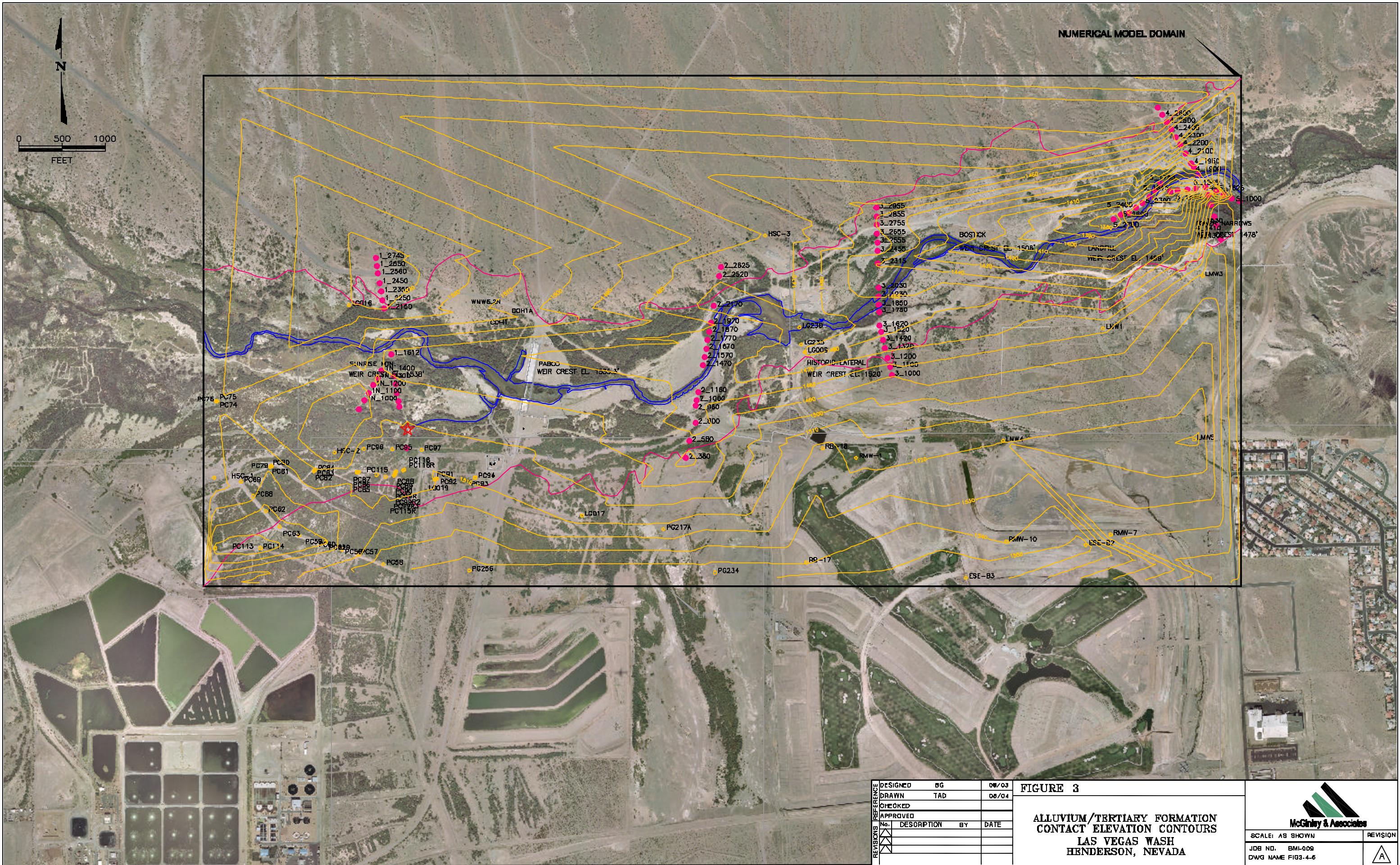
McGinley & Associates

SCALE: AS SHOWN REVISION

JOB NO. BMI-009 REVISION

DWG NAME BASE

A

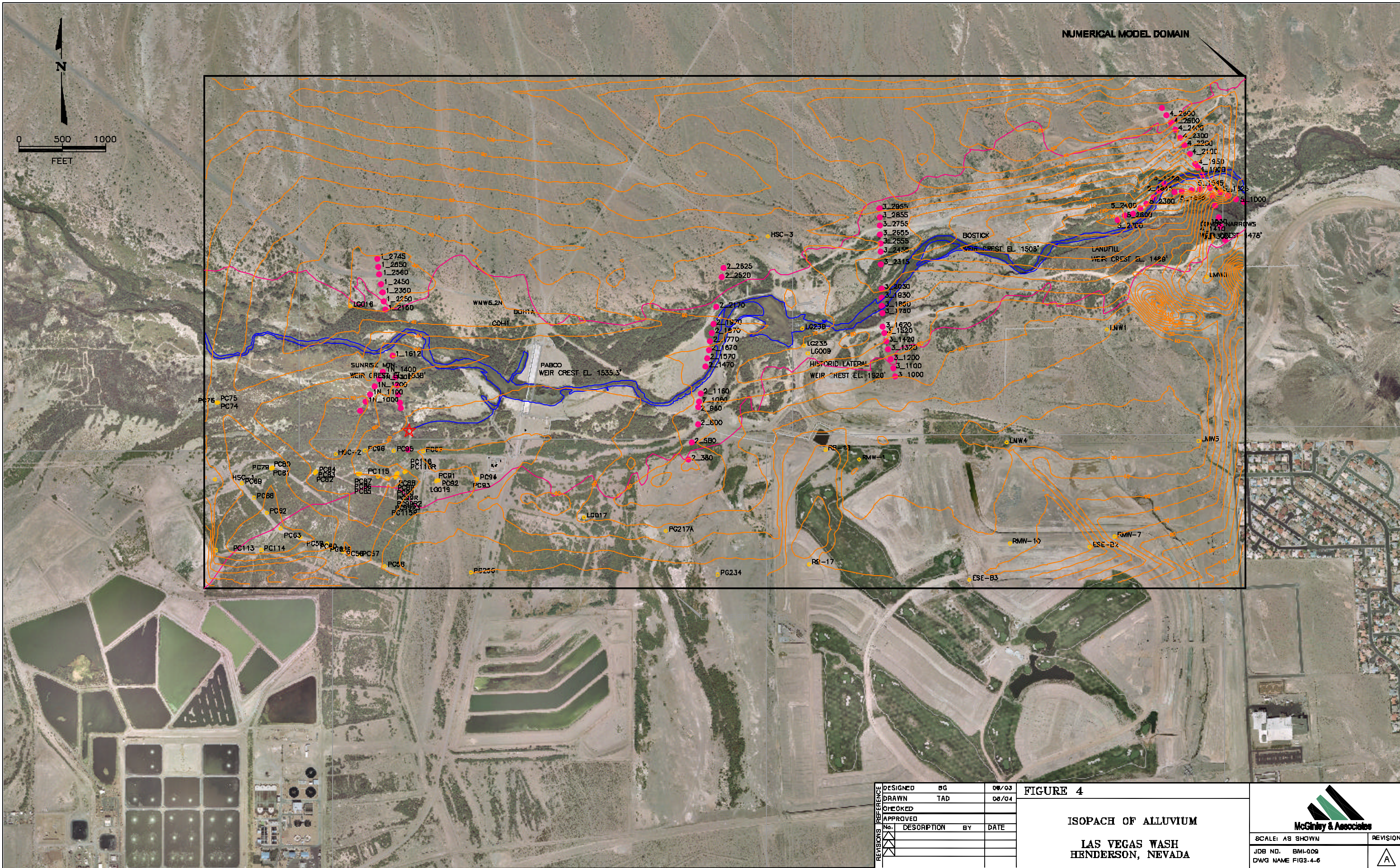


DESIGNED	BG	08/03
DRAWN	TAD	08/04
CHECKED		
APPROVED		
No.	DESCRIPTION	BY DATE

FIGURE 3
ALLUVIUM/TERTIARY FORMATION CONTACT ELEVATION CONTOURS
LAS VEGAS WASH
HENDERSON, NEVADA


McKinley & Associates

SCALE: AS SHOWN	REVISION
JOB NO. BML-009	
DWG NAME FIG3-4-6	A



DESIGNED	BG	08/03
DRAWN	TAD	08/04
CHECKED		
APPROVED		
No.	DESCRIPTION	BY DATE

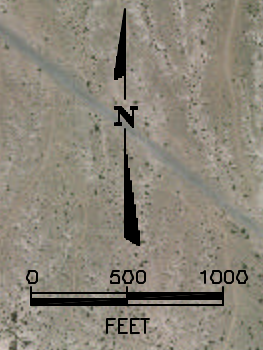
FIGURE 4
ISOPACH OF ALLUVIUM
LAS VEGAS WASH
HENDERSON, NEVADA



McKinley & Associates

SCALE: AS SHOWN	REVISION
JOB NO. BML-009	
DWG NAME FIG3-4-6	

NUMERICAL MODEL DOMAIN



DESIGNED	BG	08/03
DRAWN	TAD	08/03
CHECKED		
APPROVED		
REVISIONS	No.	DESCRIPTION BY DATE

FIGURE 5
GROUNDWATER ELEVATIONS AND
CONTOURS IN ALLUVIUM
LAS VEGAS WASH
HINDERSON, NEVADA

McKinley & Associates

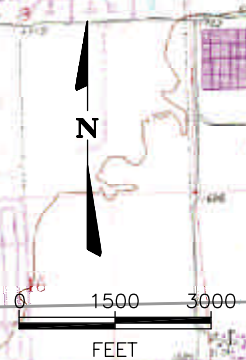
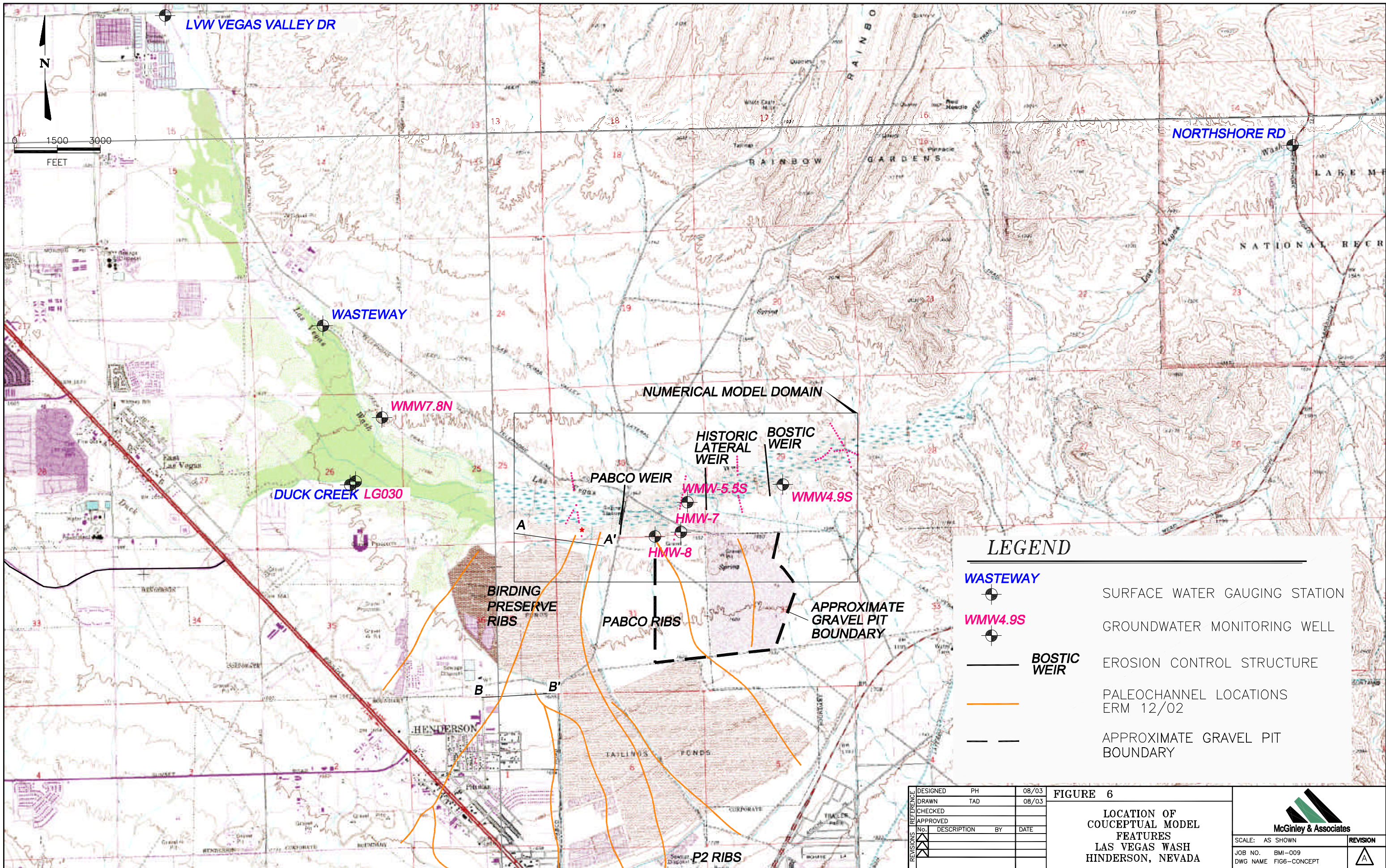
SCALE: AS SHOWN

JOB NO. BML-009

DWG NAME FIGS. 4-6

REVISION

A



LEGEND

	WASTEWAY	SURFACE WATER GAUGING STATION
	WMW4.9S	GROUNDWATER MONITORING WELL
	BOSTIC WEIR	EROSION CONTROL STRUCTURE
		PALEOCHANNEL LOCATIONS ERM 12/02
		APPROXIMATE GRAVEL PIT BOUNDARY

DESIGNED	PH	08/03
DRAWN	TAD	08/03
CHECKED		
APPROVED		
No.	DESCRIPTION	BY DATE

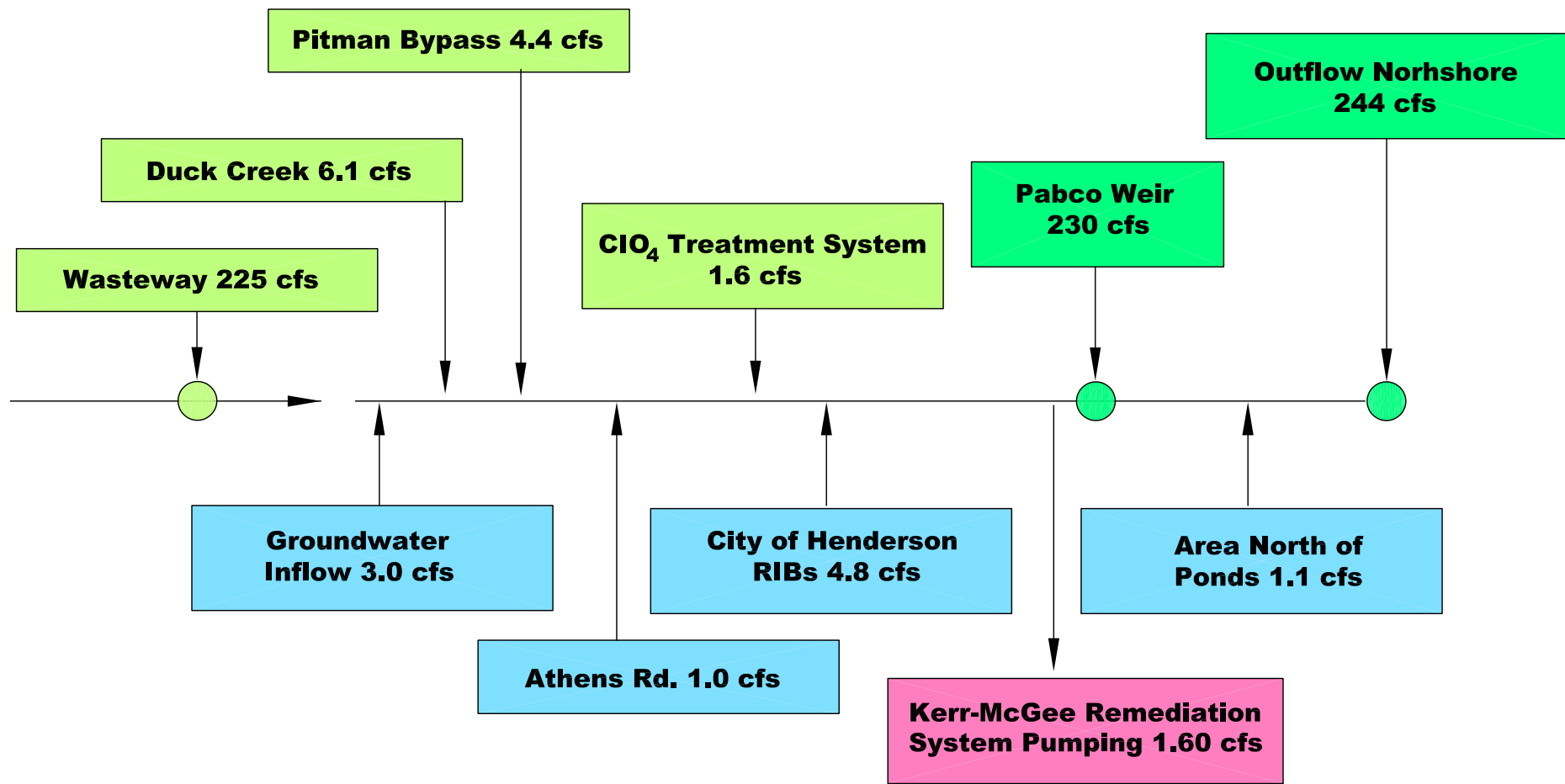
FIGURE 6
**LOCATION OF
 COUCEPTUAL MODEL
 FEATURES
 LAS VEGAS WASH
 HINDERSON, NEVADA**

SCALE: AS SHOWN

JOB NO. BMI-009


DWG NAME FIG6-CONCEPT

REVISION



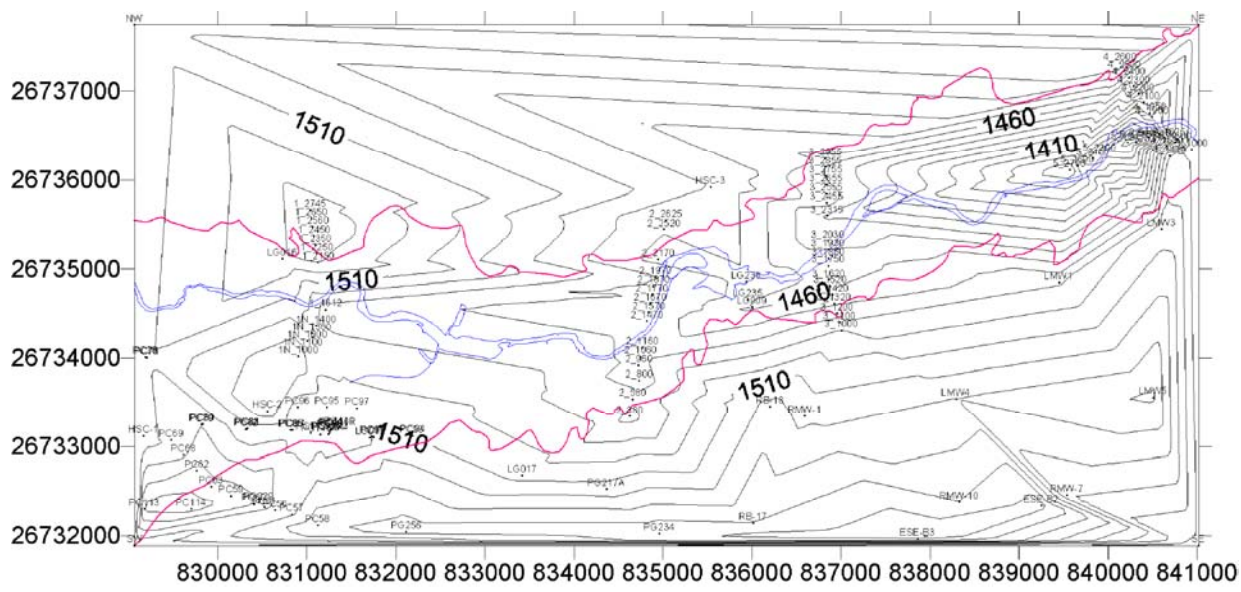
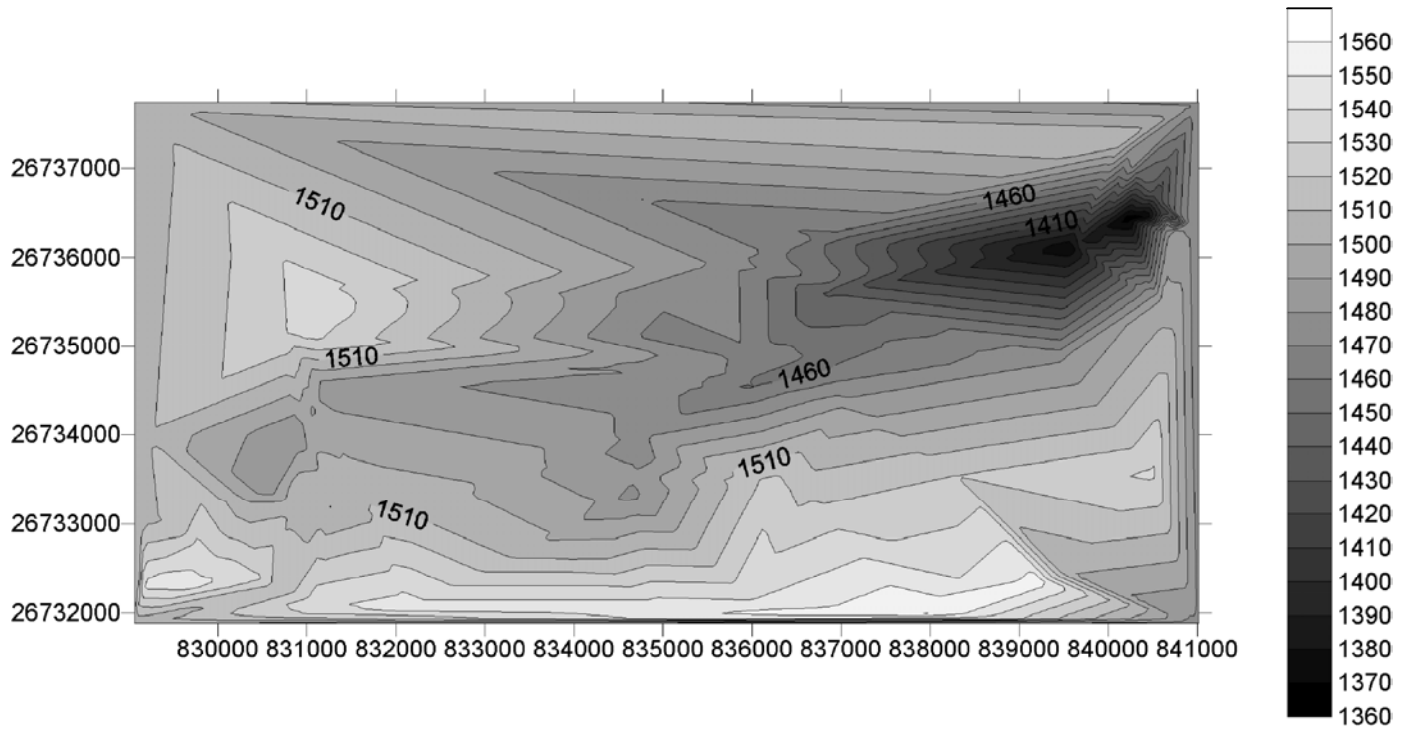
DESIGNED	PH	08/03		
	TAD	08/03		
CHECKED				
APPROVED				
REVISIONS	No.	DESCRIPTION	BY	DATE
	1			
	2			
	3			

FIGURE 7
SCHEMATIC OF CONCEPTUAL MODEL
LAS VEGAS WASH
HENDERSON, NEVADA




McGinley & Associates
 SCALE: AS SHOWN
 JOB NO. BMI-009
 DWG NAME FIG7

REVISION	△
----------	---



REFERENCE	DESIGNED	DE	08/03
	DRAWN	TAD	08/03
	CHECKED		
REVISIONS	APPROVED		
	No.	DESCRIPTION	BY DATE
	1		
	2		

FIGURE 8
NUMERICAL MODEL
GRID BOTTOM
CONTOURS
LAS VEGAS WASH
HENDERSON, NEVADA



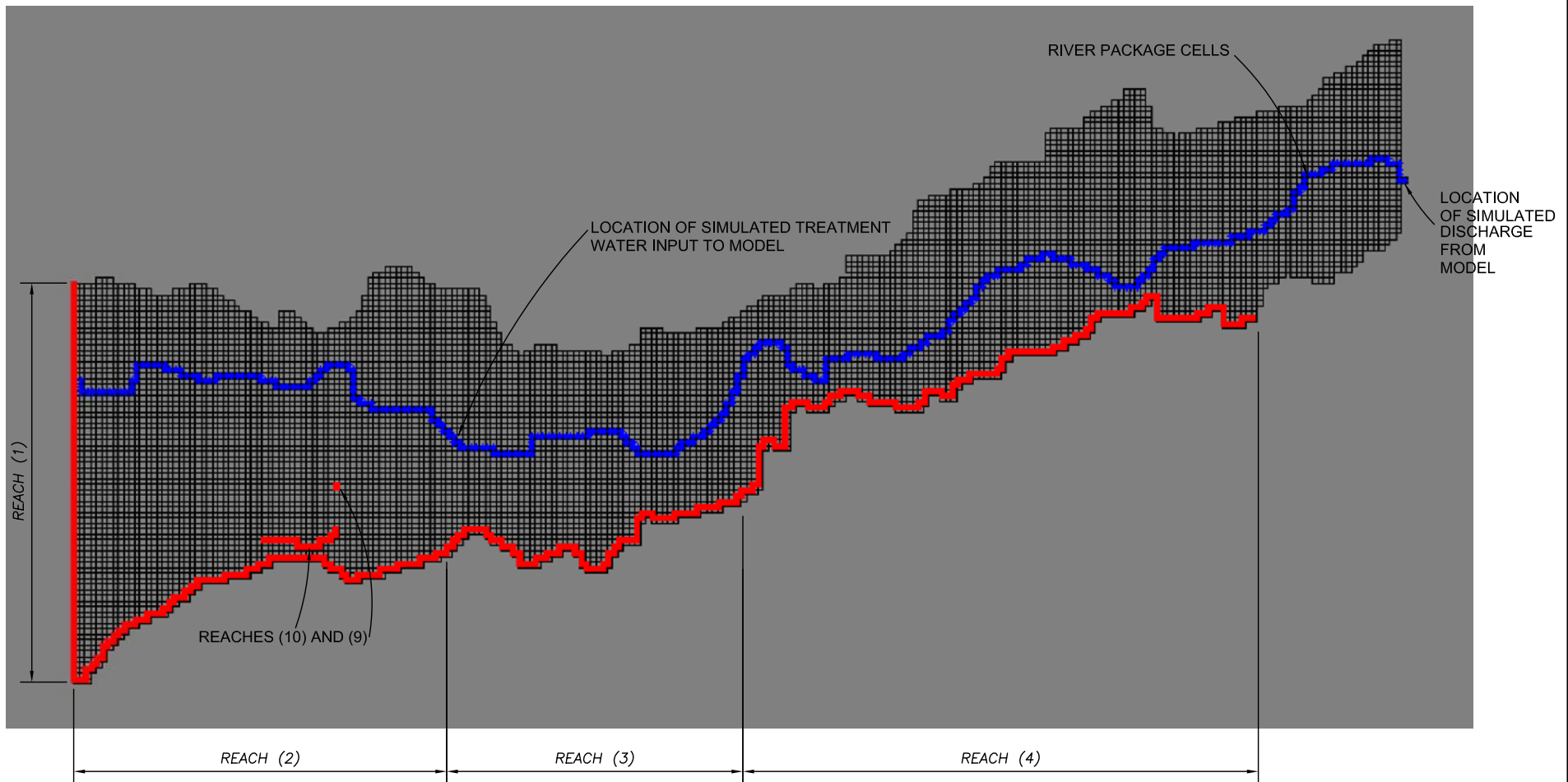
McGinley & Associates

SCALE: AS SHOWN

JOB NO. BMI-009

DWG NAME FIG7

REVISION
A



REFERENCE	DESIGNED	DE	08/03
	DRAWN	TAD	08/03
	CHECKED		
	APPROVED		
REVISIONS	No.	DESCRIPTION	BY DATE
	1		
	2		
	3		

FIGURE 9

**NUMERICAL MODEL
BOUNDARY ASSIGNMENTS
LAS VEGAS WASH
HENDERSON, NEVADA**



McGinley & Associates

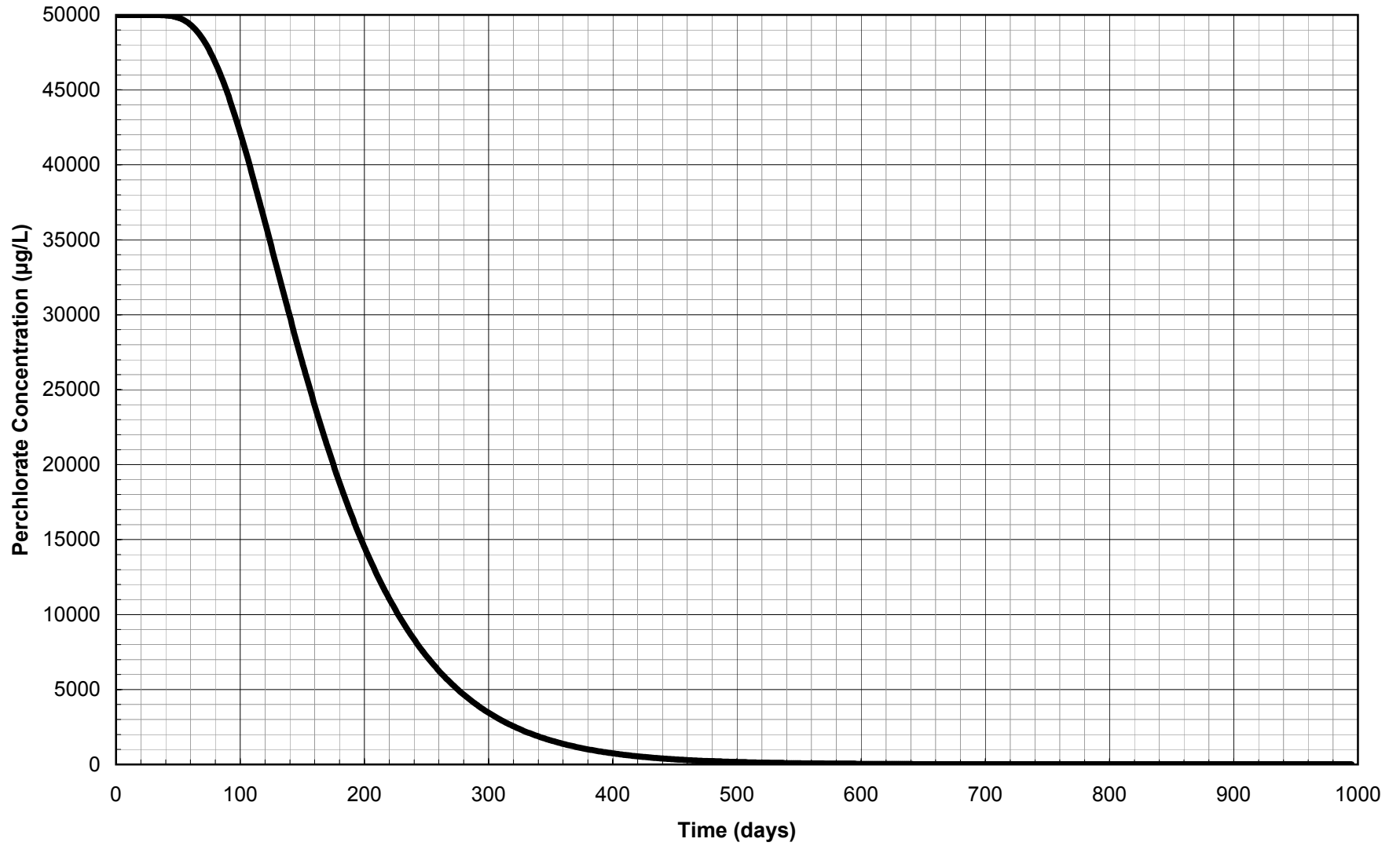
SCALE: AS SHOWN

JOB NO. BMI-009
DWG NAME FIG7

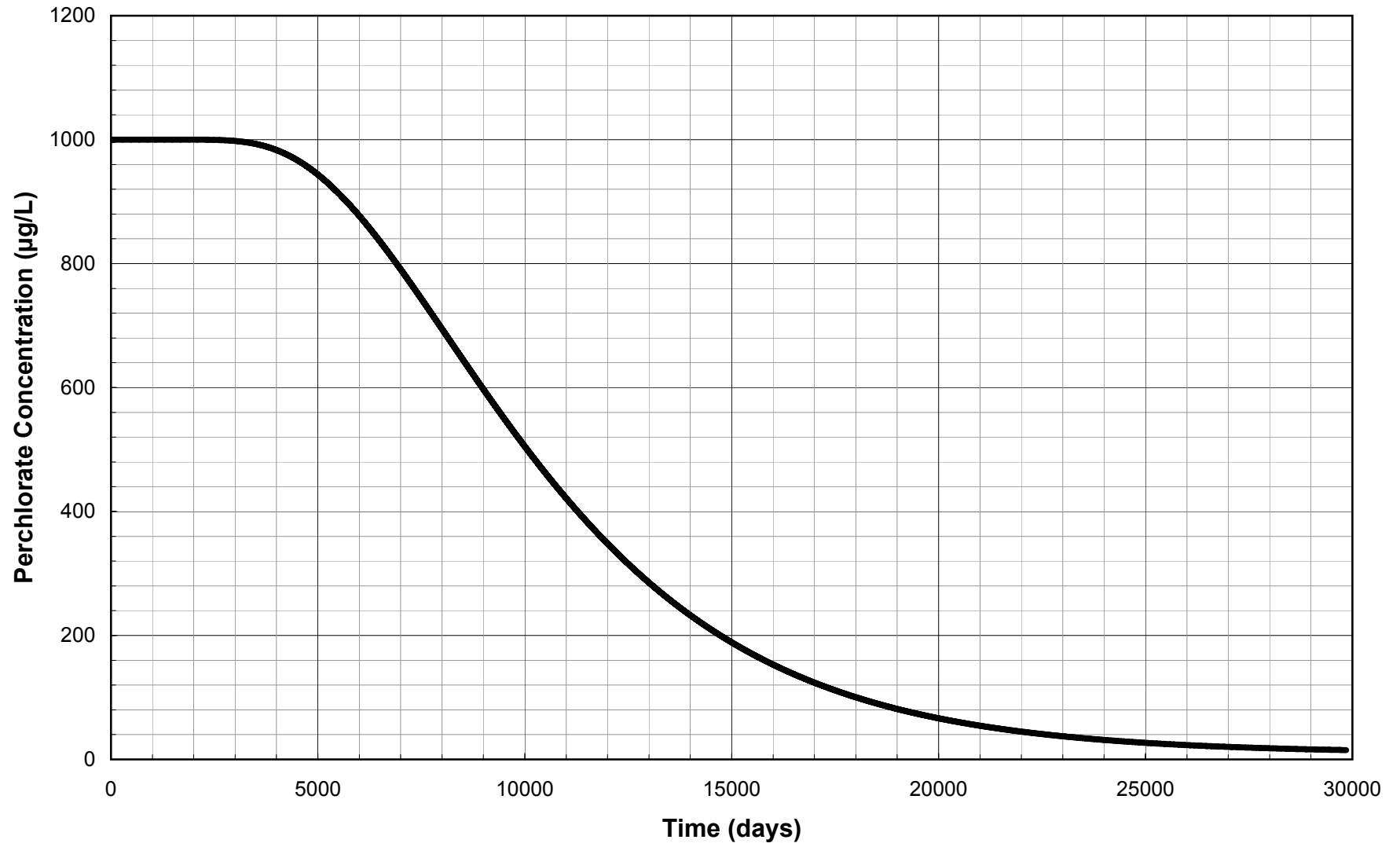
REVISION



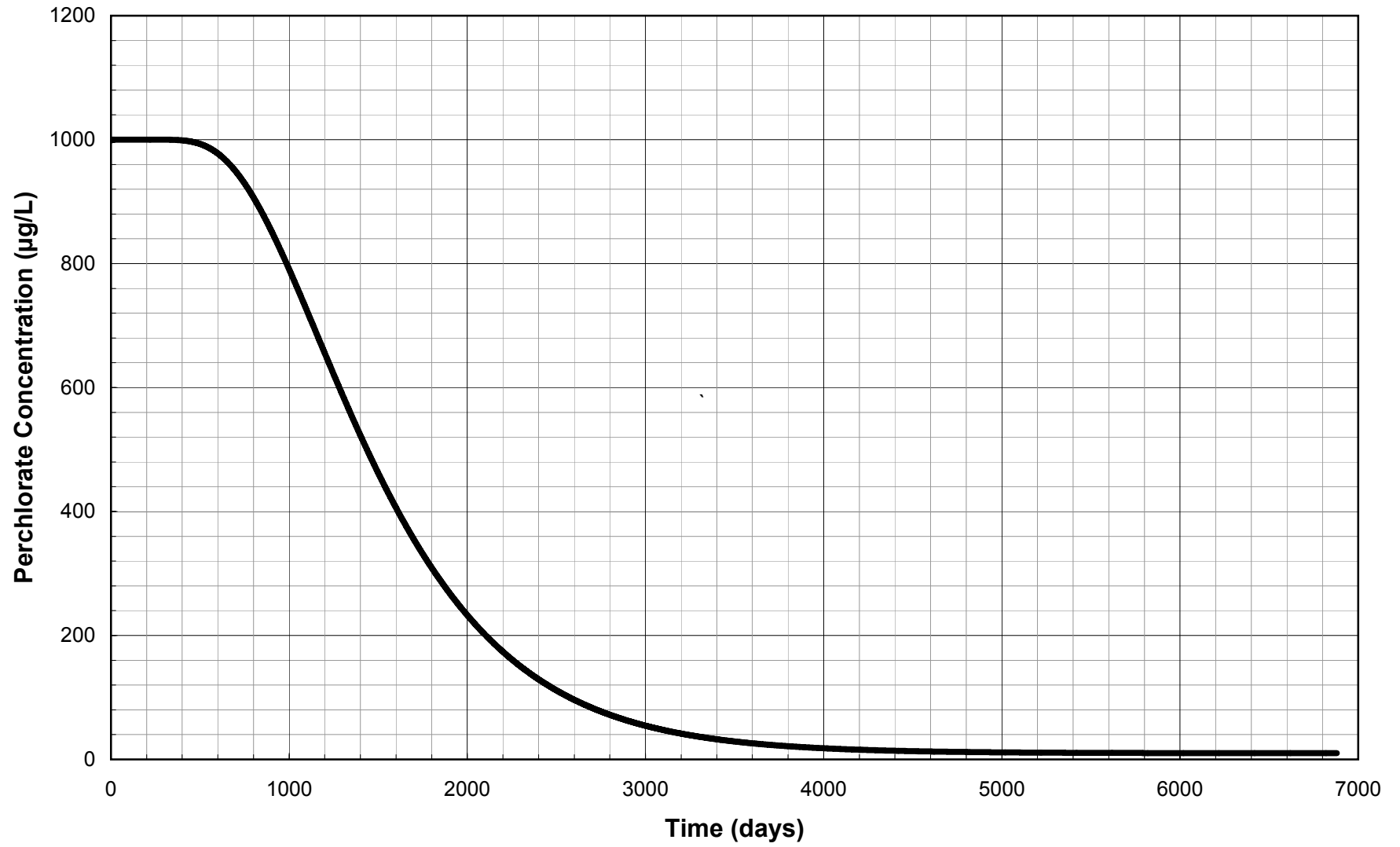
Plot 1. Reach (2) Solute Concentration Input Function



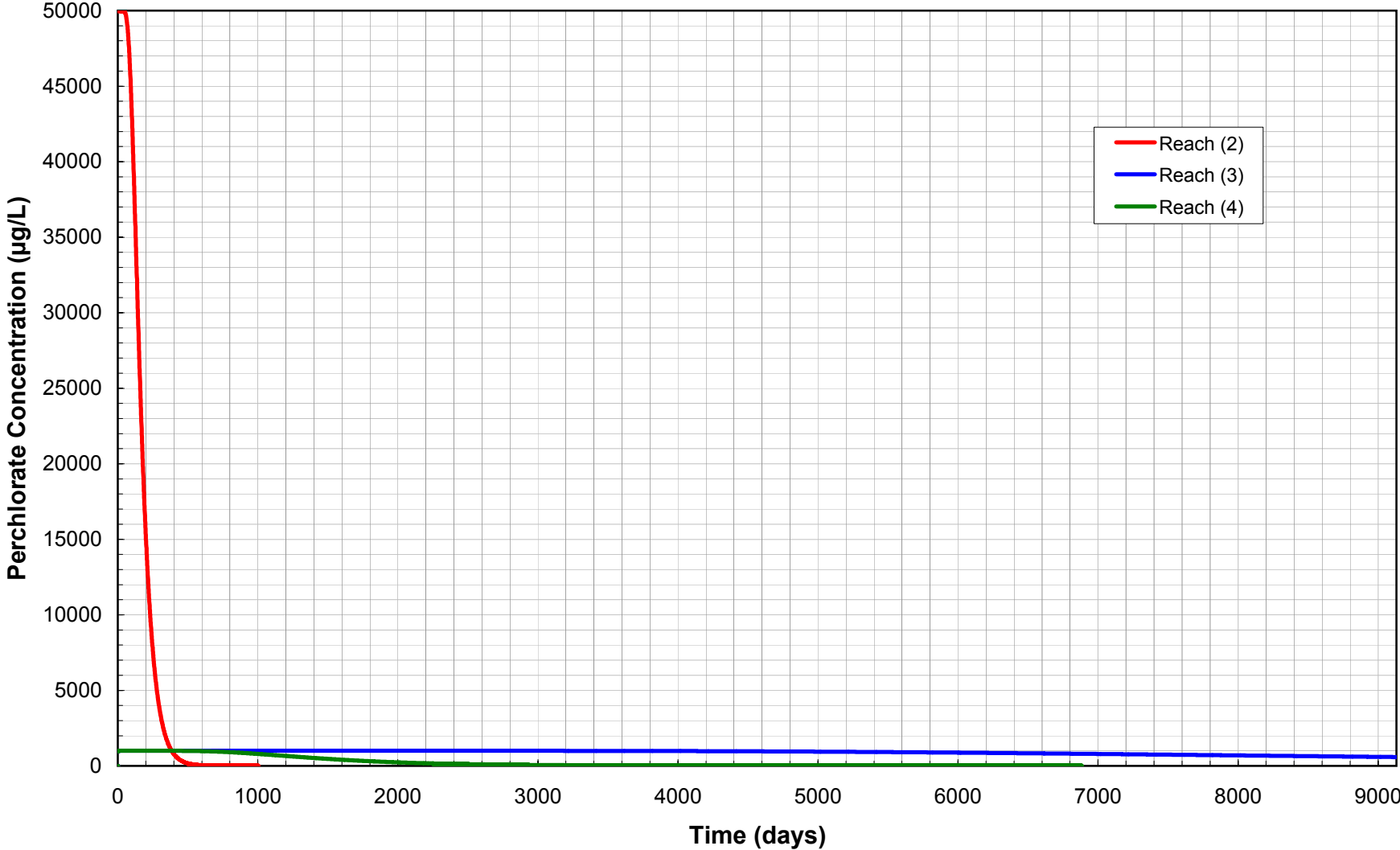
Plot 2. Reach (3) Solute Concentration Input Function



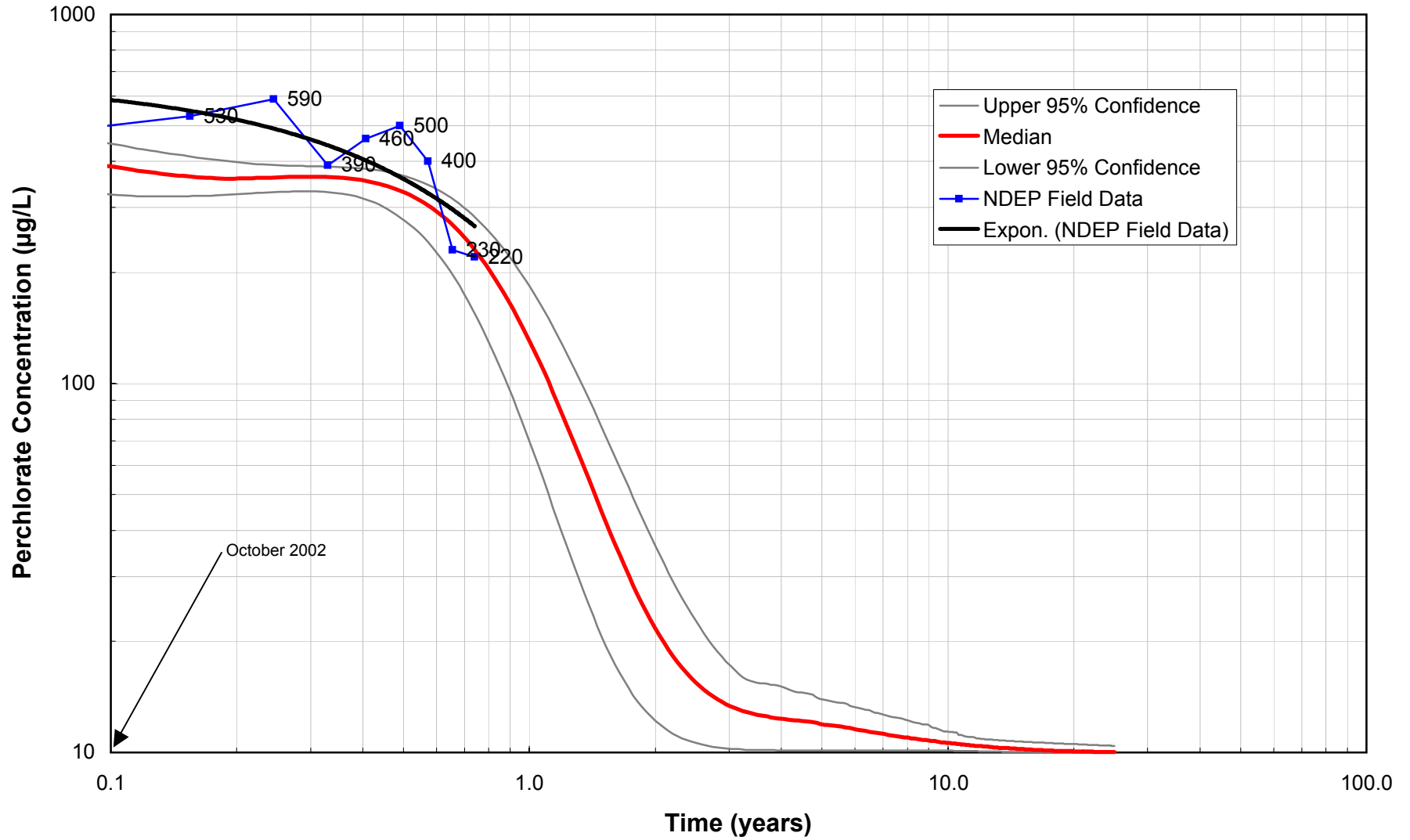
Plot 3. Reach (4) Solute Concentration Input Function



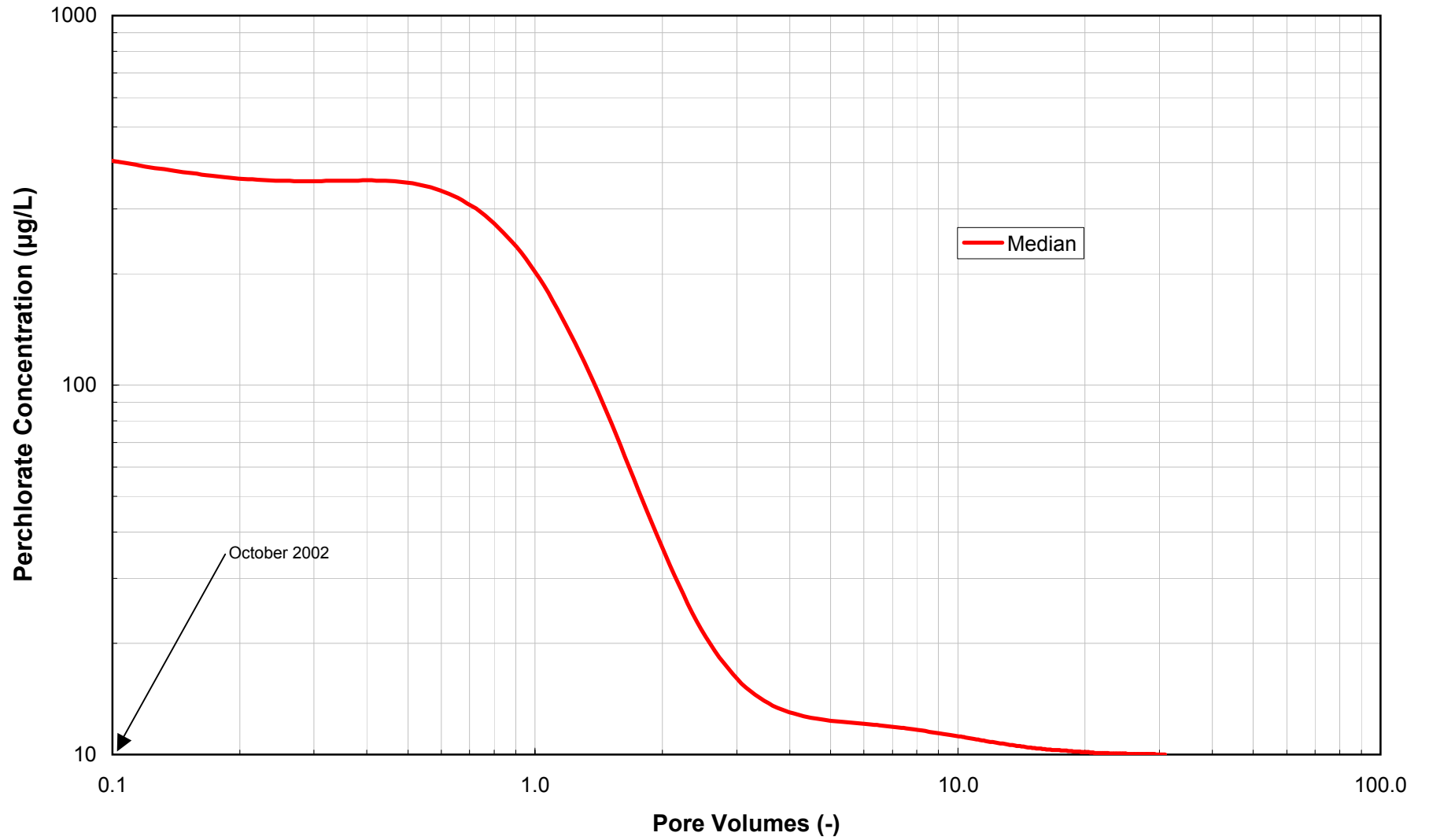
Plot 4. Relative Solute Concentration Input Functions



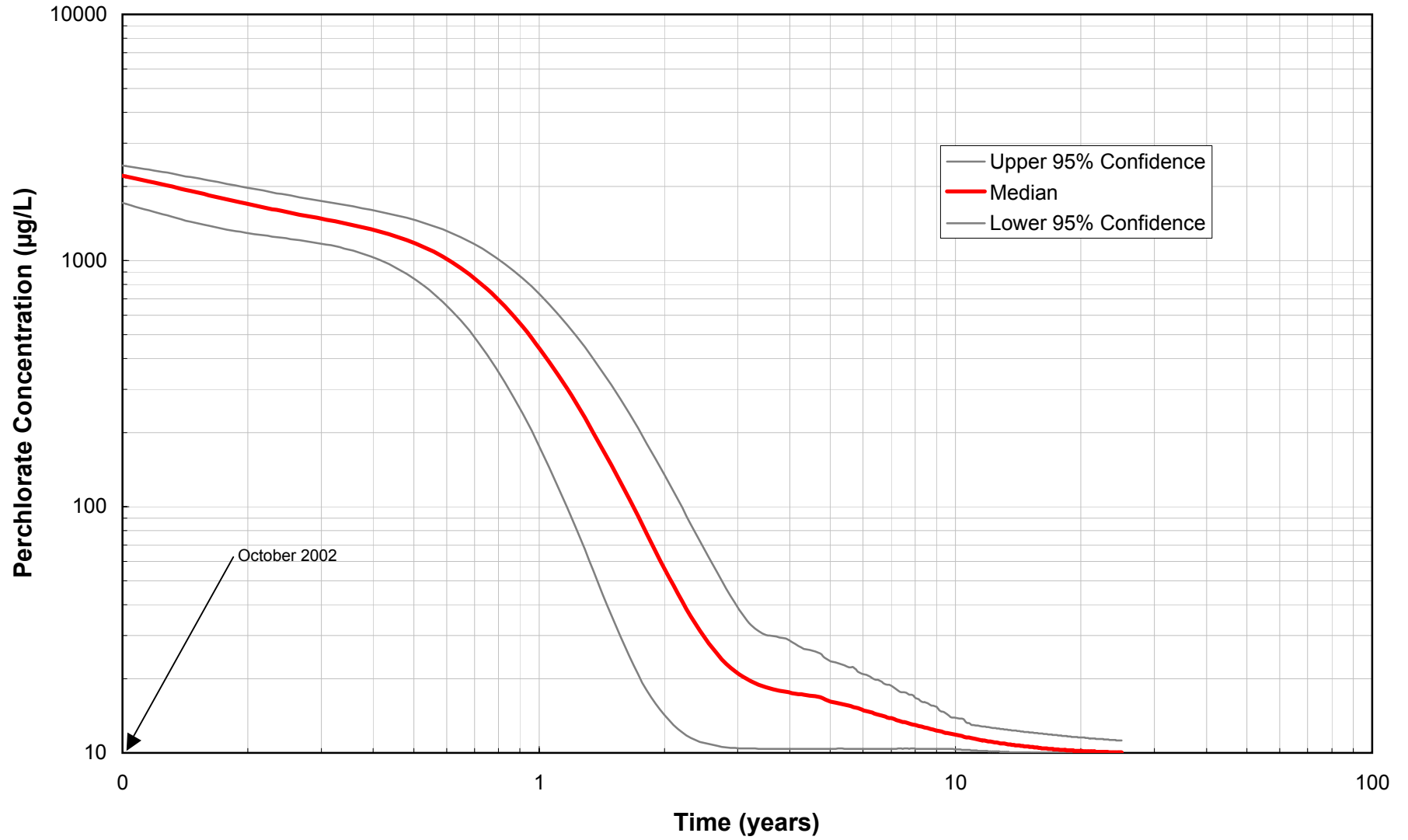
Plot 5. Breakthrough Curve: Wash Concentrations



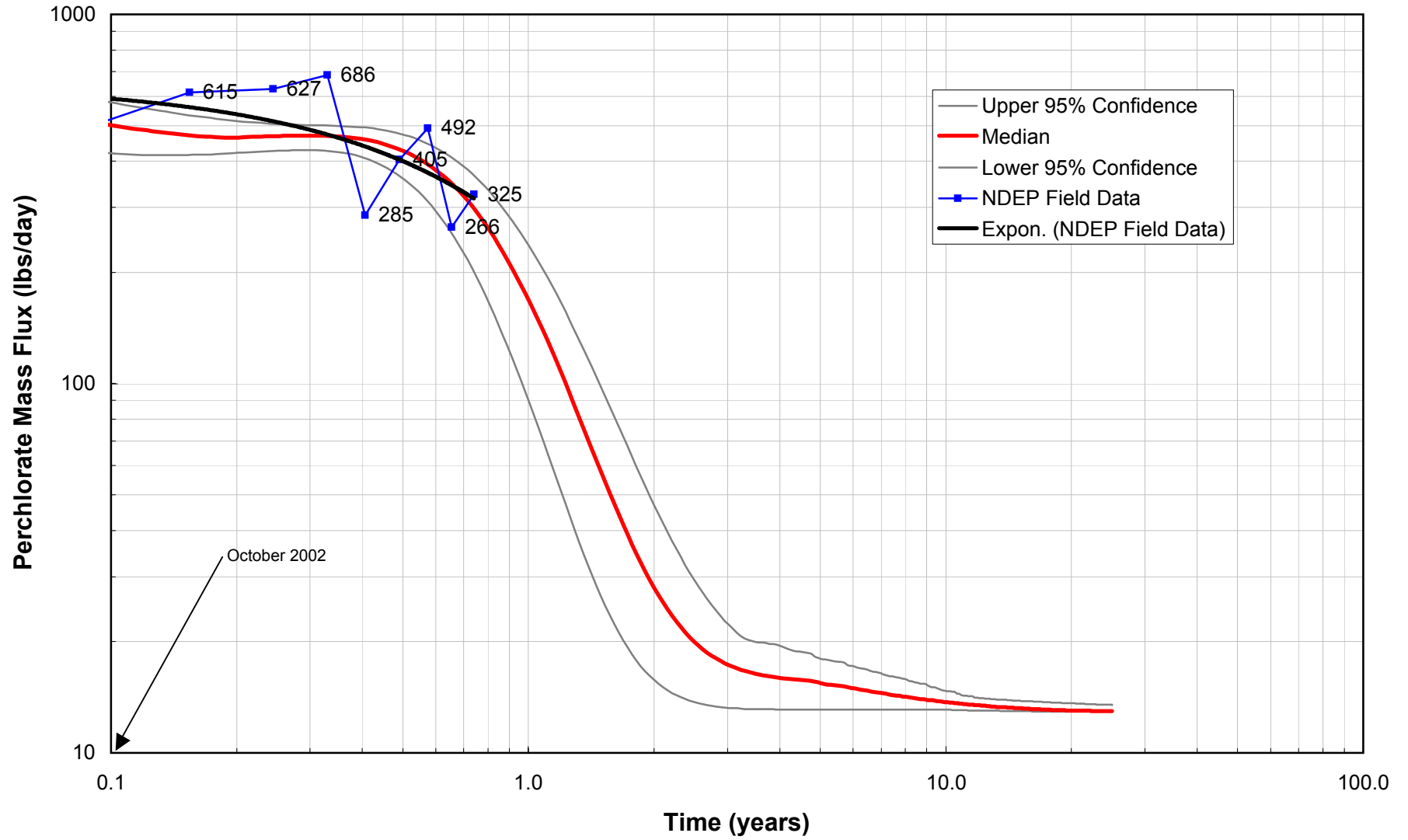
Plot 6. Breakthrough Curve: Wash Concentrations Versus Pore Volumes



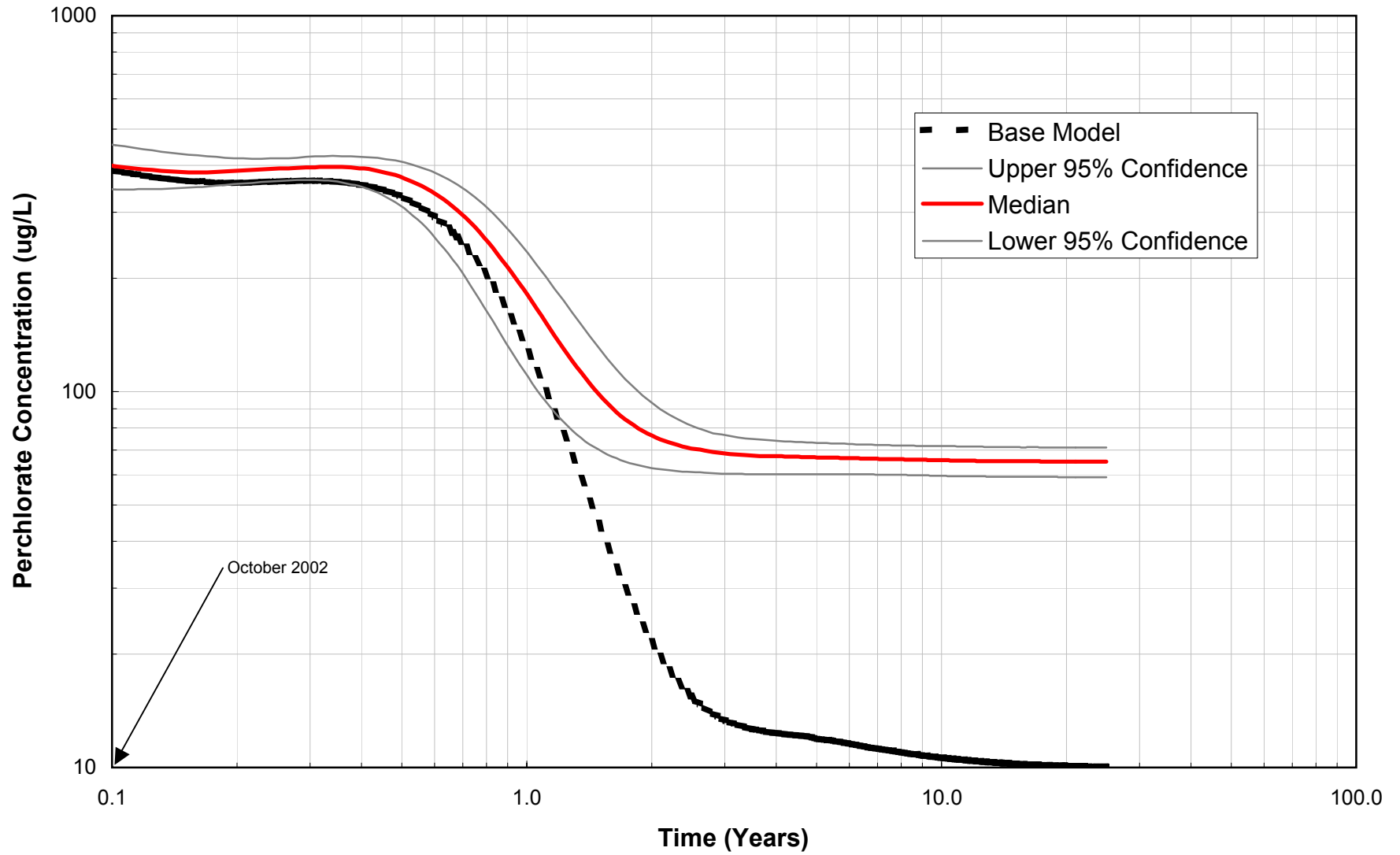
Plot 7. Breakthrough Curve: Aquifer Concentrations



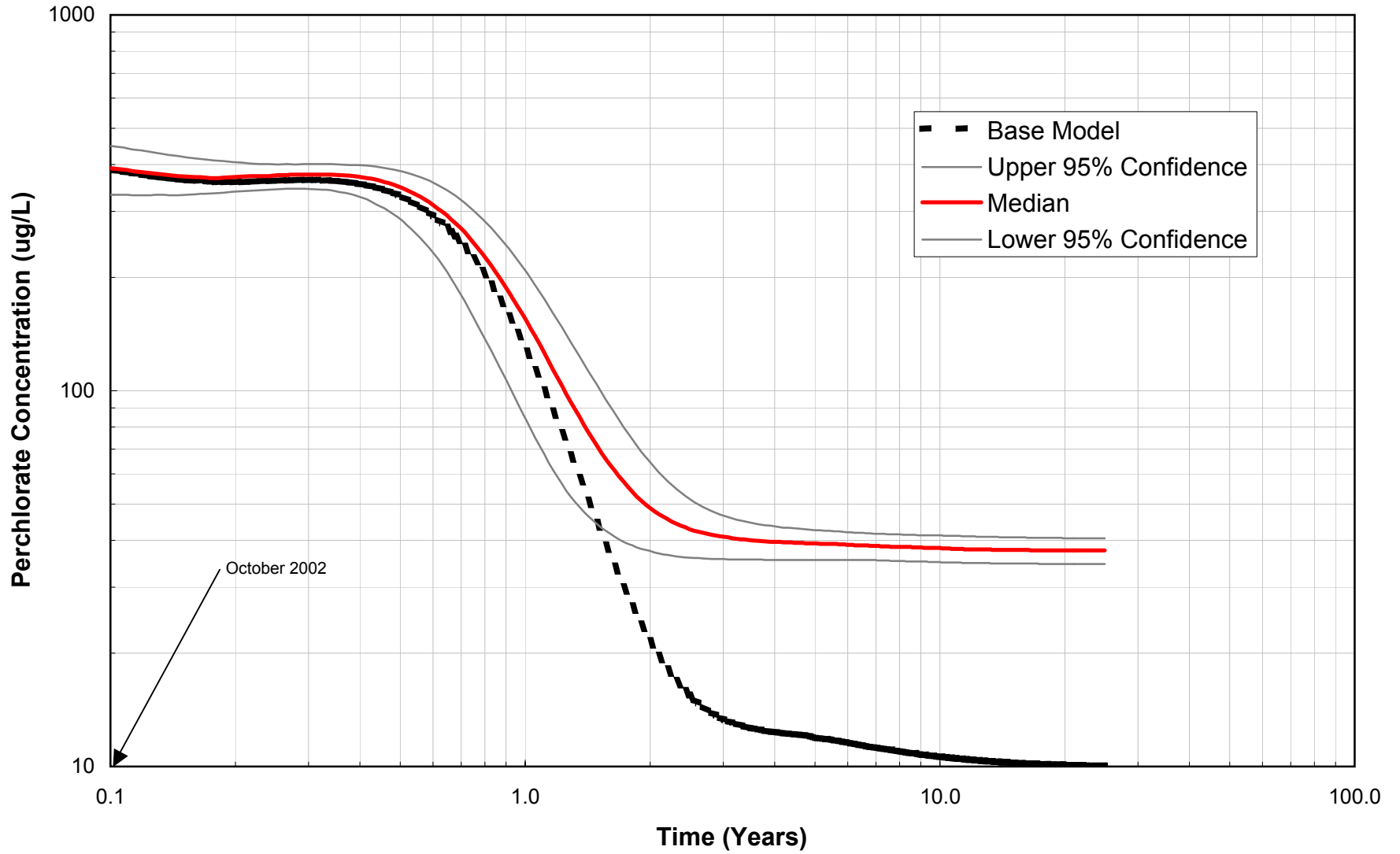
Plot 8. Breakthrough Curve: Wash Mass



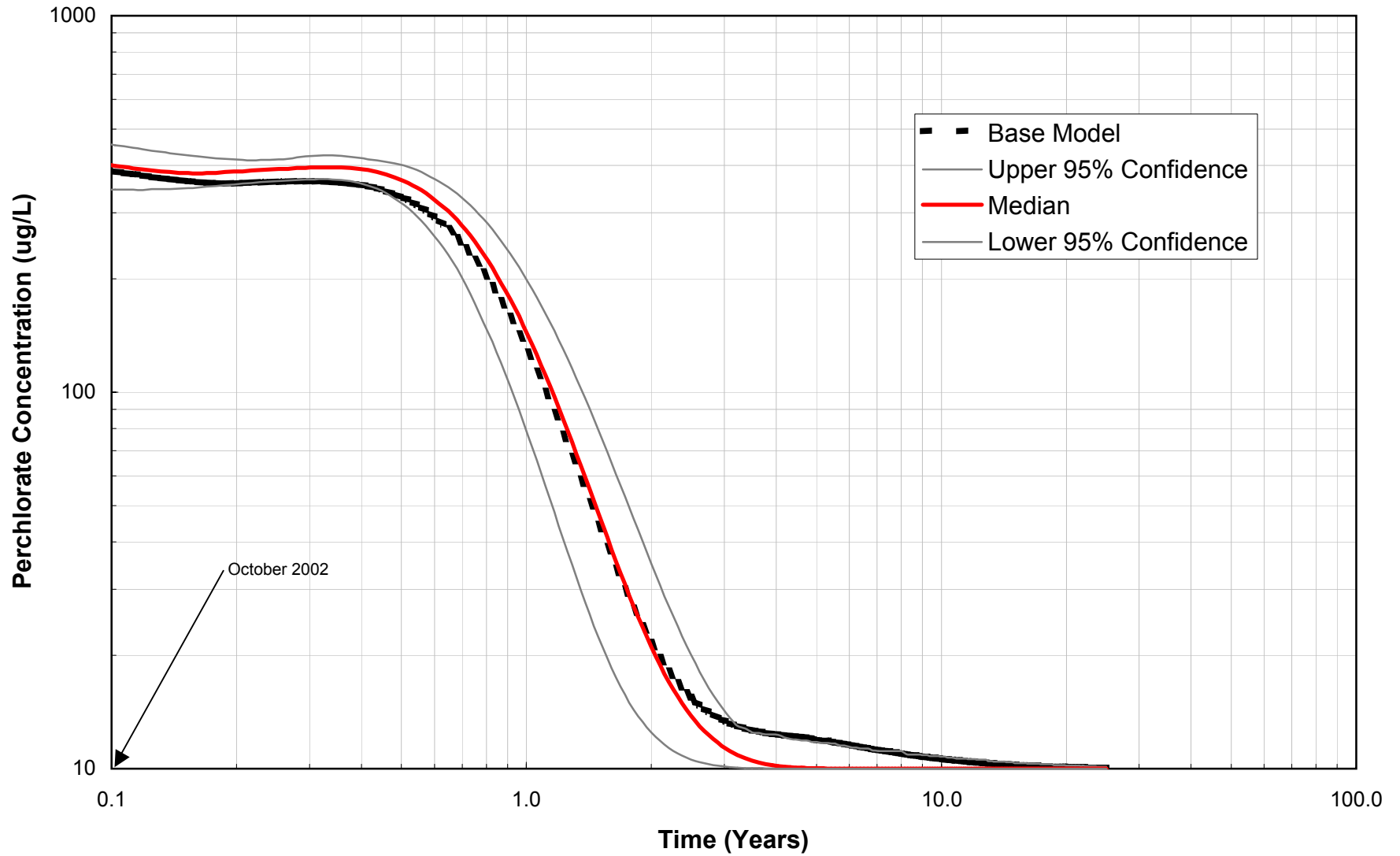
Plot 9. Breakthrough Curve: 90%-Efficient Model Results



Plot 10. Breakthrough Curve: 95%-Efficient Model Results



Plot 11. Breakthrough Curve: Reach (4) Zero-Flux Model Results



APPENDIX A

Geophysical Survey Report



**PRELIMINARY DRAFT REPORT
GEOPHYSICAL INVESTIGATION**

**Las Vegas Wash
Clark County, Nevada**

GEOVision Project No. 3209

Prepared for

McGinley & Associates
5690 Riggins Court, Suite C
Reno, Nevada 89502

Prepared by

GEOVision Geophysical Services
1151 Pomona Rd, Unit P
Corona, CA 92882
(909) 549-1234

June 2, 2003

TABLE OF CONTENTS

1	INTRODUCTION.....	1
1.1	PURPOSE.....	1
1.2	TECHNICAL APPROACH	1
1.3	GEOLOGIC BACKGROUND	1
1.4	REPORT OUTLINE	2
2	METHODOLOGY.....	3
2.1	FREQUENCY DOMAIN ELECTROMAGNETIC METHOD.....	3
2.2	TIME DOMAIN ELECTROMAGNETIC METHOD.....	4
3	FIELD PROCEDURES.....	7
3.1	SURVEY CONTROL	7
3.2	FREQUENCY DOMAIN ELECTROMAGNETIC SURVEY.....	7
3.3	TIME DOMAIN ELECTROMAGNETIC SURVEY.....	7
4	DATA PROCESSING	9
4.1	GEONICS EM-34 DATA PROCESSING.....	9
4.2	TDEM MODELING	9
5	INTERPRETATION AND RESULTS.....	11
5.1.1	<i>Line 1</i>	11
5.1.2	<i>Line 2</i>	11
5.1.3	<i>Line 3</i>	12
5.1.4	<i>Line 4</i>	12
5.1.5	<i>Line 5</i>	13
6	CONCLUSIONS AND RECOMMENDATIONS	15
7	CERTIFICATION.....	16

LIST OF TABLES

TABLE 1	LINE 1 - SURVEY DATA FOR FDEM PROFILE AND TDEM SOUNDINGS
TABLE 2	LINE 2 - SURVEY DATA FOR FDEM PROFILE AND TDEM SOUNDINGS
TABLE 3	LINE 3 - SURVEY DATA FOR FDEM PROFILE AND TDEM SOUNDINGS
TABLE 4	LINE 4 - SURVEY DATA FOR FDEM PROFILE AND TDEM SOUNDINGS
TABLE 5	LINE 5 - SURVEY DATA FOR FDEM PROFILE AND TDEM SOUNDINGS

LIST OF FIGURES

FIGURE 1	SITE MAP
FIGURE 2	GEOLOGIC MAP
FIGURE 3	GEONICS EM-47 TDEM SYSTEM AND GEONICS EM-34 CONDUCTIVITY METER
FIGURE 4	TDEM MODEL EXAMPLE
FIGURE 5	LINE 1 – GEOELECTRIC SECTION FOR 1D LAYERED MODEL INVERSION
FIGURE 6	LINE 1 – GEOELECTRIC SECTION FOR SMOOTH MODEL INVERSION AND GEONICS EM-34 PROFILE
FIGURE 7	LINE 2 – GEOELECTRIC SECTION FOR 1D LAYERED MODEL INVERSION
FIGURE 8	LINE 2 – GEOELECTRIC SECTION FOR SMOOTH MODEL INVERSION AND GEONICS EM-34 PROFILE
FIGURE 9	LINE 3 – GEOELECTRIC SECTION FOR 1D LAYERED MODEL INVERSION
FIGURE 10	LINE 3 – GEOELECTRIC SECTION FOR SMOOTH MODEL INVERSION AND GEONICS EM-34 PROFILE
FIGURE 11	LINE 4 – GEOELECTRIC SECTION FOR 1D LAYERED MODEL INVERSION
FIGURE 12	LINE 4 – GEOELECTRIC SECTION FOR SMOOTH MODEL INVERSION AND GEONICS EM-34 PROFILE
FIGURE 13	LINE 5 – GEOELECTRIC SECTION FOR 1D LAYERED MODEL INVERSION
FIGURE 14	LINE 5 – GEOELECTRIC SECTION FOR SMOOTH MODEL INVERSION AND GEONICS EM-34 PROFILE

1 INTRODUCTION

1.1 Purpose

A geophysical investigation was conducted between March 12, 2003 and March 24, 2003 in Las Vegas Wash, Clark County, Nevada. The purpose of the geophysical investigation was to map the approximate depth to the tertiary clay unit underlying the site in support of hydrogeologic site characterization efforts. Geophysical techniques used during this investigation included time domain electromagnetic (TDEM) soundings with a Geonics EM-47 and frequency domain electromagnetic (FDEM) profiles with the Geonics EM-34 terrain conductivity meter.

1.2 Technical Approach

A total of 76 TDEM soundings were conducted with the Geonics EM-47 at nominal 100 foot intervals along 5 profiles totaling 9,450 linear feet to map the depth of the clay unit. FDEM data was acquired along the profiles using the Geonics EM-34 terrain conductivity meter to map lateral changes in deep resistivity structure potentially associated with changes in depth to the clay unit. TDEM sounding and Geonics EM-34 profile locations are shown in Figure 1. Four of the profiles (Lines 1 to 4) were conducted perpendicular to the wash and the remaining profile (Line 5) was conducted parallel to the wash.

In designing the geophysical survey the following assumptions were made:

- 1) There is a large contrast in electrical resistivity/conductivity between the alluvium and underlying clay unit.
- 2) Saturated alluvium is not highly conductive (i.e. groundwater does not have a highly elevated total dissolved solids content)
- 3) Subsurface geology is relatively simple (i.e. highly resistive alluvium overlying highly conductive clay)

1.3 Geologic Background

A geologic map with the locations of the five geophysical traverses (Lines 1 to 5) is presented as Figure 1. Soils within the Las Vegas Wash are mapped as modern wash deposits (Qa). This unit is generally depicted as consisting of sands and gravels, although the wash deposits within the Las Vegas Wash predominantly consist of salt-rich silty sand. This is significant as salt-rich sands may be electrically conductive. Three separate Quaternary alluvial fan systems converge onto the Las Vegas Wash – pediment and fan deposits of Henderson (Qf1 and Qf2) and River Mountain (Qr1 and Qr2) from the south and Frenchman Mountain (Qpf1 and Qpf2) from the north.

Surface exposures of the undifferentiated coarse and fine-grained facies (Tm_{cu}) of the Tertiary Muddy Creek Formation are mapped north of the site. The coarse-grained facies of the Muddy Creek Formation (Tm_{cc}) is described as a fanglomerate primarily composed of sandy gravels. The fine-grained member of the Muddy Creek Formation (Tm_{cf}) consists of basin fill sediments

of lacustrine and subaerial origin and is primarily composed of often gypsiferous silts, sandy silts and clays. This unit and soils of similar composition is the target layer of this investigation.

A northwest to southeast trending inferred fault may be located between Lines 3 and Lines 4 and 5. Line 5 could not be extended across the projected location of this potential fault due to heavy vegetation in the wash. East of the inferred fault, the Tertiary Horse Spring (Ths) and Thumb (Tt, Ttg) Formations are mapped south and north of the Las Vegas Wash. The Horse Spring Formation is older than the Muddy Creek Formation and primarily consists of carbonate rocks with some interbedded siltstone and shale. The Thumb Formation is older than the Horse Spring Formation and in the project area is primarily composed of calcareous siltstone and sandstone, and gypsiferous shale and claystone. There are several localized outcrops of brecciated basement rock (Ttg), thought to be of landslide origin, within the Thumb Formation.

Two tertiary volcanic units (Tvr and Td) outcrop near the project area. These units generally range in composition from basalt to dacite.

1.4 Report Outline

Geophysical techniques used during the investigation are discussed in Section 2. Field procedures are described in Section 3. Data processing and modeling are discussed in Section 4. Interpretation of the geophysical data is presented in Section 5. Conclusions derived from the geophysical survey and our recommendations are presented in Section 6, and our professional certification is presented in Section 7.

2 METHODOLOGY

This section presents background information on the frequency and time domain electromagnetic methods used during this investigation.

2.1 Frequency Domain Electromagnetic Method

Frequency domain electromagnetic (FDEM) instruments consist of separate transmitter and receiver coils maintained at a constant spacing. The transmitter coil is energized with an alternating current at an audio frequency. The time-varying primary magnetic field resulting from the alternating current in the transmitter coil induces eddy currents in the earth. These eddy currents in turn generate a secondary magnetic field which is sensed along with the primary magnetic field at the receiver coil. The FDEM instrument used during this investigation consisted of a Geonics EM-34 terrain conductivity meter.

Most FDEM instruments measure the components of the secondary magnetic field both in-phase and 90-degrees out-of-phase (quadrature) with the primary EM field. The magnitude of this field is a function of the operating frequency, the intercoil spacing, and the ground conductivity. As both the operating frequency and intercoil spacing are known and fixed for each tool, and the instruments are all designed to operate at low-induction numbers, the quadrature component may be converted to apparent conductivity in millisiemens per meter (mS/m). The in-phase component is not measured by the EM-34 but is instead used to set the coil spacing. Depth of investigation of FDEM instruments is generally a function of coil spacing, electrical conductivity of subsurface soils and operating frequency; however under the low induction number approximation depth of investigation is primarily a function of coil spacing. Electrical conductivity is the inverse of electrical resistivity. Conductivity in mS/m can be converted to resistivity in ohm-meters by taking the inverse and multiplying by 1000.

Some surface FDEM instruments, such as the EM-34 can be operated in either vertical dipole (horizontal coil orientation) or horizontal dipole (vertical coil orientation) mode. In the horizontal dipole mode, measurements are most strongly affected by near-surface soils and the instrument has an effective depth of exploration (thickness contributing about 70% of the measurement) of 0.75 times the coil spacing. In the vertical dipole mode, measurements are most strongly influenced by soils at a depth of 0.5 times the coil spacing and the effective depth of exploration is 1.5 times the coil spacing.

The EM-34 is a two person FDEM tool used to measure ground conductivity (Figure 3). This instrument provides some flexibility in that the coil spacing can be varied from 10m, 20m, or 40m. For each intercoil spacing, the transmitter operates at a different set frequency (6.4 kHz for 10m, 1.60 kHz for 20m, and 0.4 kHz for 40m) to maintain the low induction number approximation. For this study, the EM-34 was operated in horizontal dipole mode (vertical coils) with either a 20m or 40m coil spacing. Effective depth of investigation was, therefore, 15m (50 ft) and 30m (100 ft) for the 20 and 40m coil spacing, respectively.

Applications of FDEM methods include:

- Locating buried tanks and pipes
- Locating buried pits and trenches containing metallic and/or metallic debris
- Delineating landfill boundaries
- Delineating oil production sumps and mud pits
- Mapping conductive soil and groundwater contamination
- Mapping soil salinity in agricultural areas
- Characterizing shallow subsurface geology
 - Mapping buried channel deposits
 - Locating sand and gravel deposits
 - Mapping conductive fault and fracture zones
 - Mapping lateral (EM-31 and EM-34) or vertical (EM-39) variations in subsurface soil type

Strengths of FDEM methods as applied to mapping subsurface geologic conditions include:

- Very rapid – data can be collected at a slow walking pace with the EM-31 or in several seconds with the EM-34
- Not very sensitive to small (relative to coil spacing) surface debris
- Do not require contact with the ground surface or borehole walls
- Can be used in PVC or Teflon cased holes (EM-39)

Limitations of EM induction methods include:

- Metallic structures such as buildings, fences, reinforced concrete, and light posts interfere with the measurements
- Susceptible to interference from high voltage power lines, radar antennas and radio transmitters
- Cannot easily resolve the difference between lateral and vertical resistivity variation
- Do not provide absolute depth information

2.2 Time Domain Electromagnetic Method

The time-domain electromagnetic (TDEM) instrument used during this investigation consisted of a Geonics EM-47 transmitter, high-frequency receiver coil and a Protem digital receiver (Figure 3). This system is designed to image to a maximum depth of about 100 m, whereas other systems such as the Geonics EM-57 and EM-37 are designed with larger transmitters and lower-frequency coils to image to greater depth.

A TDEM system consists of a separate transmitter (Tx) and receiver (Rx) coils. The Tx coil generally consists of a square loop of insulated wire laid on the surface. The Rx coil is generally placed in the center of the Tx loop (central loop sounding). The EM-47 transmitter operates at three user-selectable repetition frequencies of 285, 75, and 30 Hz and is synchronized to the Protem receiver using a reference cable.

Depending on the required resolution and depth of investigation, the dimensions of the transmitter loop may be changed. In the central loop sounding mode, 30 by 30m to 100 by 100m Tx loops can be used with the EM-47 transmitter. Larger loops allow deeper depths of investigation and reduced noise level, at some loss of resolution.

The 100-watt battery-powered EM-47 transmitter is used to drive a modified square-wave current through the Tx loop. One period of the transmitted waveform (33.3 milliseconds for the 30 Hz repetition frequency) consists of two current-on (time-on) and two current-off (time-off) cycles. At the end of the first time-on cycle, the current is abruptly switched off for a quarter period using a rapid linear ramp. During the following time-on cycle, the current flows in the opposite direction. The abrupt termination of the current induces a short-duration voltage pulse in the ground in accordance with Faraday's Law of Induction. This voltage pulse gives rise to a current loop in the ground in the immediate vicinity of the Tx loop. The location of the maximum current intensity diffuses downward and outward with time, thereby providing information on the electrical properties of successively deeper materials. The diffusing current system produces a time-varying secondary magnetic field, which is measured as a voltage induced in the receiver coil. The Geonics PROTEM receiver measures the decaying secondary magnetic field at 20 logarithmically-spaced gates during the transmitter time-off cycle only. Many hundreds to thousands of measurements are stacked to improve data quality. The measurements are converted to apparent resistivity by calculating the resistivity of a uniform half-space that would give rise to the measured voltage.

Applications of TDEM soundings include:

- Characterize subsurface hydrogeology
 - Determine depth to groundwater
 - Determine depth to bedrock/overburden thickness
 - Map stratigraphy
 - Map clay aquitards
 - Map saltwater and/or contaminant intrusions
- Mapping vertical and horizontal distribution of permafrost
- Massive sulfide target detection

Advantages of TDEM compared to FDEM are:

- Lower sensitivity to geologic noise, such as variation in overburden thickness and lateral changes in overburden conductivity
- Greater depths of penetration than conventional FDEM instrumentation
- Smaller transmitter-receiver separation for equivalent depth
- Minimal land survey requirements because the method is less sensitive to topographic relief
- More suited to mapping variation of electrical resistivity versus depth.

Advantages of TDEM compared to DC resistivity are:

- Has better lateral and vertical resolution for deeper targets
- More rapid data collection

- Electrode stakes are not necessary for electrical contact, meaning that there are no problems injecting current into a resistive surface area
- Better depth of investigation with portable equipment
- Better at mapping conductive targets, such as clay

Limitations of the TDEM method include:

- Slower data collection than conventional FDEM instrumentation
- Like all surface geophysical methods, suffers from equivalence/nonuniqueness where multiple earth models may fit the field data
- Highly resistive areas limit signal strength at depth
- Unable to image upper 5m
- Not as good as DC resistivity at mapping resistive targets

3 FIELD PROCEDURES

This section describes the field procedures used during the investigation, including site preparation, FDEM survey and the TDEM survey.

3.1 Survey Control

Survey control for this investigation was provided by PBS&J of Henderson, Nevada. The PBS&J survey team used a Trimble base and rover dual-frequency, differential global positioning system operated in radio kinematic mode for horizontal and vertical control. Five geophysical traverses, labeled 1 to 5, were surveyed and staked at 100 -ft intervals, as possible, in advance of geophysical field operations. Each station along a traverse was marked with a wooden hub or nail and staked with 4 ft survey lathe. Station number and elevation were marked on the lathe for reference by the geophysical crew.

GPS data were collected in geodetic coordinates based on the WGS84 system and transformed to Nevada State Plane Coordinates, Eastern Zone, North American Datum of 1983 (NAD 83). Ellipsoid heights measured using the GPS system were converted to NAVD 88 elevations using the Geoid Model of 1996. Maximum horizontal and vertical errors from the leveling and GPS surveying are estimated at about 0.1 feet.

A site map showing the location of the geophysical traverses is presented as Figure 1. Coordinates and elevations of geophysical station locations are presented in Tables 1 to 5.

3.2 Frequency Domain Electromagnetic Survey

Geonics EM-34 data were acquired along five (5) profile lines totaling about 9,450 linear feet as shown in Figure 1. EM-34 data were acquired to map lateral changes in the electrical properties of deeper soils to infer relative depth of the more conductive clay unit.

EM-34 measurements of conductivity were made at 50 ft intervals in horizontal dipole mode with a coil separation of 40m. The survey stations on each line, which were generally staked at 100 ft intervals, were used for spatial control for the EM-34 surveys. EM-34 data were not acquired in heavily vegetated areas or in the active portion of the wash. The EM-34 data were stored in a digital data logger along with line and station number. At the end of each field day, EM-34 data were downloaded to a laptop computer using the computer program DAT34-3 by Geonics Ltd.

3.3 Time Domain Electromagnetic Survey

A Geonics EM47 transmitter (Tx), high-frequency receiver coil and a Protem digital receiver (Rx) were used to conduct TDEM soundings. The TDEM soundings were conducted in the central-loop sounding mode where the receiver coil is placed in the center of the transmitter loop during data recording.

Where possible, TDEM soundings were made at 100 ft intervals along the five profiles for a total of 76 soundings as shown in Figure 2. The locations of all TDEM soundings are summarized in Tables 1 to 5.

At each sounding location a transmitter loop consisting of insulated 12-gauge copper wire was placed on the ground in a square loop with 100 ft sides. The receiver coil was placed in the center of the Tx loop. The center of each sounding loop was at a staked survey station. Leveling legs was used to orient the receiver coil horizontally, thereby allowing the vertical component of the decaying secondary magnetic field to be recorded. The receiver coil was connected to the Protem Receiver and a reference cable between the transmitter and receiver synchronized the system.

The 100-watt battery-powered EM-47 transmitter, placed at a corner of each wire-loop, was used to drive current pulses through the wire. The EM47 transmitter was operated at repetition frequencies of 285 and 30 Hz. Generally, transmitter currents of 1 to 3 amperes were used for the 285 and 30 Hz repetition rates, respectively. The current pulses induced eddy current flow in the subsurface. The receiver coil positioned in the center of the wire-loop is used to record the decay of the secondary magnetic field due to the eddy currents induced in the subsurface. The Geonics Protem receiver measured the decaying secondary magnetic field at 20 logarithmically-spaced gates during the transmitter time-off cycle only. The data acquired at each sounding center consisted of measurements at several different receiver gain settings for the two transmitter frequencies. This was accomplished in order to assure data quality and to obtain data over the largest possible time interval. Additionally, hundreds of measurements were stacked at each location to improve the signal to noise ratio. The measurements were converted to apparent resistivity by calculating the resistivity of a uniform half-space that would give rise to the measured voltage. The data from each sounding were stored in solid-state memory in the receiver and transferred at the end of the day to a computer for processing.

4 DATA PROCESSING

This section summarizes the data processing procedures utilized during this investigation.

4.1 Geonics EM-34 Data Processing

The EM-34 apparent conductivity data were recorded onto a data logger in the field and were transferred to a computer for editing and processing using the program DAT34-3 (Geonics Ltd), respectively. The data were exported in ASCII format and subsequently entered into the program GRAPHER (Golden Software, Inc) where profile plots were made.

The names of the files generated and the processing parameters used were recorded in project notes, which are retained in project files. All files generated during the processing sequence were archived on CD-ROM.

4.2 TDEM Modeling

The TDEM field data collected along the 5 profiles were transferred from the Geonics PROTEM receiver to a PC for editing and processing. All processing and modeling of the TDEM data was performed with the inversion program TEMIX XL (Interpex Ltd.). The initial step in processing was to input all of the soundings from a profile into the program. During data input the measurements made at the various amplifier gains and frequencies for each sounding were combined to produce one voltage decay curve (transient). Next, the data were transformed into apparent resistivity versus recorded time gate. The apparent resistivity curve was modeled by inversion to obtain a one-dimensional (1-D) geoelectric section that most closely matches the observed decay curve. Two types of inversions were utilized: a 1D layered model inversion and a 1D smooth model inversion. The 1D layered models are generally provide the most accurate depth to a specific layer (i.e. clay layer) and are used to generate geoelectric cross-sections. The smooth model inversions are generally used to generate color-enhanced images of the data. Smooth model inversions may also assist the user in determining the minimum number of layers needed to model the data.

The TEMIX XL 1D layered model inversion program requires an initial model of the geoelectric section, which includes the number of layers and the thickness and resistivity of each of the layers. The inversion program then adjusts these parameters so that the model curve converges to best fit the curve formed by the field data. The inversion program does not change the number of layers within the model curve, but allows all other parameters to change freely or they can optionally be made constant. To determine the influence and best fit of the number of layers on the solution, separate inversions with different numbers of layers are run. The model with the fewest number of layers, which best fits the data is used in the final interpretation.

The TEMIX XL smooth model inversion program requires the user to specify the number of layers, the thickness of the first layer and the depth of the final layer. Optionally, the program can calculate a default thickness of the first layer and depth of the final layer. The program increases layer thickness with depth to account for loss of vertical resolution with depth. Generally, 15 or the maximum 19 layers were used for the smooth model inversions. The

thickness of the first layer was either fixed between 3 and 8m or program defaults were used. The maximum depth was generally set to greater than 50m; however, occasionally program defaults were used to determine a realistic depth of investigation.

An example of the output of the inversion program for the TDEM sounding at Line 3, Station 1520 is presented as Figure 4. This figure shows the measured data points (in terms of apparent resistivity) superimposed on a solid line. The solid line represents the computed forward model for the geoelectric section for either the layered model or smooth model shown on the right. These geoelectric sections are the best match obtained by the inversion program. A four-layer inversion model is shown for the sounding. The upper conductive layer is interpreted as silts, clays and/or saturated sands. The underlying resistive layer is interpreted as coarse-grained alluvium and the lower two conductive layers are interpreted as the clay unit.

The interpreted geoelectric section derived from each TDEM sounding is not unique. The magnitude of each individual layer resistivity and thickness can normally be varied within a limited range with no significant change to the fit of the geoelectric model of the field data. This variation in fit parameters is termed equivalence and is a problem faced by most surface geophysical techniques. An equivalence analysis was performed for each of the TDEM soundings. Figure 4 also shows the equivalence analysis for the example sounding. This sounding is typical of the TDEM data which generally has about a plus or minus 5 to 10 % equivalence in depth determinations and about plus or minus 5 to 10% equivalence in individual layer resistivity.

Another form of analyzing equivalence is in the total number of layers used in the inversion model. In the TEMIXXL program, the interpreter sets a fixed number of layers. During the inversion process, the program adjusts the layer resistivity and thickness so the model best fits the field data. Generally, a minimum number of layers are used in the modeling program. This is determined by increasing the number of layers in the model, until additional layers do not significantly improve the fit of the model to the field data. Inversion models with three to four layers were generally used for the TDEM data collected during this investigation.

The 1D layered models for each profile were output as an ASCII file and a Visual Basic utility program was written to convert this file to a free-format ASCII containing the station number, layer resistivity and the elevation of the top of each layer. This file was subsequently entered into the program GRAPHER so that geoelectric cross-sections could be generated for each line.

The smooth model inversion data for each profile were exported as an ASCII format file containing station, and interpolated layer resistivity and elevations at about 1m increments. Layer elevations were converted to feet and resistivity was converted to conductivity in a spreadsheet and subsequently entered into the program SURFER (Golden Software, Inc) where color-enhanced images of the smooth models for each profile were generated.

5 INTERPRETATION AND RESULTS

5.1.1 Line 1

Line 1 is a 1,745 foot long, south to north trending line located along the western portion of the site (Figure 1). Geophysical data could not be acquired in the centermost 500 ft of the line due to heavy vegetation and the wash. The geoelectric section for the 1D layered model inversion is presented as Figure 5. The geoelectric section for the smooth model inversion and EM-34 profile for Line 1 are presented in Figure 6.

The geoelectric model for the site (Figures 5 and 6) is different south and north of the wash, respectively. This is not unexpected as different alluvial fan systems are located south and north of the wash. South of the wash TDEM models indicate that there is an average of about 25 ft of fine-grained soils (modeled resistivity of 5 to 8 ohm-meters) overlying a 30 to 45 ft thick coarse-grained unit (modeled resistivity of 19 to 42 ohm-meters). This unit is underlain by a very low resistivity (high conductivity) clay unit at an elevation between 1481 and 1492 ft MSL. The conductive uppermost unit south of the wash interpreted as fine-grained soils could also be interpreted as salt-rich silty sands or saturated sediments. Subsurface conditions north of the wash are different with the upper 25 to 43 ft consisting of intermediate resistivity (12 to 22 ohm-meter) silts and sands. Underlying this unit at an elevation ranging from 1530 to 1538 ft MSL is a low resistivity (6 to 8 ohm-meters) layer interpreted as silt or silty clay. This unit becomes more conductive with depth, although the smooth model inversion (Figure 6) introduces the possibility that a thin coarser-grained, less conductive unit may underlie the uppermost silt/clay, which is in turn underlain by conductive clay.

There is no available borehole control in the vicinity of this line. EM-34 data is consistent with the TDEM models. EM-34 conductivity measurements decrease to the north from 87 mS/m at the southern end of the line to 48 mS/m at the northern end of the line and appear to reflect near-surface electrical conductivity structure rather than deeper structure.

5.1.2 Line 2

Line 2 is a 2,245 foot long, south to north trending line located about 3,750 ft east of Line 1 (Figure 1). Geophysical data could not be acquired between stations 1160 and 1470 ft and 2170 and 2520 ft due to the wash and heavy vegetation, respectively. The geoelectric section for the 1D layered model inversion is presented as Figure 7. The geoelectric section for the smooth model inversion and EM-34 profile for Line 2 are presented in Figure 8.

The geoelectric model for the site (Figures 7 and 8) exhibits similar geologic conditions both south and north of the wash. TDEM models indicate that there is about 10 to 20 ft of silts and sands and/or saturated sands (modeled resistivity of 7 to 15 ohm-meters) overlying a 25 to 50 ft thick coarser grained unit (modeled resistivity of 13 to 40 ohm-meters). This unit is underlain by a very low resistivity (high conductivity) clay unit at an elevation between 1471 and 1482.5 ft MSL.

EM-34 data is consistent with the TDEM models. EM-34 conductivity measurements range from 52 to 92 mS/m and appear to reflect relative changes in depth to the subsurface clay unit. The lowest EM-34 conductivities occur at the northern end of the line where the clay unit is modeled at the greatest depth.

Geologic data from Well 5.585S located about 200 ft east of station 1770 ft encountered a clay layer at a depth of 40-58 ft. The top of the clay layer was modeled at a depth of about 45 ft for the TDEM sounding at station 1770 ft.

5.1.3 Line 3

Line 3 is a 1,955 foot long, south to north trending line located about 2,000 ft east of Line 2 (Figure 1). Geophysical data could not be acquired between stations 2131 and 2315 ft due to heavy vegetation. The geoelectric section for the 1D layered model inversion is presented as Figure 9. The geoelectric section for the smooth model inversion and EM-34 profile for Line 3 are presented in Figure 10.

The geoelectric model for the site (Figures 9 and 10) exhibits similar geologic conditions both south and north of the wash. TDEM models indicate that there is about 7 to 12 ft of silts, clays and/or salt-rich saturated sands (modeled resistivity of 6 to 8 ohm-meters) within the active wash complex (central portion of the line). This unit is not well resolved because the TDEM technique does not adequately image the upper 15 ft. A thick coarser grained unit (modeled resistivity of 16 to 54 ohm-meters) underlies the fine-grained unit and is exposed at the surface on the south and north ends of the line. This unit, which is interpreted as sands and gravels, ranges in thickness from 55 to 85 ft and is underlain by a very low resistivity (high conductivity) clay unit. The clay unit is modeled at elevations between 1443 and 1490 ft MSL, 1443 to 1456 ft MSL beneath the active portion of the wash.

EM-34 data is consistent with the TDEM models. EM-34 conductivity measurements range from 30 to 78 mS/m and appear to reflect relative changes in depth to the subsurface clay unit expect for the central portion of the line, where data is influenced by the electrically conductive surface layer. The lowest EM-34 conductivities occur at the northern end of the line where the clay unit is modeled at the greatest depth.

Boreholes drilled along a pipeline alignment between Lines 2 and 3 encountered the Tertiary clay unit at an elevation ranging from 1459 to 1471 ft MSL. This elevation range for the clay unit is intermediate to and consistent with the clay elevations modeled on Lines 2 and 3, respectively.

5.1.4 Line 4

Line 4 is a 1,700 foot long, south to north trending line located about 3,750 ft east of Line 3 (Figure 1). Geophysical data could not be acquired between stations 16+25 and 18+50 due to the wash. The geoelectric section for the 1D layered model inversion is presented as Figure 11. The geoelectric section for the smooth model inversion and EM-34 profile for Line 4 are presented in Figure 12.

The geoelectric model for this line (Figures 11 and 12) is much different than Lines 1 to 3. Line 4 is located east of an inferred fault and older Tertiary sediments (Horse Spring and Thumb Formations) outcrop south and north of the active wash complex. The geoelectric section is much more complex beneath this line than Lines 1 to 3. The Thumb Formation outcrops immediately south of station 1000 and at station 2500 ft. Near-surface soils beneath the southern portion of the line outside the active wash are conductive (low resistivity of 7 to 9 ohm-meters) and interpreted to be silts and clays. This unit is underlain by a more resistive unit (modeled resistivity of 28 to 51 ohm-meters) interpreted as sands and gravels, possibly a

sandstone member of the Thumb Formation. There is evidence of a fine-grained unit at depths exceeding 250 feet, possibly a siltstone or claystone member of the Thumb Formation. This unit is too deep to accurately resolve in this area.

Within the active wash complex (stations 1410 to 1950 ft), TDEM models indicate a 15 to 45 ft thick, conductive surficial unit (modeled resistivity of 7 to 13 ohm-meters) interpreted as silts, clays and/or saturated sands. On the southern portion of the active wash, this unit is underlain by coarser-grained sands and gravels with modeled resistivity ranging from 34 to 55 ohm-meters. These units are underlain by a thin, 10 to 15 ft thick, conductive unit interpreted as claystone or siltstone. This unit is interpreted as the upper member of the Thumb Formation as it appears to outcrop at the northern end of the line in an area mapped as Thumb Formation (Figure 2). This unit is not thick enough to accurately resolve; however TDEM models indicate that it must exist. This siltstone/claystone layer is underlain by a coarser-grained, possibly sandstone, member of the Thumb Formation, which overlies a possible claystone member of the Thumb Formation. TDEM soundings at stations 1410 to 1625 did not appear to image deep enough to model this lower fine-grained unit.

North of the active wash complex (stations 2100 to 2700 ft), TDEM models indicate a 0 to 60 ft thick, resistive surficial unit (modeled resistivity of 24 to 48 ohm-meters) interpreted as sands and gravels. This unit is underlain by a 10 to 35 ft thick, conductive unit that appears to outcrop at station 2600. This unit has a modeled resistivity of 5 to 13 ohm-meters and is interpreted as an upper siltstone/claystone member of the Thumb Formation. This siltstone/claystone layer is underlain by a 30 to 90 ft thick, coarser-grained, possibly sandstone, member of the Thumb Formation, which overlies a siltstone/claystone member of the Thumb Formation.

There is no available borehole control in the vicinity of this line. EM-34 data is consistent with the TDEM models and EM-34 conductivity measurements range from about 20 to 55 mS/m. Conductivity measurements are higher between stations 1000 and 2000, primarily as the result of electrical conductive near-surface soils. There is an abrupt drop in EM-34 conductivity at station 2100 ft corresponding to a ground surface elevation increase of about 25 ft and corresponding coarser-grained near surface soils. Conductivity then increases to the north as the Thumb Formation becomes shallower.

5.1.5 Line 5

Line 5 is a 1,695 foot long, west to east trending line located in the active wash complex, perpendicular to Line 4 (Figure 1). Station 1427 on Line 5 intersects Line 4 at station 1625 ft. Geophysical data could not be acquired between stations 18+45 and 23+07 due to the wash. The geoelectric section for the 1D layered model inversion is presented as Figure 13. The geoelectric section for the smooth model inversion and EM-34 profile for Line 5 are presented in Figure 14.

The geoelectric model for the site (Figures 13 and 14) is much different than Lines 1 to 3 and more complex. Line 5 is located east of an inferred fault and older Tertiary sediments (Horse Spring and Thumb Formations) outcrop south and north of the active wash complex. This line could not be extended across the potential fault due to heavy vegetation in the wash.

Near-surface soils beneath the southern portion of the line outside the active wash are conductive (low resistivity of 7 to 10 ohm-meters) and are interpreted to be silts and/or

saturated sands. This unit is underlain by a more resistive unit (modeled resistivity of 25 to 65 ohm-meters) interpreted as sand and gravel or possibly a limestone member to the Horse Spring Formation to the west and a sandstone member of the Thumb Formation to the east. In the central portion of the line this unit is underlain by a 10 to 25 ft thick, conductive unit (modeled resistivity of 5 to 10 ohm-meters) interpreted as an upper siltstone/claystone member of the Thumb Formation. A similar layer is present on the westernmost end of the line and is probably a siltstone/claystone layer within the Horse Spring Formation that pinches out near station 2500 ft. Both siltstone/claystone layers are underlain by resistive sandstone or limestone layers, which overly a possible siltstone/claystone unit about 200 ft deep. The contact between the Horse Spring and Thumb Formations is not clear, although the TDEM models between stations 2300 and 2500 ft differ from those to the west and east.

Interpretation of the TDEM data acquired along this line could include potential faulting; however, other geophysical or geological data is needed to make this kind of interpretation.

There is no available borehole control in the vicinity of this line. EM-34 data is consistent with the TDEM models and EM-34 conductivity measurements range from about 27 to 45 mS/m. Conductivity measurements are higher in the vicinity of station 1300 ft where the siltstone/claystone layer interpreted as the top of the Thumb Formation is shallowest and the surface conductive layer becomes thicker.

6 CONCLUSIONS AND RECOMMENDATIONS

TDEM and FDEM geophysical surveys performed in a portion of the Las Vegas Wash located in Clark County, Nevada were effective at mapping electrical properties of the subsurface. The geophysical survey was designed to map the top of the clay layer underlying the site. To meet these objectives, a total of 76 TDEM soundings were made along 5 profiles, as shown in Figure 1, to image the electrical structure to a maximum depth of about 150 ft. FDEM profiles were acquired with the Geonics EM-34 terrain conductivity meter along each of the 5 profiles for a total of about 9,450 linear-feet.

The data quality was generally excellent for the TDEM and FDEM data and there is excellent correlation between the two types of data. The top of the uppermost clay unit was modeled between elevations of 1481 and 1538, 1471 and 1483 and 1443 and 1490 feet MSL, on Lines 1, 2 and 3, respectively. TDEM models for Lines 1 to 3 indicate that the top of the clay unit decreases in elevation to the east. TDEM models for Lines 4 and 5 are much different than those for Lines 1 to 3 indicating that the inferred fault (Figure 2) exists west of the western end of Line 5. Line 5 could not be extended across this probable fault due to heavy vegetation in the wash. Sedimentary rocks of the Horse Spring and Thumb Formations are probably present at relatively shallow depth beneath Lines 4 and 5. Unfortunately, the TDEM method can not distinguish rock from soil with similar electrical properties. A thin siltstone/claystone layer was modeled at a depth of 50 ft or less beneath much of Line 4 and at a depth of between 45 and 90 ft beneath a portion of Line 5. This layer is probably at or near the top of the Thumb Formation. A more massive siltstone/claystone layer is modeled on both lines at a depth of 100 to over 200 ft.

Geologic models developed from the geophysical data acquired during this investigation could be refined by acquiring TDEM data along west to east traverses south and north of the wash to locate the inferred fault. Additionally, seismic refraction profiles could be conducted east of the fault to determine the top of the Horse Springs and Thumb Formations.

7 CERTIFICATION

All geophysical data, analysis, interpretations, conclusions, and recommendations in this document have been prepared under the supervision of and reviewed by a **GEOVision** California Registered Geophysicist.

Antony J. Martin

Date

California Registered Geophysicist GP989

GEOVision Geophysical Services

- * This geophysical investigation was conducted under the supervision of a California Registered Geophysicist using industry standard methods and equipment. A high degree of professionalism was maintained during all aspects of the project from the field investigation and data acquisition, through data processing interpretation and reporting. All original field data files, field notes and observations, and other pertinent information are maintained in the project files and are available for the client to review for a period of at least one year.

A registered geophysicist's certification of interpreted geophysical conditions comprises a declaration of his/her professional judgment. It does not constitute a warranty or guarantee, expressed or implied, nor does it relieve any other party of its responsibility to abide by contract documents, applicable codes, standards, regulations or ordinances.

TABLES

TABLE 1 LINE 1 - SURVEY DATA FOR FDEM PROFILE AND TDEM SOUNDINGS

STATION	EASTING	NORTHING	ELEVATION (ft MSL)	TDEM (Y/N)
8+79	830842.794	26733911.26	1551.938	
10+00	830903.863	26734016.38	1550.786	Y
11+00	830954.102	26734102.9	1550.59	Y
12+00	831004.211	26734189.13	1550.481	Y
13+00	831054.5	26734275.69	1550.912	Y
14+00	831104.87	26734362.08	1549.447	Y
16+13	831211.51	26734546.03	1549.448	Y
21+50	831127.709	26735076.7	1554.28	Y
22+50	831112.084	26735175.4	1558.114	Y
23+50	831096.28	26735274.03	1567.119	Y
24+50	831080.53	26735372.73	1562.958	Y
25+60	831063.712	26735481.55	1568.778	Y
26+50	831049.435	26735570.38	1573.518	Y
27+45	831034.541	26735664.06	1577.426	Y

TABLE 2 LINE 2 - SURVEY DATA FOR FDEM PROFILE AND TDEM SOUNDINGS

STATION	EASTING	NORTHING	ELEVATION (ft MSL)	TDEM (Y/N)
3+80	834624.581	26733344.6	1530.827	Y
5+80	834660.554	26733541.61	1541.398	Y
8+00	834733.858	26733751.76	1539.374	Y
9+60	834729.399	26733915.35	1531.724	Y
10+00	834736.631	26733954.52	1530.347	
10+60	834747.707	26734013.46	1529.628	Y
11+60	834765.619	26734111.96	1526.794	Y
14+70	834821.643	26734416.58	1523.919	Y
15+70	834839.847	26734514.97	1524.019	Y
16+70	834857.806	26734613.43	1523.983	Y
17+70	834876.132	26734711.77	1523.886	Y
18+70	834893.94	26734810.07	1523.181	Y
19+72	834912.501	26734910.17	1522.005	Y
21+71	834948.462	26735106.05	1521.751	Y
25+20	835011.827	26735449.19	1534.862	Y
26+25	835030.679	26735552.75	1535.443	Y

TABLE 3 LINE 3 - SURVEY DATA FOR FDEM PROFILE AND TDEM SOUNDINGS

STATION	EASTING	NORTHING	ELEVATION (ft MSL)	TDEM (Y/N)
10+00	837006.003	26734305.71	1541.614	Y
11+00	836981.816	26734402.8	1540.677	Y
12+00	836957.389	26734499.74	1537.597	Y
13+20	836928.186	26734616.12	1531.465	Y
14+20	836903.937	26734713.17	1524.231	Y
15+20	836879.716	26734809.94	1523.547	Y
15+90	836862.564	26734878.2	1523.987	Y
17+50	836858.252	26735038.03	1508.774	Y
18+30	836856.101	26735117.9	1506.903	Y
19+30	836853.382	26735217.79	1505.927	Y
20+31	836850.573	26735318.99	1506.086	Y
23+15	836842.749	26735602.79	1509.078	Y
24+56	836838.93	26735743.21	1522.61	Y
25+55	836835.926	26735842.67	1522.58	Y
26+55	836833.534	26735942.46	1522.138	Y
27+55	836830.67	26736042.46	1523.572	Y
28+55	836828.172	26736142.55	1524.503	Y
29+55	836825.283	26736242.17	1525.935	Y

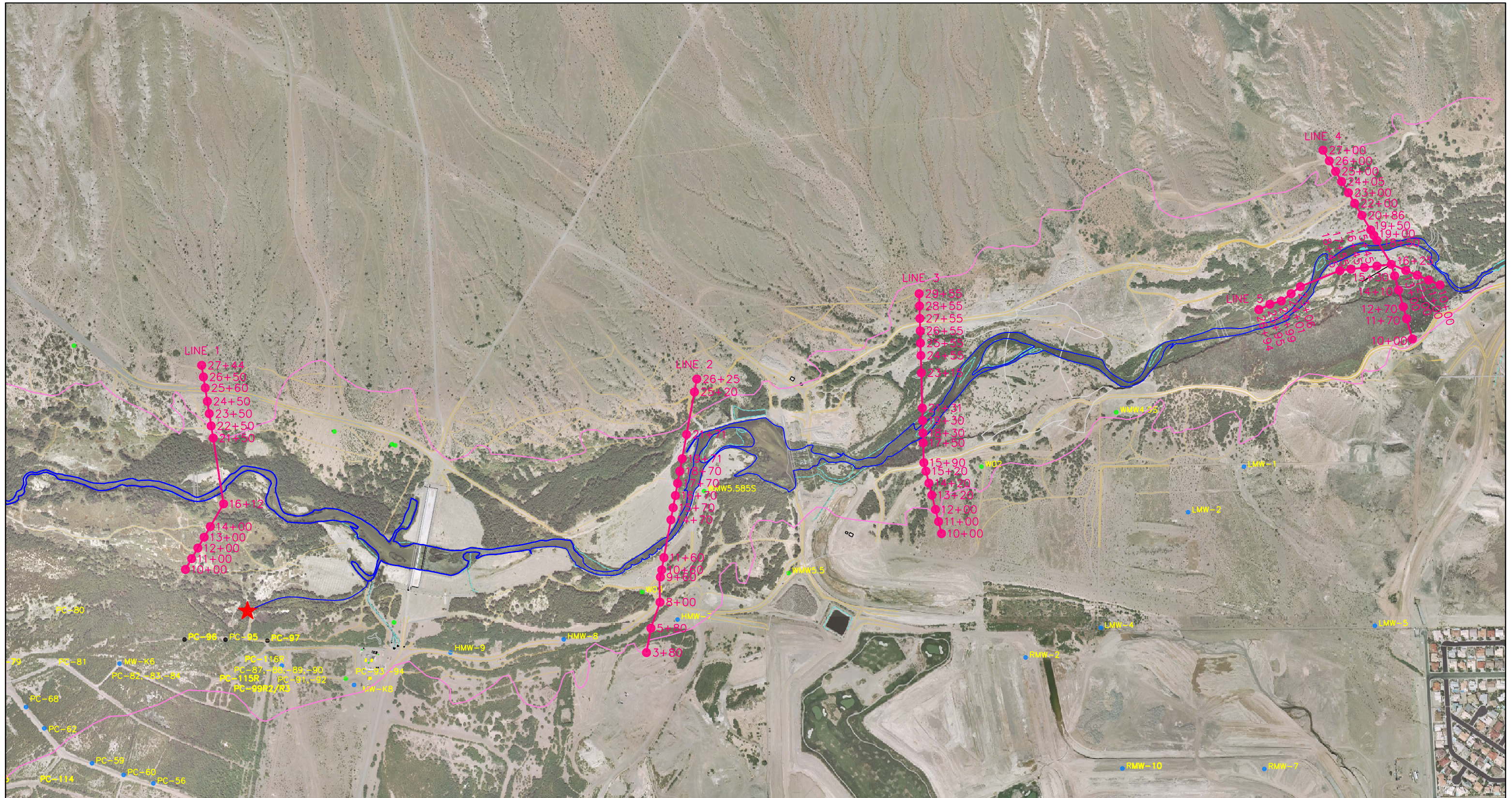
TABLE 4 LINE 4 - SURVEY DATA FOR FDEM PROFILE AND TDEM SOUNDINGS

STATION	EASTING	NORTHING	ELEVATION (ft MSL)	TDEM (Y/N)
10+00	840805.562	26735876.57	1504.388	Y
11+70	840759.367	26736040.1	1504.831	Y
12+70	840732.207	26736136.21	1504.675	Y
14+10	840693.997	26736271.1	1483.596	Y
15+30	840661.5	26736386.52	1478.338	Y
16+25	840635.364	26736478.78	1477.803	Y
18+00	840545.868	26736628.13	1476.497	Y
19+00	840494.35	26736713.92	1477.772	Y
19+50	840468.818	26736756.83	1478.361	Y
20+87	840398.528	26736874.23	1505.171	Y
22+00	840340.174	26736971.23	1505.576	Y
23+00	840288.752	26737057.23	1505.836	Y
24+05	840235.152	26737146.98	1506.752	Y
25+00	840186.372	26737228.7	1508.992	Y
26+00	840134.942	26737314.36	1510.523	Y
27+00	840083.554	26737400.08	1525.316	Y

TABLE 5 LINE 5 - SURVEY DATA FOR FDEM PROFILE AND TDEM SOUNDINGS

STATION	EASTING	NORTHING	ELEVATION (ft MSL)	TDEM (Y/N)
26+95	839566.804	26736112.87	1483.895	Y
25+96	839655.768	26736157.16	1483.241	Y
24+99	839748.24	26736183.22	1482.373	Y
24+01	839826.716	26736242.38	1481.438	Y
23+07	839901.797	26736299.32	1481.199	Y
21+97	839989.096	26736365.68	1479.801	
20+99	840047.435	26736445.28	1479.508	
19+95	840108.624	26736528.95	1478.919	
18+45	840220.558	26736429.46	1478.599	Y
17+55	840309.839	26736439.83	1481.353	Y
16+45	840418.905	26736453.2	1481.239	Y
15+45	840518.57	26736464.87	1480.998	Y
14+27	840635.364	26736478.78	1477.803	Y
13+00	840752.645	26736429.25	1476.801	Y
12+00	840844.727	26736390.78	1477.306	Y
11+00	840936.866	26736352.11	1480.086	Y
10+00	841029.053	26736313.13	1477.341	Y

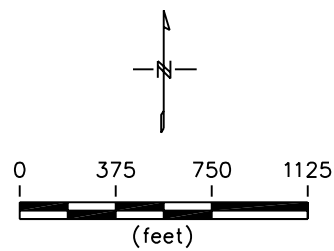
FIGURES



LEGEND

- 27+44 TDEM SOUNDING WITH STATION NUMBER
- LINE 1 GEONICS EM-34 PROFILE AND LINE NUMBER
- MW-K6 WELL LOCATION AND NAME
- ★ SEEP

NOTE: BASE MAP PROVIDED BY MCGINLEY & ASSOCIATES

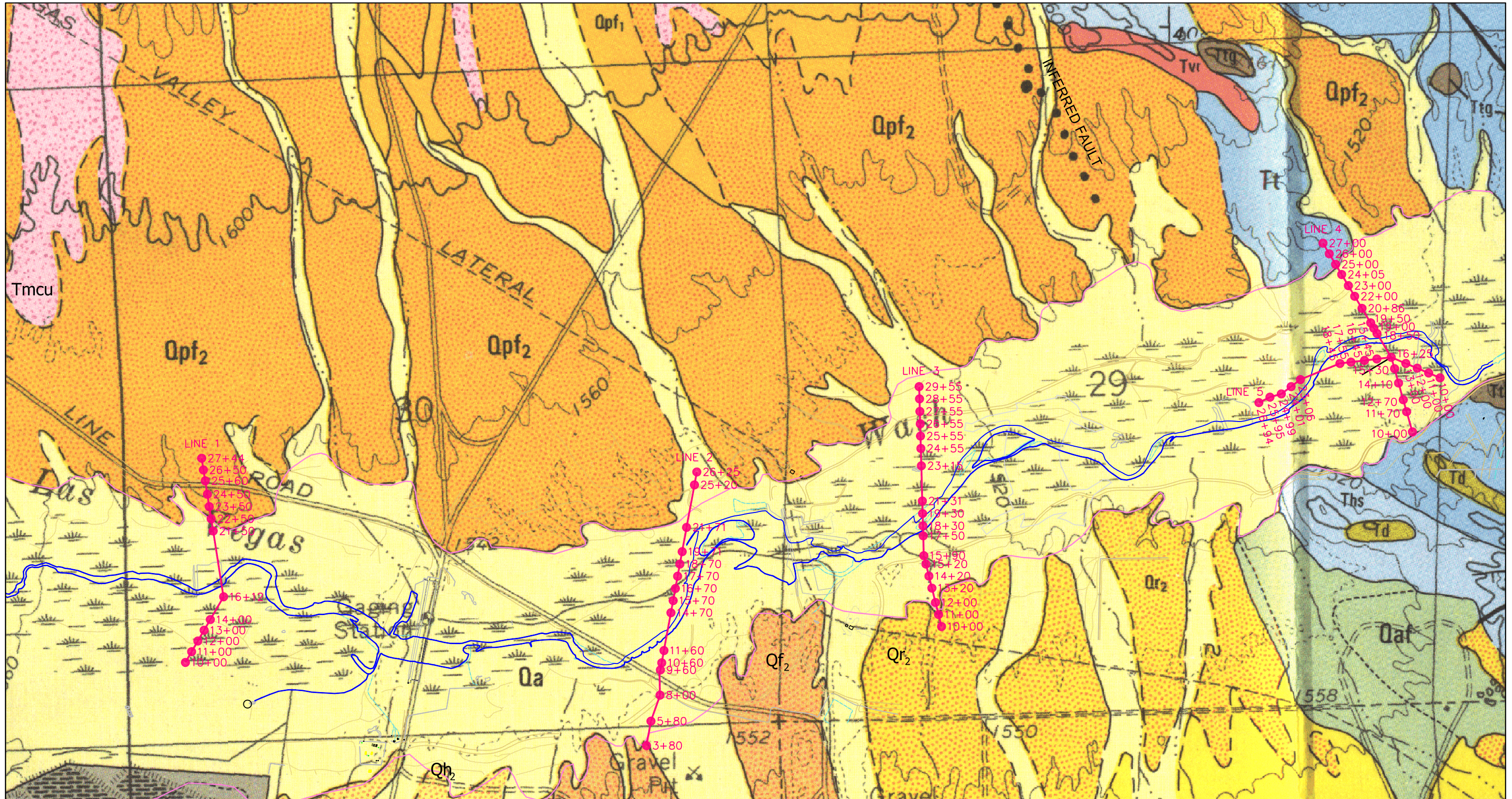


Project # 3209
 Date Jun 02, 2003
 Developed by A MARTIN
 Drawn by T RODRIGUEZ
 Approved by
 File z:\3209\3209-1.dwg

FIGURE - 1
 SITE MAP

LAS VEGAS WASH
 CLARK COUNTY, NEVADA

PREPARED FOR
 MCGINLEY & ASSOCIATES

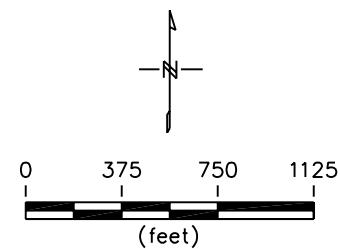


LEGEND

- 27+44 TDEM SOUNDING WITH STATION NUMBER
- LINE 1 GEONICS EM-34 PROFILE AND LINE NUMBER

NOTE: BASE MAP PROVIDED BY MCGINLEY & ASSOCIATES

REFERENCE: J.W. BELL & E.I. SMITH, 1980, GEOLOGIC MAP OF THE HENDERSON QUADRANGLE, NEVADA, NEVADA BUREAU OF MINES AND GEOLOGY, MAP 67



Project # 3209
 Date Jun 02, 2003
 Developed by A MARTIN
 Drawn by T RODRIGUEZ
 Approved by
 File z:\3209\3209-1.dwg

FIGURE - 2
 GEOLOGIC MAP

LAS VEGAS WASH
 CLARK COUNTY, NEVADA

PREPARED FOR
 MCGINLEY & ASSOCIATES



GEONICS EM-47 TRANSMITTER



GEONICS EM-47 PROTEM RECEIVER



GEONICS EM-34



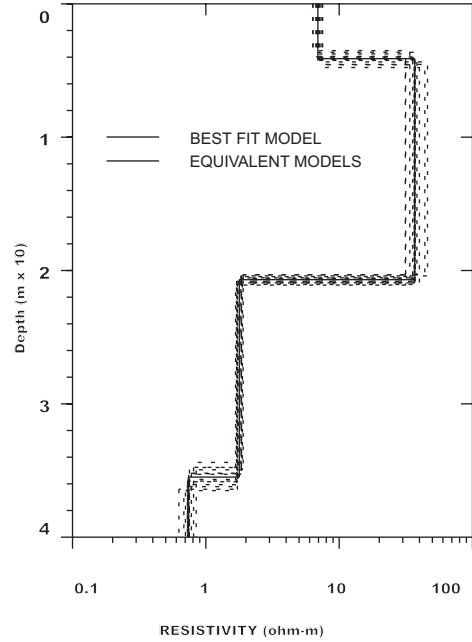
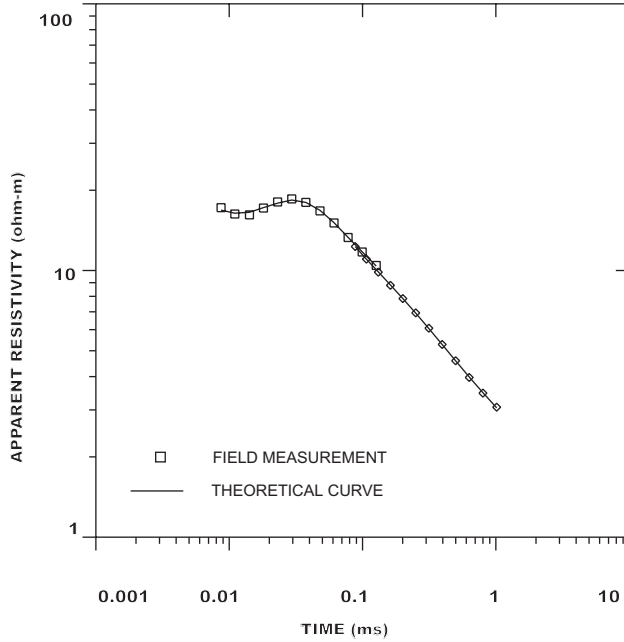
Project # 3209
 Date: May 30, 2003
 Drawn By: A MARTIN
 Approved By:
 File C:\Gvprojects\3209mgalf3.cdr

FIGURE 3
 GEONICS EM-47 TDEM SYSTEM AND
 GEONICS EM-34 CONDUCTIVITY METER

LAS VEGAS WASH
 CLARK COUNTY, NEVADA

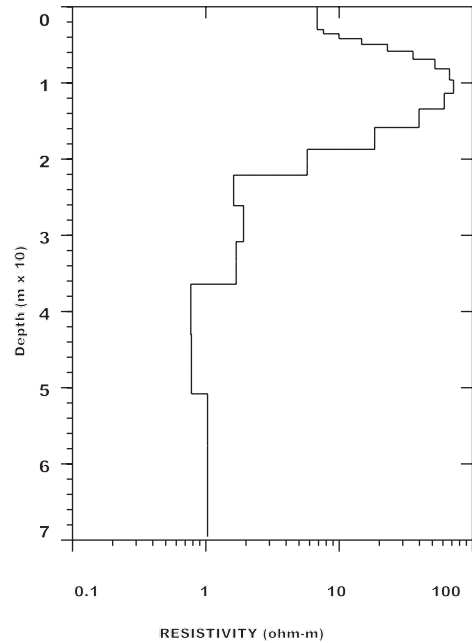
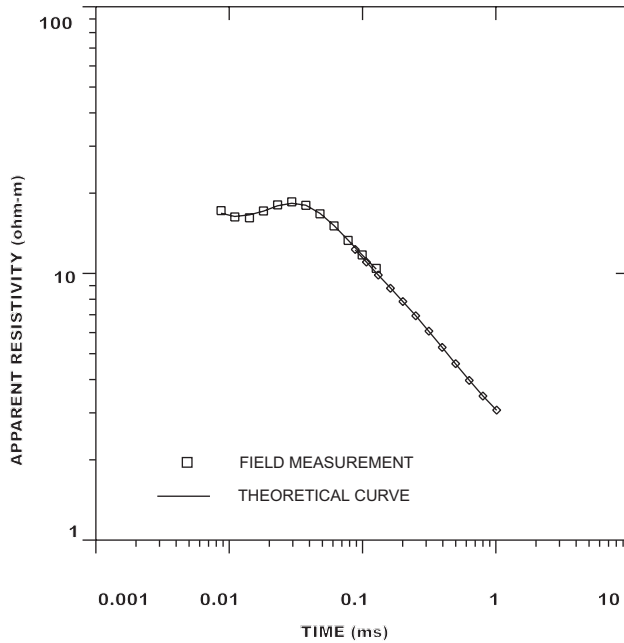
PREPARED FOR
 MCGINLEY & ASSOCIATES

L3-1520



1-D LAYERED INVERSION

L3-1520



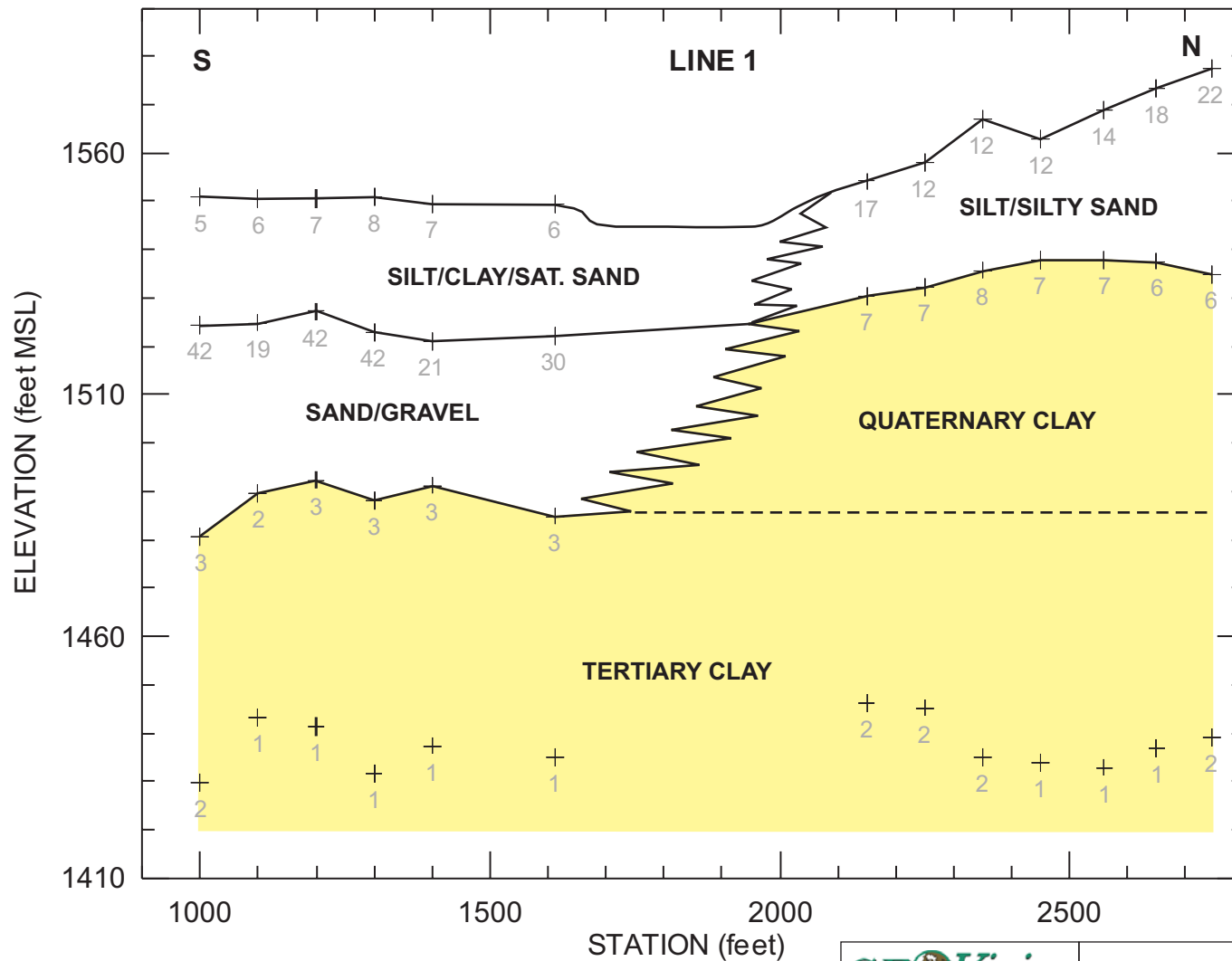
SMOOTH MODEL INVERSION

Project #	3209
Date:	May 30, 2003
Drawn By:	A MARTIN
Approved By:	
File C:\Gvprojects\3209mgalf4.cdr	

FIGURE 4
TDEM MODEL EXAMPLE

LAS VEGAS WASH
CLARK COUNTY, NEVADA

PREPARED FOR
McGINLEY & ASSOCIATES



LEGEND

2 LAYER BOUNDARY AND RESISTIVITY OF UNDERLYING LAYER IN OHM-METERS

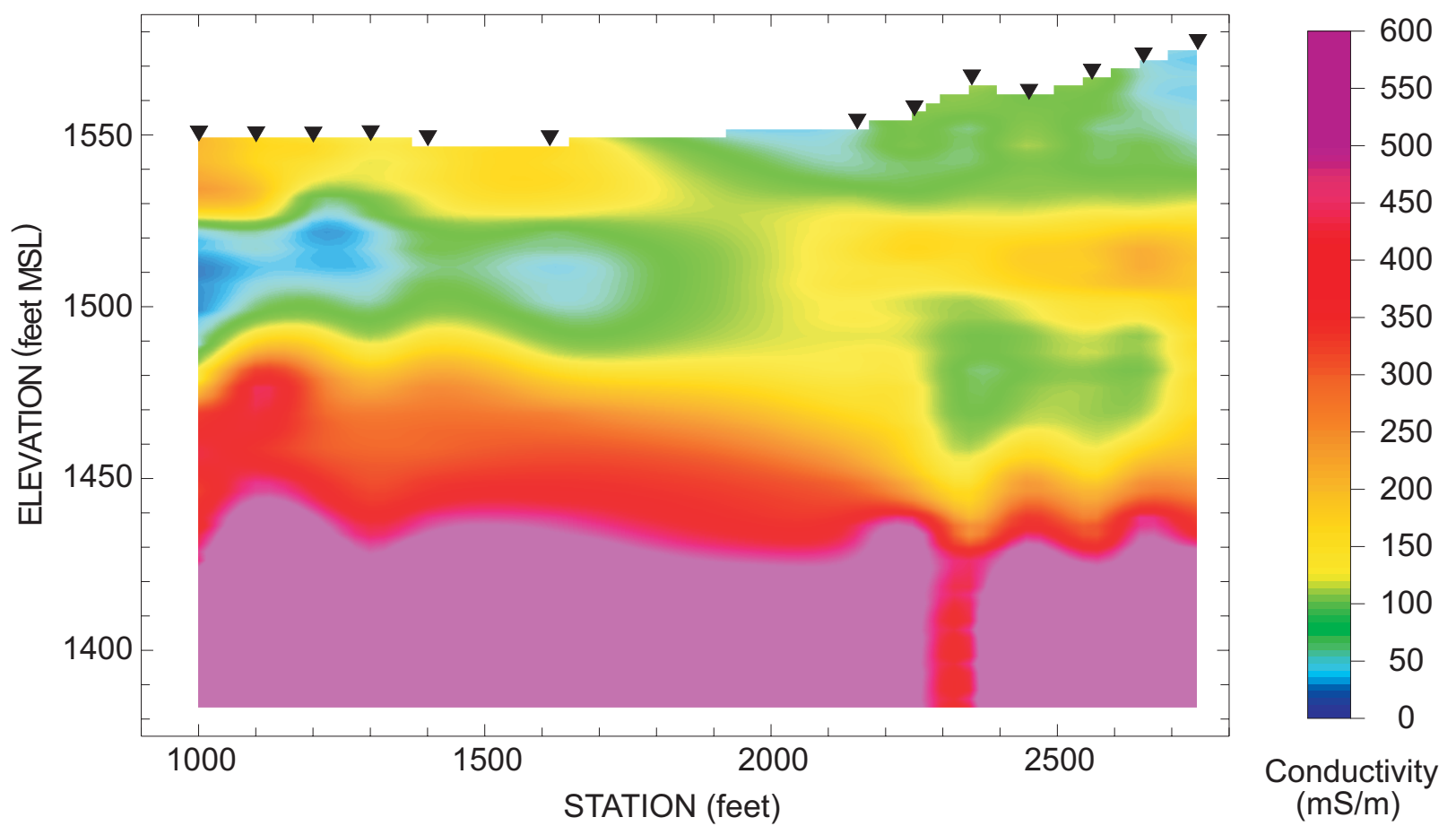
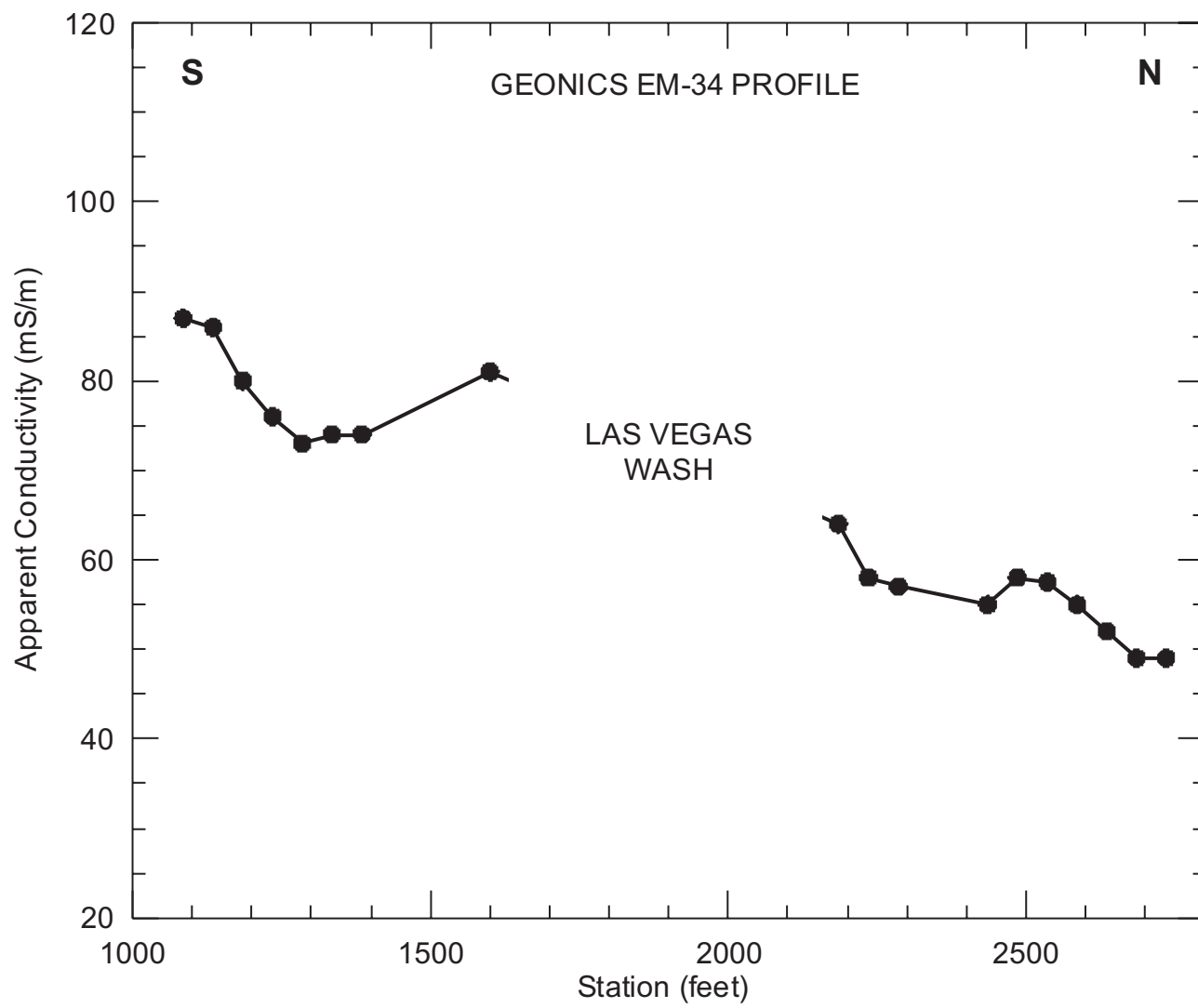


Project # 3209
 Date: May 30, 2003
 Drawn By: A MARTIN
 Approved By:
 File C:\Gvprojects\3209mgalf5.cdr

FIGURE 5
 LINE 1 - GEOELECTRIC SECTION FOR
 1D LAYERED MODEL INVERSION

LAS VEGAS WASH
 CLARK COUNTY, NEVADA

PREPARED FOR
 MCGINLEY & ASSOCIATES

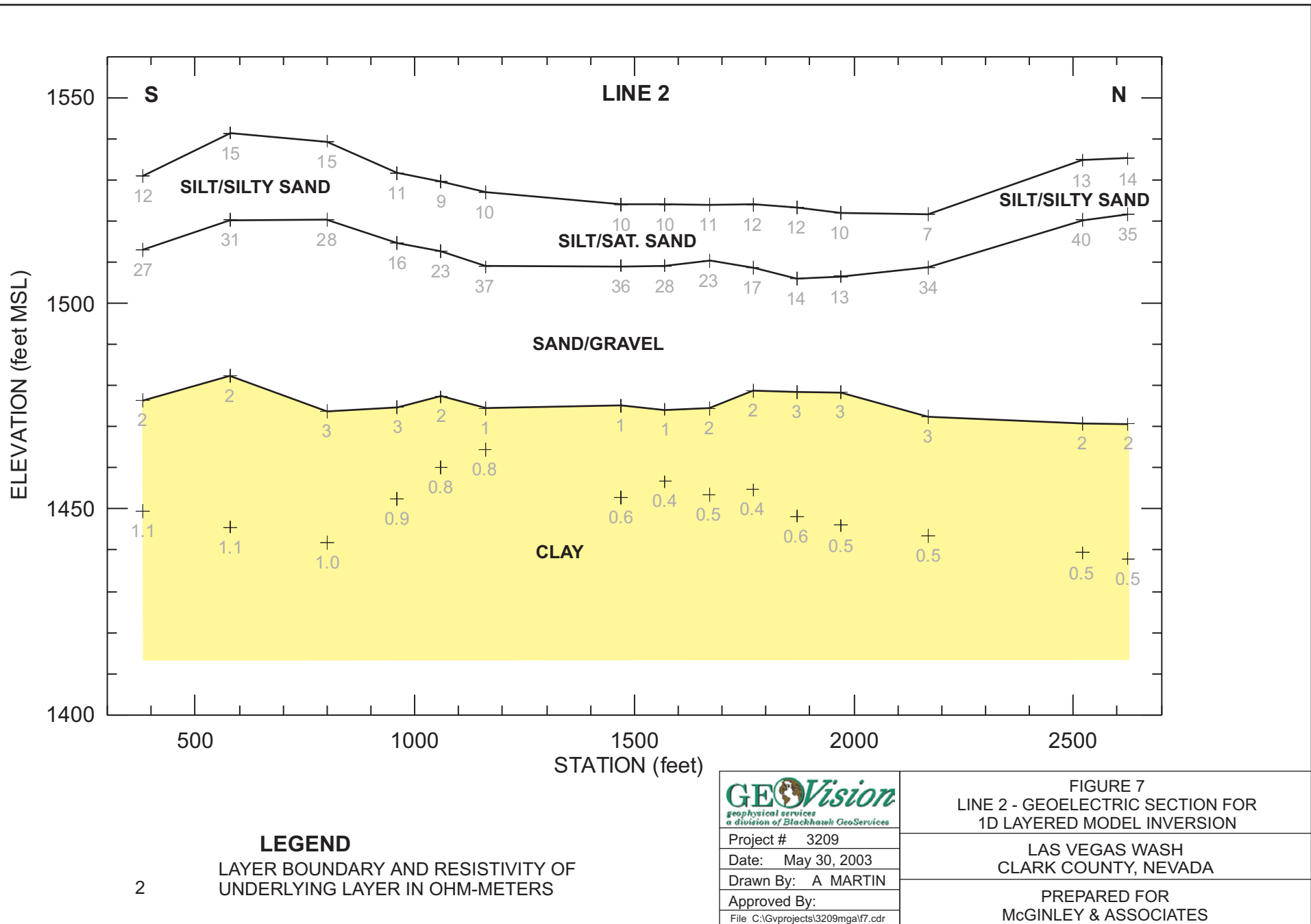


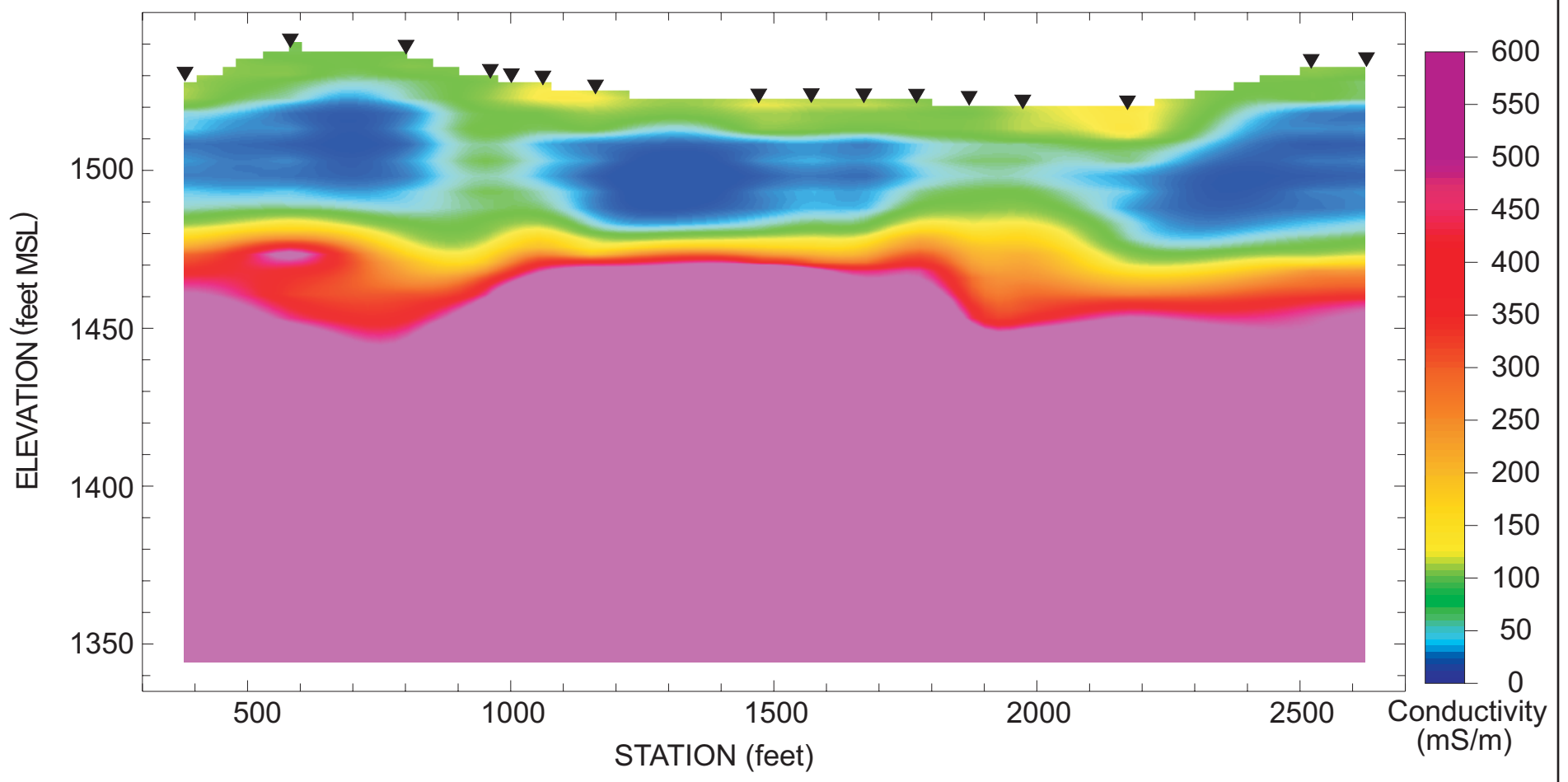
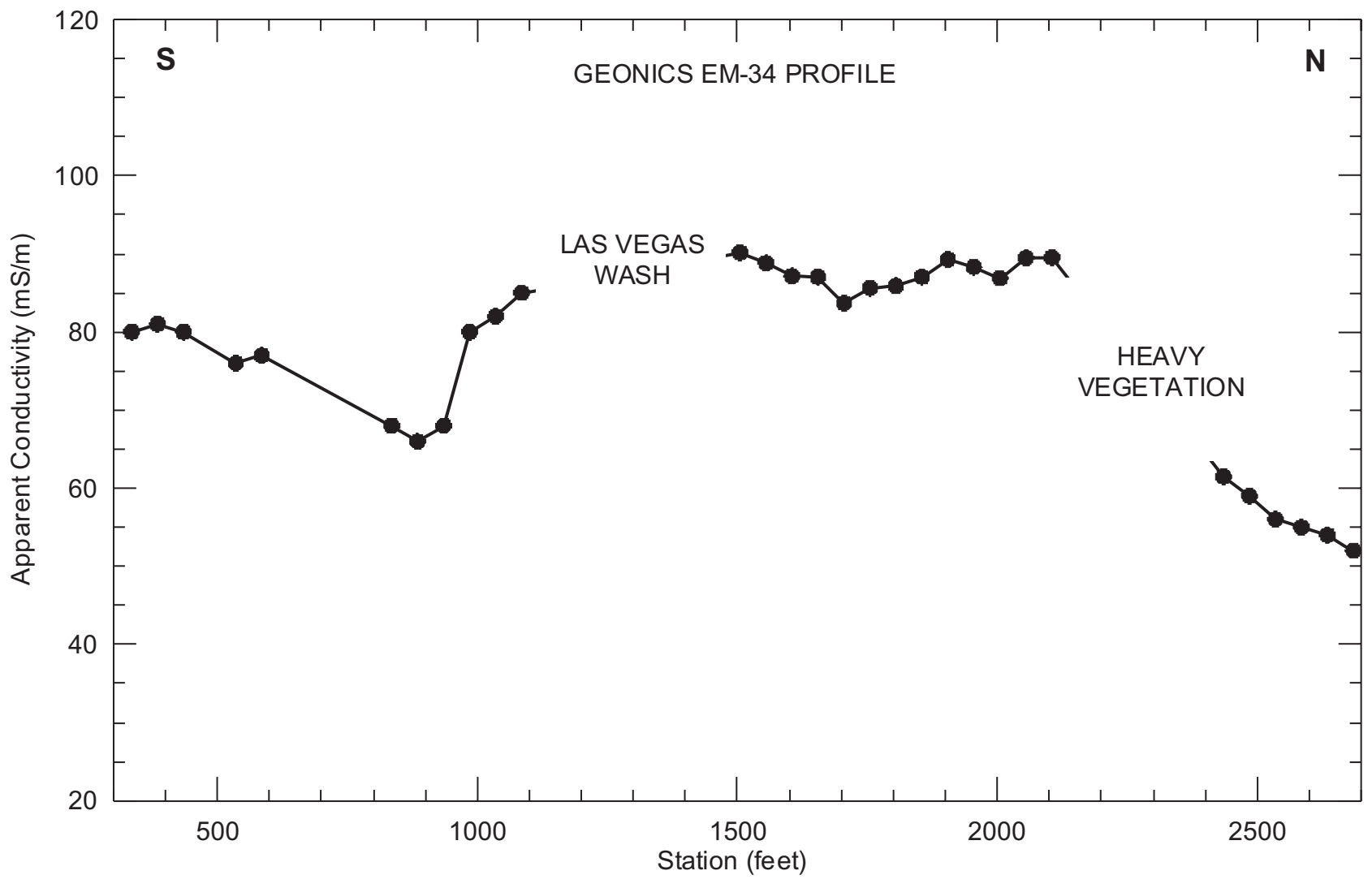
Project # 3209
 Date: May 30, 2003
 Drawn By: A MARTIN
 Approved By:
 File C:\Gvprojects\3209mga\vf6.cdr

FIGURE 6
 LINE 1 - GEOELECTRIC SECTION FOR SMOOTH
 MODEL INVERSION AND GEONICS EM-34 PROFILE

LAS VEGAS WASH
 CLARK COUNTY, NEVADA

PREPARED FOR
 MCGINLEY & ASSOCIATES





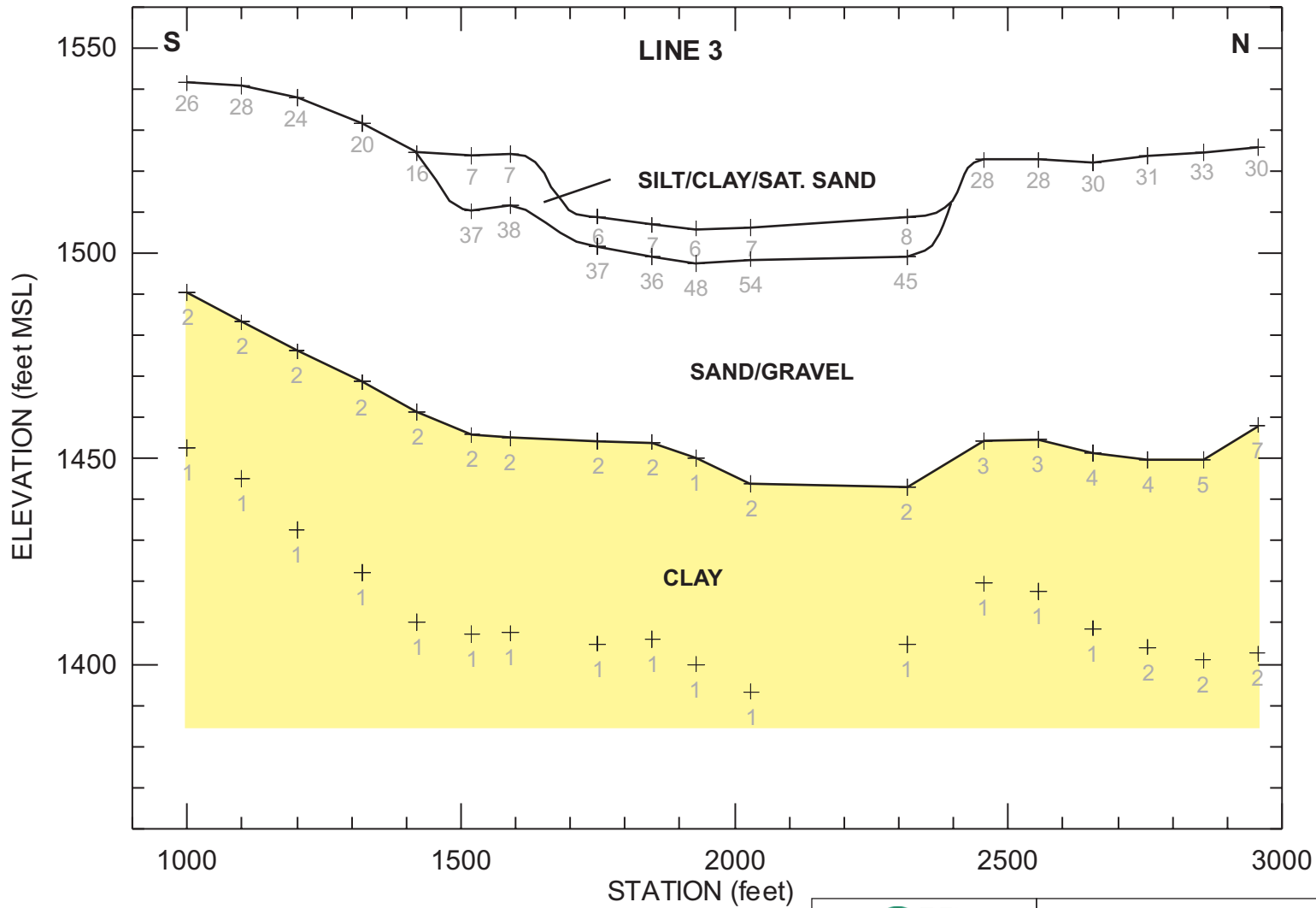
GEOVision
 geophysical services
 a division of Blackhawk GeoServices

Project # 3209
 Date: May 30, 2003
 Drawn By: A MARTIN
 Approved By:
 File C:\Gvprojects\3209mga\8.cdr

FIGURE 8
 LINE 2 - GEOELECTRIC SECTION FOR SMOOTH
 MODEL INVERSION AND GEONICS EM-34 PROFILE

LAS VEGAS WASH
 CLARK COUNTY, NEVADA

PREPARED FOR
 MCGINLEY & ASSOCIATES



LEGEND

2 LAYER BOUNDARY AND RESISTIVITY OF UNDERLYING LAYER IN OHM-METERS

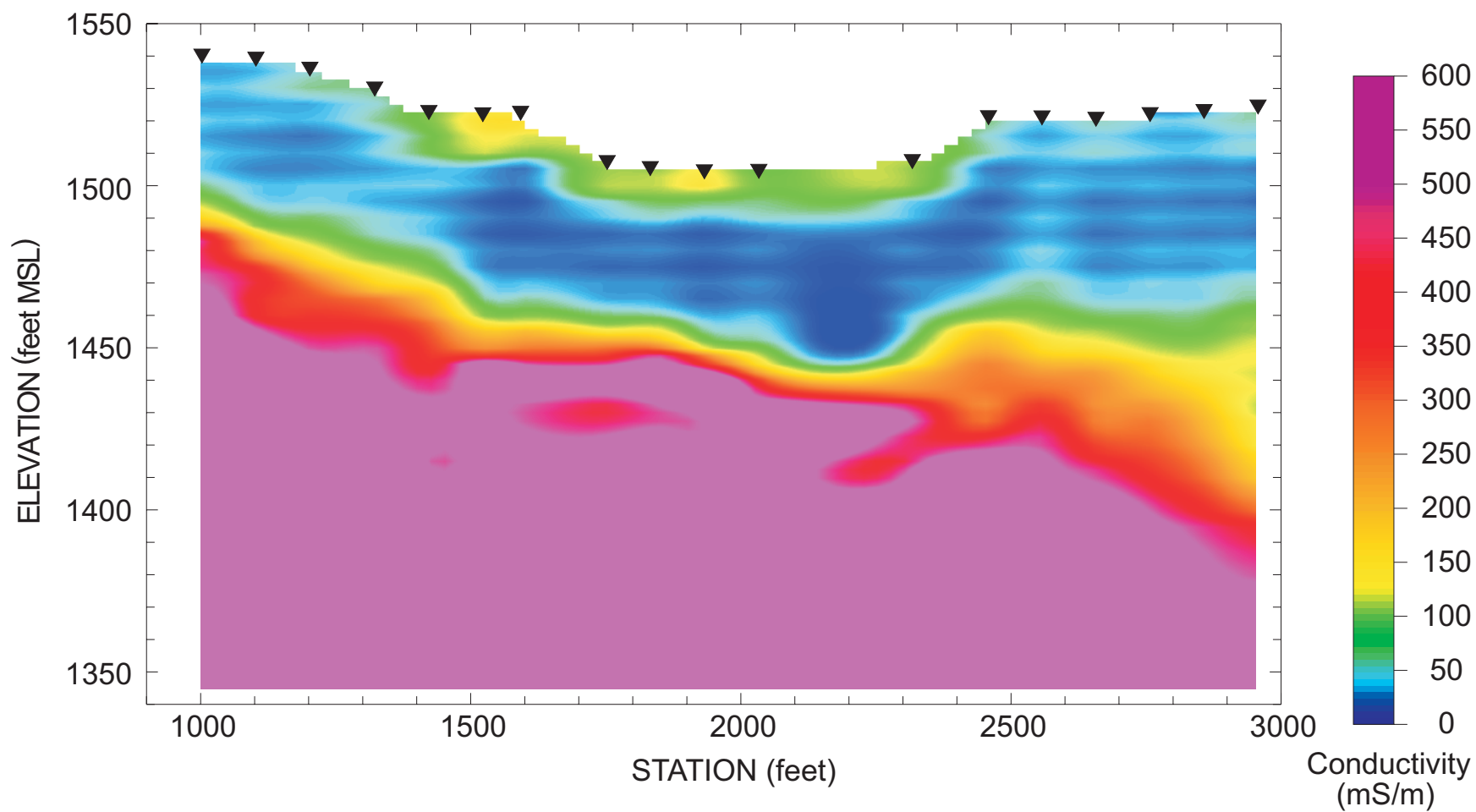
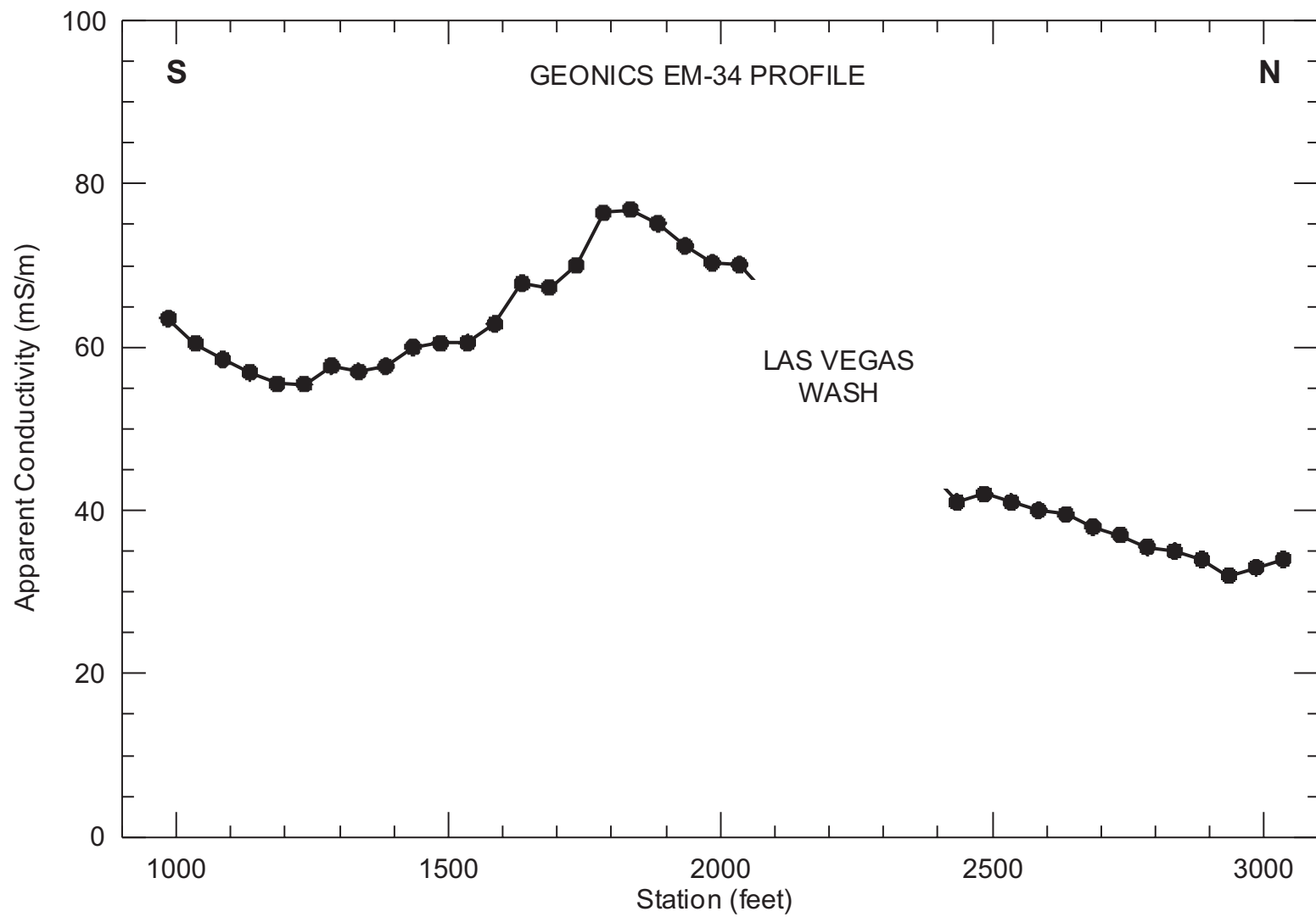


Project # 3209
 Date: May 30, 2003
 Drawn By: A MARTIN
 Approved By:
 File C:\Gvprojects\3209mgalf9.cdr

FIGURE 9
 LINE 3 - GEOELECTRIC SECTION FOR 1D LAYERED MODEL INVERSION

LAS VEGAS WASH
 CLARK COUNTY, NEVADA

PREPARED FOR
 MCGINLEY & ASSOCIATES

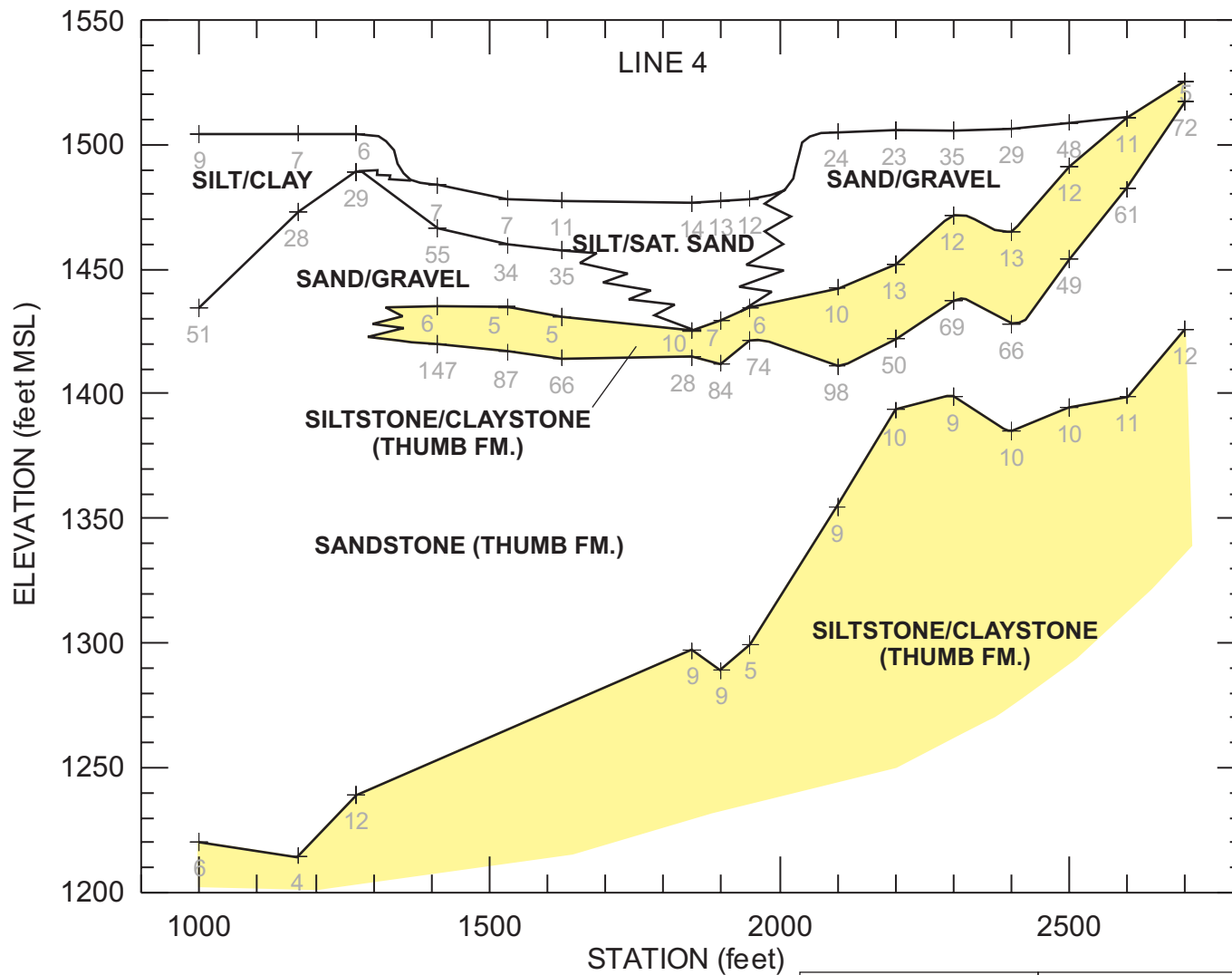


Project # 3209
 Date: May 30, 2003
 Drawn By: A MARTIN
 Approved By:
 File C:\Gvprojects\3209mga\10.cdr

FIGURE 10
 LINE 3 - GEOELECTRIC SECTION FOR SMOOTH
 MODEL INVERSION AND GEONICS EM-34 PROFILE

LAS VEGAS WASH
 CLARK COUNTY, NEVADA

PREPARED FOR
 MCGINLEY & ASSOCIATES

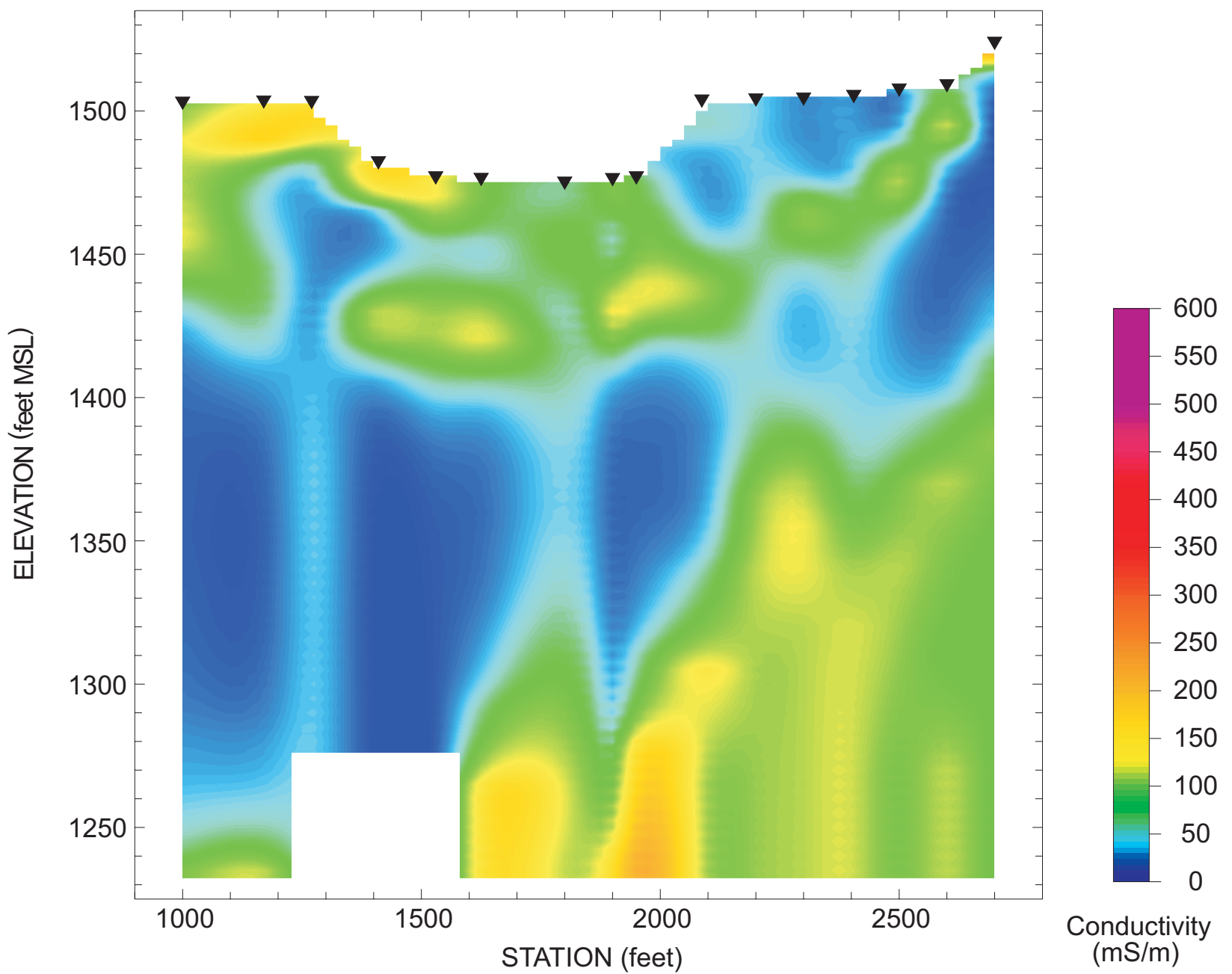
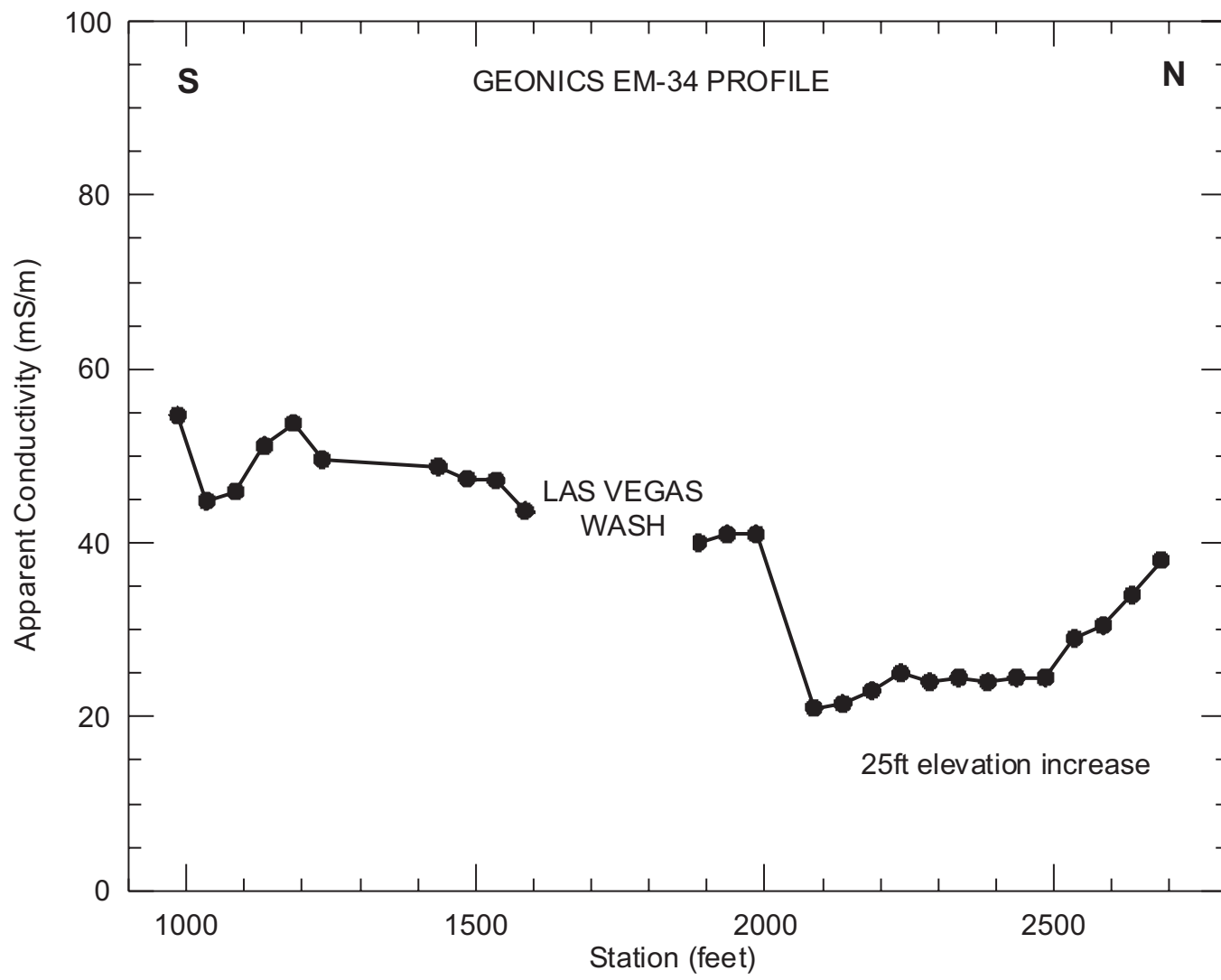


Project # 3209
 Date: May 30, 2003
 Drawn By: A MARTIN
 Approved By:
 File C:\Gvprojects\3209mgalf11.cdr

FIGURE 11
 LINE 4 - GEOELECTRIC SECTION FOR
 1D LAYERED MODEL INVERSION

LAS VEGAS WASH
 CLARK COUNTY, NEVADA

PREPARED FOR
 MCGINLEY & ASSOCIATES

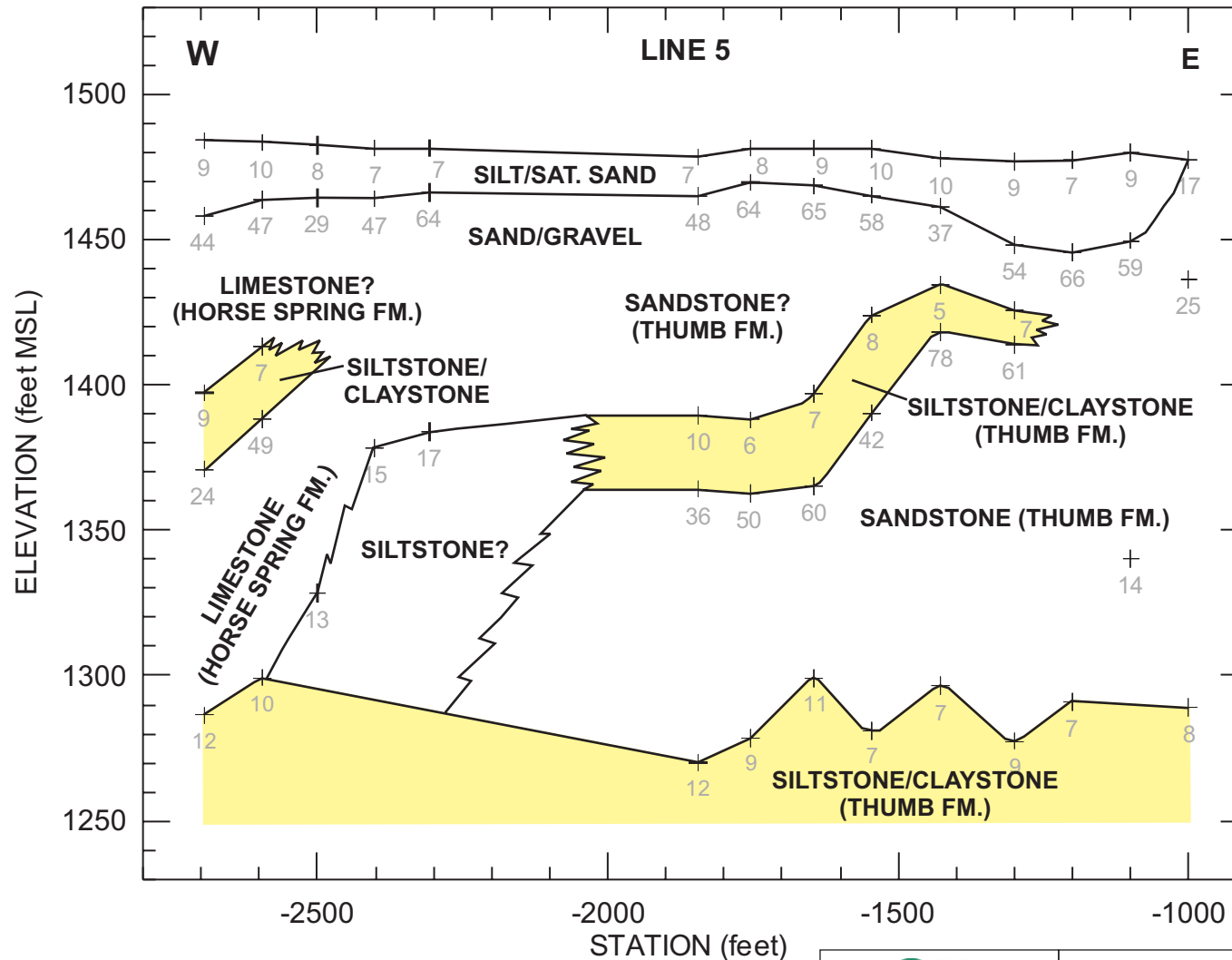


Project # 3209
 Date: May 30, 2003
 Drawn By: A MARTIN
 Approved By:
 File C:\Gvprojects\3209mga\12.cdr

FIGURE 12
 LINE 4 - GEOELECTRIC SECTION FOR SMOOTH
 MODEL INVERSION AND GEONICS EM-34 PROFILE

LAS VEGAS WASH
 CLARK COUNTY, NEVADA

PREPARED FOR
 MCGINLEY & ASSOCIATES

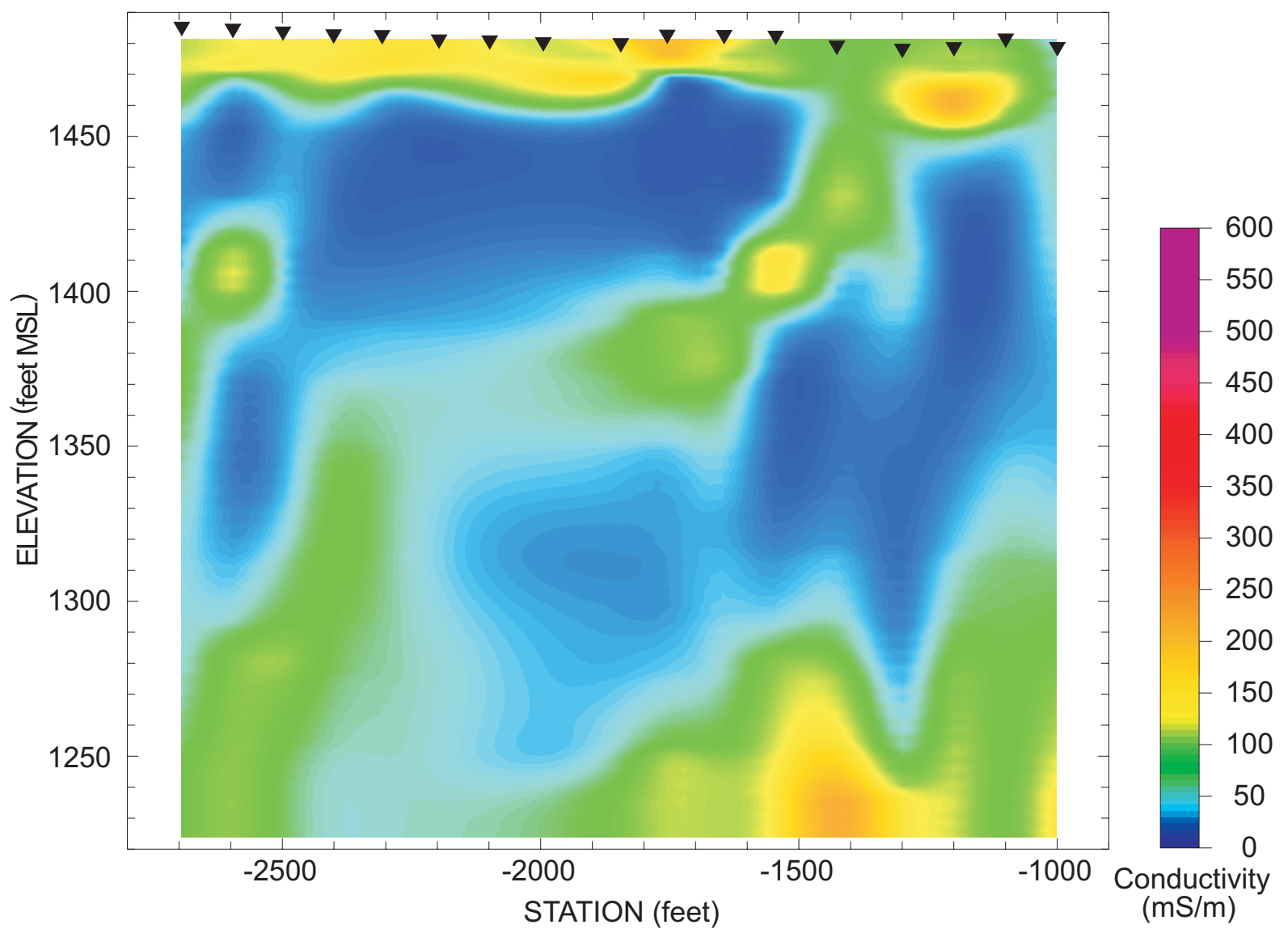
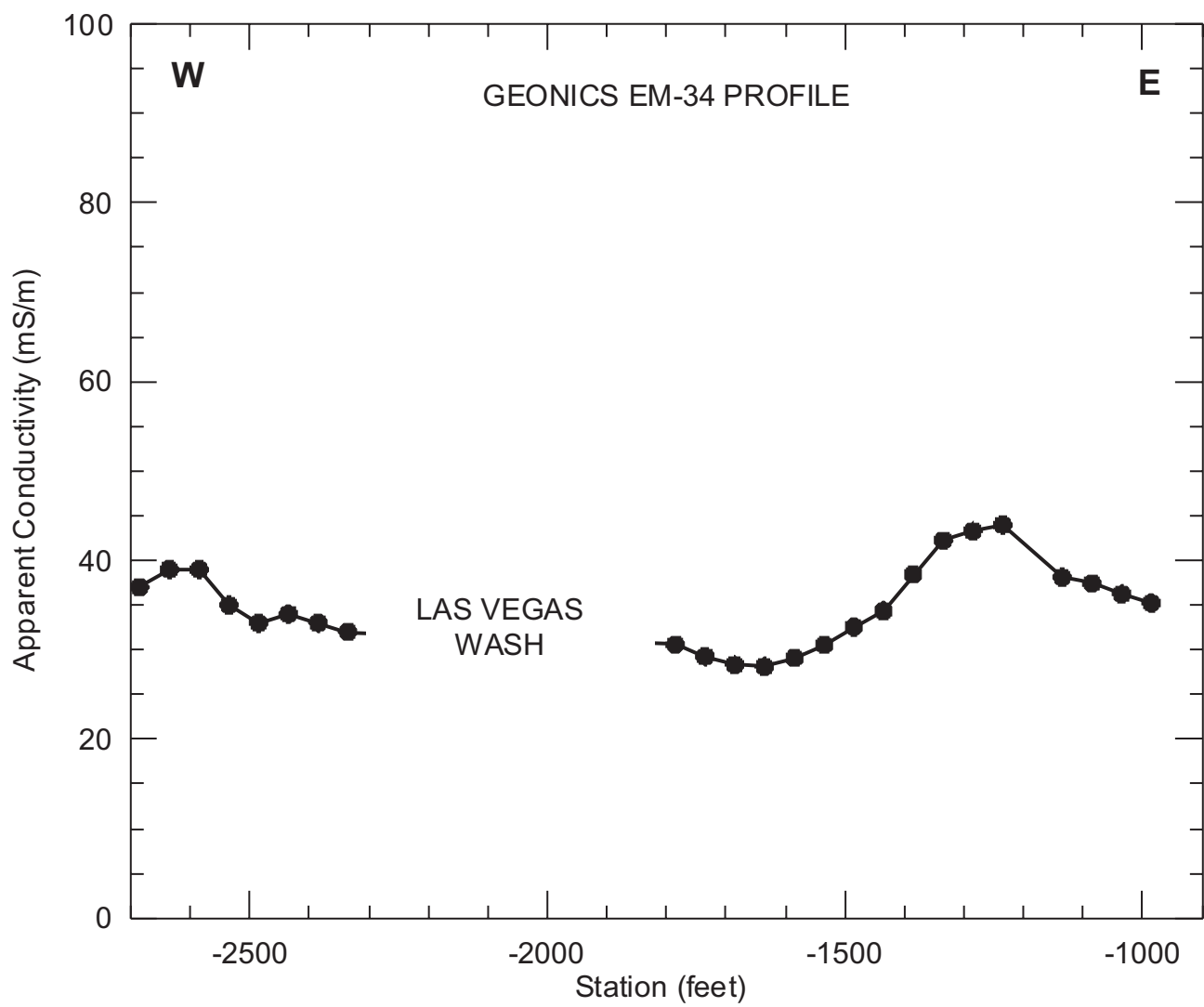


2

LEGEND
 LAYER BOUNDARY AND RESISTIVITY OF UNDERLYING LAYER IN OHM-METERS

Project #	3209
Date:	May 30, 2003
Drawn By:	A. MARTIN
Approved By:	
File C:\Gvprojects\3209mgaf13.cdr	

<p>FIGURE 13 LINE 5 - GEOELECTRIC SECTION FOR 1D LAYERED MODEL INVERSION</p>
<p>LAS VEGAS WASH CLARK COUNTY, NEVADA</p>
<p>PREPARED FOR MCGINLEY & ASSOCIATES</p>



GEOVision
 geophysical services
 a division of Blackhawk GeoServices

Project # 3209
 Date: May 30, 2003
 Drawn By: A MARTIN
 Approved By:
 File C:\Gvprojects\3209mgalf14.cdr

FIGURE 14
 LINE 5 - GEOELECTRIC SECTION FOR SMOOTH
 MODEL INVERSION AND GEONICS EM-34 PROFILE

LAS VEGAS WASH
 CLARK COUNTY, NEVADA

PREPARED FOR
 MCGINLEY & ASSOCIATES

APPENDIX B

Modifications and New Source Code for MT3D

Two of the existing source files were modified (note: all modifications are labeled with a c gp start and c gp end within the code):

- mt3dms4.for
- mt_ssm4.for

Three new source files were created:

- ade.for
- erfc.for
- river_flow.for

MT3DMS4.FOR - Main Program

Lines 76 – 83:

```
c gp start
c added additional variables for river calculations
  real          :: wash_flow(0:1000), wash_up_conc
  real          :: conc_river_outlet, conc_aq_output
  real          :: dec_par(3,5)
  character(len=18) :: dum
  integer       :: imont, igp, jgp
c gp end
```

Lines 117 -136:

```
c gp start
c open required files
  open(210, file='monte.dat', status='old')
  read(210, *) imont
  close(210)
  write(dum, 888) imont
888  format('output\outlet.', i4.4)
  open(211, file=dum, status='unknown')
  open(212, file='wash.in', status='old')
c read ade input data
c paleochannel section first
  do jgp=1,3
    do igp=1,5
      read(212, *) dec_par(jgp, igp)
    enddo
  enddo
  read(212, *) wash_flow(0)
  read(212, *) wash_up_conc
  close(212)
c gp end
```

Lines 406 – 410:

```
c gp start
c calculating river flows at each river cell
  call river_flow(x(lcss), x(lcdelr), x(lcdelc), x(lcdh), ncol, nrow,
```

```
1 nlay,ntss,mxss,wash_flow)
c gp end
```

Lines 516 – 525:

```
c gp start
  IF (TRNOP(3) .AND. ICOMP.LE.MCOMP)
  & CALL SSM4FM(NCOL,NROW,NLAY,NCOMP,ICOMP,IX(LCIB),
  & X(LCDELRL),X(LCDELCL),X(LCDHL),IX(LCIRCH),X(LCRECH),X(LCCRCH),
  & IX(LCIEVT),X(LCEVTR),X(LCCEVT),MXSS,NTSS,X(LCSS),X(LCSSMC),
  & X(LCQSTO),X(LCCNEW),ISS,X(LCA),X(LCRHS),NODES,UPDLHS,MIXELM,
  & wash_flow,wash_up_conc,
  & conc_river_outlet,conc_aq_output,
  & dec_par,time2)
c gp end
```

Lines 596 – 600:

```
c gp start
c save concentrations at outlet to unit 211
  write(211,3011) time2,conc_river_outlet,conc_aq_output
3011 format(f8.2,1x,4(e15.7,1x))
c gp end
```

MT_SSM4.FOR - SUBROUTINE SSM4FM

(note: line number refer to file line numbers not individual subroutine line numbers)

Lines 600 – 607:

```
c gp start
c initial new variables for river concentration calculations
  real :: wash_flow(0:1000),wash_up_conc,wash_conc(0:1000)
  real :: conc_river_outlet,conc_aq_output,qsss
  real :: dec_par(3,5)
  real :: time2,c1,c2,c3
  integer :: icnt
c gp end
```

Lines 663 – 739:

```
c gp start
c calculate concentrations on flux boundaries based on ade solution
c note that c1 is paleochannel conc and c2 is pond conc
c calculate river concentrations
  20 continue
c reach 2
  call ade(dec_par(1,1),dec_par(1,2),dec_par(1,3),dec_par(1,4),
  1 dec_par(1,5),time2,c1)
c reach 3
  call ade(dec_par(2,1),dec_par(2,2),dec_par(2,3),dec_par(2,4),
  1 dec_par(2,5),time2,c2)
c reach 4
```

```

    call ade(dec_par(3,1),dec_par(3,2),dec_par(3,3),dec_par(3,4),
1      dec_par(3,5),time2,c3)
    icnt=0
    wash_conc(0)=wash_up_conc
    DO NUM=1,NTSS
      K=SS(1,NUM)
      I=SS(2,NUM)
      J=SS(3,NUM)
      QSS=SS(5,NUM)
      qsss=ss(5,num)*DELR(J)*DELC(I)*DH(J,I,K)
      IQ=SS(6,NUM)
      if(IQ==4) then
        icnt=icnt+1
c calculate wash concentration for river cells only
c flow from aquifer to river (use mixing equation)
c note that ctmp is not used in this case
        if(QSS<0.0) then
          if(j==69.and.i==74) then
            wash_conc(icnt)=(wash_flow(icnt-1)*wash_conc(icnt-1)+
1              abs(qsss)*cnew(j,i,k,1)+138240.*20.)/
2              wash_flow(icnt)
          else
            wash_conc(icnt)=(wash_flow(icnt-1)*wash_conc(icnt-1)+
1              abs(QSSS)*cnew(j,i,k,1))/
2              wash_flow(icnt)
          endif
        else
c flow from river to aquifer (use upstream concentration)
          wash_conc(icnt)=wash_conc(icnt-1)
          ctmp=wash_conc(icnt)
        endif
c save downstream river and aquifer concentrations for printing in main
          conc_river_outlet=wash_conc(icnt)
          conc_aq_output=cnew(j,i,k,1)
        else
c concentration for flux boundaries
          if(ss(4,num)>49000..and.ss(4,num)<51000.) then
c paleochannels
            ctmp=c1
          elseif(ss(4,num)>999..and.ss(4,num)<1001.) then
c pond section
            ctmp=c2
          elseif(ss(4,num)>49..and.ss(4,num)<51.) then
c central section
            ctmp=c3
          else
c western boundary -- constant 10 micrograms per liter
            ctmp=ss(4,num)
          endif
        endif
      endif
    IF(NCOMP.GT.1) CTMP=SSMC(ICOMP,NUM)

    IF(IQ.EQ.15) QSS=1./(DELR(J)*DELC(I)*DH(J,I,K))
    IF(ICBUND(J,I,K,ICOMP).GT.0.AND.IQ.GT.0) THEN
      N=(K-1)*NCOL*NROW+(I-1)*NCOL+J
    IF(QSS.LT.0) THEN

```

```

        IF (UPDLHS) A(N)=A(N)+QSS*DELR(J)*DELC(I)*DH(J,I,K)
    ELSE
        RHS(N)=RHS(N)-QSS*CTMP*DELR(J)*DELC(I)*DH(J,I,K)
    ENDIF
ENDIF
ENDDO
c gp end

```

ADE.FOR

```

subroutine ade(L,v,d1,c1,c0,t,c)
    real    :: L
    t1=(L-v*t)/sqrt(4.0*d1*t)
    c=0.5*erfc(t1)*(c1-c0)+c0
return
end subroutine ade

```

ERFC.FOR – Taken from Numerical Recipes

```

FUNCTION erfc(x)
REAL erfc,x
CU  USES gammp,gammq
REAL gammp,gammq
if(x.lt.0.)then
    erfc=1.+gammp(.5,x**2)
else
    erfc=gammq(.5,x**2)
endif
return
END

FUNCTION gammp(a,x)
REAL a,gammp,x
CU  USES gcf,gser
REAL gammcf,gamser,gln
if(x.lt.0..or.a.le.0.)pause 'bad arguments in gammp'
if(x.lt.a+1.)then
    call gser(gamser,a,x,gln)
    gammp=gamser
else
    call gcf(gammcf,a,x,gln)
    gammp=1.-gammcf
endif
return
END

FUNCTION gammq(a,x)
REAL a,gammq,x
CU  USES gcf,gser
REAL gammcf,gamser,gln
if(x.lt.0..or.a.le.0.)pause 'bad arguments in gammq'
if(x.lt.a+1.)then
    call gser(gamser,a,x,gln)
    gammq=1.-gamser
else

```

```

        call gcf(gammcf,a,x,gln)
        gammq=gammcf
    endif
    return
END
SUBROUTINE gcf(gammcf,a,x,gln)
    INTEGER ITMAX
    REAL a,gammcf,gln,x,EPS,FPMIN
    PARAMETER (ITMAX=100,EPS=3.e-7,FPMIN=1.e-30)
CU    USES gammln
    INTEGER i
    REAL an,b,c,d,del,h,gammln
    gln=gammln(a)
    b=x+1.-a
    c=1./FPMIN
    d=1./b
    h=d
    do 11 i=1,ITMAX
        an=-i*(i-a)
        b=b+2.
        d=an*d+b
        if(abs(d).lt.FPMIN)d=FPMIN
        c=b+an/c
        if(abs(c).lt.FPMIN)c=FPMIN
        d=1./d
        del=d*c
        h=h*del
        if(abs(del-1.).lt.EPS)goto 1
11    continue
    pause 'a too large, ITMAX too small in gcf'
1    gammcf=exp(-x+a*log(x)-gln)*h
    return
END
SUBROUTINE gser(gamser,a,x,gln)
    INTEGER ITMAX
    REAL a,gamser,gln,x,EPS
    PARAMETER (ITMAX=100,EPS=3.e-7)
CU    USES gammln
    INTEGER n
    REAL ap,del,sum,gammln
    gln=gammln(a)
    if(x.le.0.)then
        if(x.lt.0.)pause 'x < 0 in gser'
        gamser=0.
        return
    endif
    ap=a
    sum=1./a
    del=sum
    do 11 n=1,ITMAX
        ap=ap+1.
        del=del*x/ap
        sum=sum+del
        if(abs(del).lt.abs(sum)*EPS)goto 1
11    continue
    pause 'a too large, ITMAX too small in gser'
1    gamser=sum*exp(-x+a*log(x)-gln)

```

```

return
END
FUNCTION gammln(xx)
REAL gammln,xx
INTEGER j
DOUBLE PRECISION ser,stp,tmp,x,y,cof(6)
SAVE cof,stp
DATA cof,stp/76.18009172947146d0,-86.50532032941677d0,
*24.01409824083091d0,-1.231739572450155d0,.1208650973866179d-2,
*-.5395239384953d-5,2.5066282746310005d0/
x=xx
y=x
tmp=x+5.5d0
tmp=(x+0.5d0)*log(tmp)-tmp
ser=1.000000000190015d0
do 11 j=1,6
  y=y+1.d0
  ser=ser+cof(j)/y
11 continue
gammln=tmp+log(stp*ser/x)
return
END

```

RIVER_FLOW.FOR

```

subroutine river_flow(ss,delr,delc,dh,ncol,nrow,nlay,
1 ntss,mxss,wash_flow)
c subroutine to read in wash flow directions and
c to calculate wash flows in all river cells
c notes: 1. positive ss(5,i) represents flow from river to aquifer (i.e.
lossing reach)
c 2. negative ss(5,i) represents flow from aquifer to river (i.e.
gaining reach)
c 3. ss(1,i) = river layer number (z)
c 4. ss(2,i) = river row number (y)
c 5. ss(3,i) = river column number (x)
c 6. ss(4,i) = river concentration, note that this will be updated
within SSM4FM subroutine
c 7. ss(5,i) = volumetric flow rate from river to aquifer
c 8. ss(6,i) = integer flag noting source/sink type, river cells must
be = "4"
c 9. wash_flow = array of wash volumetric flows (cubic feet per day)
c 10. wash_up_conc = upstream wash concentration (micrograms per
liter)
c 11. iwash = number of river cells in modflow model
c 12. current version allows for a maximum of 1000 river cells
c 13. wash_index: 1=reach #, 2=row#(y),3=col#,4=layer#
c
c written by: greg pohll - desert research institute
c
c date: July 9, 2003
c
c initialize variables
real :: ss(6,mxss)
real :: delr(ncol)

```

```

real      :: delc(nrow)
real      :: dh(ncol,nrow,nlay)
real      :: wash_flow(0:1000)
integer   :: wash_index(3,1000)
icnt=0
do num=1,ntss
  K=SS(1,NUM)
  I=SS(2,NUM)
  J=SS(3,NUM)
  if(ss(6,num)==4) then
    icnt=icnt+1
    VOLAQU=DELR(J)*DELC(I)*DH(J,I,K)
    if(j==69.and.i==74) then
      wash_flow(icnt)=wash_flow(icnt-1)-ss(5,num)*volaqu+138240.
    else
      wash_flow(icnt)=wash_flow(icnt-1)-ss(5,num)*volaqu
    endif
  endif
enddo
10 continue
return
end

```

APPENDIX C

Model Results: Time-Series Data

Appendix C. Model Results

Time		Pore Vol	Wash (ug/L)			Aquifer (ug/L)			Wash Mass Flux (lbs/day)		
(d)	(yr)	(-)	Low 95%	Median	High 95%	Low 95%	Median	High 95%	Low 95%	Median	High 95%
1.00E-01	2.74E-04	3.38E-04	6.13E+02	6.54E+02	6.95E+02	3.00E+03	3.00E+03	3.00E+03	7.93E+02	8.46E+02	8.98E+02
2.00E-01	5.48E-04	6.77E-04	6.12E+02	6.58E+02	7.00E+02	3.00E+03	3.00E+03	3.00E+03	7.91E+02	8.50E+02	9.06E+02
3.20E-01	8.76E-04	1.08E-03	6.01E+02	6.51E+02	6.96E+02	3.00E+03	3.00E+03	3.00E+03	7.77E+02	8.42E+02	9.00E+02
4.30E-01	1.18E-03	1.45E-03	5.90E+02	6.44E+02	6.90E+02	3.00E+03	3.00E+03	3.00E+03	7.63E+02	8.32E+02	8.93E+02
5.50E-01	1.51E-03	1.86E-03	5.80E+02	6.37E+02	6.84E+02	3.00E+03	3.00E+03	3.00E+03	7.50E+02	8.23E+02	8.85E+02
6.80E-01	1.86E-03	2.30E-03	5.71E+02	6.30E+02	6.79E+02	3.00E+03	3.00E+03	3.00E+03	7.38E+02	8.15E+02	8.78E+02
8.10E-01	2.22E-03	2.74E-03	5.62E+02	6.24E+02	6.74E+02	3.00E+03	3.00E+03	3.00E+03	7.27E+02	8.06E+02	8.71E+02
9.50E-01	2.60E-03	3.21E-03	5.54E+02	6.18E+02	6.69E+02	3.00E+03	3.00E+03	3.00E+03	7.17E+02	7.99E+02	8.65E+02
1.10E+00	3.01E-03	3.72E-03	5.47E+02	6.12E+02	6.64E+02	3.00E+03	3.00E+03	3.00E+03	7.08E+02	7.91E+02	8.58E+02
1.26E+00	3.45E-03	4.26E-03	5.40E+02	6.07E+02	6.59E+02	3.00E+03	3.00E+03	3.00E+03	6.99E+02	7.84E+02	8.52E+02
1.42E+00	3.89E-03	4.80E-03	5.34E+02	6.01E+02	6.54E+02	3.00E+03	3.00E+03	3.00E+03	6.90E+02	7.78E+02	8.46E+02
1.59E+00	4.35E-03	5.38E-03	5.28E+02	5.96E+02	6.50E+02	3.00E+03	3.00E+03	3.00E+03	6.83E+02	7.71E+02	8.41E+02
1.77E+00	4.85E-03	5.99E-03	5.22E+02	5.91E+02	6.46E+02	3.00E+03	3.00E+03	3.00E+03	6.75E+02	7.65E+02	8.35E+02
1.96E+00	5.37E-03	6.63E-03	5.16E+02	5.87E+02	6.42E+02	3.00E+03	3.00E+03	3.00E+03	6.68E+02	7.59E+02	8.30E+02
2.16E+00	5.91E-03	7.31E-03	5.11E+02	5.82E+02	6.38E+02	3.00E+03	3.00E+03	3.00E+03	6.61E+02	7.53E+02	8.24E+02
2.37E+00	6.49E-03	8.02E-03	5.06E+02	5.78E+02	6.34E+02	2.99E+03	3.00E+03	3.00E+03	6.54E+02	7.47E+02	8.19E+02
2.58E+00	7.06E-03	8.73E-03	5.01E+02	5.73E+02	6.30E+02	2.99E+03	3.00E+03	3.00E+03	6.47E+02	7.41E+02	8.14E+02
2.81E+00	7.69E-03	9.50E-03	4.96E+02	5.69E+02	6.26E+02	2.99E+03	2.99E+03	3.00E+03	6.41E+02	7.36E+02	8.09E+02
3.05E+00	8.35E-03	1.03E-02	4.91E+02	5.65E+02	6.22E+02	2.99E+03	2.99E+03	2.99E+03	6.34E+02	7.30E+02	8.04E+02
3.31E+00	9.06E-03	1.12E-02	4.86E+02	5.60E+02	6.18E+02	2.98E+03	2.99E+03	2.99E+03	6.28E+02	7.25E+02	7.99E+02
3.57E+00	9.77E-03	1.21E-02	4.81E+02	5.56E+02	6.14E+02	2.98E+03	2.99E+03	2.99E+03	6.22E+02	7.19E+02	7.94E+02
3.85E+00	1.05E-02	1.30E-02	4.76E+02	5.52E+02	6.10E+02	2.97E+03	2.99E+03	2.99E+03	6.16E+02	7.14E+02	7.89E+02
4.14E+00	1.13E-02	1.40E-02	4.72E+02	5.48E+02	6.07E+02	2.96E+03	2.99E+03	2.99E+03	6.10E+02	7.08E+02	7.85E+02
4.45E+00	1.22E-02	1.51E-02	4.67E+02	5.44E+02	6.03E+02	2.95E+03	2.98E+03	2.99E+03	6.04E+02	7.03E+02	7.80E+02
4.77E+00	1.31E-02	1.61E-02	4.62E+02	5.40E+02	5.99E+02	2.95E+03	2.98E+03	2.98E+03	5.98E+02	6.98E+02	7.75E+02
5.11E+00	1.40E-02	1.73E-02	4.58E+02	5.36E+02	5.95E+02	2.93E+03	2.98E+03	2.98E+03	5.92E+02	6.93E+02	7.70E+02
5.47E+00	1.50E-02	1.85E-02	4.53E+02	5.31E+02	5.92E+02	2.92E+03	2.97E+03	2.98E+03	5.86E+02	6.87E+02	7.65E+02
5.84E+00	1.60E-02	1.98E-02	4.48E+02	5.27E+02	5.88E+02	2.91E+03	2.97E+03	2.98E+03	5.80E+02	6.82E+02	7.60E+02
6.23E+00	1.71E-02	2.11E-02	4.44E+02	5.23E+02	5.84E+02	2.89E+03	2.96E+03	2.97E+03	5.74E+02	6.77E+02	7.55E+02
6.64E+00	1.82E-02	2.25E-02	4.39E+02	5.19E+02	5.80E+02	2.88E+03	2.95E+03	2.97E+03	5.68E+02	6.71E+02	7.50E+02
7.08E+00	1.94E-02	2.39E-02	4.35E+02	5.15E+02	5.76E+02	2.86E+03	2.95E+03	2.96E+03	5.62E+02	6.66E+02	7.45E+02
7.53E+00	2.06E-02	2.55E-02	4.30E+02	5.11E+02	5.72E+02	2.84E+03	2.94E+03	2.96E+03	5.56E+02	6.60E+02	7.40E+02
8.01E+00	2.19E-02	2.71E-02	4.25E+02	5.07E+02	5.68E+02	2.82E+03	2.93E+03	2.95E+03	5.50E+02	6.55E+02	7.35E+02
8.51E+00	2.33E-02	2.88E-02	4.21E+02	5.02E+02	5.65E+02	2.79E+03	2.92E+03	2.94E+03	5.44E+02	6.50E+02	7.30E+02
9.03E+00	2.47E-02	3.05E-02	4.16E+02	4.98E+02	5.60E+02	2.77E+03	2.90E+03	2.94E+03	5.38E+02	6.44E+02	7.25E+02
9.58E+00	2.62E-02	3.24E-02	4.12E+02	4.94E+02	5.56E+02	2.74E+03	2.89E+03	2.93E+03	5.32E+02	6.38E+02	7.20E+02
1.02E+01	2.78E-02	3.44E-02	4.07E+02	4.89E+02	5.52E+02	2.71E+03	2.88E+03	2.92E+03	5.26E+02	6.33E+02	7.14E+02
1.08E+01	2.95E-02	3.64E-02	4.03E+02	4.85E+02	5.48E+02	2.68E+03	2.86E+03	2.91E+03	5.21E+02	6.27E+02	7.09E+02
1.14E+01	3.12E-02	3.86E-02	3.98E+02	4.81E+02	5.44E+02	2.65E+03	2.85E+03	2.90E+03	5.15E+02	6.22E+02	7.03E+02

Appendix C. Model Results

Time		Pore Vol	Wash (ug/L)			Aquifer (ug/L)			Wash Mass Flux (lbs/day)		
(d)	(yr)	(-)	Low 95%	Median	High 95%	Low 95%	Median	High 95%	Low 95%	Median	High 95%
1.21E+01	3.31E-02	4.09E-02	3.94E+02	4.76E+02	5.40E+02	2.62E+03	2.83E+03	2.89E+03	5.09E+02	6.16E+02	6.98E+02
1.28E+01	3.50E-02	4.32E-02	3.89E+02	4.72E+02	5.35E+02	2.58E+03	2.81E+03	2.87E+03	5.03E+02	6.10E+02	6.92E+02
1.35E+01	3.70E-02	4.57E-02	3.85E+02	4.67E+02	5.31E+02	2.55E+03	2.79E+03	2.86E+03	4.98E+02	6.04E+02	6.87E+02
1.43E+01	3.92E-02	4.84E-02	3.80E+02	4.63E+02	5.27E+02	2.51E+03	2.77E+03	2.85E+03	4.92E+02	5.99E+02	6.81E+02
1.51E+01	4.14E-02	5.11E-02	3.76E+02	4.58E+02	5.22E+02	2.47E+03	2.75E+03	2.83E+03	4.86E+02	5.93E+02	6.75E+02
1.60E+01	4.37E-02	5.40E-02	3.72E+02	4.54E+02	5.18E+02	2.43E+03	2.72E+03	2.82E+03	4.81E+02	5.87E+02	6.70E+02
1.69E+01	4.62E-02	5.71E-02	3.68E+02	4.49E+02	5.13E+02	2.39E+03	2.70E+03	2.80E+03	4.76E+02	5.81E+02	6.64E+02
1.78E+01	4.88E-02	6.02E-02	3.64E+02	4.45E+02	5.09E+02	2.34E+03	2.67E+03	2.78E+03	4.70E+02	5.75E+02	6.58E+02
1.88E+01	5.15E-02	6.36E-02	3.60E+02	4.40E+02	5.04E+02	2.30E+03	2.65E+03	2.76E+03	4.65E+02	5.69E+02	6.52E+02
1.98E+01	5.43E-02	6.71E-02	3.56E+02	4.36E+02	5.00E+02	2.25E+03	2.62E+03	2.74E+03	4.61E+02	5.64E+02	6.46E+02
2.09E+01	5.73E-02	7.08E-02	3.53E+02	4.31E+02	4.95E+02	2.21E+03	2.59E+03	2.72E+03	4.56E+02	5.58E+02	6.40E+02
2.21E+01	6.05E-02	7.47E-02	3.50E+02	4.27E+02	4.91E+02	2.16E+03	2.56E+03	2.70E+03	4.52E+02	5.52E+02	6.34E+02
2.33E+01	6.38E-02	7.88E-02	3.47E+02	4.23E+02	4.86E+02	2.11E+03	2.52E+03	2.67E+03	4.48E+02	5.47E+02	6.28E+02
2.46E+01	6.72E-02	8.30E-02	3.43E+02	4.18E+02	4.81E+02	2.07E+03	2.49E+03	2.65E+03	4.44E+02	5.41E+02	6.22E+02
2.59E+01	7.09E-02	8.75E-02	3.40E+02	4.14E+02	4.77E+02	2.02E+03	2.46E+03	2.62E+03	4.40E+02	5.35E+02	6.16E+02
2.73E+01	7.47E-02	9.22E-02	3.37E+02	4.10E+02	4.72E+02	1.97E+03	2.42E+03	2.60E+03	4.36E+02	5.30E+02	6.10E+02
2.87E+01	7.87E-02	9.72E-02	3.35E+02	4.06E+02	4.67E+02	1.92E+03	2.39E+03	2.57E+03	4.33E+02	5.24E+02	6.04E+02
3.03E+01	8.29E-02	1.02E-01	3.32E+02	4.01E+02	4.63E+02	1.88E+03	2.35E+03	2.54E+03	4.30E+02	5.19E+02	5.98E+02
3.19E+01	8.73E-02	1.08E-01	3.30E+02	3.97E+02	4.58E+02	1.83E+03	2.31E+03	2.51E+03	4.27E+02	5.14E+02	5.92E+02
3.36E+01	9.19E-02	1.14E-01	3.28E+02	3.93E+02	4.53E+02	1.79E+03	2.27E+03	2.48E+03	4.25E+02	5.09E+02	5.86E+02
3.54E+01	9.68E-02	1.20E-01	3.26E+02	3.90E+02	4.49E+02	1.74E+03	2.23E+03	2.45E+03	4.22E+02	5.04E+02	5.81E+02
3.72E+01	1.02E-01	1.26E-01	3.25E+02	3.86E+02	4.45E+02	1.70E+03	2.19E+03	2.42E+03	4.20E+02	4.99E+02	5.75E+02
3.92E+01	1.07E-01	1.33E-01	3.23E+02	3.83E+02	4.40E+02	1.66E+03	2.15E+03	2.39E+03	4.18E+02	4.95E+02	5.69E+02
4.13E+01	1.13E-01	1.40E-01	3.22E+02	3.79E+02	4.36E+02	1.62E+03	2.12E+03	2.35E+03	4.17E+02	4.91E+02	5.64E+02
4.34E+01	1.19E-01	1.47E-01	3.22E+02	3.76E+02	4.32E+02	1.58E+03	2.08E+03	2.32E+03	4.16E+02	4.86E+02	5.58E+02
4.57E+01	1.25E-01	1.55E-01	3.21E+02	3.73E+02	4.28E+02	1.54E+03	2.04E+03	2.29E+03	4.15E+02	4.82E+02	5.53E+02
4.81E+01	1.32E-01	1.63E-01	3.21E+02	3.70E+02	4.24E+02	1.50E+03	2.00E+03	2.25E+03	4.16E+02	4.79E+02	5.48E+02
5.06E+01	1.38E-01	1.71E-01	3.21E+02	3.68E+02	4.20E+02	1.47E+03	1.96E+03	2.22E+03	4.15E+02	4.76E+02	5.43E+02
5.32E+01	1.46E-01	1.80E-01	3.21E+02	3.66E+02	4.16E+02	1.44E+03	1.92E+03	2.18E+03	4.15E+02	4.73E+02	5.38E+02
5.60E+01	1.53E-01	1.89E-01	3.21E+02	3.64E+02	4.13E+02	1.41E+03	1.88E+03	2.15E+03	4.16E+02	4.70E+02	5.34E+02
5.89E+01	1.61E-01	1.99E-01	3.22E+02	3.62E+02	4.10E+02	1.38E+03	1.84E+03	2.12E+03	4.17E+02	4.68E+02	5.30E+02
6.19E+01	1.69E-01	2.09E-01	3.23E+02	3.61E+02	4.06E+02	1.36E+03	1.81E+03	2.08E+03	4.17E+02	4.66E+02	5.26E+02
6.51E+01	1.78E-01	2.20E-01	3.23E+02	3.59E+02	4.03E+02	1.34E+03	1.77E+03	2.05E+03	4.18E+02	4.65E+02	5.22E+02
6.84E+01	1.87E-01	2.32E-01	3.24E+02	3.59E+02	4.01E+02	1.32E+03	1.74E+03	2.02E+03	4.20E+02	4.64E+02	5.18E+02
7.20E+01	1.97E-01	2.43E-01	3.25E+02	3.59E+02	3.98E+02	1.30E+03	1.71E+03	1.99E+03	4.21E+02	4.64E+02	5.15E+02
7.57E+01	2.07E-01	2.56E-01	3.27E+02	3.59E+02	3.96E+02	1.28E+03	1.68E+03	1.96E+03	4.22E+02	4.65E+02	5.13E+02
7.96E+01	2.18E-01	2.69E-01	3.27E+02	3.60E+02	3.95E+02	1.27E+03	1.65E+03	1.92E+03	4.23E+02	4.66E+02	5.10E+02
8.36E+01	2.29E-01	2.83E-01	3.29E+02	3.61E+02	3.93E+02	1.25E+03	1.62E+03	1.89E+03	4.25E+02	4.67E+02	5.08E+02
8.79E+01	2.41E-01	2.97E-01	3.29E+02	3.61E+02	3.91E+02	1.24E+03	1.59E+03	1.87E+03	4.26E+02	4.67E+02	5.06E+02

Appendix C. Model Results

Time		Pore Vol	Wash (ug/L)			Aquifer (ug/L)			Wash Mass Flux (lbs/day)		
(d)	(yr)	(-)	Low 95%	Median	High 95%	Low 95%	Median	High 95%	Low 95%	Median	High 95%
9.24E+01	2.53E-01	3.13E-01	3.30E+02	3.62E+02	3.90E+02	1.22E+03	1.56E+03	1.84E+03	4.27E+02	4.68E+02	5.04E+02
9.71E+01	2.66E-01	3.29E-01	3.31E+02	3.63E+02	3.89E+02	1.21E+03	1.54E+03	1.81E+03	4.28E+02	4.69E+02	5.03E+02
1.02E+02	2.80E-01	3.45E-01	3.32E+02	3.63E+02	3.88E+02	1.19E+03	1.51E+03	1.78E+03	4.29E+02	4.69E+02	5.02E+02
1.07E+02	2.94E-01	3.63E-01	3.32E+02	3.63E+02	3.88E+02	1.18E+03	1.49E+03	1.76E+03	4.29E+02	4.70E+02	5.02E+02
1.13E+02	3.09E-01	3.81E-01	3.31E+02	3.63E+02	3.87E+02	1.16E+03	1.47E+03	1.73E+03	4.28E+02	4.70E+02	5.01E+02
1.19E+02	3.24E-01	4.01E-01	3.30E+02	3.63E+02	3.87E+02	1.14E+03	1.44E+03	1.71E+03	4.27E+02	4.69E+02	5.00E+02
1.25E+02	3.41E-01	4.21E-01	3.29E+02	3.62E+02	3.86E+02	1.12E+03	1.42E+03	1.68E+03	4.25E+02	4.68E+02	4.99E+02
1.31E+02	3.58E-01	4.43E-01	3.26E+02	3.61E+02	3.85E+02	1.10E+03	1.39E+03	1.66E+03	4.22E+02	4.66E+02	4.98E+02
1.38E+02	3.76E-01	4.65E-01	3.23E+02	3.59E+02	3.84E+02	1.07E+03	1.37E+03	1.63E+03	4.18E+02	4.64E+02	4.97E+02
1.44E+02	3.95E-01	4.89E-01	3.19E+02	3.56E+02	3.83E+02	1.04E+03	1.34E+03	1.61E+03	4.12E+02	4.60E+02	4.95E+02
1.52E+02	4.16E-01	5.13E-01	3.13E+02	3.53E+02	3.81E+02	1.00E+03	1.31E+03	1.58E+03	4.05E+02	4.56E+02	4.92E+02
1.60E+02	4.37E-01	5.39E-01	3.05E+02	3.48E+02	3.78E+02	9.66E+02	1.28E+03	1.55E+03	3.95E+02	4.50E+02	4.89E+02
1.68E+02	4.59E-01	5.67E-01	2.97E+02	3.42E+02	3.75E+02	9.25E+02	1.25E+03	1.52E+03	3.84E+02	4.43E+02	4.84E+02
1.76E+02	4.82E-01	5.95E-01	2.87E+02	3.36E+02	3.70E+02	8.80E+02	1.21E+03	1.49E+03	3.71E+02	4.35E+02	4.79E+02
1.85E+02	5.06E-01	6.25E-01	2.75E+02	3.29E+02	3.64E+02	8.33E+02	1.17E+03	1.46E+03	3.56E+02	4.25E+02	4.71E+02
1.94E+02	5.32E-01	6.57E-01	2.63E+02	3.20E+02	3.58E+02	7.84E+02	1.13E+03	1.42E+03	3.40E+02	4.13E+02	4.63E+02
2.04E+02	5.59E-01	6.90E-01	2.49E+02	3.10E+02	3.50E+02	7.33E+02	1.09E+03	1.38E+03	3.23E+02	4.00E+02	4.53E+02
2.14E+02	5.87E-01	7.25E-01	2.34E+02	2.98E+02	3.41E+02	6.80E+02	1.04E+03	1.34E+03	3.03E+02	3.86E+02	4.41E+02
2.25E+02	6.17E-01	7.62E-01	2.17E+02	2.86E+02	3.31E+02	6.26E+02	9.87E+02	1.29E+03	2.81E+02	3.70E+02	4.27E+02
2.37E+02	6.48E-01	8.00E-01	2.01E+02	2.72E+02	3.20E+02	5.72E+02	9.35E+02	1.25E+03	2.60E+02	3.52E+02	4.13E+02
2.49E+02	6.80E-01	8.40E-01	1.84E+02	2.58E+02	3.07E+02	5.19E+02	8.80E+02	1.20E+03	2.38E+02	3.33E+02	3.97E+02
2.61E+02	7.15E-01	8.83E-01	1.68E+02	2.42E+02	2.93E+02	4.67E+02	8.24E+02	1.14E+03	2.17E+02	3.13E+02	3.79E+02
2.74E+02	7.50E-01	9.27E-01	1.50E+02	2.26E+02	2.79E+02	4.15E+02	7.67E+02	1.09E+03	1.95E+02	2.92E+02	3.60E+02
2.88E+02	7.89E-01	9.74E-01	1.34E+02	2.09E+02	2.63E+02	3.66E+02	7.09E+02	1.03E+03	1.73E+02	2.71E+02	3.41E+02
3.03E+02	8.28E-01	1.02E+00	1.19E+02	1.92E+02	2.47E+02	3.20E+02	6.52E+02	9.69E+02	1.53E+02	2.49E+02	3.20E+02
3.18E+02	8.70E-01	1.07E+00	1.04E+02	1.75E+02	2.31E+02	2.77E+02	5.94E+02	9.08E+02	1.35E+02	2.27E+02	2.98E+02
3.34E+02	9.14E-01	1.13E+00	9.12E+01	1.59E+02	2.14E+02	2.39E+02	5.39E+02	8.47E+02	1.18E+02	2.06E+02	2.77E+02
3.51E+02	9.60E-01	1.19E+00	7.92E+01	1.43E+02	1.98E+02	2.04E+02	4.85E+02	7.85E+02	1.02E+02	1.85E+02	2.55E+02
3.68E+02	1.01E+00	1.25E+00	6.83E+01	1.28E+02	1.81E+02	1.72E+02	4.35E+02	7.24E+02	8.83E+01	1.66E+02	2.34E+02
3.87E+02	1.06E+00	1.31E+00	5.86E+01	1.14E+02	1.65E+02	1.44E+02	3.88E+02	6.64E+02	7.58E+01	1.48E+02	2.14E+02
4.06E+02	1.11E+00	1.37E+00	5.01E+01	1.01E+02	1.50E+02	1.20E+02	3.43E+02	6.06E+02	6.48E+01	1.31E+02	1.94E+02
4.26E+02	1.17E+00	1.44E+00	4.27E+01	8.87E+01	1.35E+02	9.96E+01	3.02E+02	5.50E+02	5.52E+01	1.15E+02	1.75E+02
4.48E+02	1.23E+00	1.51E+00	3.66E+01	7.76E+01	1.21E+02	8.20E+01	2.64E+02	4.96E+02	4.73E+01	1.00E+02	1.57E+02
4.70E+02	1.29E+00	1.59E+00	3.14E+01	6.77E+01	1.08E+02	6.71E+01	2.30E+02	4.46E+02	4.06E+01	8.76E+01	1.40E+02
4.94E+02	1.35E+00	1.67E+00	2.70E+01	5.90E+01	9.65E+01	5.48E+01	1.99E+02	3.98E+02	3.49E+01	7.63E+01	1.25E+02
5.19E+02	1.42E+00	1.75E+00	2.35E+01	5.13E+01	8.57E+01	4.43E+01	1.72E+02	3.53E+02	3.04E+01	6.64E+01	1.11E+02
5.45E+02	1.49E+00	1.84E+00	2.05E+01	4.48E+01	7.58E+01	3.63E+01	1.48E+02	3.12E+02	2.66E+01	5.79E+01	9.80E+01
5.72E+02	1.57E+00	1.94E+00	1.82E+01	3.90E+01	6.70E+01	2.99E+01	1.26E+02	2.74E+02	2.36E+01	5.05E+01	8.66E+01
6.01E+02	1.64E+00	2.03E+00	1.64E+01	3.42E+01	5.91E+01	2.48E+01	1.08E+02	2.40E+02	2.12E+01	4.43E+01	7.64E+01

Appendix C. Model Results

Time		Pore Vol	Wash (ug/L)			Aquifer (ug/L)			Wash Mass Flux (lbs/day)		
(d)	(yr)	(-)	Low 95%	Median	High 95%	Low 95%	Median	High 95%	Low 95%	Median	High 95%
6.31E+02	1.73E+00	2.13E+00	1.49E+01	3.02E+01	5.22E+01	2.09E+01	9.16E+01	2.09E+02	1.93E+01	3.90E+01	6.75E+01
6.63E+02	1.81E+00	2.24E+00	1.38E+01	2.68E+01	4.61E+01	1.80E+01	7.77E+01	1.81E+02	1.78E+01	3.47E+01	5.97E+01
6.96E+02	1.90E+00	2.35E+00	1.29E+01	2.40E+01	4.09E+01	1.59E+01	6.59E+01	1.56E+02	1.66E+01	3.10E+01	5.29E+01
7.31E+02	2.00E+00	2.47E+00	1.22E+01	2.17E+01	3.63E+01	1.42E+01	5.60E+01	1.35E+02	1.58E+01	2.80E+01	4.69E+01
7.67E+02	2.10E+00	2.60E+00	1.16E+01	1.98E+01	3.24E+01	1.30E+01	4.79E+01	1.16E+02	1.51E+01	2.56E+01	4.18E+01
8.06E+02	2.21E+00	2.73E+00	1.12E+01	1.82E+01	2.90E+01	1.21E+01	4.11E+01	9.90E+01	1.45E+01	2.35E+01	3.75E+01
8.46E+02	2.32E+00	2.86E+00	1.09E+01	1.69E+01	2.62E+01	1.15E+01	3.58E+01	8.48E+01	1.41E+01	2.19E+01	3.39E+01
8.89E+02	2.43E+00	3.01E+00	1.07E+01	1.59E+01	2.39E+01	1.11E+01	3.14E+01	7.25E+01	1.38E+01	2.06E+01	3.08E+01
9.33E+02	2.55E+00	3.16E+00	1.05E+01	1.51E+01	2.19E+01	1.09E+01	2.78E+01	6.21E+01	1.36E+01	1.95E+01	2.83E+01
9.80E+02	2.68E+00	3.31E+00	1.04E+01	1.44E+01	2.02E+01	1.07E+01	2.51E+01	5.35E+01	1.35E+01	1.87E+01	2.61E+01
1.03E+03	2.82E+00	3.48E+00	1.03E+01	1.39E+01	1.88E+01	1.05E+01	2.30E+01	4.64E+01	1.33E+01	1.80E+01	2.43E+01
1.08E+03	2.95E+00	3.65E+00	1.03E+01	1.35E+01	1.76E+01	1.05E+01	2.14E+01	4.05E+01	1.33E+01	1.75E+01	2.27E+01
1.13E+03	3.09E+00	3.82E+00	1.02E+01	1.32E+01	1.68E+01	1.04E+01	2.03E+01	3.63E+01	1.32E+01	1.71E+01	2.17E+01
1.18E+03	3.23E+00	3.99E+00	1.02E+01	1.30E+01	1.60E+01	1.04E+01	1.95E+01	3.30E+01	1.32E+01	1.68E+01	2.07E+01
1.23E+03	3.36E+00	4.16E+00	1.02E+01	1.28E+01	1.57E+01	1.04E+01	1.89E+01	3.13E+01	1.32E+01	1.66E+01	2.02E+01
1.28E+03	3.50E+00	4.33E+00	1.02E+01	1.27E+01	1.55E+01	1.04E+01	1.85E+01	3.01E+01	1.31E+01	1.64E+01	2.00E+01
1.33E+03	3.64E+00	4.50E+00	1.02E+01	1.26E+01	1.54E+01	1.04E+01	1.81E+01	2.98E+01	1.31E+01	1.62E+01	1.99E+01
1.38E+03	3.78E+00	4.66E+00	1.02E+01	1.25E+01	1.53E+01	1.04E+01	1.79E+01	2.94E+01	1.31E+01	1.61E+01	1.97E+01
1.43E+03	3.91E+00	4.83E+00	1.01E+01	1.24E+01	1.52E+01	1.04E+01	1.77E+01	2.91E+01	1.31E+01	1.60E+01	1.97E+01
1.48E+03	4.05E+00	5.00E+00	1.01E+01	1.23E+01	1.50E+01	1.04E+01	1.75E+01	2.82E+01	1.31E+01	1.59E+01	1.94E+01
1.53E+03	4.19E+00	5.17E+00	1.01E+01	1.23E+01	1.48E+01	1.04E+01	1.74E+01	2.72E+01	1.31E+01	1.59E+01	1.91E+01
1.58E+03	4.32E+00	5.34E+00	1.01E+01	1.22E+01	1.46E+01	1.04E+01	1.72E+01	2.64E+01	1.31E+01	1.58E+01	1.89E+01
1.63E+03	4.46E+00	5.51E+00	1.01E+01	1.22E+01	1.46E+01	1.04E+01	1.71E+01	2.62E+01	1.31E+01	1.58E+01	1.88E+01
1.68E+03	4.60E+00	5.68E+00	1.01E+01	1.22E+01	1.45E+01	1.04E+01	1.70E+01	2.59E+01	1.31E+01	1.57E+01	1.87E+01
1.73E+03	4.73E+00	5.85E+00	1.01E+01	1.21E+01	1.44E+01	1.04E+01	1.68E+01	2.54E+01	1.31E+01	1.57E+01	1.86E+01
1.78E+03	4.87E+00	6.02E+00	1.01E+01	1.20E+01	1.41E+01	1.04E+01	1.65E+01	2.42E+01	1.31E+01	1.56E+01	1.82E+01
1.83E+03	5.01E+00	6.19E+00	1.01E+01	1.19E+01	1.39E+01	1.04E+01	1.62E+01	2.35E+01	1.31E+01	1.54E+01	1.80E+01
1.88E+03	5.14E+00	6.36E+00	1.01E+01	1.19E+01	1.39E+01	1.04E+01	1.60E+01	2.33E+01	1.31E+01	1.54E+01	1.79E+01
1.93E+03	5.28E+00	6.52E+00	1.01E+01	1.18E+01	1.38E+01	1.04E+01	1.59E+01	2.30E+01	1.31E+01	1.53E+01	1.78E+01
1.98E+03	5.42E+00	6.69E+00	1.01E+01	1.18E+01	1.37E+01	1.04E+01	1.57E+01	2.27E+01	1.31E+01	1.53E+01	1.77E+01
2.03E+03	5.56E+00	6.86E+00	1.01E+01	1.18E+01	1.36E+01	1.04E+01	1.56E+01	2.23E+01	1.31E+01	1.52E+01	1.76E+01
2.08E+03	5.69E+00	7.03E+00	1.01E+01	1.17E+01	1.36E+01	1.04E+01	1.54E+01	2.22E+01	1.31E+01	1.51E+01	1.76E+01
2.13E+03	5.83E+00	7.20E+00	1.01E+01	1.16E+01	1.34E+01	1.04E+01	1.52E+01	2.13E+01	1.31E+01	1.51E+01	1.73E+01
2.18E+03	5.97E+00	7.37E+00	1.01E+01	1.16E+01	1.33E+01	1.04E+01	1.50E+01	2.10E+01	1.31E+01	1.50E+01	1.72E+01
2.23E+03	6.10E+00	7.54E+00	1.01E+01	1.15E+01	1.32E+01	1.04E+01	1.48E+01	2.08E+01	1.31E+01	1.49E+01	1.71E+01
2.28E+03	6.24E+00	7.71E+00	1.01E+01	1.15E+01	1.31E+01	1.04E+01	1.46E+01	2.03E+01	1.31E+01	1.48E+01	1.70E+01
2.33E+03	6.38E+00	7.88E+00	1.01E+01	1.14E+01	1.30E+01	1.04E+01	1.45E+01	1.99E+01	1.31E+01	1.48E+01	1.69E+01
2.38E+03	6.51E+00	8.05E+00	1.01E+01	1.14E+01	1.30E+01	1.04E+01	1.43E+01	1.99E+01	1.31E+01	1.47E+01	1.68E+01
2.43E+03	6.65E+00	8.22E+00	1.01E+01	1.13E+01	1.29E+01	1.04E+01	1.42E+01	1.94E+01	1.31E+01	1.47E+01	1.66E+01

Appendix C. Model Results

Time		Pore Vol	Wash (ug/L)			Aquifer (ug/L)			Wash Mass Flux (lbs/day)		
(d)	(yr)	(-)	Low 95%	Median	High 95%	Low 95%	Median	High 95%	Low 95%	Median	High 95%
2.48E+03	6.79E+00	8.39E+00	1.01E+01	1.13E+01	1.28E+01	1.04E+01	1.40E+01	1.90E+01	1.31E+01	1.46E+01	1.66E+01
2.53E+03	6.92E+00	8.55E+00	1.01E+01	1.13E+01	1.27E+01	1.04E+01	1.39E+01	1.89E+01	1.31E+01	1.45E+01	1.65E+01
2.58E+03	7.06E+00	8.72E+00	1.01E+01	1.12E+01	1.26E+01	1.04E+01	1.38E+01	1.85E+01	1.31E+01	1.45E+01	1.63E+01
2.63E+03	7.20E+00	8.89E+00	1.01E+01	1.12E+01	1.26E+01	1.04E+01	1.36E+01	1.81E+01	1.31E+01	1.44E+01	1.62E+01
2.68E+03	7.33E+00	9.06E+00	1.01E+01	1.11E+01	1.25E+01	1.04E+01	1.35E+01	1.77E+01	1.31E+01	1.44E+01	1.61E+01
2.73E+03	7.47E+00	9.23E+00	1.01E+01	1.11E+01	1.25E+01	1.04E+01	1.34E+01	1.76E+01	1.31E+01	1.43E+01	1.61E+01
2.78E+03	7.61E+00	9.40E+00	1.01E+01	1.11E+01	1.24E+01	1.04E+01	1.33E+01	1.76E+01	1.31E+01	1.43E+01	1.60E+01
2.83E+03	7.75E+00	9.57E+00	1.01E+01	1.10E+01	1.24E+01	1.04E+01	1.32E+01	1.72E+01	1.31E+01	1.43E+01	1.60E+01
2.88E+03	7.88E+00	9.74E+00	1.01E+01	1.10E+01	1.23E+01	1.04E+01	1.31E+01	1.72E+01	1.31E+01	1.42E+01	1.59E+01
2.93E+03	8.02E+00	9.91E+00	1.01E+01	1.10E+01	1.22E+01	1.04E+01	1.30E+01	1.67E+01	1.31E+01	1.42E+01	1.58E+01
2.98E+03	8.16E+00	1.01E+01	1.01E+01	1.09E+01	1.21E+01	1.04E+01	1.29E+01	1.65E+01	1.31E+01	1.41E+01	1.57E+01
3.03E+03	8.29E+00	1.02E+01	1.01E+01	1.09E+01	1.21E+01	1.04E+01	1.28E+01	1.61E+01	1.31E+01	1.41E+01	1.56E+01
3.08E+03	8.43E+00	1.04E+01	1.01E+01	1.09E+01	1.20E+01	1.04E+01	1.27E+01	1.61E+01	1.31E+01	1.41E+01	1.55E+01
3.13E+03	8.57E+00	1.06E+01	1.01E+01	1.09E+01	1.20E+01	1.04E+01	1.26E+01	1.59E+01	1.31E+01	1.40E+01	1.55E+01
3.18E+03	8.70E+00	1.08E+01	1.01E+01	1.08E+01	1.19E+01	1.04E+01	1.25E+01	1.57E+01	1.31E+01	1.40E+01	1.54E+01
3.23E+03	8.84E+00	1.09E+01	1.01E+01	1.08E+01	1.19E+01	1.04E+01	1.24E+01	1.56E+01	1.31E+01	1.40E+01	1.54E+01
3.28E+03	8.98E+00	1.11E+01	1.01E+01	1.08E+01	1.19E+01	1.04E+01	1.23E+01	1.54E+01	1.31E+01	1.39E+01	1.54E+01
3.33E+03	9.11E+00	1.13E+01	1.01E+01	1.08E+01	1.17E+01	1.04E+01	1.23E+01	1.49E+01	1.31E+01	1.39E+01	1.52E+01
3.38E+03	9.25E+00	1.14E+01	1.01E+01	1.07E+01	1.17E+01	1.04E+01	1.22E+01	1.47E+01	1.31E+01	1.39E+01	1.51E+01
3.43E+03	9.39E+00	1.16E+01	1.01E+01	1.07E+01	1.16E+01	1.04E+01	1.21E+01	1.47E+01	1.31E+01	1.38E+01	1.50E+01
3.48E+03	9.52E+00	1.18E+01	1.01E+01	1.07E+01	1.16E+01	1.04E+01	1.21E+01	1.44E+01	1.31E+01	1.38E+01	1.50E+01
3.53E+03	9.66E+00	1.19E+01	1.01E+01	1.07E+01	1.15E+01	1.04E+01	1.20E+01	1.41E+01	1.31E+01	1.38E+01	1.49E+01
3.58E+03	9.80E+00	1.21E+01	1.01E+01	1.06E+01	1.14E+01	1.04E+01	1.19E+01	1.39E+01	1.31E+01	1.38E+01	1.48E+01
3.63E+03	9.94E+00	1.23E+01	1.01E+01	1.06E+01	1.14E+01	1.04E+01	1.19E+01	1.39E+01	1.31E+01	1.37E+01	1.47E+01
3.68E+03	1.01E+01	1.24E+01	1.01E+01	1.06E+01	1.14E+01	1.03E+01	1.18E+01	1.38E+01	1.31E+01	1.37E+01	1.47E+01
3.73E+03	1.02E+01	1.26E+01	1.01E+01	1.06E+01	1.14E+01	1.03E+01	1.18E+01	1.38E+01	1.31E+01	1.37E+01	1.47E+01
3.78E+03	1.03E+01	1.28E+01	1.01E+01	1.06E+01	1.13E+01	1.03E+01	1.17E+01	1.38E+01	1.31E+01	1.37E+01	1.47E+01
3.83E+03	1.05E+01	1.30E+01	1.01E+01	1.06E+01	1.13E+01	1.03E+01	1.16E+01	1.36E+01	1.31E+01	1.36E+01	1.46E+01
3.88E+03	1.06E+01	1.31E+01	1.01E+01	1.05E+01	1.12E+01	1.03E+01	1.16E+01	1.33E+01	1.31E+01	1.36E+01	1.44E+01
3.93E+03	1.08E+01	1.33E+01	1.01E+01	1.05E+01	1.12E+01	1.03E+01	1.15E+01	1.32E+01	1.31E+01	1.36E+01	1.44E+01
3.98E+03	1.09E+01	1.35E+01	1.01E+01	1.05E+01	1.11E+01	1.03E+01	1.15E+01	1.30E+01	1.31E+01	1.36E+01	1.43E+01
4.03E+03	1.10E+01	1.36E+01	1.01E+01	1.05E+01	1.10E+01	1.03E+01	1.14E+01	1.30E+01	1.31E+01	1.36E+01	1.43E+01
4.08E+03	1.12E+01	1.38E+01	1.01E+01	1.05E+01	1.10E+01	1.02E+01	1.14E+01	1.29E+01	1.30E+01	1.35E+01	1.43E+01
4.13E+03	1.13E+01	1.40E+01	1.01E+01	1.05E+01	1.10E+01	1.02E+01	1.13E+01	1.29E+01	1.30E+01	1.35E+01	1.43E+01
4.18E+03	1.14E+01	1.41E+01	1.01E+01	1.05E+01	1.10E+01	1.02E+01	1.13E+01	1.29E+01	1.30E+01	1.35E+01	1.42E+01
4.23E+03	1.16E+01	1.43E+01	1.01E+01	1.04E+01	1.10E+01	1.02E+01	1.13E+01	1.28E+01	1.30E+01	1.35E+01	1.42E+01
4.28E+03	1.17E+01	1.45E+01	1.01E+01	1.04E+01	1.09E+01	1.02E+01	1.12E+01	1.28E+01	1.30E+01	1.35E+01	1.41E+01
4.33E+03	1.19E+01	1.46E+01	1.01E+01	1.04E+01	1.09E+01	1.02E+01	1.12E+01	1.28E+01	1.30E+01	1.35E+01	1.41E+01
4.38E+03	1.20E+01	1.48E+01	1.01E+01	1.04E+01	1.09E+01	1.02E+01	1.11E+01	1.27E+01	1.30E+01	1.34E+01	1.41E+01

Appendix C. Model Results

Time		Pore Vol	Wash (ug/L)			Aquifer (ug/L)			Wash Mass Flux (lbs/day)		
(d)	(yr)	(-)	Low 95%	Median	High 95%	Low 95%	Median	High 95%	Low 95%	Median	High 95%
4.43E+03	1.21E+01	1.50E+01	1.01E+01	1.04E+01	1.09E+01	1.02E+01	1.11E+01	1.27E+01	1.30E+01	1.34E+01	1.41E+01
4.48E+03	1.23E+01	1.52E+01	1.01E+01	1.04E+01	1.09E+01	1.02E+01	1.11E+01	1.26E+01	1.30E+01	1.34E+01	1.40E+01
4.53E+03	1.24E+01	1.53E+01	1.01E+01	1.04E+01	1.09E+01	1.01E+01	1.10E+01	1.26E+01	1.30E+01	1.34E+01	1.40E+01
4.58E+03	1.25E+01	1.55E+01	1.01E+01	1.04E+01	1.08E+01	1.01E+01	1.10E+01	1.26E+01	1.30E+01	1.34E+01	1.40E+01
4.63E+03	1.27E+01	1.57E+01	1.01E+01	1.03E+01	1.08E+01	1.01E+01	1.10E+01	1.26E+01	1.30E+01	1.34E+01	1.40E+01
4.68E+03	1.28E+01	1.58E+01	1.01E+01	1.03E+01	1.08E+01	1.01E+01	1.09E+01	1.25E+01	1.30E+01	1.34E+01	1.40E+01
4.73E+03	1.29E+01	1.60E+01	1.01E+01	1.03E+01	1.08E+01	1.01E+01	1.09E+01	1.25E+01	1.30E+01	1.33E+01	1.40E+01
4.78E+03	1.31E+01	1.62E+01	1.01E+01	1.03E+01	1.08E+01	1.01E+01	1.09E+01	1.25E+01	1.30E+01	1.33E+01	1.40E+01
4.83E+03	1.32E+01	1.63E+01	1.01E+01	1.03E+01	1.08E+01	1.01E+01	1.09E+01	1.24E+01	1.30E+01	1.33E+01	1.40E+01
4.88E+03	1.34E+01	1.65E+01	1.01E+01	1.03E+01	1.08E+01	1.01E+01	1.08E+01	1.24E+01	1.30E+01	1.33E+01	1.40E+01
4.93E+03	1.35E+01	1.67E+01	1.00E+01	1.03E+01	1.08E+01	1.01E+01	1.08E+01	1.24E+01	1.30E+01	1.33E+01	1.39E+01
4.98E+03	1.36E+01	1.68E+01	1.00E+01	1.03E+01	1.08E+01	1.01E+01	1.08E+01	1.24E+01	1.30E+01	1.33E+01	1.39E+01
5.03E+03	1.38E+01	1.70E+01	1.00E+01	1.03E+01	1.08E+01	1.01E+01	1.08E+01	1.23E+01	1.30E+01	1.33E+01	1.39E+01
5.08E+03	1.39E+01	1.72E+01	1.00E+01	1.03E+01	1.08E+01	1.01E+01	1.07E+01	1.23E+01	1.30E+01	1.33E+01	1.39E+01
5.13E+03	1.40E+01	1.73E+01	1.00E+01	1.03E+01	1.08E+01	1.01E+01	1.07E+01	1.23E+01	1.30E+01	1.33E+01	1.39E+01
5.18E+03	1.42E+01	1.75E+01	1.00E+01	1.03E+01	1.07E+01	1.01E+01	1.07E+01	1.23E+01	1.30E+01	1.33E+01	1.39E+01
5.23E+03	1.43E+01	1.77E+01	1.00E+01	1.03E+01	1.07E+01	1.00E+01	1.07E+01	1.22E+01	1.30E+01	1.33E+01	1.39E+01
5.28E+03	1.45E+01	1.79E+01	1.00E+01	1.02E+01	1.07E+01	1.00E+01	1.07E+01	1.22E+01	1.30E+01	1.32E+01	1.39E+01
5.33E+03	1.46E+01	1.80E+01	1.00E+01	1.02E+01	1.07E+01	1.00E+01	1.06E+01	1.22E+01	1.30E+01	1.32E+01	1.39E+01
5.38E+03	1.47E+01	1.82E+01	1.00E+01	1.02E+01	1.07E+01	1.00E+01	1.06E+01	1.22E+01	1.30E+01	1.32E+01	1.39E+01
5.43E+03	1.49E+01	1.84E+01	1.00E+01	1.02E+01	1.07E+01	1.00E+01	1.06E+01	1.21E+01	1.30E+01	1.32E+01	1.39E+01
5.48E+03	1.50E+01	1.85E+01	1.00E+01	1.02E+01	1.07E+01	1.00E+01	1.06E+01	1.21E+01	1.30E+01	1.32E+01	1.38E+01
5.53E+03	1.51E+01	1.87E+01	1.00E+01	1.02E+01	1.07E+01	1.00E+01	1.06E+01	1.21E+01	1.30E+01	1.32E+01	1.38E+01
5.58E+03	1.53E+01	1.89E+01	1.00E+01	1.02E+01	1.07E+01	1.00E+01	1.06E+01	1.21E+01	1.30E+01	1.32E+01	1.38E+01
5.63E+03	1.54E+01	1.90E+01	1.00E+01	1.02E+01	1.07E+01	1.00E+01	1.05E+01	1.21E+01	1.30E+01	1.32E+01	1.38E+01
5.68E+03	1.55E+01	1.92E+01	1.00E+01	1.02E+01	1.07E+01	1.00E+01	1.05E+01	1.21E+01	1.30E+01	1.32E+01	1.38E+01
5.73E+03	1.57E+01	1.94E+01	1.00E+01	1.02E+01	1.07E+01	1.00E+01	1.05E+01	1.20E+01	1.30E+01	1.32E+01	1.38E+01
5.78E+03	1.58E+01	1.95E+01	1.00E+01	1.02E+01	1.07E+01	1.00E+01	1.05E+01	1.20E+01	1.30E+01	1.32E+01	1.38E+01
5.83E+03	1.60E+01	1.97E+01	1.00E+01	1.02E+01	1.07E+01	1.00E+01	1.05E+01	1.20E+01	1.30E+01	1.32E+01	1.38E+01
5.88E+03	1.61E+01	1.99E+01	1.00E+01	1.02E+01	1.07E+01	1.00E+01	1.05E+01	1.20E+01	1.29E+01	1.32E+01	1.38E+01
5.93E+03	1.62E+01	2.01E+01	1.00E+01	1.02E+01	1.07E+01	1.00E+01	1.04E+01	1.20E+01	1.29E+01	1.31E+01	1.38E+01
5.98E+03	1.64E+01	2.02E+01	1.00E+01	1.02E+01	1.07E+01	1.00E+01	1.04E+01	1.19E+01	1.29E+01	1.31E+01	1.38E+01
6.03E+03	1.65E+01	2.04E+01	1.00E+01	1.02E+01	1.06E+01	1.00E+01	1.04E+01	1.19E+01	1.29E+01	1.31E+01	1.38E+01
6.08E+03	1.66E+01	2.06E+01	1.00E+01	1.02E+01	1.06E+01	1.00E+01	1.04E+01	1.19E+01	1.29E+01	1.31E+01	1.38E+01
6.13E+03	1.68E+01	2.07E+01	1.00E+01	1.02E+01	1.06E+01	1.00E+01	1.04E+01	1.19E+01	1.29E+01	1.31E+01	1.37E+01
6.18E+03	1.69E+01	2.09E+01	1.00E+01	1.01E+01	1.06E+01	1.00E+01	1.04E+01	1.19E+01	1.29E+01	1.31E+01	1.37E+01
6.23E+03	1.71E+01	2.11E+01	1.00E+01	1.01E+01	1.06E+01	1.00E+01	1.04E+01	1.19E+01	1.29E+01	1.31E+01	1.37E+01
6.28E+03	1.72E+01	2.12E+01	1.00E+01	1.01E+01	1.06E+01	1.00E+01	1.04E+01	1.18E+01	1.29E+01	1.31E+01	1.37E+01
6.33E+03	1.73E+01	2.14E+01	1.00E+01	1.01E+01	1.06E+01	1.00E+01	1.03E+01	1.18E+01	1.29E+01	1.31E+01	1.37E+01

Appendix C. Model Results

Time		Pore Vol	Wash (ug/L)			Aquifer (ug/L)			Wash Mass Flux (lbs/day)		
(d)	(yr)	(-)	Low 95%	Median	High 95%	Low 95%	Median	High 95%	Low 95%	Median	High 95%
6.38E+03	1.75E+01	2.16E+01	1.00E+01	1.01E+01	1.06E+01	9.99E+00	1.03E+01	1.18E+01	1.29E+01	1.31E+01	1.37E+01
6.43E+03	1.76E+01	2.17E+01	1.00E+01	1.01E+01	1.06E+01	9.99E+00	1.03E+01	1.18E+01	1.29E+01	1.31E+01	1.37E+01
6.48E+03	1.77E+01	2.19E+01	1.00E+01	1.01E+01	1.06E+01	9.99E+00	1.03E+01	1.18E+01	1.29E+01	1.31E+01	1.37E+01
6.53E+03	1.79E+01	2.21E+01	1.00E+01	1.01E+01	1.06E+01	9.99E+00	1.03E+01	1.18E+01	1.29E+01	1.31E+01	1.37E+01
6.58E+03	1.80E+01	2.23E+01	1.00E+01	1.01E+01	1.06E+01	9.99E+00	1.03E+01	1.17E+01	1.29E+01	1.31E+01	1.37E+01
6.63E+03	1.81E+01	2.24E+01	1.00E+01	1.01E+01	1.06E+01	9.99E+00	1.03E+01	1.17E+01	1.29E+01	1.31E+01	1.37E+01
6.68E+03	1.83E+01	2.26E+01	1.00E+01	1.01E+01	1.06E+01	9.99E+00	1.03E+01	1.17E+01	1.29E+01	1.31E+01	1.37E+01
6.73E+03	1.84E+01	2.28E+01	1.00E+01	1.01E+01	1.06E+01	9.98E+00	1.03E+01	1.17E+01	1.29E+01	1.31E+01	1.37E+01
6.78E+03	1.86E+01	2.29E+01	1.00E+01	1.01E+01	1.06E+01	9.99E+00	1.02E+01	1.17E+01	1.29E+01	1.31E+01	1.37E+01
6.83E+03	1.87E+01	2.31E+01	1.00E+01	1.01E+01	1.06E+01	9.99E+00	1.02E+01	1.17E+01	1.29E+01	1.30E+01	1.37E+01
6.88E+03	1.88E+01	2.33E+01	1.00E+01	1.01E+01	1.06E+01	9.99E+00	1.02E+01	1.17E+01	1.29E+01	1.30E+01	1.37E+01
6.93E+03	1.90E+01	2.34E+01	1.00E+01	1.01E+01	1.06E+01	9.98E+00	1.02E+01	1.16E+01	1.29E+01	1.30E+01	1.37E+01
6.98E+03	1.91E+01	2.36E+01	1.00E+01	1.01E+01	1.06E+01	9.99E+00	1.02E+01	1.16E+01	1.29E+01	1.30E+01	1.37E+01
7.03E+03	1.92E+01	2.38E+01	1.00E+01	1.01E+01	1.06E+01	9.98E+00	1.02E+01	1.16E+01	1.29E+01	1.30E+01	1.36E+01
7.08E+03	1.94E+01	2.39E+01	1.00E+01	1.01E+01	1.06E+01	9.98E+00	1.02E+01	1.16E+01	1.29E+01	1.30E+01	1.36E+01
7.13E+03	1.95E+01	2.41E+01	1.00E+01	1.01E+01	1.06E+01	9.99E+00	1.02E+01	1.16E+01	1.29E+01	1.30E+01	1.36E+01
7.18E+03	1.97E+01	2.43E+01	1.00E+01	1.01E+01	1.05E+01	9.98E+00	1.02E+01	1.16E+01	1.29E+01	1.30E+01	1.36E+01
7.23E+03	1.98E+01	2.45E+01	1.00E+01	1.01E+01	1.05E+01	9.98E+00	1.02E+01	1.16E+01	1.29E+01	1.30E+01	1.36E+01
7.28E+03	1.99E+01	2.46E+01	1.00E+01	1.01E+01	1.05E+01	9.98E+00	1.02E+01	1.16E+01	1.29E+01	1.30E+01	1.36E+01
7.33E+03	2.01E+01	2.48E+01	1.00E+01	1.01E+01	1.05E+01	9.98E+00	1.02E+01	1.16E+01	1.29E+01	1.30E+01	1.36E+01
7.38E+03	2.02E+01	2.50E+01	1.00E+01	1.01E+01	1.05E+01	9.98E+00	1.02E+01	1.15E+01	1.29E+01	1.30E+01	1.36E+01
7.43E+03	2.03E+01	2.51E+01	1.00E+01	1.01E+01	1.05E+01	9.98E+00	1.02E+01	1.15E+01	1.29E+01	1.30E+01	1.36E+01
7.48E+03	2.05E+01	2.53E+01	1.00E+01	1.01E+01	1.05E+01	9.98E+00	1.02E+01	1.15E+01	1.29E+01	1.30E+01	1.36E+01
7.53E+03	2.06E+01	2.55E+01	1.00E+01	1.01E+01	1.05E+01	9.98E+00	1.02E+01	1.15E+01	1.29E+01	1.30E+01	1.36E+01
7.58E+03	2.08E+01	2.56E+01	1.00E+01	1.01E+01	1.05E+01	9.98E+00	1.02E+01	1.15E+01	1.29E+01	1.30E+01	1.36E+01
7.63E+03	2.09E+01	2.58E+01	1.00E+01	1.01E+01	1.05E+01	9.98E+00	1.01E+01	1.15E+01	1.29E+01	1.30E+01	1.36E+01
7.68E+03	2.10E+01	2.60E+01	1.00E+01	1.01E+01	1.05E+01	9.98E+00	1.01E+01	1.15E+01	1.29E+01	1.30E+01	1.36E+01
7.73E+03	2.12E+01	2.61E+01	1.00E+01	1.01E+01	1.05E+01	9.98E+00	1.01E+01	1.15E+01	1.29E+01	1.30E+01	1.36E+01
7.78E+03	2.13E+01	2.63E+01	1.00E+01	1.01E+01	1.05E+01	9.98E+00	1.01E+01	1.15E+01	1.29E+01	1.30E+01	1.36E+01
7.83E+03	2.14E+01	2.65E+01	1.00E+01	1.01E+01	1.05E+01	9.98E+00	1.01E+01	1.14E+01	1.29E+01	1.30E+01	1.36E+01
7.88E+03	2.16E+01	2.67E+01	1.00E+01	1.01E+01	1.05E+01	9.98E+00	1.01E+01	1.14E+01	1.29E+01	1.30E+01	1.36E+01
7.93E+03	2.17E+01	2.68E+01	1.00E+01	1.01E+01	1.05E+01	9.98E+00	1.01E+01	1.14E+01	1.29E+01	1.30E+01	1.36E+01
7.98E+03	2.18E+01	2.70E+01	1.00E+01	1.01E+01	1.05E+01	9.98E+00	1.01E+01	1.14E+01	1.29E+01	1.30E+01	1.36E+01
8.03E+03	2.20E+01	2.72E+01	1.00E+01	1.01E+01	1.05E+01	9.98E+00	1.01E+01	1.14E+01	1.29E+01	1.30E+01	1.36E+01
8.08E+03	2.21E+01	2.73E+01	1.00E+01	1.01E+01	1.05E+01	9.98E+00	1.01E+01	1.14E+01	1.29E+01	1.30E+01	1.36E+01
8.13E+03	2.23E+01	2.75E+01	1.00E+01	1.00E+01	1.05E+01	9.98E+00	1.01E+01	1.14E+01	1.29E+01	1.30E+01	1.36E+01
8.18E+03	2.24E+01	2.77E+01	1.00E+01	1.00E+01	1.05E+01	9.97E+00	1.01E+01	1.14E+01	1.29E+01	1.30E+01	1.35E+01
8.23E+03	2.25E+01	2.78E+01	1.00E+01	1.00E+01	1.05E+01	9.97E+00	1.01E+01	1.14E+01	1.29E+01	1.30E+01	1.35E+01
8.28E+03	2.27E+01	2.80E+01	1.00E+01	1.00E+01	1.05E+01	9.98E+00	1.01E+01	1.14E+01	1.29E+01	1.30E+01	1.35E+01

Appendix C. Model Results

Time		Pore Vol	Wash (ug/L)			Aquifer (ug/L)			Wash Mass Flux (lbs/day)		
(d)	(yr)	(-)	Low 95%	Median	High 95%	Low 95%	Median	High 95%	Low 95%	Median	High 95%
8.33E+03	2.28E+01	2.82E+01	1.00E+01	1.00E+01	1.05E+01	9.98E+00	1.01E+01	1.13E+01	1.29E+01	1.30E+01	1.35E+01
8.38E+03	2.29E+01	2.83E+01	1.00E+01	1.00E+01	1.05E+01	9.98E+00	1.01E+01	1.13E+01	1.29E+01	1.30E+01	1.35E+01
8.43E+03	2.31E+01	2.85E+01	1.00E+01	1.00E+01	1.05E+01	9.98E+00	1.01E+01	1.13E+01	1.29E+01	1.30E+01	1.35E+01
8.48E+03	2.32E+01	2.87E+01	1.00E+01	1.00E+01	1.05E+01	9.98E+00	1.01E+01	1.13E+01	1.29E+01	1.30E+01	1.35E+01
8.53E+03	2.34E+01	2.88E+01	1.00E+01	1.00E+01	1.05E+01	9.98E+00	1.01E+01	1.13E+01	1.29E+01	1.30E+01	1.35E+01
8.58E+03	2.35E+01	2.90E+01	1.00E+01	1.00E+01	1.05E+01	9.98E+00	1.01E+01	1.13E+01	1.29E+01	1.30E+01	1.35E+01
8.63E+03	2.36E+01	2.92E+01	1.00E+01	1.00E+01	1.05E+01	9.98E+00	1.01E+01	1.13E+01	1.29E+01	1.30E+01	1.35E+01
8.68E+03	2.38E+01	2.94E+01	1.00E+01	1.00E+01	1.05E+01	9.98E+00	1.01E+01	1.13E+01	1.29E+01	1.30E+01	1.35E+01
8.73E+03	2.39E+01	2.95E+01	1.00E+01	1.00E+01	1.04E+01	9.98E+00	1.01E+01	1.13E+01	1.29E+01	1.30E+01	1.35E+01
8.78E+03	2.40E+01	2.97E+01	1.00E+01	1.00E+01	1.04E+01	9.97E+00	1.01E+01	1.13E+01	1.29E+01	1.30E+01	1.35E+01
8.83E+03	2.42E+01	2.99E+01	1.00E+01	1.00E+01	1.04E+01	9.97E+00	1.01E+01	1.13E+01	1.29E+01	1.30E+01	1.35E+01
8.88E+03	2.43E+01	3.00E+01	1.00E+01	1.00E+01	1.04E+01	9.98E+00	1.01E+01	1.13E+01	1.29E+01	1.30E+01	1.35E+01
8.93E+03	2.44E+01	3.02E+01	1.00E+01	1.00E+01	1.04E+01	9.98E+00	1.01E+01	1.13E+01	1.29E+01	1.30E+01	1.35E+01
8.98E+03	2.46E+01	3.04E+01	1.00E+01	1.00E+01	1.04E+01	9.98E+00	1.01E+01	1.12E+01	1.29E+01	1.30E+01	1.35E+01
9.03E+03	2.47E+01	3.05E+01	1.00E+01	1.00E+01	1.04E+01	9.98E+00	1.01E+01	1.12E+01	1.29E+01	1.30E+01	1.35E+01
9.08E+03	2.49E+01	3.07E+01	1.00E+01	1.00E+01	1.04E+01	9.98E+00	1.00E+01	1.12E+01	1.29E+01	1.30E+01	1.35E+01
9.13E+03	2.50E+01	3.09E+01	1.00E+01	1.00E+01	1.04E+01	9.98E+00	1.00E+01	1.12E+01	1.29E+01	1.30E+01	1.35E+01
9.13E+03	2.50E+01	3.09E+01	1.00E+01	1.00E+01	1.04E+01	9.97E+00	1.00E+01	1.12E+01	1.29E+01	1.30E+01	1.35E+01

APPENDIX D

Sensitivity Analyses Results: Time-Series Data

Appendix D. Sensitivity Analyses Results

Time		Wash Conc (ug/L)								
(d)	(yr)	90% Effective Remediation			95% Effective Remediation			No Southeast Flux		
		Low 95%	Median	High 95%	Low 95%	Median	High 95%	Low 95%	Median	High 95%
1.00E-01	2.74E-04	6.13E+02	6.54E+02	6.94E+02	6.13E+02	6.54E+02	6.94E+02	6.21E+02	6.60E+02	6.98E+02
2.00E-01	5.48E-04	6.12E+02	6.57E+02	7.00E+02	6.12E+02	6.57E+02	7.00E+02	6.20E+02	6.63E+02	7.04E+02
3.20E-01	8.76E-04	6.01E+02	6.50E+02	6.96E+02	6.01E+02	6.51E+02	6.96E+02	6.09E+02	6.57E+02	6.99E+02
4.30E-01	1.18E-03	5.90E+02	6.43E+02	6.90E+02	5.90E+02	6.43E+02	6.90E+02	5.98E+02	6.50E+02	6.93E+02
5.50E-01	1.51E-03	5.80E+02	6.36E+02	6.84E+02	5.80E+02	6.36E+02	6.84E+02	5.88E+02	6.43E+02	6.88E+02
6.80E-01	1.86E-03	5.70E+02	6.29E+02	6.79E+02	5.70E+02	6.29E+02	6.79E+02	5.79E+02	6.36E+02	6.82E+02
8.10E-01	2.22E-03	5.62E+02	6.23E+02	6.73E+02	5.62E+02	6.23E+02	6.73E+02	5.70E+02	6.30E+02	6.77E+02
9.50E-01	2.60E-03	5.54E+02	6.17E+02	6.68E+02	5.54E+02	6.17E+02	6.68E+02	5.63E+02	6.24E+02	6.72E+02
1.10E+00	3.01E-03	5.47E+02	6.11E+02	6.63E+02	5.47E+02	6.11E+02	6.63E+02	5.56E+02	6.18E+02	6.67E+02
1.26E+00	3.45E-03	5.40E+02	6.06E+02	6.59E+02	5.40E+02	6.06E+02	6.59E+02	5.49E+02	6.13E+02	6.62E+02
1.42E+00	3.89E-03	5.34E+02	6.01E+02	6.54E+02	5.34E+02	6.01E+02	6.54E+02	5.43E+02	6.08E+02	6.58E+02
1.59E+00	4.35E-03	5.28E+02	5.96E+02	6.50E+02	5.28E+02	5.96E+02	6.50E+02	5.37E+02	6.03E+02	6.54E+02
1.77E+00	4.85E-03	5.22E+02	5.91E+02	6.46E+02	5.22E+02	5.91E+02	6.46E+02	5.31E+02	5.98E+02	6.49E+02
1.96E+00	5.37E-03	5.16E+02	5.86E+02	6.41E+02	5.16E+02	5.86E+02	6.41E+02	5.25E+02	5.93E+02	6.45E+02
2.16E+00	5.91E-03	5.11E+02	5.81E+02	6.37E+02	5.11E+02	5.81E+02	6.37E+02	5.20E+02	5.89E+02	6.41E+02
2.37E+00	6.49E-03	5.05E+02	5.77E+02	6.33E+02	5.05E+02	5.77E+02	6.33E+02	5.15E+02	5.84E+02	6.37E+02
2.58E+00	7.06E-03	5.00E+02	5.72E+02	6.29E+02	5.00E+02	5.73E+02	6.29E+02	5.10E+02	5.80E+02	6.33E+02
2.81E+00	7.69E-03	4.95E+02	5.68E+02	6.25E+02	4.95E+02	5.68E+02	6.25E+02	5.05E+02	5.75E+02	6.30E+02
3.05E+00	8.35E-03	4.90E+02	5.64E+02	6.22E+02	4.90E+02	5.64E+02	6.22E+02	5.00E+02	5.71E+02	6.26E+02
3.31E+00	9.06E-03	4.86E+02	5.60E+02	6.18E+02	4.86E+02	5.60E+02	6.18E+02	4.95E+02	5.67E+02	6.22E+02
3.57E+00	9.77E-03	4.81E+02	5.55E+02	6.14E+02	4.81E+02	5.56E+02	6.14E+02	4.91E+02	5.63E+02	6.18E+02
3.85E+00	1.05E-02	4.76E+02	5.51E+02	6.10E+02	4.76E+02	5.51E+02	6.10E+02	4.86E+02	5.59E+02	6.15E+02
4.14E+00	1.13E-02	4.72E+02	5.47E+02	6.06E+02	4.71E+02	5.47E+02	6.06E+02	4.81E+02	5.55E+02	6.11E+02
4.45E+00	1.22E-02	4.67E+02	5.43E+02	6.03E+02	4.67E+02	5.43E+02	6.03E+02	4.77E+02	5.51E+02	6.07E+02
4.77E+00	1.31E-02	4.62E+02	5.39E+02	5.99E+02	4.62E+02	5.39E+02	5.99E+02	4.72E+02	5.47E+02	6.03E+02
5.11E+00	1.40E-02	4.58E+02	5.35E+02	5.95E+02	4.58E+02	5.35E+02	5.95E+02	4.68E+02	5.43E+02	6.00E+02
5.47E+00	1.50E-02	4.53E+02	5.31E+02	5.91E+02	4.53E+02	5.31E+02	5.91E+02	4.63E+02	5.39E+02	5.96E+02
5.84E+00	1.60E-02	4.49E+02	5.27E+02	5.88E+02	4.48E+02	5.27E+02	5.88E+02	4.59E+02	5.35E+02	5.92E+02
6.23E+00	1.71E-02	4.44E+02	5.23E+02	5.84E+02	4.44E+02	5.23E+02	5.84E+02	4.54E+02	5.31E+02	5.89E+02
6.64E+00	1.82E-02	4.40E+02	5.18E+02	5.80E+02	4.39E+02	5.19E+02	5.80E+02	4.50E+02	5.27E+02	5.85E+02
7.08E+00	1.94E-02	4.36E+02	5.14E+02	5.76E+02	4.35E+02	5.14E+02	5.76E+02	4.45E+02	5.23E+02	5.81E+02
7.53E+00	2.06E-02	4.31E+02	5.10E+02	5.72E+02	4.30E+02	5.10E+02	5.72E+02	4.41E+02	5.19E+02	5.77E+02
8.01E+00	2.19E-02	4.27E+02	5.06E+02	5.68E+02	4.26E+02	5.06E+02	5.68E+02	4.36E+02	5.14E+02	5.73E+02

Appendix D. Sensitivity Analyses Results

Time		Wash Conc (ug/L)								
(d)	(yr)	90% Effective Remediation			95% Effective Remediation			No Southeast Flux		
		Low 95%	Median	High 95%	Low 95%	Median	High 95%	Low 95%	Median	High 95%
8.51E+00	2.33E-02	4.22E+02	5.02E+02	5.64E+02	4.21E+02	5.02E+02	5.64E+02	4.32E+02	5.10E+02	5.69E+02
9.03E+00	2.47E-02	4.18E+02	4.98E+02	5.61E+02	4.17E+02	4.98E+02	5.60E+02	4.27E+02	5.06E+02	5.65E+02
9.58E+00	2.62E-02	4.14E+02	4.94E+02	5.57E+02	4.12E+02	4.93E+02	5.56E+02	4.23E+02	5.02E+02	5.61E+02
1.02E+01	2.78E-02	4.09E+02	4.89E+02	5.52E+02	4.08E+02	4.89E+02	5.52E+02	4.18E+02	4.98E+02	5.57E+02
1.08E+01	2.95E-02	4.05E+02	4.85E+02	5.48E+02	4.03E+02	4.85E+02	5.48E+02	4.14E+02	4.93E+02	5.53E+02
1.14E+01	3.12E-02	4.01E+02	4.81E+02	5.44E+02	3.99E+02	4.81E+02	5.44E+02	4.09E+02	4.89E+02	5.49E+02
1.21E+01	3.31E-02	3.97E+02	4.77E+02	5.40E+02	3.95E+02	4.76E+02	5.40E+02	4.05E+02	4.85E+02	5.45E+02
1.28E+01	3.50E-02	3.93E+02	4.73E+02	5.36E+02	3.90E+02	4.72E+02	5.35E+02	4.01E+02	4.80E+02	5.41E+02
1.35E+01	3.70E-02	3.89E+02	4.68E+02	5.32E+02	3.86E+02	4.68E+02	5.31E+02	3.96E+02	4.76E+02	5.37E+02
1.43E+01	3.92E-02	3.86E+02	4.64E+02	5.28E+02	3.82E+02	4.63E+02	5.27E+02	3.92E+02	4.72E+02	5.32E+02
1.51E+01	4.14E-02	3.83E+02	4.60E+02	5.23E+02	3.78E+02	4.59E+02	5.23E+02	3.88E+02	4.67E+02	5.28E+02
1.60E+01	4.37E-02	3.79E+02	4.56E+02	5.19E+02	3.74E+02	4.55E+02	5.18E+02	3.84E+02	4.63E+02	5.24E+02
1.69E+01	4.62E-02	3.76E+02	4.52E+02	5.15E+02	3.71E+02	4.50E+02	5.14E+02	3.80E+02	4.59E+02	5.20E+02
1.78E+01	4.88E-02	3.73E+02	4.48E+02	5.11E+02	3.67E+02	4.46E+02	5.09E+02	3.77E+02	4.54E+02	5.15E+02
1.88E+01	5.15E-02	3.70E+02	4.44E+02	5.06E+02	3.64E+02	4.42E+02	5.05E+02	3.74E+02	4.50E+02	5.11E+02
1.98E+01	5.43E-02	3.67E+02	4.40E+02	5.02E+02	3.61E+02	4.37E+02	5.00E+02	3.70E+02	4.45E+02	5.06E+02
2.09E+01	5.73E-02	3.64E+02	4.36E+02	4.98E+02	3.58E+02	4.33E+02	4.96E+02	3.67E+02	4.41E+02	5.02E+02
2.21E+01	6.05E-02	3.61E+02	4.32E+02	4.94E+02	3.54E+02	4.29E+02	4.92E+02	3.64E+02	4.37E+02	4.97E+02
2.33E+01	6.38E-02	3.58E+02	4.28E+02	4.89E+02	3.51E+02	4.25E+02	4.87E+02	3.61E+02	4.33E+02	4.93E+02
2.46E+01	6.72E-02	3.56E+02	4.24E+02	4.85E+02	3.48E+02	4.21E+02	4.83E+02	3.58E+02	4.29E+02	4.89E+02
2.59E+01	7.09E-02	3.53E+02	4.21E+02	4.81E+02	3.45E+02	4.17E+02	4.78E+02	3.55E+02	4.25E+02	4.84E+02
2.73E+01	7.47E-02	3.51E+02	4.17E+02	4.77E+02	3.42E+02	4.13E+02	4.74E+02	3.53E+02	4.21E+02	4.80E+02
2.87E+01	7.87E-02	3.50E+02	4.13E+02	4.72E+02	3.40E+02	4.08E+02	4.69E+02	3.50E+02	4.17E+02	4.75E+02
3.03E+01	8.29E-02	3.48E+02	4.10E+02	4.68E+02	3.38E+02	4.05E+02	4.65E+02	3.48E+02	4.13E+02	4.71E+02
3.19E+01	8.73E-02	3.47E+02	4.07E+02	4.64E+02	3.36E+02	4.01E+02	4.60E+02	3.47E+02	4.09E+02	4.67E+02
3.36E+01	9.19E-02	3.46E+02	4.04E+02	4.60E+02	3.35E+02	3.97E+02	4.56E+02	3.46E+02	4.06E+02	4.62E+02
3.54E+01	9.68E-02	3.46E+02	4.01E+02	4.56E+02	3.33E+02	3.94E+02	4.51E+02	3.45E+02	4.02E+02	4.58E+02
3.72E+01	1.02E-01	3.46E+02	3.98E+02	4.52E+02	3.32E+02	3.91E+02	4.47E+02	3.45E+02	3.99E+02	4.54E+02
3.92E+01	1.07E-01	3.45E+02	3.95E+02	4.49E+02	3.32E+02	3.88E+02	4.43E+02	3.46E+02	3.96E+02	4.50E+02
4.13E+01	1.13E-01	3.45E+02	3.93E+02	4.45E+02	3.32E+02	3.84E+02	4.39E+02	3.45E+02	3.93E+02	4.46E+02
4.34E+01	1.19E-01	3.45E+02	3.91E+02	4.42E+02	3.31E+02	3.82E+02	4.35E+02	3.45E+02	3.91E+02	4.42E+02
4.57E+01	1.25E-01	3.46E+02	3.88E+02	4.38E+02	3.31E+02	3.79E+02	4.31E+02	3.46E+02	3.88E+02	4.38E+02
4.81E+01	1.32E-01	3.46E+02	3.87E+02	4.35E+02	3.31E+02	3.77E+02	4.28E+02	3.46E+02	3.86E+02	4.35E+02

Appendix D. Sensitivity Analyses Results

Time		Wash Conc (ug/L)								
(d)	(yr)	90% Effective Remediation			95% Effective Remediation			No Southeast Flux		
		Low 95%	Median	High 95%	Low 95%	Median	High 95%	Low 95%	Median	High 95%
5.06E+01	1.38E-01	3.46E+02	3.86E+02	4.32E+02	3.32E+02	3.75E+02	4.24E+02	3.46E+02	3.84E+02	4.31E+02
5.32E+01	1.46E-01	3.47E+02	3.84E+02	4.30E+02	3.32E+02	3.72E+02	4.21E+02	3.47E+02	3.83E+02	4.28E+02
5.60E+01	1.53E-01	3.48E+02	3.83E+02	4.27E+02	3.32E+02	3.71E+02	4.18E+02	3.48E+02	3.82E+02	4.25E+02
5.89E+01	1.61E-01	3.49E+02	3.83E+02	4.25E+02	3.33E+02	3.70E+02	4.15E+02	3.50E+02	3.81E+02	4.23E+02
6.19E+01	1.69E-01	3.50E+02	3.83E+02	4.23E+02	3.33E+02	3.69E+02	4.12E+02	3.51E+02	3.82E+02	4.20E+02
6.51E+01	1.78E-01	3.52E+02	3.85E+02	4.21E+02	3.34E+02	3.68E+02	4.10E+02	3.53E+02	3.83E+02	4.18E+02
6.84E+01	1.87E-01	3.53E+02	3.86E+02	4.19E+02	3.35E+02	3.69E+02	4.08E+02	3.55E+02	3.84E+02	4.17E+02
7.20E+01	1.97E-01	3.55E+02	3.87E+02	4.18E+02	3.37E+02	3.70E+02	4.06E+02	3.56E+02	3.86E+02	4.16E+02
7.57E+01	2.07E-01	3.56E+02	3.88E+02	4.17E+02	3.38E+02	3.71E+02	4.05E+02	3.58E+02	3.86E+02	4.14E+02
7.96E+01	2.18E-01	3.57E+02	3.89E+02	4.16E+02	3.39E+02	3.72E+02	4.03E+02	3.60E+02	3.88E+02	4.13E+02
8.36E+01	2.29E-01	3.59E+02	3.90E+02	4.16E+02	3.41E+02	3.73E+02	4.02E+02	3.62E+02	3.89E+02	4.14E+02
8.79E+01	2.41E-01	3.61E+02	3.92E+02	4.17E+02	3.42E+02	3.73E+02	4.01E+02	3.63E+02	3.91E+02	4.14E+02
9.24E+01	2.53E-01	3.62E+02	3.92E+02	4.17E+02	3.43E+02	3.74E+02	4.00E+02	3.64E+02	3.91E+02	4.16E+02
9.71E+01	2.66E-01	3.63E+02	3.93E+02	4.18E+02	3.44E+02	3.75E+02	4.01E+02	3.65E+02	3.92E+02	4.17E+02
1.02E+02	2.80E-01	3.65E+02	3.94E+02	4.19E+02	3.44E+02	3.76E+02	4.00E+02	3.67E+02	3.94E+02	4.20E+02
1.07E+02	2.94E-01	3.65E+02	3.95E+02	4.21E+02	3.45E+02	3.75E+02	4.01E+02	3.67E+02	3.95E+02	4.23E+02
1.13E+02	3.09E-01	3.65E+02	3.95E+02	4.23E+02	3.45E+02	3.76E+02	4.01E+02	3.68E+02	3.95E+02	4.25E+02
1.19E+02	3.24E-01	3.65E+02	3.96E+02	4.23E+02	3.44E+02	3.76E+02	4.01E+02	3.68E+02	3.96E+02	4.26E+02
1.25E+02	3.41E-01	3.65E+02	3.96E+02	4.24E+02	3.43E+02	3.76E+02	4.01E+02	3.67E+02	3.96E+02	4.26E+02
1.31E+02	3.58E-01	3.64E+02	3.96E+02	4.23E+02	3.41E+02	3.75E+02	4.00E+02	3.66E+02	3.95E+02	4.24E+02
1.38E+02	3.76E-01	3.60E+02	3.95E+02	4.23E+02	3.37E+02	3.74E+02	3.99E+02	3.64E+02	3.94E+02	4.22E+02
1.44E+02	3.95E-01	3.56E+02	3.93E+02	4.21E+02	3.34E+02	3.71E+02	3.98E+02	3.59E+02	3.92E+02	4.19E+02
1.52E+02	4.16E-01	3.52E+02	3.91E+02	4.20E+02	3.29E+02	3.68E+02	3.97E+02	3.54E+02	3.89E+02	4.16E+02
1.60E+02	4.37E-01	3.46E+02	3.87E+02	4.18E+02	3.23E+02	3.64E+02	3.95E+02	3.47E+02	3.85E+02	4.13E+02
1.68E+02	4.59E-01	3.38E+02	3.82E+02	4.15E+02	3.14E+02	3.59E+02	3.92E+02	3.38E+02	3.79E+02	4.10E+02
1.76E+02	4.82E-01	3.29E+02	3.77E+02	4.12E+02	3.05E+02	3.53E+02	3.88E+02	3.27E+02	3.72E+02	4.05E+02
1.85E+02	5.06E-01	3.19E+02	3.70E+02	4.08E+02	2.94E+02	3.46E+02	3.83E+02	3.14E+02	3.64E+02	4.00E+02
1.94E+02	5.32E-01	3.07E+02	3.62E+02	4.01E+02	2.83E+02	3.38E+02	3.77E+02	3.00E+02	3.54E+02	3.93E+02
2.04E+02	5.59E-01	2.94E+02	3.52E+02	3.94E+02	2.69E+02	3.28E+02	3.70E+02	2.85E+02	3.44E+02	3.84E+02
2.14E+02	5.87E-01	2.81E+02	3.42E+02	3.86E+02	2.55E+02	3.17E+02	3.62E+02	2.67E+02	3.31E+02	3.73E+02
2.25E+02	6.17E-01	2.64E+02	3.30E+02	3.78E+02	2.39E+02	3.05E+02	3.52E+02	2.51E+02	3.17E+02	3.63E+02
2.37E+02	6.48E-01	2.48E+02	3.17E+02	3.67E+02	2.24E+02	2.93E+02	3.42E+02	2.32E+02	3.03E+02	3.51E+02
2.49E+02	6.80E-01	2.32E+02	3.04E+02	3.55E+02	2.07E+02	2.78E+02	3.30E+02	2.13E+02	2.87E+02	3.37E+02

Appendix D. Sensitivity Analyses Results

Time		Wash Conc (ug/L)								
(d)	(yr)	90% Effective Remediation			95% Effective Remediation			No Southeast Flux		
		Low 95%	Median	High 95%	Low 95%	Median	High 95%	Low 95%	Median	High 95%
2.61E+02	7.15E-01	2.17E+02	2.89E+02	3.43E+02	1.90E+02	2.64E+02	3.16E+02	1.93E+02	2.70E+02	3.22E+02
2.74E+02	7.50E-01	2.00E+02	2.75E+02	3.29E+02	1.73E+02	2.48E+02	3.02E+02	1.72E+02	2.52E+02	3.05E+02
2.88E+02	7.89E-01	1.84E+02	2.58E+02	3.14E+02	1.57E+02	2.31E+02	2.87E+02	1.53E+02	2.33E+02	2.88E+02
3.03E+02	8.28E-01	1.68E+02	2.41E+02	2.98E+02	1.42E+02	2.15E+02	2.71E+02	1.36E+02	2.14E+02	2.71E+02
3.18E+02	8.70E-01	1.54E+02	2.25E+02	2.82E+02	1.28E+02	1.99E+02	2.55E+02	1.19E+02	1.95E+02	2.52E+02
3.34E+02	9.14E-01	1.41E+02	2.09E+02	2.66E+02	1.15E+02	1.83E+02	2.39E+02	1.04E+02	1.77E+02	2.34E+02
3.51E+02	9.60E-01	1.29E+02	1.94E+02	2.49E+02	1.03E+02	1.67E+02	2.23E+02	8.95E+01	1.59E+02	2.15E+02
3.68E+02	1.01E+00	1.19E+02	1.80E+02	2.33E+02	9.25E+01	1.53E+02	2.06E+02	7.69E+01	1.42E+02	1.97E+02
3.87E+02	1.06E+00	1.09E+02	1.66E+02	2.17E+02	8.31E+01	1.39E+02	1.91E+02	6.59E+01	1.26E+02	1.79E+02
4.06E+02	1.11E+00	1.01E+02	1.53E+02	2.02E+02	7.48E+01	1.26E+02	1.75E+02	5.63E+01	1.11E+02	1.62E+02
4.26E+02	1.17E+00	9.41E+01	1.41E+02	1.88E+02	6.78E+01	1.14E+02	1.61E+02	4.80E+01	9.73E+01	1.46E+02
4.48E+02	1.23E+00	8.82E+01	1.30E+02	1.75E+02	6.17E+01	1.03E+02	1.48E+02	4.08E+01	8.49E+01	1.30E+02
4.70E+02	1.29E+00	8.32E+01	1.21E+02	1.62E+02	5.65E+01	9.36E+01	1.35E+02	3.48E+01	7.38E+01	1.16E+02
4.94E+02	1.35E+00	7.89E+01	1.12E+02	1.51E+02	5.24E+01	8.51E+01	1.24E+02	2.98E+01	6.39E+01	1.02E+02
5.19E+02	1.42E+00	7.52E+01	1.05E+02	1.40E+02	4.90E+01	7.76E+01	1.13E+02	2.57E+01	5.52E+01	9.04E+01
5.45E+02	1.49E+00	7.23E+01	9.86E+01	1.31E+02	4.63E+01	7.12E+01	1.03E+02	2.24E+01	4.77E+01	7.93E+01
5.72E+02	1.57E+00	7.01E+01	9.30E+01	1.22E+02	4.42E+01	6.58E+01	9.47E+01	1.97E+01	4.12E+01	6.94E+01
6.01E+02	1.64E+00	6.81E+01	8.82E+01	1.15E+02	4.24E+01	6.12E+01	8.69E+01	1.75E+01	3.55E+01	6.05E+01
6.31E+02	1.73E+00	6.64E+01	8.45E+01	1.08E+02	4.08E+01	5.73E+01	8.01E+01	1.58E+01	3.09E+01	5.28E+01
6.63E+02	1.81E+00	6.52E+01	8.13E+01	1.02E+02	3.96E+01	5.38E+01	7.41E+01	1.44E+01	2.70E+01	4.61E+01
6.96E+02	1.90E+00	6.42E+01	7.87E+01	9.75E+01	3.87E+01	5.10E+01	6.89E+01	1.33E+01	2.38E+01	4.02E+01
7.31E+02	2.00E+00	6.34E+01	7.64E+01	9.34E+01	3.80E+01	4.88E+01	6.44E+01	1.25E+01	2.11E+01	3.51E+01
7.67E+02	2.10E+00	6.26E+01	7.47E+01	8.98E+01	3.74E+01	4.70E+01	6.06E+01	1.19E+01	1.88E+01	3.07E+01
8.06E+02	2.21E+00	6.21E+01	7.32E+01	8.68E+01	3.70E+01	4.55E+01	5.74E+01	1.14E+01	1.70E+01	2.70E+01
8.46E+02	2.32E+00	6.17E+01	7.22E+01	8.43E+01	3.65E+01	4.43E+01	5.48E+01	1.10E+01	1.56E+01	2.38E+01
8.89E+02	2.43E+00	6.14E+01	7.11E+01	8.21E+01	3.62E+01	4.33E+01	5.25E+01	1.07E+01	1.44E+01	2.12E+01
9.33E+02	2.55E+00	6.12E+01	7.03E+01	8.03E+01	3.60E+01	4.25E+01	5.06E+01	1.05E+01	1.34E+01	1.90E+01
9.80E+02	2.68E+00	6.10E+01	6.96E+01	7.88E+01	3.59E+01	4.19E+01	4.91E+01	1.03E+01	1.26E+01	1.72E+01
1.03E+03	2.82E+00	6.08E+01	6.91E+01	7.74E+01	3.58E+01	4.14E+01	4.78E+01	1.02E+01	1.20E+01	1.57E+01
1.08E+03	2.95E+00	6.06E+01	6.86E+01	7.68E+01	3.57E+01	4.10E+01	4.68E+01	1.02E+01	1.15E+01	1.46E+01
1.13E+03	3.09E+00	6.05E+01	6.82E+01	7.61E+01	3.57E+01	4.07E+01	4.61E+01	1.01E+01	1.11E+01	1.37E+01
1.18E+03	3.23E+00	6.04E+01	6.79E+01	7.55E+01	3.56E+01	4.04E+01	4.54E+01	1.01E+01	1.09E+01	1.30E+01
1.23E+03	3.36E+00	6.04E+01	6.77E+01	7.51E+01	3.56E+01	4.02E+01	4.50E+01	1.00E+01	1.07E+01	1.28E+01

Appendix D. Sensitivity Analyses Results

Time		Wash Conc (ug/L)								
(d)	(yr)	90% Effective Remediation			95% Effective Remediation			No Southeast Flux		
		Low 95%	Median	High 95%	Low 95%	Median	High 95%	Low 95%	Median	High 95%
1.28E+03	3.50E+00	6.04E+01	6.75E+01	7.47E+01	3.55E+01	4.00E+01	4.45E+01	1.00E+01	1.05E+01	1.25E+01
1.33E+03	3.64E+00	6.04E+01	6.74E+01	7.45E+01	3.55E+01	3.98E+01	4.42E+01	1.00E+01	1.04E+01	1.25E+01
1.38E+03	3.78E+00	6.04E+01	6.74E+01	7.43E+01	3.55E+01	3.97E+01	4.39E+01	1.00E+01	1.03E+01	1.23E+01
1.43E+03	3.91E+00	6.04E+01	6.73E+01	7.40E+01	3.55E+01	3.97E+01	4.37E+01	1.00E+01	1.02E+01	1.23E+01
1.48E+03	4.05E+00	6.03E+01	6.73E+01	7.39E+01	3.55E+01	3.96E+01	4.34E+01	1.00E+01	1.02E+01	1.23E+01
1.53E+03	4.19E+00	6.03E+01	6.72E+01	7.38E+01	3.55E+01	3.96E+01	4.32E+01	1.00E+01	1.01E+01	1.21E+01
1.58E+03	4.32E+00	6.03E+01	6.72E+01	7.37E+01	3.55E+01	3.95E+01	4.32E+01	1.00E+01	1.01E+01	1.20E+01
1.63E+03	4.46E+00	6.03E+01	6.71E+01	7.35E+01	3.55E+01	3.94E+01	4.30E+01	1.00E+01	1.01E+01	1.20E+01
1.68E+03	4.60E+00	6.03E+01	6.70E+01	7.34E+01	3.55E+01	3.93E+01	4.29E+01	1.00E+01	1.01E+01	1.19E+01
1.73E+03	4.73E+00	6.03E+01	6.70E+01	7.33E+01	3.55E+01	3.93E+01	4.28E+01	1.00E+01	1.00E+01	1.19E+01
1.78E+03	4.87E+00	6.03E+01	6.69E+01	7.32E+01	3.55E+01	3.92E+01	4.27E+01	1.00E+01	1.00E+01	1.18E+01
1.83E+03	5.01E+00	6.03E+01	6.68E+01	7.30E+01	3.55E+01	3.92E+01	4.26E+01	1.00E+01	1.00E+01	1.18E+01
1.88E+03	5.14E+00	6.03E+01	6.68E+01	7.30E+01	3.55E+01	3.92E+01	4.25E+01	1.00E+01	1.00E+01	1.17E+01
1.93E+03	5.28E+00	6.03E+01	6.67E+01	7.29E+01	3.55E+01	3.92E+01	4.25E+01	1.00E+01	1.00E+01	1.17E+01
1.98E+03	5.42E+00	6.03E+01	6.67E+01	7.29E+01	3.55E+01	3.91E+01	4.24E+01	1.00E+01	1.00E+01	1.17E+01
2.03E+03	5.56E+00	6.03E+01	6.67E+01	7.28E+01	3.55E+01	3.91E+01	4.22E+01	1.00E+01	1.00E+01	1.17E+01
2.08E+03	5.69E+00	6.03E+01	6.66E+01	7.27E+01	3.55E+01	3.90E+01	4.22E+01	1.00E+01	1.00E+01	1.15E+01
2.13E+03	5.83E+00	6.03E+01	6.65E+01	7.27E+01	3.55E+01	3.90E+01	4.21E+01	1.00E+01	1.00E+01	1.15E+01
2.18E+03	5.97E+00	6.03E+01	6.65E+01	7.26E+01	3.55E+01	3.89E+01	4.21E+01	1.00E+01	1.00E+01	1.14E+01
2.23E+03	6.10E+00	6.03E+01	6.65E+01	7.25E+01	3.55E+01	3.88E+01	4.20E+01	1.00E+01	1.00E+01	1.14E+01
2.28E+03	6.24E+00	6.03E+01	6.65E+01	7.24E+01	3.55E+01	3.88E+01	4.19E+01	1.00E+01	1.00E+01	1.14E+01
2.33E+03	6.38E+00	6.03E+01	6.64E+01	7.24E+01	3.55E+01	3.88E+01	4.19E+01	1.00E+01	1.00E+01	1.13E+01
2.38E+03	6.51E+00	6.03E+01	6.64E+01	7.23E+01	3.55E+01	3.87E+01	4.18E+01	1.00E+01	1.00E+01	1.13E+01
2.43E+03	6.65E+00	6.03E+01	6.63E+01	7.23E+01	3.55E+01	3.87E+01	4.18E+01	1.00E+01	1.00E+01	1.13E+01
2.48E+03	6.79E+00	6.02E+01	6.63E+01	7.22E+01	3.55E+01	3.87E+01	4.17E+01	1.00E+01	1.00E+01	1.12E+01
2.53E+03	6.92E+00	6.02E+01	6.63E+01	7.22E+01	3.54E+01	3.86E+01	4.16E+01	1.00E+01	1.00E+01	1.12E+01
2.58E+03	7.06E+00	6.02E+01	6.62E+01	7.22E+01	3.54E+01	3.86E+01	4.16E+01	1.00E+01	1.00E+01	1.12E+01
2.63E+03	7.20E+00	6.02E+01	6.62E+01	7.21E+01	3.53E+01	3.86E+01	4.16E+01	1.00E+01	1.00E+01	1.12E+01
2.68E+03	7.33E+00	6.01E+01	6.62E+01	7.21E+01	3.53E+01	3.85E+01	4.16E+01	1.00E+01	1.00E+01	1.12E+01
2.73E+03	7.47E+00	6.01E+01	6.62E+01	7.20E+01	3.53E+01	3.85E+01	4.15E+01	1.00E+01	1.00E+01	1.11E+01
2.78E+03	7.61E+00	6.01E+01	6.62E+01	7.20E+01	3.53E+01	3.85E+01	4.15E+01	1.00E+01	1.00E+01	1.11E+01
2.83E+03	7.75E+00	6.00E+01	6.61E+01	7.20E+01	3.52E+01	3.85E+01	4.15E+01	1.00E+01	1.00E+01	1.11E+01
2.88E+03	7.88E+00	6.00E+01	6.61E+01	7.19E+01	3.52E+01	3.84E+01	4.14E+01	1.00E+01	1.00E+01	1.11E+01

Appendix D. Sensitivity Analyses Results

Time		Wash Conc (ug/L)								
(d)	(yr)	90% Effective Remediation			95% Effective Remediation			No Southeast Flux		
		Low 95%	Median	High 95%	Low 95%	Median	High 95%	Low 95%	Median	High 95%
2.93E+03	8.02E+00	6.00E+01	6.61E+01	7.19E+01	3.52E+01	3.84E+01	4.14E+01	1.00E+01	1.00E+01	1.11E+01
2.98E+03	8.16E+00	6.00E+01	6.60E+01	7.19E+01	3.52E+01	3.84E+01	4.14E+01	1.00E+01	1.00E+01	1.10E+01
3.03E+03	8.29E+00	6.00E+01	6.60E+01	7.18E+01	3.52E+01	3.84E+01	4.14E+01	1.00E+01	1.00E+01	1.09E+01
3.08E+03	8.43E+00	6.00E+01	6.60E+01	7.18E+01	3.52E+01	3.84E+01	4.14E+01	1.00E+01	1.00E+01	1.09E+01
3.13E+03	8.57E+00	6.00E+01	6.59E+01	7.18E+01	3.52E+01	3.83E+01	4.13E+01	1.00E+01	1.00E+01	1.09E+01
3.18E+03	8.70E+00	6.00E+01	6.59E+01	7.18E+01	3.51E+01	3.83E+01	4.13E+01	1.00E+01	1.00E+01	1.09E+01
3.23E+03	8.84E+00	5.99E+01	6.59E+01	7.18E+01	3.51E+01	3.83E+01	4.13E+01	1.00E+01	1.00E+01	1.09E+01
3.28E+03	8.98E+00	5.99E+01	6.59E+01	7.17E+01	3.51E+01	3.83E+01	4.13E+01	1.00E+01	1.00E+01	1.09E+01
3.33E+03	9.11E+00	5.99E+01	6.58E+01	7.17E+01	3.51E+01	3.82E+01	4.13E+01	1.00E+01	1.00E+01	1.09E+01
3.38E+03	9.25E+00	5.98E+01	6.58E+01	7.17E+01	3.51E+01	3.82E+01	4.13E+01	1.00E+01	1.00E+01	1.09E+01
3.43E+03	9.39E+00	5.98E+01	6.58E+01	7.17E+01	3.51E+01	3.82E+01	4.12E+01	1.00E+01	1.00E+01	1.08E+01
3.48E+03	9.52E+00	5.98E+01	6.58E+01	7.17E+01	3.51E+01	3.82E+01	4.12E+01	1.00E+01	1.00E+01	1.08E+01
3.53E+03	9.66E+00	5.98E+01	6.57E+01	7.17E+01	3.51E+01	3.82E+01	4.12E+01	1.00E+01	1.00E+01	1.08E+01
3.58E+03	9.80E+00	5.97E+01	6.57E+01	7.17E+01	3.50E+01	3.81E+01	4.12E+01	1.00E+01	1.00E+01	1.08E+01
3.63E+03	9.94E+00	5.97E+01	6.57E+01	7.16E+01	3.50E+01	3.81E+01	4.12E+01	1.00E+01	1.00E+01	1.08E+01
3.68E+03	1.01E+01	5.97E+01	6.57E+01	7.16E+01	3.50E+01	3.81E+01	4.12E+01	1.00E+01	1.00E+01	1.08E+01
3.73E+03	1.02E+01	5.97E+01	6.57E+01	7.16E+01	3.50E+01	3.81E+01	4.12E+01	1.00E+01	1.00E+01	1.08E+01
3.78E+03	1.03E+01	5.96E+01	6.56E+01	7.16E+01	3.50E+01	3.80E+01	4.12E+01	1.00E+01	1.00E+01	1.07E+01
3.83E+03	1.05E+01	5.96E+01	6.56E+01	7.16E+01	3.49E+01	3.80E+01	4.11E+01	1.00E+01	1.00E+01	1.07E+01
3.88E+03	1.06E+01	5.96E+01	6.56E+01	7.16E+01	3.49E+01	3.80E+01	4.11E+01	1.00E+01	1.00E+01	1.07E+01
3.93E+03	1.08E+01	5.96E+01	6.56E+01	7.16E+01	3.49E+01	3.80E+01	4.11E+01	1.00E+01	1.00E+01	1.07E+01
3.98E+03	1.09E+01	5.96E+01	6.56E+01	7.15E+01	3.49E+01	3.80E+01	4.11E+01	1.00E+01	1.00E+01	1.06E+01
4.03E+03	1.10E+01	5.96E+01	6.55E+01	7.15E+01	3.49E+01	3.80E+01	4.11E+01	1.00E+01	1.00E+01	1.06E+01
4.08E+03	1.12E+01	5.96E+01	6.55E+01	7.15E+01	3.49E+01	3.79E+01	4.11E+01	1.00E+01	1.00E+01	1.06E+01
4.13E+03	1.13E+01	5.96E+01	6.55E+01	7.15E+01	3.49E+01	3.79E+01	4.10E+01	1.00E+01	1.00E+01	1.06E+01
4.18E+03	1.14E+01	5.96E+01	6.55E+01	7.15E+01	3.48E+01	3.79E+01	4.10E+01	1.00E+01	1.00E+01	1.06E+01
4.23E+03	1.16E+01	5.96E+01	6.55E+01	7.14E+01	3.48E+01	3.79E+01	4.10E+01	1.00E+01	1.00E+01	1.06E+01
4.28E+03	1.17E+01	5.96E+01	6.55E+01	7.14E+01	3.48E+01	3.79E+01	4.10E+01	1.00E+01	1.00E+01	1.06E+01
4.33E+03	1.19E+01	5.96E+01	6.55E+01	7.14E+01	3.48E+01	3.78E+01	4.10E+01	1.00E+01	1.00E+01	1.06E+01
4.38E+03	1.20E+01	5.95E+01	6.55E+01	7.14E+01	3.48E+01	3.78E+01	4.10E+01	1.00E+01	1.00E+01	1.06E+01
4.43E+03	1.21E+01	5.95E+01	6.54E+01	7.14E+01	3.48E+01	3.78E+01	4.09E+01	1.00E+01	1.00E+01	1.06E+01
4.48E+03	1.23E+01	5.95E+01	6.54E+01	7.14E+01	3.48E+01	3.78E+01	4.09E+01	1.00E+01	1.00E+01	1.06E+01
4.53E+03	1.24E+01	5.95E+01	6.54E+01	7.14E+01	3.48E+01	3.78E+01	4.09E+01	1.00E+01	1.00E+01	1.06E+01

Appendix D. Sensitivity Analyses Results

Time		Wash Conc (ug/L)								
(d)	(yr)	90% Effective Remediation			95% Effective Remediation			No Southeast Flux		
		Low 95%	Median	High 95%	Low 95%	Median	High 95%	Low 95%	Median	High 95%
4.58E+03	1.25E+01	5.95E+01	6.54E+01	7.13E+01	3.48E+01	3.78E+01	4.09E+01	1.00E+01	1.00E+01	1.06E+01
4.63E+03	1.27E+01	5.95E+01	6.54E+01	7.13E+01	3.48E+01	3.78E+01	4.09E+01	1.00E+01	1.00E+01	1.06E+01
4.68E+03	1.28E+01	5.95E+01	6.54E+01	7.13E+01	3.48E+01	3.78E+01	4.09E+01	1.00E+01	1.00E+01	1.06E+01
4.73E+03	1.29E+01	5.94E+01	6.54E+01	7.13E+01	3.48E+01	3.78E+01	4.08E+01	1.00E+01	1.00E+01	1.05E+01
4.78E+03	1.31E+01	5.94E+01	6.54E+01	7.13E+01	3.48E+01	3.78E+01	4.08E+01	1.00E+01	1.00E+01	1.05E+01
4.83E+03	1.32E+01	5.94E+01	6.54E+01	7.13E+01	3.48E+01	3.78E+01	4.08E+01	1.00E+01	1.00E+01	1.05E+01
4.88E+03	1.34E+01	5.94E+01	6.54E+01	7.13E+01	3.47E+01	3.78E+01	4.08E+01	1.00E+01	1.00E+01	1.05E+01
4.93E+03	1.35E+01	5.94E+01	6.54E+01	7.13E+01	3.47E+01	3.77E+01	4.08E+01	1.00E+01	1.00E+01	1.05E+01
4.98E+03	1.36E+01	5.94E+01	6.54E+01	7.12E+01	3.47E+01	3.77E+01	4.08E+01	1.00E+01	1.00E+01	1.05E+01
5.03E+03	1.38E+01	5.94E+01	6.53E+01	7.12E+01	3.47E+01	3.77E+01	4.08E+01	1.00E+01	1.00E+01	1.05E+01
5.08E+03	1.39E+01	5.94E+01	6.53E+01	7.12E+01	3.47E+01	3.77E+01	4.08E+01	1.00E+01	1.00E+01	1.05E+01
5.13E+03	1.40E+01	5.94E+01	6.53E+01	7.12E+01	3.47E+01	3.77E+01	4.08E+01	1.00E+01	1.00E+01	1.05E+01
5.18E+03	1.42E+01	5.94E+01	6.53E+01	7.12E+01	3.47E+01	3.77E+01	4.08E+01	1.00E+01	1.00E+01	1.04E+01
5.23E+03	1.43E+01	5.94E+01	6.53E+01	7.12E+01	3.47E+01	3.77E+01	4.08E+01	1.00E+01	1.00E+01	1.04E+01
5.28E+03	1.45E+01	5.94E+01	6.53E+01	7.12E+01	3.47E+01	3.77E+01	4.08E+01	1.00E+01	1.00E+01	1.04E+01
5.33E+03	1.46E+01	5.94E+01	6.53E+01	7.12E+01	3.47E+01	3.77E+01	4.08E+01	1.00E+01	1.00E+01	1.04E+01
5.38E+03	1.47E+01	5.94E+01	6.53E+01	7.11E+01	3.47E+01	3.77E+01	4.08E+01	1.00E+01	1.00E+01	1.04E+01
5.43E+03	1.49E+01	5.94E+01	6.53E+01	7.11E+01	3.47E+01	3.77E+01	4.08E+01	1.00E+01	1.00E+01	1.04E+01
5.48E+03	1.50E+01	5.94E+01	6.53E+01	7.11E+01	3.47E+01	3.77E+01	4.08E+01	1.00E+01	1.00E+01	1.03E+01
5.53E+03	1.51E+01	5.94E+01	6.53E+01	7.11E+01	3.47E+01	3.77E+01	4.08E+01	1.00E+01	1.00E+01	1.03E+01
5.58E+03	1.53E+01	5.94E+01	6.53E+01	7.11E+01	3.47E+01	3.77E+01	4.07E+01	1.00E+01	1.00E+01	1.03E+01
5.63E+03	1.54E+01	5.94E+01	6.53E+01	7.11E+01	3.47E+01	3.77E+01	4.07E+01	1.00E+01	1.00E+01	1.03E+01
5.68E+03	1.55E+01	5.94E+01	6.53E+01	7.11E+01	3.47E+01	3.77E+01	4.07E+01	1.00E+01	1.00E+01	1.03E+01
5.73E+03	1.57E+01	5.94E+01	6.53E+01	7.11E+01	3.47E+01	3.77E+01	4.07E+01	1.00E+01	1.00E+01	1.03E+01
5.78E+03	1.58E+01	5.94E+01	6.53E+01	7.11E+01	3.47E+01	3.77E+01	4.07E+01	1.00E+01	1.00E+01	1.03E+01
5.83E+03	1.60E+01	5.93E+01	6.53E+01	7.11E+01	3.47E+01	3.77E+01	4.07E+01	1.00E+01	1.00E+01	1.03E+01
5.88E+03	1.61E+01	5.93E+01	6.53E+01	7.11E+01	3.47E+01	3.77E+01	4.07E+01	1.00E+01	1.00E+01	1.03E+01
5.93E+03	1.62E+01	5.93E+01	6.53E+01	7.11E+01	3.47E+01	3.77E+01	4.07E+01	1.00E+01	1.00E+01	1.03E+01
5.98E+03	1.64E+01	5.93E+01	6.53E+01	7.11E+01	3.47E+01	3.77E+01	4.07E+01	1.00E+01	1.00E+01	1.03E+01
6.03E+03	1.65E+01	5.93E+01	6.53E+01	7.11E+01	3.47E+01	3.76E+01	4.07E+01	1.00E+01	1.00E+01	1.03E+01
6.08E+03	1.66E+01	5.93E+01	6.52E+01	7.11E+01	3.47E+01	3.76E+01	4.06E+01	1.00E+01	1.00E+01	1.03E+01
6.13E+03	1.68E+01	5.93E+01	6.52E+01	7.11E+01	3.46E+01	3.76E+01	4.06E+01	1.00E+01	1.00E+01	1.03E+01
6.18E+03	1.69E+01	5.93E+01	6.52E+01	7.11E+01	3.46E+01	3.76E+01	4.06E+01	1.00E+01	1.00E+01	1.03E+01

Appendix D. Sensitivity Analyses Results

Time		Wash Conc (ug/L)								
(d)	(yr)	90% Effective Remediation			95% Effective Remediation			No Southeast Flux		
		Low 95%	Median	High 95%	Low 95%	Median	High 95%	Low 95%	Median	High 95%
6.23E+03	1.71E+01	5.93E+01	6.52E+01	7.11E+01	3.46E+01	3.76E+01	4.06E+01	1.00E+01	1.00E+01	1.03E+01
6.28E+03	1.72E+01	5.93E+01	6.52E+01	7.11E+01	3.46E+01	3.76E+01	4.06E+01	1.00E+01	1.00E+01	1.03E+01
6.33E+03	1.73E+01	5.93E+01	6.52E+01	7.11E+01	3.46E+01	3.76E+01	4.06E+01	1.00E+01	1.00E+01	1.03E+01
6.38E+03	1.75E+01	5.93E+01	6.52E+01	7.11E+01	3.46E+01	3.76E+01	4.06E+01	1.00E+01	1.00E+01	1.03E+01
6.43E+03	1.76E+01	5.93E+01	6.52E+01	7.11E+01	3.46E+01	3.76E+01	4.06E+01	1.00E+01	1.00E+01	1.03E+01
6.48E+03	1.77E+01	5.93E+01	6.52E+01	7.11E+01	3.46E+01	3.76E+01	4.06E+01	1.00E+01	1.00E+01	1.03E+01
6.53E+03	1.79E+01	5.93E+01	6.52E+01	7.11E+01	3.46E+01	3.76E+01	4.06E+01	1.00E+01	1.00E+01	1.03E+01
6.58E+03	1.80E+01	5.93E+01	6.52E+01	7.11E+01	3.46E+01	3.76E+01	4.06E+01	1.00E+01	1.00E+01	1.03E+01
6.63E+03	1.81E+01	5.93E+01	6.52E+01	7.11E+01	3.46E+01	3.76E+01	4.06E+01	1.00E+01	1.00E+01	1.03E+01
6.68E+03	1.83E+01	5.93E+01	6.52E+01	7.11E+01	3.46E+01	3.76E+01	4.06E+01	1.00E+01	1.00E+01	1.03E+01
6.73E+03	1.84E+01	5.93E+01	6.52E+01	7.11E+01	3.46E+01	3.76E+01	4.06E+01	1.00E+01	1.00E+01	1.03E+01
6.78E+03	1.86E+01	5.93E+01	6.52E+01	7.11E+01	3.46E+01	3.76E+01	4.06E+01	1.00E+01	1.00E+01	1.03E+01
6.83E+03	1.87E+01	5.93E+01	6.52E+01	7.11E+01	3.46E+01	3.76E+01	4.06E+01	1.00E+01	1.00E+01	1.02E+01
6.88E+03	1.88E+01	5.93E+01	6.52E+01	7.11E+01	3.46E+01	3.76E+01	4.06E+01	1.00E+01	1.00E+01	1.02E+01
6.93E+03	1.90E+01	5.93E+01	6.52E+01	7.11E+01	3.46E+01	3.76E+01	4.06E+01	1.00E+01	1.00E+01	1.02E+01
6.98E+03	1.91E+01	5.93E+01	6.52E+01	7.10E+01	3.46E+01	3.76E+01	4.06E+01	1.00E+01	1.00E+01	1.02E+01
7.03E+03	1.92E+01	5.93E+01	6.52E+01	7.10E+01	3.46E+01	3.76E+01	4.06E+01	1.00E+01	1.00E+01	1.02E+01
7.08E+03	1.94E+01	5.93E+01	6.52E+01	7.10E+01	3.46E+01	3.76E+01	4.06E+01	1.00E+01	1.00E+01	1.02E+01
7.13E+03	1.95E+01	5.93E+01	6.52E+01	7.10E+01	3.46E+01	3.76E+01	4.06E+01	1.00E+01	1.00E+01	1.02E+01
7.18E+03	1.97E+01	5.93E+01	6.52E+01	7.10E+01	3.46E+01	3.76E+01	4.06E+01	1.00E+01	1.00E+01	1.02E+01
7.23E+03	1.98E+01	5.92E+01	6.51E+01	7.10E+01	3.46E+01	3.76E+01	4.05E+01	1.00E+01	1.00E+01	1.02E+01
7.28E+03	1.99E+01	5.92E+01	6.51E+01	7.10E+01	3.46E+01	3.76E+01	4.05E+01	1.00E+01	1.00E+01	1.02E+01
7.33E+03	2.01E+01	5.92E+01	6.51E+01	7.10E+01	3.46E+01	3.76E+01	4.05E+01	1.00E+01	1.00E+01	1.02E+01
7.38E+03	2.02E+01	5.92E+01	6.51E+01	7.10E+01	3.46E+01	3.76E+01	4.05E+01	1.00E+01	1.00E+01	1.02E+01
7.43E+03	2.03E+01	5.92E+01	6.51E+01	7.10E+01	3.46E+01	3.76E+01	4.05E+01	1.00E+01	1.00E+01	1.02E+01
7.48E+03	2.05E+01	5.92E+01	6.51E+01	7.10E+01	3.46E+01	3.76E+01	4.05E+01	1.00E+01	1.00E+01	1.02E+01
7.53E+03	2.06E+01	5.92E+01	6.51E+01	7.10E+01	3.46E+01	3.76E+01	4.05E+01	1.00E+01	1.00E+01	1.02E+01
7.58E+03	2.08E+01	5.92E+01	6.51E+01	7.10E+01	3.46E+01	3.76E+01	4.05E+01	1.00E+01	1.00E+01	1.02E+01
7.63E+03	2.09E+01	5.92E+01	6.51E+01	7.10E+01	3.46E+01	3.76E+01	4.05E+01	1.00E+01	1.00E+01	1.02E+01
7.68E+03	2.10E+01	5.92E+01	6.51E+01	7.10E+01	3.46E+01	3.76E+01	4.05E+01	1.00E+01	1.00E+01	1.02E+01
7.73E+03	2.12E+01	5.92E+01	6.51E+01	7.10E+01	3.46E+01	3.76E+01	4.05E+01	1.00E+01	1.00E+01	1.02E+01
7.78E+03	2.13E+01	5.92E+01	6.51E+01	7.10E+01	3.46E+01	3.76E+01	4.05E+01	1.00E+01	1.00E+01	1.02E+01
7.83E+03	2.14E+01	5.92E+01	6.51E+01	7.10E+01	3.46E+01	3.76E+01	4.05E+01	1.00E+01	1.00E+01	1.02E+01

Appendix D. Sensitivity Analyses Results

Time		Wash Conc (ug/L)								
(d)	(yr)	90% Effective Remediation			95% Effective Remediation			No Southeast Flux		
		Low 95%	Median	High 95%	Low 95%	Median	High 95%	Low 95%	Median	High 95%
7.88E+03	2.16E+01	5.92E+01	6.51E+01	7.10E+01	3.46E+01	3.76E+01	4.05E+01	1.00E+01	1.00E+01	1.02E+01
7.93E+03	2.17E+01	5.92E+01	6.51E+01	7.09E+01	3.46E+01	3.76E+01	4.05E+01	1.00E+01	1.00E+01	1.02E+01
7.98E+03	2.18E+01	5.92E+01	6.51E+01	7.09E+01	3.46E+01	3.76E+01	4.05E+01	1.00E+01	1.00E+01	1.02E+01
8.03E+03	2.20E+01	5.92E+01	6.51E+01	7.09E+01	3.46E+01	3.76E+01	4.05E+01	1.00E+01	1.00E+01	1.02E+01
8.08E+03	2.21E+01	5.92E+01	6.51E+01	7.09E+01	3.46E+01	3.76E+01	4.05E+01	1.00E+01	1.00E+01	1.02E+01
8.13E+03	2.23E+01	5.92E+01	6.51E+01	7.09E+01	3.46E+01	3.76E+01	4.05E+01	1.00E+01	1.00E+01	1.02E+01
8.18E+03	2.24E+01	5.92E+01	6.51E+01	7.09E+01	3.46E+01	3.76E+01	4.05E+01	1.00E+01	1.00E+01	1.02E+01
8.23E+03	2.25E+01	5.92E+01	6.51E+01	7.09E+01	3.46E+01	3.76E+01	4.05E+01	1.00E+01	1.00E+01	1.02E+01
8.28E+03	2.27E+01	5.92E+01	6.51E+01	7.09E+01	3.46E+01	3.76E+01	4.05E+01	1.00E+01	1.00E+01	1.02E+01
8.33E+03	2.28E+01	5.92E+01	6.51E+01	7.09E+01	3.46E+01	3.76E+01	4.05E+01	1.00E+01	1.00E+01	1.02E+01
8.38E+03	2.29E+01	5.92E+01	6.51E+01	7.09E+01	3.46E+01	3.76E+01	4.05E+01	1.00E+01	1.00E+01	1.02E+01
8.43E+03	2.31E+01	5.92E+01	6.51E+01	7.09E+01	3.46E+01	3.76E+01	4.05E+01	1.00E+01	1.00E+01	1.02E+01
8.48E+03	2.32E+01	5.92E+01	6.51E+01	7.09E+01	3.46E+01	3.76E+01	4.05E+01	1.00E+01	1.00E+01	1.02E+01
8.53E+03	2.34E+01	5.92E+01	6.51E+01	7.09E+01	3.46E+01	3.76E+01	4.05E+01	1.00E+01	1.00E+01	1.02E+01
8.58E+03	2.35E+01	5.92E+01	6.51E+01	7.09E+01	3.46E+01	3.76E+01	4.05E+01	1.00E+01	1.00E+01	1.02E+01
8.63E+03	2.36E+01	5.92E+01	6.51E+01	7.09E+01	3.46E+01	3.76E+01	4.05E+01	1.00E+01	1.00E+01	1.01E+01
8.68E+03	2.38E+01	5.92E+01	6.51E+01	7.09E+01	3.46E+01	3.76E+01	4.05E+01	1.00E+01	1.00E+01	1.01E+01
8.73E+03	2.39E+01	5.92E+01	6.51E+01	7.09E+01	3.46E+01	3.76E+01	4.05E+01	1.00E+01	1.00E+01	1.01E+01
8.78E+03	2.40E+01	5.92E+01	6.51E+01	7.09E+01	3.46E+01	3.76E+01	4.05E+01	1.00E+01	1.00E+01	1.01E+01
8.83E+03	2.42E+01	5.92E+01	6.51E+01	7.09E+01	3.46E+01	3.76E+01	4.05E+01	1.00E+01	1.00E+01	1.01E+01
8.88E+03	2.43E+01	5.92E+01	6.51E+01	7.09E+01	3.46E+01	3.76E+01	4.05E+01	1.00E+01	1.00E+01	1.01E+01
8.93E+03	2.44E+01	5.92E+01	6.51E+01	7.09E+01	3.46E+01	3.76E+01	4.05E+01	1.00E+01	1.00E+01	1.01E+01
8.98E+03	2.46E+01	5.92E+01	6.51E+01	7.09E+01	3.46E+01	3.76E+01	4.05E+01	1.00E+01	1.00E+01	1.01E+01
9.03E+03	2.47E+01	5.92E+01	6.51E+01	7.09E+01	3.46E+01	3.76E+01	4.05E+01	1.00E+01	1.00E+01	1.01E+01
9.08E+03	2.49E+01	5.92E+01	6.51E+01	7.09E+01	3.46E+01	3.76E+01	4.05E+01	1.00E+01	1.00E+01	1.01E+01
9.13E+03	2.50E+01	5.92E+01	6.51E+01	7.09E+01	3.46E+01	3.76E+01	4.05E+01	1.00E+01	1.00E+01	1.01E+01
9.13E+03	2.50E+01	5.92E+01	6.51E+01	7.09E+01	3.46E+01	3.76E+01	4.05E+01	1.00E+01	1.00E+01	1.01E+01